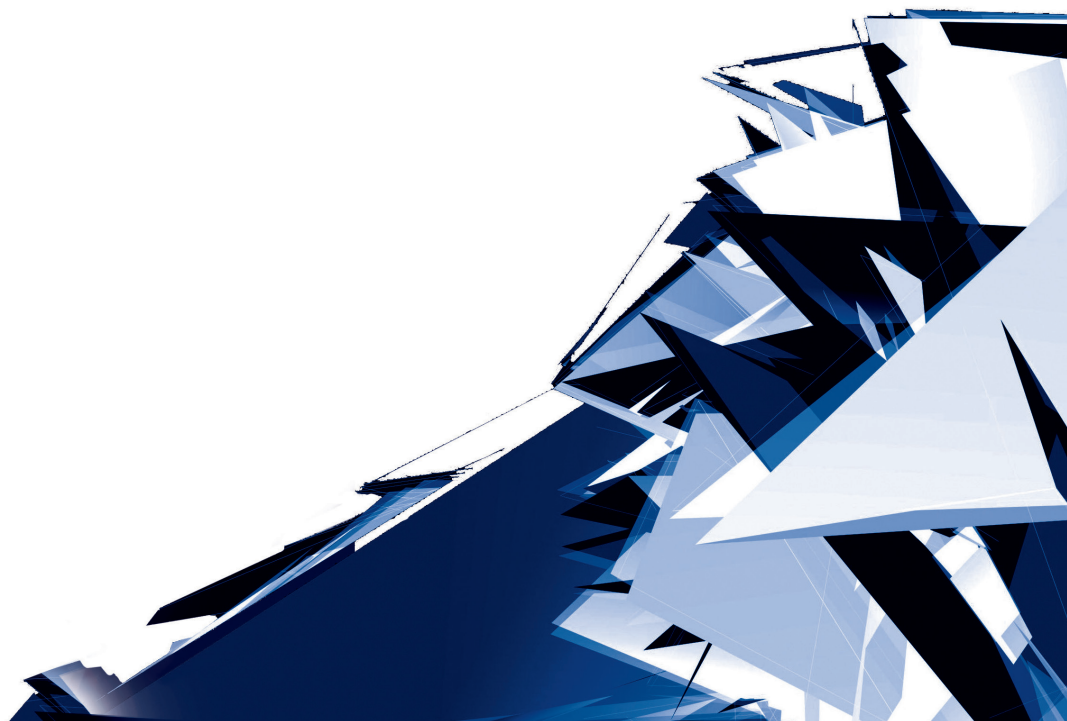


Technical Transactions

Czasopismo Techniczne

Volume 9

Year 2017 (114)



Chairman of the Cracow University of Technology Press Editorial Board
Przewodniczący Kolegium Redakcyjnego Wydawnictwa Politechniki Krakowskiej

Tadeusz Tatara

Editor-in-chief
Redaktor naczelny

Józef Gawlik
(jgawlik@mech.pk.edu.pl)

Scientific Council
Rada Naukowa

Jan Blachut – University of Liverpool (UK)
Wojciech Bonenberg – Poznan University of Technology (Poland)
Tadeusz Burczyński – Silesian University of Technology (Poland)
Massimo Corcione – Sapienza University of Rome (Italy)
Leszek Demkowicz – The University of Texas at Austin (USA)
Joseph El Hayek – University of Applied Sciences (Switzerland)
Ameen Farooq – Technical University of Atlanta (USA)
Zbigniew Florjańczyk – Warsaw University of Technology (Poland)
Marian Giżejowski – Warsaw University of Technology (Poland)
Sławomir Gzell – Warsaw University of Technology (Poland)
Allan N. Hayhurst – University of Cambridge (UK)
Maria Kuśnierowa – Slovak Academy of Sciences (Slovakia)
Krzysztof Magnucki – Poznan University of Technology (Poland)
Herbert Mang – Vienna University of Technology (Austria)
Arthur E. McGarity – Swarthmore College (USA)
Antonio Monestiroli – Polytechnic of Milan (Italy)
Ivor Samuels – University of Birmingham (UK)
Mirosław J. Skibniewski – University of Maryland (USA)
Günter Wozny – Technical University in Berlin (Germany)
Roman Zarzycki – Lodz University of Technology (Poland)

Native Speakers

Weryfikacja językowa

Tim Churcher
Justin Nnorom

Section Editor
Sekretarz Sekcji

Dorota Sapek
(dsapek@wydawnictwo.pk.edu.pl)

Editorial Compilation
Opracowanie redakcyjne

Aleksandra Urzędowska
(aurzedowska@pk.edu.pl)

Typesetting
Skład i lamanie

Anna Basista

Design
Projekt graficzny

Michał Graffstein

Series Editors
Redaktorzy Serii

ARCHITECTURE AND URBAN PLANNING

Mateusz Gyurkovich
(mgyurkovich@pk.edu.pl)

CHEMISTRY

Radomir Jasiński
(radomir@chemia.pk.edu.pl)

CIVIL ENGINEERING

Marek Piekarczyk
(mpiekar@pk.edu.pl)

ELECTRICAL ENGINEERING

Piotr Drozdowski
(pdrozdow@usk.pk.edu.pl)

ENVIRONMENTAL ENGINEERING

Michał Zielina
(mziel@vistula.wis.pk.edu.pl)

**PHYSICS, MATHEMATICS
AND COMPUTER SCIENCES**

Włodzimierz Wójcik
(puwojcik@cyf-kr.edu.pl)

MECHANICS

Andrzej Sobczyk
(andrzej.sobczyk@mech.pk.edu.pl)

www.ejournals.eu/Czasopismo-Techniczne
www.technicaltransactions.com
www.czasopismotechniczne.pl

Contents

ARCHITECTURE AND URBAN PLANNING

Rafał Blazy	
<i>Deformation of the city</i>	5
Piotr Langer	
<i>Life and death of a colliery. The condition and significance of former coal mining facilities in the transborder region of Saarland-Moselle</i>	23
Wojciech Kujawski	
<i>New role of buildings as contributors to the infrastructure</i>	43

CIVIL ENGINEERING

Magdalena Rogalska, Zdzisław Hejducki	
<i>The application of time coupling methods in the engineering of construction projects</i>	67
Janusz Kogut, Jakub Zięba	
<i>The modification of the dynamic properties of cohesive soil resulting from triaxial consolidation</i>	75
Maria Kośmiejka, Jerzy Paślowski	
<i>A flexible approach to the evaluation of the cost effectiveness of investment projects</i>	91
Dorota Olszewska	
<i>The acceleration response spectra for Legnica-Głogow copper district</i>	99
Dariusz Skorupka, Artur Duchaczek, Agnieszka Waniewska	
<i>Optimisation of the choice of UAV intended to control the implementation of construction projects and works using the AHP method</i>	117
Andrzej Więckowski	
<i>Modelling the delivery and laying of concrete mix</i>	127

ENVIRONMENTAL ENGINEERING

Maciej Knapik	
<i>Analysis of influence of LEED certification process to achieve the passive house standard</i> ...	137

MATHEMATICS

Ludwik Byszewski	
<i>Continuous dependence of mild solutions, on initial nonlocal data, of the nonlocal semilinear evolution Cauchy problems</i>	151

MECHANICS

Mariusz Domagała, Hassan Momeni	
<i>CFD simulation of cavitation over water turbine hydrofoils</i>	159

Joanna Fabiś-Domagala	
<i>Quality function deployment method for selected website usability analysis</i>	165
Renata Filipowska	
<i>Homotopy perturbation method for solving fourth – order boundary value problems with additional boundary condition</i>	173
Ewa Koziń	
<i>Application of approximation technique to on-line updating of the actual cost curve in the earned value method</i>	181
Stanislaw Krenich	
<i>Multi-thread evolutionary computation for design optimization</i>	197
Marek A. Książek, Janusz Tarnowski	
<i>Influence of dual vibrations on control of percussive hand-operated power tools – experimental investigations</i>	207
Filip Lisowski	
<i>Optimization of thread root undercut in the planetary roller screw</i>	219
Przemysław Młynarczyk, Piotr Cyklis	
<i>Application of porous media flow model for the regenerator fluidised bed simulation</i>	229
Andrzej Skowronek	
<i>Application of the multi-generating method to support the quality of smart designs of experiment</i>	237

Rafał Blazy (r_j_blazy@wp.pl)

Faculty of Architecture, Institute of Cities and Region Designing,
Cracow University of Technology

DEFORMATION OF THE CITY

DEFORMOWANIE MIASTA

Abstract

Cities in the present time are developing in a very vivid and dynamic way. At the same time, in Polish reality, many cities are physically losing the characteristics of buildings that defined the urban space for centuries. It seems that some cases of Polish cities are heading towards „formlessness”, and their structure instead of being crystallized is deformed and destroyed. The problem of the loss of the cities' urban form was named by the author as the deformation of the city. The article presents social, cultural and legislative phenomena which cause negative processes, also points out the chances and possibilities of real prevention of urban structure's break up.

Keywords: Chaos, shapeless city, deformed city, city without city, future of cities, city deformation, city creation, city formation

Streszczenie

Miasta w obecnym czasie rozwijają się w sposób bardzo dynamiczny i żywiołowy. Jednocześnie w rzeczywistości polskiej wiele miast fizycznie traci cechy zabudowy, która od wieków definiowała przestrzeń miejską. Wydaje się, że niektóre przypadki miast polskich zmierzają w kierunku „bezformia”, a ich struktura zamiast podlegać krystalizacji ulega deformacji i destrukcji. Problem utraty miejskiej formy miast został nazwany przez autora deformowaniem miasta. W artykule zaprezentowano zjawiska społeczne, kulturowe i legislacyjne, które wywołują niekorzystne procesy, wskazano także na szanse i możliwości realnego zapobiegania rozbijaniu struktury miejskiej.

Słowa kluczowe: Chaos, bezkształtne miasto, zdeformowane miasto, miasto bez miasta, przyszłość miast, deformowanie miasta, kreowanie miasta, formowanie miasta

1. Background

Nowadays, the cities are developing in a very vivid and dynamic way. At the same time, in Polish reality, a lot of cities physically lose the character of buildings, which defined so far the space considered as urban. It seems that some Polish cities are heading towards “formlessness”, and their structure, instead of being crystallized, is subject to deformation and destruction. The processes visible in the context of urban transformation are largely reflected in the changes that are taking place in our society and the broadly understood culture. A number of publications including *Living in the Endless City* [22] and *Drosscape – Wasting Land in Urban America* [6] point the problems of city deformation and reconfiguration, making it a reference to issues in a broader European-Atlantic context.

In the contemporary literature it can be noticed that there is a constant search for the formula of the city: the following projects can be included within the above mentioned topic: *Kartal – Pendik Masterplan of Istanbul* by Zaha Hadid, *Masdar City* by Norman Foster, *Songdo* – studio Kohn Pedersen Fox and *Seven Mountains on Zira Island near Baku* by the Danish studio Bjarke Ingels Group (BIG). In all of them the city is treated as an experimental field [22, p. 44–55].

On the other hand, we more often look at traditional urban arrangements with some nostalgia. Remo Koolhaas publications or Marta Schwartz¹. We also observe a strong movement of urban renewal which is a counterbalance to modernism – seeking to correct their own misconceptions and assumptions of modernism. This move aims to restore the old form of cities and the “meaning of the city”. According to the developers, what shaped the cities was not the need to meet housing needs nor to create infrastructure. Examples of this type of activity in Poland are *Elblag city center plan*, *Germany plans for Gladbeck* (Michael Stojan Projects), *Kirchsteigfeld (Drewitz) in Potcheid*, *Rieselfeld and Vauban in Freiburg*, and *Great Britain in Poundsbury, Poundbury, Aberdeen and Coed Darcy*.

Sociologists have noted that in many cities their indigenous – rooted communities live in internal opposition to the existing and proposed changes in the scale of the city and the proliferation of its territory which destroy the traditional, fine texture of the building tissue. In practice of spatial management, in order to ensure social acceptance for the uncontrolled spread of development, the local population is presented with positive equivalents of the inconvenience caused in the form of the development of road and technical infrastructure. It is also argued that the territorial development associated with the new investment areas brings profits into a significant increase in the budget of the municipality which should be reflected in the well-being of its inhabitants.

Sociologists also point out that uncontrolled development produces untamed social phenomena and processes – similar to those in Biology. They point out that under natural conditions, a foreign implant – a new organ or invasion of a hostile virus – encounters natural resistance from the body. The organism is trying to reject what it defines as an intruder in

¹ The emerging terms “city within a city” or “non-existent urbanism” are also reflections of the processes that have arisen in cities, [27].

Entropic Indicators

Houston, Texas

The Houston Ship Channel (due east of downtown to the water) is the region's densest concentration of intermodal sites, manufacturing establishments, and contaminated land. This region exhibits a classic drosscape signature with the majority of wasted deindustrialized land near the city center and the wasteful low density land around the city's periphery. The urbanized region also contains over 4,200 closed municipal solid waste landfills that may potentially be redeveloped.

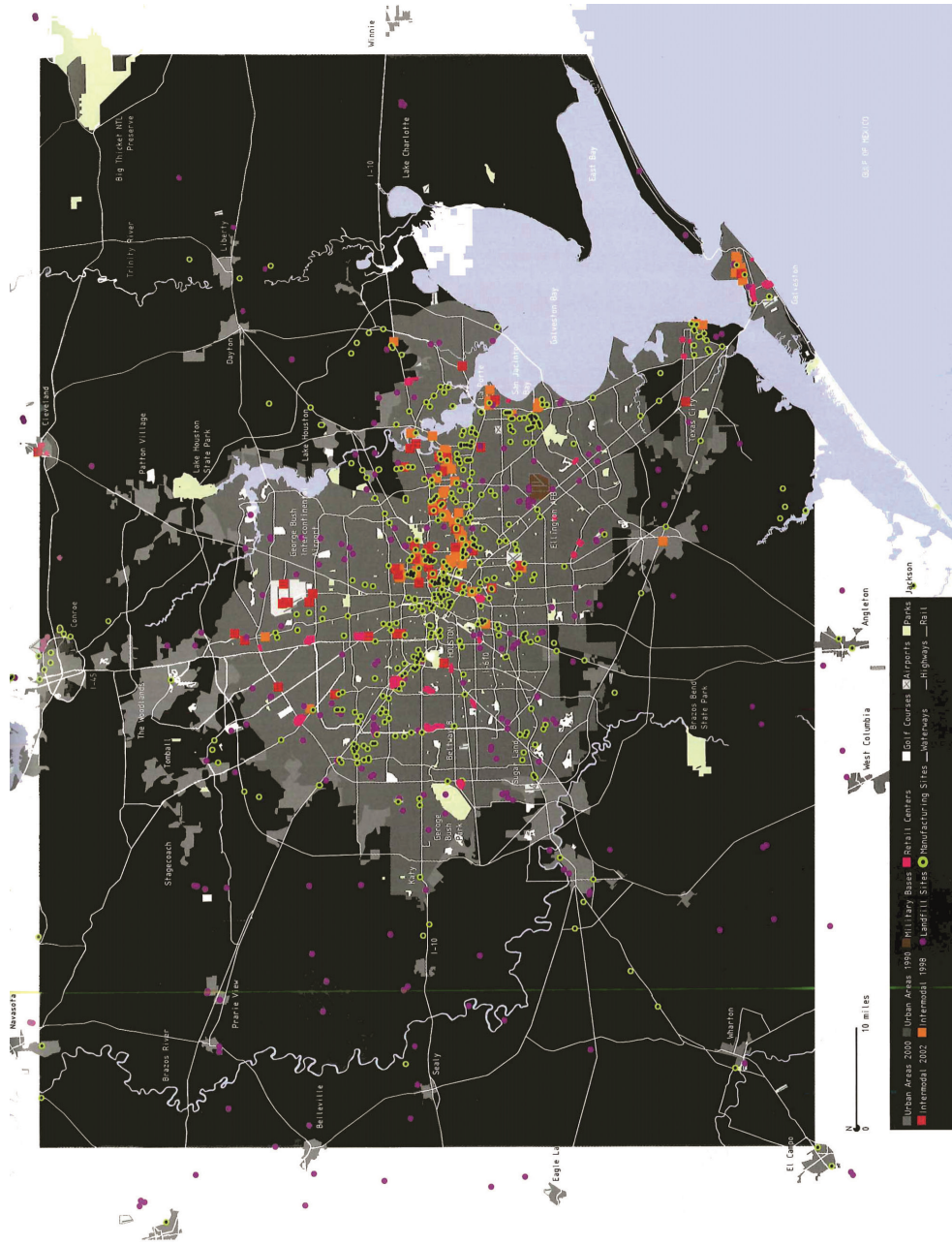


Fig. 1. Analysis and determination of entropic sites and coefficients for Houston, Texas (source: [6, p. 123])

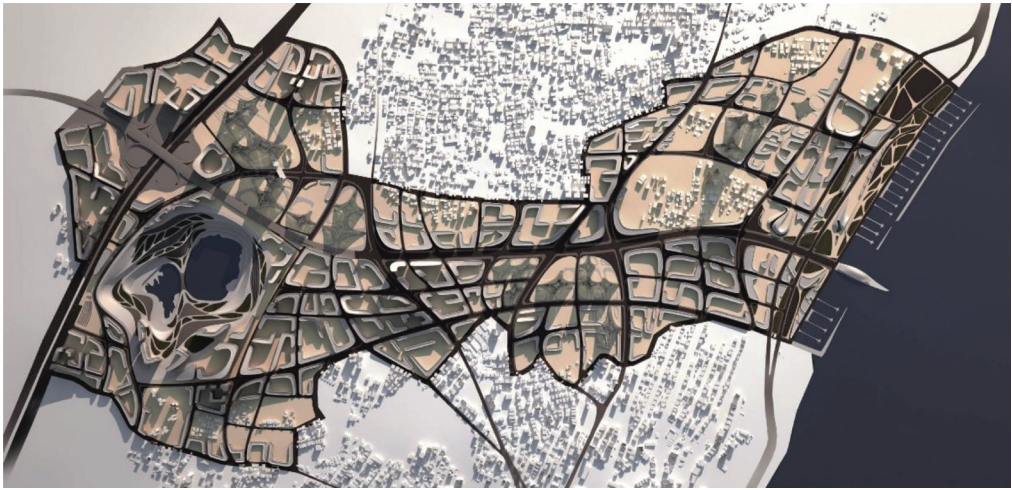


Fig. 2. A project of urban tissue transformation for the Kartal Region in the Metropolis of Istanbul, under the direction of Zaha Hadid (source: [36])

the system. Immunosuppressants are used to overcome the body's resistance to induce it to receive a transplanted organ. Similarly, there is a local community existing in the territory which is forced to operate in the new socio-spatial conditions. Behaviorists argue that, as with immunosuppressive drugs, the side effect of violent and unnatural spatial changes may be the destruction of natural protective systems and constituting the community at sociological level.

Persistent damage to the immune system in biology is that the body is unable to resist any infection or danger. Accordingly, they assume that the damage and disruption of existing social relationships, especially in small towns, can have similar effects.

In many small Polish cities we observe the lack of use in the planning work of existing and previously planned plans and analyzes. Marjan Kloosterboer in *Lessons of Informality* writes that actions taken in the context of new plans are based more on the tabula rasa approach than on the continuation or refinement of existing documents [19, p. 62–70]. The effects of this type of “approach” is observed in many municipalities outside the urban agglomerations such as Łomianki, Otwock, Wolomin near Warsaw, Zielonka, Zabierzów or Mogilany near Krakow. In this way there is no respect for the value of the current spatial layout and the existing landscape. There is also no appreciation of the values resulting from the band, concentric, knot or stripe-node layout of land invested in combination with high natural and recreational values with a surrounding, harmonious and already existing small urban scale.

Undoubtedly, contemporary culture is characterized by some degree of undermining tradition and authority. Looking more broadly, it seems to be the result of the dominant ways and styles in Art and Philosophy in the twentieth century. Modernism, cubism, postmodernism, and deconstructivism are the directions that have definitely broken with tradition. Modernism strongly connected with conceptualism has been called a modern movement in architecture. Kubism developing in the early twentieth century, predominantly in art, broke with the traditional representation of reality in favor of abstraction, which was

expressed by drawing lines, colors and contours. Postmodernism, although drawing on historical resources, using different stylistic styles, does not take cultural heritage seriously, it further strengthens the conviction of relativity depending on the subjective perceptions of the individual. In turn deconstructivism from its assumption is a deformation of form. Not too far from the truth is therefore the statement that modern culture, which grew mainly on the basis of postmodernism, it is a deconstruction of culture and social values. This is stated by Maria Miczyńska-Kowalska in the book *Values in postmodernism. The concept of deconstruction of social reality – critical analysis*.

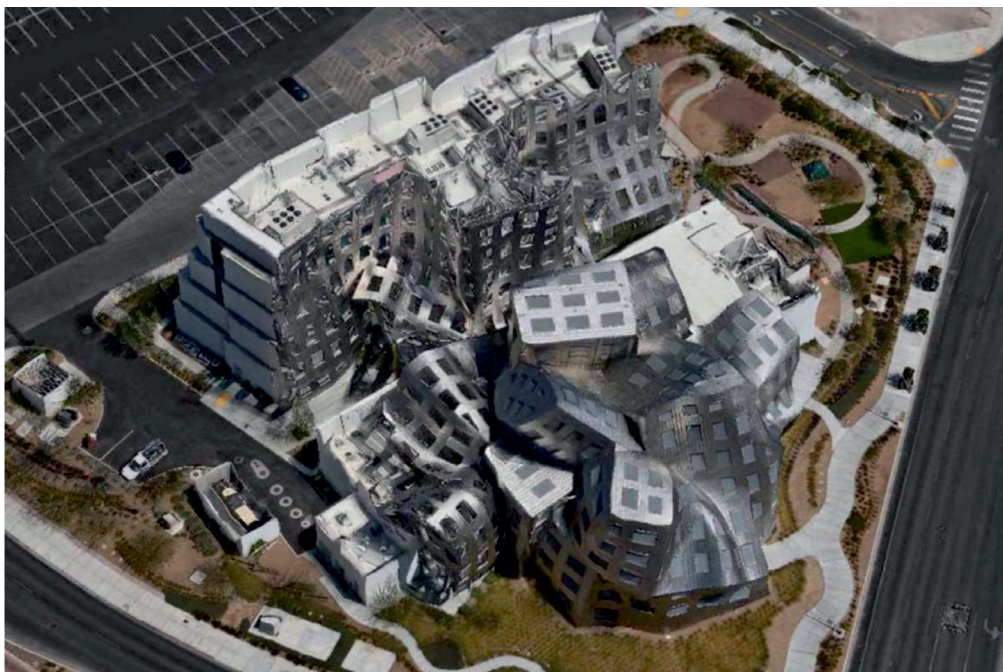


Fig. 3. Example of the deconstructive foundation by Frank Gehry's of Lou Ruvo Center for Brain Health (source: [37])

Looking at the world from the perspective of civilization development, it is clear that in each of the epochs a slightly different image of man has been formed. Undoubtedly, the culture influences man and their values and patterns of behavior. The extreme and even militant individualism which is exposed by the media, in the example of politicians and even scholars, makes everything seems subjective and relative (compared by Milena Banasiak: *Beauty as a subjective and objective value* [2]). It can also be noted that what is new and modern is increasingly important. Media exerts a tremendous impact on human beings by boosting momentum to continuous change. We often behave like a spectator in front of a television that jumps from the canal to the canal, unable to stop for longer period of time, unable to concentrate for a while, and we do not enjoy our achievements and gifts for more than a few minutes.

2. Problem

Chaos in the world of culture, aesthetics and ethics results not only in conceptual chaos but also in spatial chaos. Many contemporary urbanists, architectural theoreticians and planners emphasize the fact that the structure of the city has been broken down [18, p. 125–133]. The uncontrolled spread of urban organisms in the form of distracting growth and suburban hyperplasia is one of the fundamental problems of the modern city². In fact, today's city could be compared to a clay pot. In literature, we find statements describing this phenomenon as island urbanism, urban chaos and city explosion. More broadly, looking at the disintegration of the urban structure on its fragments leads to the dysfunctionality resulting from the lack of interaction between the related parts of one organism, which is each city. In living biological organisms, it is difficult to imagine, for example, the development of the left part of the body in the case of hypopituitarism and underdevelopment of the right part. This problem is well characterized by the statements made by the Commission of the European Union: "The future of cities" quoting "Urban sprawl and the spread of low population density housing is one of the main threats to sustainable territorial development. Public services are getting more and more expensive and difficult, natural resources are over-exploited, public transport networks are insufficient, and the dependence on cars and traffic in cities and towns is very high" [13, p. VI].

The contextual approach (in the analysis of the problem) presented in this text attempts to state (present) the current city against the background of the prevailing culture, social transformation and image of the present man. Reflecting on the future of the city in our surroundings, we should ask ourselves a few questions: how to prevent the city from growing, how to control the dynamism causing the breakdown of the city form as it does not lead to city formlessness³?

3. Antidotum – theoretical part

Theoreticians of aesthetics and philosophers emphasize that to shape something, one has to shape something. This is a creationist approach, based on the assumption that there must be an entity that undertakes the creation act of the so-creator. The evolutionary approach, on the other hand, is based on the assumption that everything is happening in the same way that nature can manage itself. Life, however, shows that in the case of a city form cannot

² The modern man seems to say, "I'm free, because I am free", and he is sure of his own right and is convinced of his infallibility. It conforms to a media standard, living momentarily and most often without consequences. The world of advertising seems to imply the principle of "I consume, so I am". Much individualistic and even selfish attitudes are promoted and praised largely. The paradigm of individual economic success and material values is one of the foundations of our collective existence. Man becomes more of a pilgrim or a constantly moving nomad in a dynamic and permanently changing reality. Psychology and pedagogy confirm that it is increasingly difficult for us to reach a state of harmony, peace and balance.

³ The attempt to answer and solve these problems cannot remain in the world of moralizing appeals that "should be" that "it is necessary" and that "it is", the modern man who hears that "something must" – shudders at the very thought of it this type of statement reacts almost allergically.

give up only the elements. The process of creation has analyzed precisely St. Augustine. The philosopher of creation is the same as the formation. According to him, creation is the giving or materializing of essences in a given object, in other words, giving the most essential and characteristic of a given object. St. Augustine writes that creation requires participation, that is the participation and engagement. Without this participation nothing can happen. In his opinion, each form also requires measure⁴. The conclusion of his vision is to say that only in a proper form we achieve the fullness of the proper existence of the given object. The penetration of the above analysis St. Augustine urges that the definition of urban development from the perspective of form is indispensable. Trying to apply these principles to the city, it should be stated that without the active participation of the local community, the form of a city cannot itself be realized; there must also be an entity that will take responsibility and act to create a model of a city. At present, such a symbolic entity is the designer of the Local Plan of Spatial Development, however; its powers in the sphere of influence on the shape of space are small because formally responsible for the development of the plan is the head of the mayor or the president. You also need to adopt a specific (forming) principle. In spatial terms, the essence of urban form is concentration – the compactness of buildings while the coexistence of public spaces. The measure of the city is the quantity, density and intensification of buildings, and the number, form and area of public space proportional to that quantity.

For the author, in terms of urban form, these qualities seem to be fundamental to urbanism. Lastly, as in every composition, and also for the author it is the city as well, for the introduction of order we need, like in music, a specific rhythm, which would additionally organize and systematize the material that is the matter of buildings and their interstates. For example, if the width of a building plots for single-family housing starts to be greater than 30 m, then we cannot speak at this stage about urban development. Interesting insights concerning the width of plots are provided by Jacek Kozinski's lecture entitled "The social costs of the current urbanization model borne by other groups outside the local government"⁵.

As it was said, the form requires a certain principle, therefore the world without principles is a deformed world, and the emerging towns are areas filled with formlessness, in other words, amorphous cities. The powerlessness associated with lack of composition in the city results from the lack of a shared sense of duty to take care of its form. The authorities are not directly and explicitly obliged to take care of the beauty of the village. The provisions of the Land Use Planning Act do not in any way oblige the authorities in the Local Spatial Development Plans to make compositional rules for agglomeration⁶. Finally, they are not competing with each

⁴ Referring these visions to a simple example, it is important to note that only a collection of pages or pages of the appropriate layout combined with the cover, the cover page and the content in the chapters gives – defines the book [1, p. 34–42].

⁵ Jacek Kozinski's lecture: Social costs of the current urbanization model borne by other groups outside the local government. Financial effects of abandonment of land consolidation. Profitability of urbanization processes. Conference material entitled: The financial implications of the Polish spatial planning system [31].

⁶ This problem was discussed and described by prof. Barbara Bartkovicz, among others [3, 32]; Problems of harmonizing the space of Polish cities and areas in the light of internal conditions and integration with the European Union [30].

other and we have lost the feeling that they have to be representative. This problem was largely described by Alan Berger in *The Production of Waste Landscape* [6, p. 46–63].

Choosing in practice Polish “cheaper designers” developing the planning work results in simpler, easier and incomplete solutions. On the other hand, beauty, aesthetics and representativeness require time, resources and inputs, which we still lack. Often, somewhere in the interior we envy some of their beautiful cities, without making any effort to embellish our city and its immediate surroundings. Meanwhile, spatial order, as some studies show, is one of the catalysts of development. Alicja Kopeć (Spatial order catalyses the development of Gdansk) writes about this in her article. It must be remembered that beauty is self-promoting [20].

As studies show, housing development decisions are not procedures that stop urban sprawl. These decisions largely favor the atomization and breakdown of the urban structure into sets of independent monitors. In 97% applications for housing development decisions are considered positively – according to the proposals and plans of the investors. A filter and document that has a real impact on the city is the Local Spatial Development Plan (MPZP). This is one of the reasons why it is such an important piece of local law that translates into the form of our cities. No local land use plans or their incorrect – incomplete studies have a destructive effect on our space.

On the other hand, in analytical and specialist studies, the classification of urban spaces is often incorrect. The statistical adoption and recognition in European Union documents that population density of 3 persons/ha is equivalent to the suburbs, and the indicator of 15 persons per ha is characteristic for the city as the minimum indicator of urbanization, contrary to any of the principles described in the books on spatial planning and urban planning⁷. It should be noted that for single-family housing it is assumed that the density of the population oscillates from 40–100 persons/ha, and for the built-up 70–200 persons/ha⁸[8]. Estimation based on the aforementioned indicators of the number of urban and suburban areas in Europe casts doubt on the reliability of conducted research and analysis. In pre-war Warsaw, population density was 243 persons/ha, with no space for squares and gardens about 500 persons/ha.

4. Antidotum – practical part

unrestrained desire to build new areas at city borders seems to be a very important issue. It is a mental problem to give up the ability to build “my-own” terrain for many people. Looking for an answer to the question of when and why we are able to give up our reason, the author in psychological and pedagogical literature has found the answer why man resigns from his rights to:

⁷ The intensity of conflicts is, for example, inversely proportional to the [5, 31].

⁸ Data compiled by the author on the basis of indicators [from:] Table 1. Defining cities by population density, p. 3, [13].

- ▶ ideas (love, victory, truth, good).
- ▶ health,
- ▶ better future.

It seems therefore that, in order to strengthen the argument for non-development of a given area, it would be necessary to address these three issues. It is worth to take care of the idea a bit earlier than at the time of developing the Local Spatial Development Plan. Creating a proper image of the city over the years results not only in its appearance but also in its commitment to the promotion of the city. In this way, the feelings of pride, belonging, respect, values of the place and social self-consciousness are strengthened. One example is Copenhagen's multi-annual and systematic approach to making it a child-friendly city [14, 15].

The author tried on the basis of conversations with various investors and students and on the basis of his own experience to compile features which we are difficult to give up in the case of having own plot, or larger area for investment. These features are also described in the literature, among others, in the articles by K.C. Sivaramakrishmanna [29]⁹, where they are ranked from the hardest to the easiest.

1. Resignation from the possibility of any development of the plot,
2. Abandonment of certain building functions,
3. Resignation from a certain building size,
4. Resignation from the form of the building,
5. Resignation from parking by the building,
6. Resignation from the shape of the roof,
7. Resignation from the color of the building,
8. Resignation from the form of advertising.

The selected feature set shows the degree of difficulty and degree of resistance we encounter when developing the Local Spatial Development Plan. At the same time, the comparison shows that practically without special loads we are able to regulate and unify the buildings with the colors and shapes of the roofs. Examples of cities whose beautiful landscape is the synergy of these two traits may be Polish Masurian Ryn, and Italian Tuscany, also Florence and Siena. Even less would seem to limit the amount of usable colors and narrowing their spectrum can significantly standardize the building¹⁰.

Turning to the issue of abandoning the possibility of building a plot clearly visible that this is an extremely difficult problem. Contemporary man with constantly taught economic principles is not inclined to altruistic actions. Payment of compensation in the event of a change of management plan to the disadvantage of the investor, involving the reduction of investment opportunities in a given area, in practice is very rarely used as means of ordering

⁹ It describes different levels of democracy including various privileges and entitlements for a given level. Democracy at the level of the state, region (voivodeship) and city. It also demonstrates that the state interest cannot be undermined by the interest of lower-level democracy, i.e. regional interest, while the regional interest cannot be affected by the urban interest.

¹⁰ The choice of aesthetic as a possible basis - the mother of ethical choices, write in his book [25].



space at the stage of implementation of the Local Plan of Spatial Development. There are no common procedures for consolidation and exchange of the land by Jacek Koziński¹¹.

On the other hand, the lack of borders in many areas of life is not conducive to the belief that there should be such a limit in the development of the city and the spread of its development.¹² The evolution of cities should rely more heavily on transformation, understood as the stratification and transformation of the inner structure and form of cities. To a lesser extent, it should be the search for new forms in the suburbs or in areas not yet invested.

Because of the high fees and prices of properties in large cities such as Warsaw, Poznań, Cracow, Katowice, Wrocław, Łódź, their suburbs (outside the administrative borders) develop much faster than suburbs in administrative urban areas. In addition, due to the relatively constant travel costs, a large proportion of the population chooses larger, more comfortable and cheaper housing and homes under the city than smaller, more narrow, less comfortable and more expensive homes and houses in the city. Confronting even the two choices shows that homes and houses in the city should be more modernized and their cost of living (taxes, media charges) should be lower than in the suburbs¹³.

Another principle promoted by the state should be the principle of common good. Researchers studying the so-called. Common goods undermine the principles of modern economics that every human being is selfish. The basic thesis of common good is that while cooperation and altruism can be “locally unfavorable” for individuals, then groups can bring many evolutionary benefits. Edward O. Wilson and David Sloan Wilson put it this way: “Egoist wins with the altruist within the group. Groups of altruists win with selfish groups” [33]. “Already in the 1970s, Elinor Ostrom demonstrated in his empirical studies that hypotheses made by some economists that” people are incapable of long-term, stable co-operation “are false and unfounded. By researching various communities and even African tribes including Ethiopian farmers, rubber collectors in the Amazon, Indonesian fishermen, Töbel villagers in Switzerland, Ostrom has developed a set of rules for the so-shared resources ie those to which no community has exclusive rights”¹⁴. These principles according to Elinor Ostrom are as follows:

¹¹ “The social costs of the current urbanization model borne by other groups outside the local government. Financial effects of abandonment of land consolidation. Profitability of urbanization processes” [35].

¹² The situation of unstopable development of the city clearly illuminates the following statement: “The measure of love is not how much we are able to give to another person, but from what we are able to give up”. The folk proverb says that habit is a second nature, so if we were used to the clear boundaries of our city for years, accepting it would be easier for us.

¹³ Such a description of the system of property taxes wrote in her work Barbara Bartkovicz. The author also at several scientific conferences and several articles cited arguments for the tax increase as he moved away from the center, but in Polish realities are not yet known examples of cities that the amount of property tax inversely proportional to the distance of a given property from the center.

¹⁴ The basic questions that accompanied Elinor Ostrom during the research: (1) How to organize and manage for constant shared benefits when everyone is facing the temptation of goosebumps, avoidance of duty, and other opportunistic actions? (2) How to increase the initial opportunities for self-organization? (3) How to improve self-sustainability in the long run? (3) How to extend the possibilities of solving problems while using shared resources through self-organization without the need for continuous external support?

1. It is necessary to clearly define the limits of the common good, including who grants the right to use the resource,
2. Outsiders who do not contribute to maintaining the resources do not have the right to access and benefit or to use common goods,
3. The rules of benefit must take into account local conditions, as well as the limits of benefits – and what can be used,
4. The Kommoners, or beneficiaries of the common good, must be able to create or co-create the rules for the management of the common good – without interference by the external authorities,
5. Convoys must supervise themselves as to how their resources are shared or used,
6. The Kommoners must also develop a system of penalties for breaking rules, preferably with graduated sanctions, more and more annoying,
7. In the event of a dispute, the committees must be able to easily use the conflict resolution mechanism,
8. In the case of common goods, which are part of a larger management system, all rules must be multilayered polycentric and multilevel with benefits, monitoring, enforcement, conflict resolution and other entitlements - from local to regional level up to the domestic level [7, p. 26–28].

Although it is difficult to quantify the benefits of using the common good in the city, parks, green spaces, water reservoirs, public spaces, open spaces, but also a broader image of the city and its character, should qualify for these common goods. Many examples show that the cities in which an impersonal investor is ruling, even if the investor only piles public terrains, lose their citizenship and become somehow a corporate city. This largely endangers the attractive downtown areas in conurbations such as Katowice, Warsaw, Łódź or Poznań.

It seems that today we should at some time redefine the scope of the land use right and make a new codification of it, as described in part in *Recorded City. Co-creating Urban Futures* [12] and in Martin Baum's "Re-use" (reuse) process of urban renewal and revitalization [4, p. 145–154]. Examples of this type of activity are the Canning Town plan (a plan for parts of the eastern London district) and the Clear Willage program for Essex in eastern England.

Interesting action, shortly after World War II, was undertaken by Peter and Alison Smithson. This was an attempt to "re-identify the city". Already in the 50s of the last century, young CIAM members Peter and Alison Smithsons expressed their criticism of the ruling modernist dogma of a rational city with separate, distinct functions and disordered urban tissue. Working with photographer Nigel Hendersen tried, based on visual experience, to change the approach to urban planning. The essence of their founding was the experience accompanying man in urban space. This search for a new spatial coding appealed to architectural intuitions, employing human behavior similar to unrestricted children's play. It used the emotional reception of space as the key to its new codification. The impressionable experience of the city - going from house to street prompted them to formulate the idea of a hierarchy of relations, connections and social associations from home through the street to the urban districts. Their aim was to achieve social cohesion of the city by using proper tissue with a culturally recognized pattern of behavior.

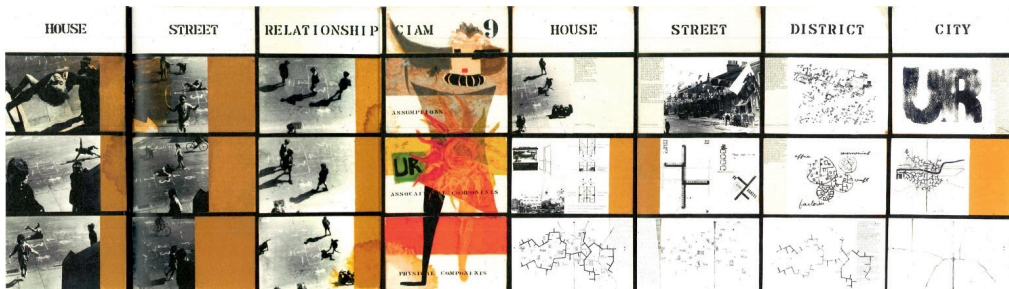


Fig. 4. Presentation of urban space identification by Peter and Alison Smithsons at the CIAM conference in Aix-en-Provence in 1953

5. Conclusion

Stabilization maintained for centuries through faith, culture and tradition by the modern world is treated as anachronism. Challenging the foundations of ethical Christianity and natural law causes ethical and moral emancipation. In this way we are increasingly suspended in the ideological vacuum. However, in order to avoid total destabilization and destruction of culture and state, attempts to replace ethics are becoming increasingly commonplace – political ethics, based on the thesis that the only and ultimate measure of ethics is the law in force. The conviction that modern law is capable of shaping attitudes and controlling social behavior is in essence erroneous. In politics itself, especially at the local level, looking through the prism of individual good and career limits the field of vision only to the present, cutting off from the past and not looking to the future. The current effect is a measure of policy effectiveness. The words of the Danish philosopher Søren Kierkegaard are more and more emphatic that “our existence goes beyond logic”.

If we want our cities to be re-urbanized, we must abandon passivity. Caring for any “form” requires effort and continuous effort – it is no different with the city. Examples of cities that have been leading a policy of shaping a particular image and form for a long time are Paris, Copenhagen and Berlin. Particularly in small towns, special attention should be paid to the outer areas - the coast and all the areas where investment pressures occur. These are areas where there is usually a rapid and uncontrolled development. It is important to put a stop sign for territorial expansion, in turn, to allow the downtown area to undergo further refinement and reconstruction. We have to give up the informality and indeterminacy that allows for any activity within urban and suburban spaces. It is not allowed to continue to allow the ill-considered wastage of space, which allows for free and inconsistent spillage of urban areas¹⁵. It seems important to focus on determinism and creationism in philosophy and culture, but also on closeness, rationality, completeness, harmony, clarity, uniqueness, legitimacy, as well

¹⁵ In English-language literature we deal with two terms: on the one hand there is term “waste” meaning waste, and the term “vast” means “vast” meaning large and vast urban areas.

as the reality and normativity that lead to the synthesis of culture and not to the culture of deconstruction¹⁶.

Observation of urban phenomena, however, suggests that we prefer beauty instead of formlessness and ugliness. Therefore cities like buildings should be carefully designed in terms of form and composition [11, p. 18–25]. In turn, in terms of functionality, the city was formed primarily as a community and a tool for meeting various social needs. According to New Urbanism theorists, unrestricted spatial and demographic development of cities consequently leads to their catastrophe. The pattern to which they claim to refer is the historic layout of the city with its central square and the quarterly surrounding it.

Slawomir Gzell made the right thesis that “in the liberal economy (in Poland after 1989) planning was considered as a tool of oppression”. At the same time treating the private property of the land as an inviolable property [17]. This approach in the long run leads to the depletion of open space in some small towns and suburban communities. This process may be akin to an energy policy that causes the depletion of non-renewable goods, to which some extent also undeveloped space belongs. In addition, the negation of the need and practice of urban planning and design leads to the formation of fragmentary and amorphous spaces, and in the areas of neighboring cities – overlapping amorphous urban areas¹⁷.

The impact of neoliberal doctrine in the economy, using the slogans of “better housing in a green habitat”, not only results in the outflow of population from the city, but also the outflow of capital and its relocation to suburban areas. It would be appropriate to change the structure or form of ownership of space, in which there should not be entities, i.e. very small and independent municipalities, which pursue spatial policy completely independent of large cities, consisting solely of investing in further free space.

Nowadays, the authorities try to be softly postmodern, pretending not to notice that in the physical sense, the outflow of people and capital in the long run means slow but consistent and time-bound agony of the city.

In Polish reality, in the absence of Local Spatial Development Plans, scattering of buildings continues, leading to the entropy of the settlement system of the city, resulting in system inefficiency and increasing costs of its maintenance in the sparse area. It seems that in the Polish spatial reality, At the very least, it is necessary to initialize the order, i.e., the sequences of actions consistent with the logic of reaching the desired and assumed result. These actions, if implemented, will ensure consistency in the creation of real and real urban space. At the beginning of this process should be the vision – “Idea”, which is the basis for the formulation of strategic objectives. In other words, without a substantively prepared and developed idea, what city vision we want to achieve and why, there is no question of its rational development, and even more of a planned and balanced development. The idea should include a “concept”

¹⁶ At the same time, it is important to deny the fear of making a mistake at the time of making such a decision. Such an anxiety leads to the failure to take any decision or to make a decision so general that nothing is wrong and, in addition, usually very populist.

¹⁷ In Polish reality, in the absence of Local Spatial Development Plans, scattering of buildings leads to further entropy of the city’s settlement system, resulting in system inefficiencies and increased costs of maintenance in sparse areas.

that must include operational objectives. Finally, on the basis of a precise and clear concept, you can execute the “Plan”, which will in a detail solve a predetermined concept and sanction the findings and assumptions. This orderly design process is in contrast to the action that treats chaos as a synonym for dynamism, potential, and opportunity for more interesting development.

In the adopted solutions it is necessary to clearly translate the individual spatial decisions into concrete urban forms. First and foremost, they should be solutions consisting in complementing elements, and in addition, they create order and harmony. In particular urban reality, especially in small towns as a rule, one should accept:

- ▶ respect for the local identity (identity) of urban tissue based on the synthesis of the cultural, social and urban environment,
- ▶ maintenance of the area and size of the spatial units¹⁸,
- ▶ the distinctiveness of the character of the teams and the readability of the nodal points,
- ▶ uniqueness of borders,
- ▶ creation of characteristic points of the system along with new dominant.

The above mentioned features are nothing more than a consistent translation of the principles of urban composition presented among others. By K. Lynch, K. Wejchert or J. Żórawski.

At the same time, in thinking about the design of urban space, one must follow the principle of complementarity, taking into account the complexity and harmony of the whole system. This type of attempt was made by Shasa Delz during the implementation of the Adis Abeby Revitalization Program (GTZ 2006, Addis Ababa: GTZ 2006) [10].

He developed the rules of social dialogue accompanying the planning process, laying down the following principles:

- ▶ From “control to chance”,
- ▶ From “nostalgia to reality and rationality”,
- ▶ From “argumentation to dialogue and dialectical discussion”,
- ▶ From “thinking in what direction to thinking: what if – and what will be the effects of concrete decisions”¹⁹.

At the very end, Bartłomiej Gutowski could say that every city represents in the sphere an iconic expression of human strength and greatness, but at the same time its weaknesses and deficiencies. The city is an expression of our aspirations and desires and a testimony of the culture in which it was born. It would be good if the cities that left us would be a testament to harmony and order, not dissolution and romance [16].

¹⁸ Unit size should be adequate to units occurring in a populated, existing area.

¹⁹ The proposed strategy of action according to Felix Heisel and Bisrat Kifle, consisting in changes of attitude during spatial planning, described in accordance with the following principles: from simplicity towards immersion, from control towards possibilities, from nostalgia towards reality, from dialectic argument towards dialogic discussion [21, p. 190–200].

a)



b)

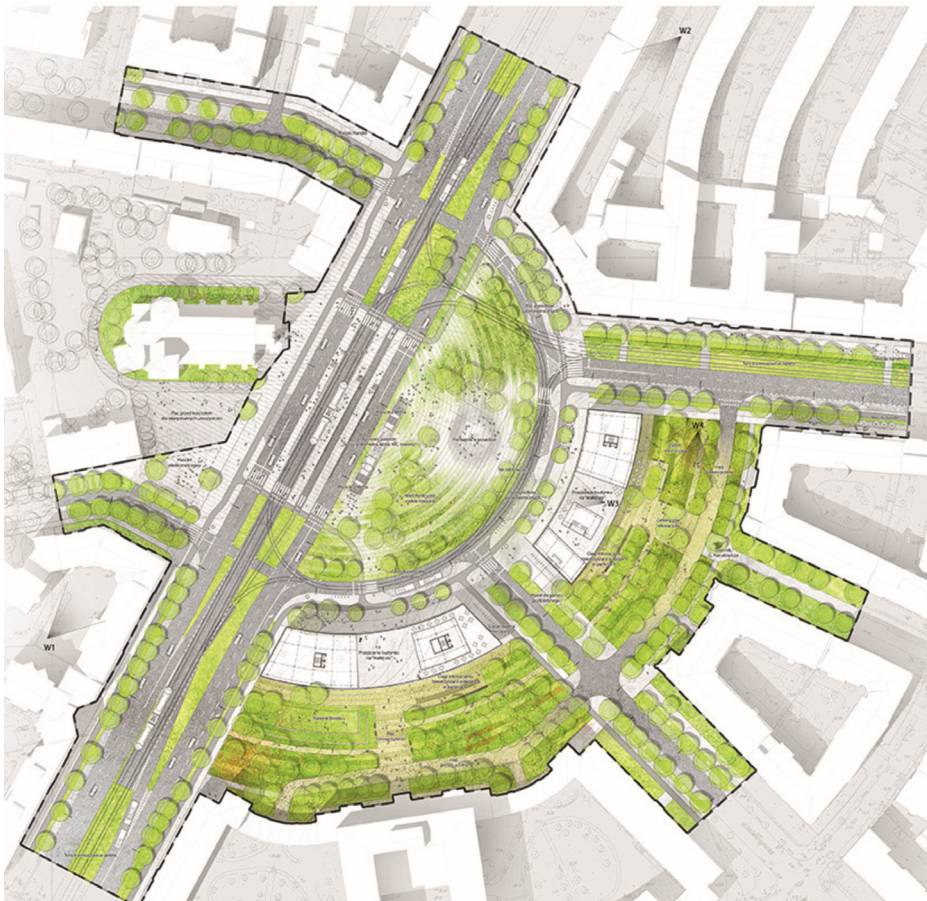


Fig. 5a, b. Expressive and consistent vision of urban space presented by the 4AM team Architects in the competition for the project pl. Narutowicza in Warsaw. The work awarded by the jury of the competition (source: [34])



Bibliography

- [1] Anderson J.F., *St. Augustine and Being. A Metaphysical Essay*, Villanova University, Martinus Ni Hoff, Hague 1965.
- [2] Banasiak M., *Beauty as a subjective and objective value*, May 17–20, 2010, Chair of the UKSW, <http://katedra.uksw.edu.pl/posiedzenia/17pos.htm> (access: 12.12.2016).
- [3] Bartkowicz B., *Przyczyny braku kompozycji i piękna w przeobrażeniach i rozwoju miast*, Teka Komisji UiA PAN, Vol. XXXIII, Kraków 2001.
- [4] Baum M., *Re-use. From Exception to Normality: Re-use in Urban Development*, [in:] *The city as Resource*, T. Rieniets, N. Kretschmann, M. Perret, J. Verlag (eds.), GmbH, Berlin 2014, 145–154.
- [5] Bednarek-Szczepańska M., Więckowski M., Komornicki T., *Spatial Conflicts in Selected Communes*, [in:] P. Śleszyński and J. Solon (eds.), *Planning and Spatial Conflicts in Municipalities*, Studia KPZK PAN, 130, Warszawa 2010, 90–120.
- [6] Berger A., *Drosscape – Wasting Land in Urban America*, Princeton Architectural Press, New York 2006.
- [7] Bollier D., *The Commons, The Commons, Dobro wspólne dla każdego*, Faktoria, Zielonka 2014.
- [8] Borsa M., *Indicators for urban development*, <http://www.m-borsa.net/edu/ranslationsUrbanistyczne.pdf> (access: 12.12.2016).
- [9] Chiodelli F., *Typology of spaces and topology of tolerance: city, pluralism, ownership*, *Gran Sasso Science Institute, L'aquila, Stefano Moroni, Politecnico di Milano*, “Journal of Urban Affairs”, Vol. 0/2013, 1–16.
- [10] Delz S., *Spatial Dialogic. An integrative approach to urban development in rapidly transforming cities Lessons of informality*, 190–200.
- [11] Eisenschmidt A., *The City's Architectural Project from Formless City to Architects*, [in:] *Architectural Design, Special Issue: City Catalyst: Architecture in the Age of Extreme Urbanization*, Vol. 82, Issue 5, September/October 2012.
- [12] Emacora T., Bullivant L., *Recoded City. Co-creating Urban Futures*, Routledge Taylor & Francis Group, London-New York 2016.
- [13] European Commission, Directorate-General for Regional Policy: *Cities of the future. Challenges, visions, perspectives. European Union, Amsterdam October 2011*, Amsterdam, October 2011.
- [14] Gehl J., lectures on *Changing mindsets about urban planning and living*, <http://www.youtube.com/watch?v=Lid9ELzzT8Y> (access: 12.12.2016).
- [15] Gehl J., lectures on *Cities for people*, http://www.youtube.com/watch?v=KL_RYm8zs28 (access: 12.12.2016).
- [16] Gutowski B., *The space of dreamers. City as a Utopian project*, Warszawa 2006.
- [17] Gzell S., *Urban doctrine in times of plague*, “Urban Review”, <http://www.przegladurbanistyczny.pl/gzell> (access: 12.12.2016).
- [18] Hawrylak M., Hawrylak P., *Fragmentaryzacja Miasta*, „Czasopismo Techniczne”, 2-A/2007, 125–133.

- [19] Kloosterboer M., *Lessons of Informality*, [in:] *Lessons of Informality. Architecture and Urban Planning for Emerging Territories – Concepts form Ethiopia*, F. Heisel, B. Kifle (eds.), Birkhäuser Verlag GmbH, Basel 2016.
- [20] Kopeć A., *Spatial order catalyst for the development of Gdansk?*, “Pomeranian space”, 2/2007 (31), [in:] <http://ppg.ibngr.pl/pomorska-spaces/post-space-atylst-development-gdanska> (access: 12.12.2016).
- [21] *Lessons of Informality. Architecture and Urban Planning for Emerging Territories – Concepts form Ethiopia*, F. Heisel, B. Kifle (eds.), Birkhäuser Verlag GmbH, Basel 2016.
- [22] *Living in the endless city*, R. Burett, D. Sudjic (eds.), Urban Age Production Team, Phaidon Press. Ltd., London 2011.
- [23] Lyons F., *Przyszłość Miasta, Gestaltizm Miasto*, „Czasopismo Techniczne”, 1-A/1/2012, 473–483.
- [24] Maciocco G., *Fundamental trends in city development*, [in:] *Springer Science + Business Media B.V.*, 2008.
- [25] Maciocco G., Tagliagambe S., *People and Space. New Forms of Interaction in the City Project. Urban and Landscape Perspectives*, Springer Science + Business Media B.V., p. 3.
- [26] Merrifield A., *The Urban Question, Urbanization and Regional Research*, Vol. 37.3, May 2013, 909–922.
- [27] *Recycling Spaces*, Marta Schwartz Partners, Thames Hudson, London 2011.
- [28] Rubinowicz P., *Chaos jako porządek wyższego rzędu w wybranych trendach współczesnej architektury*, Ph.D. Dissertation, Faculty of Architecture, Cracow University of Technology, Kraków 2010.
- [29] Sivaramakrishmann K.C., *Democracy and self-interest*, [in:] *Living in the endless city. Urban Age Produciuon Team*, Phaidon Press, Ltd. London 2011, 90–93.
- [30] *Spatial Planning and Leveling Opportunities in the Enlarged Areas of the European Union*, Kraków 2005.
- [31] *The spatial planning in gminas: state, dynamics, conditions*, Co-author: Institute of Geography and Spatial Organization of the Polish Academy of Sciences, Sedno, Warszawa 2012 .
- [32] *What is a city*, Essays, Yearbook of Architecture and 2000, Wydawnictwo Politechniki Krakowskiej, Kraków 2000.
- [33] Wilson E.O., Wilson D.S., *Evolution for the Good of the Group*, “American Scientist”, Vol. 96, September 2008, 380–389.
- [34] http://www.a-ronet.pl/index.php?mod=nagroda&n_id=3184 (access: 12.12.2016).
- [35] <http://www.finansewurbanizacja.pl/konferencja> (access: 12.12.2016).
- [36] <http://www.skyscrapercity.com/showthread.php?t=569079> (access: 12.12.2016).
- [37] <http://www.widewalls.ch/deconstructivism-buildings> (access: 12.12.2016).



Piotr Langer (piotrlanger@pro.onet.pl)

Chair of Spatial Planning and Environment Protection of the Institute of City and Regional Planning, Faculty of Architecture, Cracow University of Technology

LIFE AND DEATH OF A COLLIERY. THE CONDITION AND SIGNIFICANCE OF FORMER COAL MINING FACILITIES IN THE TRANSBORDER REGION OF SAARLAND-MOSELLE

ŚMIERĆ I ŻYCIE KOPALNI. STAN ORAZ ZNACZENIE OBIEKTÓW POGÓRNICZYCH W TRANSGRANICZNYM REGIONIE SAARLAND-MOSELLE

Abstract

The region of the Saar Basin in Germany and Moselle in France used to be one of the most important centres of coal mining. Spatial transformations of the region are related to the close-down of collieries and to the redevelopment of the former mining facilities. The research carried out by the Author in 2015 enabled an analysis of mines, taking into account the mode and scope of their redevelopment, as well as significance of these facilities. Several types of transformations have been distinguished – ranging from demolition of the former mining facilities to their adaptation for a new use. The analysis has given grounds for an evaluation of the observed processes, also in the aspect of the significance of the mines for revitalisation of the degraded areas. The conclusions primarily refer to the mining facilities in the Saarland-Moselle region, yet they may provide a reference point in the evaluation of transformations of similar European regions.

Keywords: coal mining, colliery, former mining facilities, revitalisation, cultural heritage

Streszczenie

Transgraniczny region Zagłębia Saary w Niemczech i Moselle we Francji to obszar dawnej eksploatacji węgla kamiennego. Przeobrażenia tego regionu mają związek z likwidacją kopalni oraz zagospodarowaniem obiektów pogórnich. Autorskie badania terenowe, przeprowadzone w 2015 roku, pozwoliły na analizę reprezentatywnej części kopalni regionu Saarland-Moselle, z uwzględnieniem sposobu i zakresu ich przebudowy po zakończeniu eksploatacji oraz przestrzennego, użytkowego i krajobrazowego znaczenia tych elementów. Wyszczególniono podstawowe kierunki działań - od całkowitej likwidacji obiektów pogórnich aż po ich adaptację dla nowych potrzeb. Dokonano oceny zaobserwowanych procesów i zjawisk, również pod kątem znaczenia kopalni dla rewitalizacji obszarów zdegradowanych oraz wykorzystania dziedzictwa pogórnego w kreowaniu przestrzeni postindustrialnej. Sformułowane wnioski odnoszą się do obiektów w regionie Saarland-Moselle, ale mogą stanowić odniesienie do oceny przeobrażeń innych regionów górnictwa podziemnego w Europie, także w Polsce.

Słowa kluczowe: górnictwo węgla kamiennego, kopalnia węgla, obiekty pogórnice, rewitalizacja, dziedzictwo kulturowe

1. Introduction. The Saarland-Moselle region as the area of underground coal mining industry transformation

A special place among all problems related to spatial revitalisation is occupied by the problems of transformations taking place in former industrial areas, including the sites of underground mining of raw materials. The significance and validity of these problems stem primarily from the transformation of the mining industry, observed in many European countries, which is reflected not only in economic and social processes, but also in initial changes in the space and in the functioning of traditional mining areas.

An example illustrating the problems accompanying contemporary transformations of areas with an underground mining industry, including a review of diverse approaches to the process of closing defunct collieries and to using the former mining facilities, is the trans-border region of the Saar Basin – located in the western part of Germany and the French region of Moselle – jointly constituting one of the biggest areas of underground coal mining in Europe. The area comprises several dozens of collieries located on both sides of the Saar River running along the French-German border, in the zone outlined by the network of towns: Saarlouis, Neunkirchen and Saarbrücken in Germany and Creutzwald, Stiring-Wendel and Folschviller in France (Fig. 1).

The history of coal mining in the Saar Basin and the Moselle region goes back to the 14th century, and the industrial scale mining of “black gold” began in these areas in the early 19th century. From that time on, the region was experiencing dynamic growth, playing a significant role in the post-war industrialisation process of the whole continent, based mainly on heavy industry, such as coal mining, coke production and their accompanying industries – steel metallurgy and conventional power generation. Until the mid-20th century, German and French coal mining industries were key economic sectors in both countries. Coal production in the Saarland-Moselle region reached its historic peak in the 50s of the last century [8]¹. However, since that time on, the amount of mined coal was continually diminishing until June 2012, when the last underground colliery in the Saar Basin was finally shut down.²

¹ As may be found in statistical data, the German coal mining industry recorded its historic highest level of raw material extraction in the first decade after the end of the II world war and in the mid-50s of the last century, it reached 125 m tonnes a year. Over 150 underground collieries were functioning in the area of then Germany at that time, employing jointly almost 600 thousand miners.

² The main reason of coal mining industry liquidation in Germany was the systematically decreasing profitability of coal extraction, as the industry was unable to compete with the considerably cheaper stock imported from abroad, among others from Russia, Columbia, the USA, Canada and Poland [9]. Contrary to popular belief, German collieries were not shut down due to pro-environmental policy of the government and, which follows, the desire to limit the amount of energy generated in conventional power plants [4]. Admittedly, the share of renewable energy in the total energy production in Germany is continuously growing, but at the same time, by the decision of the federal government, Germany is going to withdraw completely from nuclear power generation by 2022 [6]. In such situation, the demand for coal used for energy production in modern conventional power plants has been stable in recent years and amounts to approximately 60 m tonnes per year, the significantly major part of which is imported. Coal mining in Germany will definitely cease to exist in 2018, when the domestic mining industry will no longer receive subsidies. The last two active underground collieries – in Bottrop in the Ruhr Basin area and in Ibbenbueren (North Rhine-Westphalia) – will have

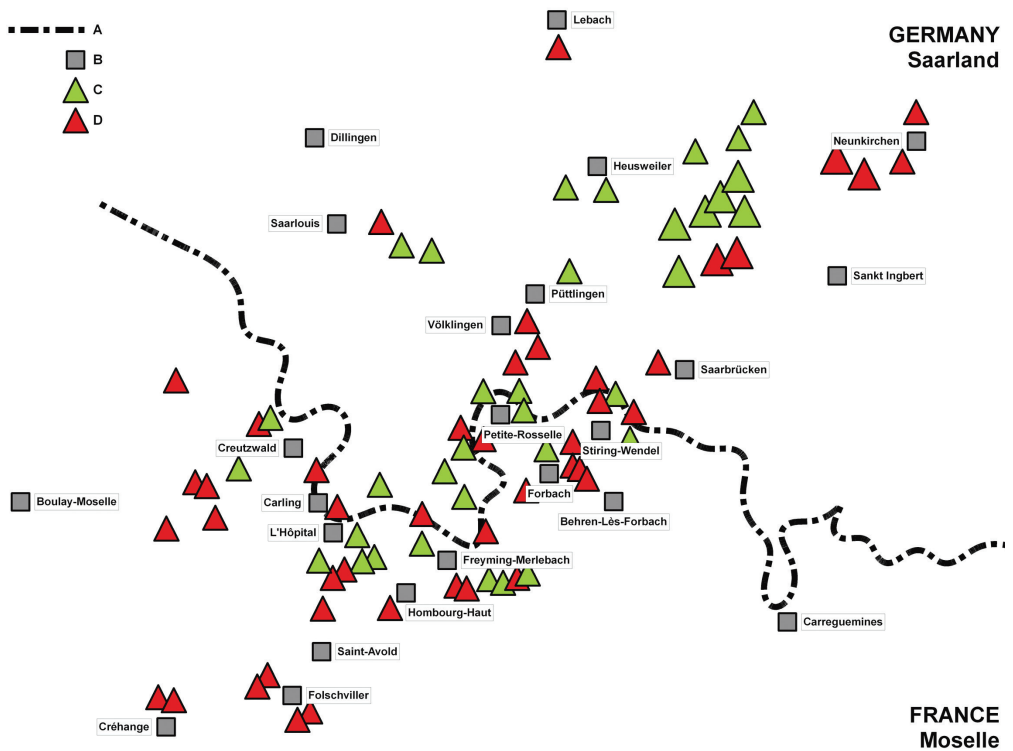


Fig. 1. Location of defunct coalmine shafts in the Saarland-Moselle region in Germany and France (graphics by the author based on the permanent exhibition in the museum of mining at the site of former *Wendel* colliery in Petite-Rosselle): A – German-French border; B – major towns; C – locations of mining shafts included in the field research; D – locations of the remaining mining shafts (preserved and non-preserved)

The ongoing transformation of the former mining region of Saarland-Moselle and its related spatial phenomena and problems have inspired the author to undertake research work comprising field research carried out in July and August 2015 at over thirty sites of coal extraction (listed in Fig. 1). The selected locations reflect the distribution of mining infrastructure, i.e. complexes of shaft headframes and their accompanying facilities of industrial, administrative and economic function related to the operation of a dozen or so separate collieries. Taking into account the stage of liquidation of individual collieries at the time of the research as well as the degree of preservation and the scope of use of the former mining facilities, the studied objects may be classified into two basic groups:

been closed by that time [8]. The situation of coal mining in France used to be the same as in Germany, the only difference being that the process of coal mining industry liquidation took place a little earlier and was stretched over a longer period of time. In France, environment protection was indeed a strong argument for shutting down underground collieries extracting coal. It is worth noting that both in Germany and in France, the process of coal mining industry liquidation is accompanied by comprehensive government programmes alleviating the social effects of definitive closure of all underground collieries in the Saarland-Moselle region.

- a) collieries, which have been definitely closed, now in various degrees of preservation and used as former industrial facilities;
- b) collieries currently in the process of being shut down, undergoing spatial and functional transformations.

With reference to the classification outlined above, the aim of the field research was to identify certain properties and phenomena that are important for the space and functioning of the former mining region of Saarland-Moselle in the face of the ongoing or completed process of liquidating defunct collieries. The following issues were the focus of the research work:

- ▶ spatial effects of liquidating the defunct underground collieries, with emphasis placed on the degree of preservation of the infrastructure characteristic of underground mining;
- ▶ the potential of the preserved mining facilities to be used for other purposes, with special attention paid to using defunct collieries for the function of services;
- ▶ landscape, scenic and compositional role of former mining facilities, including shaft headframes and dumping grounds;
- ▶ relation between the direction in which the colliery liquidation proceeded as well as the preservation and display of specific culture-related values connected with mining in the region.

2. The current situation of underground collieries in the Saarland-Moselle region

The main objective of liquidating collieries, in which industrial extraction of natural stock, including coal, has ceased, is to neutralise the negative effects of their operation as well as to prevent the emergence of such effects in the future. In the technical sense, liquidation of underground collieries includes securing the underground post-excitation spaces, which is aimed at limiting the influence of the colliery on its surrounding areas above ground. The final stage of liquidation is filling up the shafts, or at least sealing off the shaft openings above ground. The process is, as a rule, irreversible, so it may be assumed that a colliery liquidation usually entails permanent and total loss of the underground workings in spite of the fact that there are a number of options of how these spaces could be adapted and reused, also for commercial purposes.

The liquidation mode presented above is typical of the great majority of shutdown procedures applied to collieries in the Saarland-Moselle region. Of all the researched cases, only the German colliery *Velsen* located in the area of Grossrosseln has made a fragment of its former underground workings available for mass tourism (Fig. 2).

Given the complete liquidation of underground workings in almost all collieries in the Saarland-Moselle region, the analysis of the current condition and significance of these facilities must automatically be restricted to an evaluation of mining components located above ground – individual buildings, complexes of buildings, engineering facilities and undeveloped areas in the past connected with the operations of the colliery.



Fig. 2. Entrance to the underground tourist route created in a part of the former underground workings of the now defunct colliery *Velsen* in the vicinity of the German town of Grossrosseln (photo by P. Langer, 2015)

2.1. Collieries in the Saarland-Moselle region after completion of the liquidation process

Liquidation of a great majority of collieries in the Saarland-Moselle region has already been completed. Nonetheless, they differ considerably from one another in respect of the degree of preservation and their current functional, spatial and scenic significance.

In extreme cases, the liquidation has led to complete demolition and clearance of aboveground mining infrastructure, including the structures of shaft headframes. At present, the only reminder that such collieries or parts thereof – in the form of scattered clusters of shafts – ever existed are information boards presenting a short outline of the colliery history, old photos and basic technical data of the facility. Such is the situation of, among others, the *Südschacht* shaft headframe in the *Saar* colliery close to the German town of Heusweiler, or the *Josefschacht* headframe in Altenkessel located near Völklingen. Some of the closed mining shafts are marked out in the space by installations mounted above ground in order to degas the closed underground workings, such as in the case of twin shafts *Neuhaus 1* and *Neuhaus 2* as well as the *Lauterbach* shaft located just off the German-French border (Fig. 3). The cases presented above constitute a minority. Most often, some of the aboveground mining infrastructure is preserved, including the now totally useless shaft headframes. It makes economic sense as it reduces the cost of colliery liquidation, even if the former mining facilities are not going to be adapted for new functions.

A large group among the closed collieries in the Saarland-Moselle region are facilities with a partly preserved aboveground infrastructure, which has remained unused since the liquidation process completion. Development complexes, in the past servicing the mining shaft, are usually fenced away and frequently screened by high greenery; access to them is difficult or there is no access at all. In numerous cases, locations of defunct shafts are highlighted by their still



Fig. 3. An installation for degassing liquidated coal workings – the only element marking the former location of mining shaft *Lauterbach* on the border between Saarland and the Moselle district (photo by P. Langer, 2015)

existing headframes, which constitute characteristic dominant elements of the view. Remnants of liquidated collieries – in the form of abandoned and useless mining facilities – may be found both in Saarland, e.g. *Elm* shaft, *Erkershöhe* shaft in the vicinity of Friedrichstahl, *Itzenplitz* shafts near Schiffweiler or remnants of *Landsweiler-Reden* colliery (Fig. 4), and on the French side of the border: shafts in Stiring-Wendel, *Saint-Charles 1* shaft between Grossrosseln and Petite-Rosselle, *Troise* shaft in L'Hôpital and others (Fig. 5).



Fig. 4. Headframes and disused facilities of *Itzenplitz* shafts in the Saar Basin (photo by P. Langer, 2015)



Fig. 5. Useless remnants of a colliery in Stiring-Wendel in the French district of Moselle (photo by P. Langer, 2015)

A separate category of facilities falling within the scope of this research are collieries, which, following the completion of the liquidation process, have undergone functional adaptation of the preserved former mining facilities. This category may be divided into two subgroups. The first one comprises shaft headframe complexes, which are used in a way that has no connection to their original function. It refers primarily to large-scale buildings used by local companies for purposes related to their business operations. The following complexes of former shaft facilities are used in this way: *Neuschacht*, the collieries in Holz, Hirtel and Putlingen in the Saarland area, and in the French part of the region – *inter alia* the *Saint-Charles 2* shaft facilities in Petite-Rosselle and the shutdown colliery *Ste-Fontaine* in Freyming-Merlebach (Fig. 6).



Fig. 6. The area and buildings of the shut down colliery in Holz (Saarland, Germany) used by a local building company to purposes totally unconnected with the former function of the preserved facilities (photo by P. Langer, 2015)

In some cases, like e.g. in German Dilsburg, the former colliery sites have become the cores of modern industrial zones, where the preserved headframes play the role of compositional dominants testifying to the mining past of the region, yet they are not incorporated into the functional programme of the new areas, nor have they been turned into a tourist attraction.

A different way of putting defunct Saarland-Moselle collieries back to use is their functional adaptation for public services, which is accompanied by rebuilding and spatial restructuring guided by intentional use of former mining facilities highlighting them as components of the region's specific cultural heritage. Such mode of transforming shutdown collieries is described by the author as their revitalisation.

Analysing the process of former collieries revitalisation, both on the French and on the German side of the border, we cannot fail to notice how much attention is paid to preserving the authentic character of these facilities, which manifests itself, among others, by keeping their original form and layout, conservation, as the facilities are not always in good technical condition, preserving the old furnishings, materials and colour schemes, while at the same time introducing new components – remaining in clear contrast with the traditional form of the former colliery buildings (Fig. 7).



Fig. 7. Colliery *Wendel* in Petite-Rosselle in the French district of Moselle, after revitalisation playing the role of an interactive museum of mining (Musée La Mine – Carreau Wendel and Musée Les Mineurs Wendel) housed both in the original mining facilities and in contemporary pavilions built within the framework of the revitalisation process. The areas of the former colliery are used as open-air stage for mass cultural and entertainment events as well as an open-air exhibition of mining machines and devices (photo by P. Langer, 2015)

The research done in the Saarland-Moselle region has demonstrated that revitalisation of defunct collieries refers not only to the built development located at the mining shafts, but also – in equal measure – to the open areas surrounding these shafts. An example to illustrate the above is the *Schiffweiler-Reden* colliery in the Saar Basin, where the revitalisation project comprised creating a park whose main axis is the natural, though partly arranged, watercourse flowing under the main headframe of the colliery adapted for a museum and an exhibition area – *Das ERBE* (Fig. 8). The recreation and leisure areas of the revitalised colliery also incorporate the colliery’s external dumping ground, the top of which has been turned into an extensive area destined for mass events, complete with a stage, gastronomic infrastructure and viewing terraces over the vast panorama of the Basin. The revitalisation activities at the dumping grounds are part of the programme aiming at turning this area into a multifunctional park-garden (*Reden-Haldengarten*) exhibiting the natural and cultural assets, which are specific for the land related to coal mining. An interesting example of modern redevelopment of former mining facilities in the Saarland-Moselle region is the site of the former colliery in Saarbrücken-Burbach. The area surrounding the now defunct shaft complex has been transformed into a modern technological park with works of architecture and public spaces designed and executed to high technological and aesthetic standards. Admittedly, the preserved mining facilities are not incorporated into the functional programme of the park, yet they constitute a key element in shaping its composition and visual connections. The shaft steel headframe as well as two ventilation exhaust vents of the former underground workings make interesting features in the spatial structure of the former industrial part of Saarbrücken – the second largest city in the Saar Basin (Fig. 9).



Fig. 8. Open areas of the revitalised colliery in Schiffweiler (Saarland, Germany) arranged as a contemporary park with a natural watercourse and an artificial water canal along the main compositional axis of the site (photo by P. Langer, 2015)



Fig. 9. The site of a former colliery in Saarbrücken-Burbach (Saar Basin, Germany) now transformed into a technology park. Besides new buildings, an important component of the new urban development are former mining facilities, including air exhaust vents ventilating the underground coal workings (photo by P. Langer, 2015)

2.2. Collieries in the Saarland-Moselle region currently undergoing the liquidation process

The collieries discussed so far are facilities for which the liquidation process has already been completed. Therefore, it is possible to undertake a preliminary analysis of the effects that this process has produced. However, there are still mining companies in the Saarland-

Moselle region, which are currently going through the process of liquidation and are subject to intensive functional and spatial transformations. One of such collieries is *Göttelborn*, located a few kilometres to the west of Heusweiler (Fig. 10).



Fig. 10. Fragment of the aboveground infrastructure of *Göttelborn* colliery (the Saar Basin, Germany) now undergoing intensive spatial and functional transformation (photo by P. Langer, 2015)

Movements in the area of the main shaft of the colliery and, in particular, the working hoist in the headframe reveal that works related to sealing off the coal workings are still continued underground. Meanwhile, a part of the preserved aboveground infrastructure has been transformed into modern commercial facilities.

New buildings, although blended into the former excavation infrastructure, stand out because of their architectural form and applied materials. Generally accessible spaces, gradually incorporated into the system of public areas, are characterised by carefully designed details of the urban plan referring to the now defunct industrial plant. An interesting component of the *Göttelborn* colliery's new development is the educational trail linking the main complex of buildings with the dumping ground, which features a viewing platform offering views over the whole development complex of the shaft and extensive panoramas of the region, at the same time allowing for observation of the mining works carried out within the dumping site itself (Fig. 11).

Another example of a facility, which is undergoing the process of liquidation, is the *Saar* colliery, whose shaft complexes (already partially inactivated) are located in the vicinity of the region's capital – Saarlouis. The colliery, where the liquidation works are still continuing, maintains its mining function, but its accompanying dumping grounds are being gradually regenerated and made accessible to new users. The crown of the dumping site is a perfect viewing point offering an extensive panorama of the Saar valley and the industrial sites located therein (Fig. 12). The flattened top of the hill is a convenient starting point for air

sports lovers, and the slopes perform the function of public green areas in which camping is permitted. The southern slopes of the dumping grounds have also been used as the site of experimental vineyards, which apparently yield excellent fruit due to the soil, which is rich in carbon compounds.



Fig. 11. View from the platform located at the end of the educational trail created in the area of the *Göttelborn* colliery on the slopes of the dumping site, a water reservoir and the local power plant set against the panorama of the region (photo by P. Langer, 2015)



Fig. 12. View over the Saar valley and the city of Saarlouis – the capital of the Saar Basin – from the top of the dumping site heaped up at one of the shaft complexes of the Saar colliery, now in liquidation (photo by P. Langer, 2015)

3. Evaluation of the contemporary condition and significance of collieries in the Saarland-Moselle region. Discussion of the research results

The examination carried out by the Author has unveiled a certain image of the collieries covered by his field research. It may be noticed that the present condition and contemporary significance of the analysed facilities differ considerably. All the collieries have ceased their industrial mining operations; however, some of them still continue underground works within the closedown process. The research enables a general assessment of the liquidation outcomes as well as the spatial, functional and scenic significance of the collieries in which the liquidation process has been completed. When it comes to the facilities, which are still undergoing liquidation, we may only monitor the tendencies in their transformation, but the final results of the ongoing metamorphosis remain unknown.

Table 1.

Stage of the liquidation process and the present mode of using the colliery	Examined feature				Sample facilities (names of collieries or towns/cities in which collieries are located (G) – facilities located in the area of Germany, Saarland (F) – facilities located in the area of France, Moselle)
	Degree of mining infrastructure preservation	Functional significance of defunct collieries	Landscape-related role of former mining facilities	Influence of the liquidation on the culture-related value of former industrial facilities	
Completely dismantled and cleared	unpreserved	no functional significance	no landscape-related significance	immediate loss of culture-related assets	Südschacht, Josefschacht, Neuhaus 1 i 2, Lauterbach (G)
Liquidated collieries and complexes of shafts	partly preserved, subject to ongoing technical degradation	no functional significance	limited landscape-related and compositional role of the preserved former mining facilities	gradually progressing degradation of culture-related assets	Elm, Erkershöhe, Itzenplitz, Landsweiler-Reden (G) Stiring-Wendel, Saint-Charles 1, Troise (F)
	preserved, maintained in satisfactory technical condition	commercial function with no connection to the mining function	considerable landscape-related significance and important compositional and scenic role of the preserved former mining facilities	maintaining former industrial units as part of cultural heritage without showcasing the preserved assets (static role)	Neuschacht, Holz, Hirtel, Puttingen, Dilsburg (G) Saint-Charles 2, Ste-Fontaine (F)

<p>Liquidated collieries and complexes of shafts</p>	<p>Revitalised</p>	<p>preserved, renovated and technically modernised</p>	<p>comprehensively redeveloped for public utility purposes closely related to the mining function</p>	<p>considerable landscape-related significance and important compositional and scenic role of the preserved former mining facilities</p>	<p>maintaining former industrial facilities as part of cultural heritage and showcasing the preserved assets (dynamic role)</p>	<p>Schiffweiler-Reden, Saarbrücken-Burbach (G) Wendel (F)</p>
<p>Collieries undergoing the liquidation process</p>	<p>preserved, subject to successive renovation and technical modernisation</p>	<p>gradually adapted for commercial functions, using the specific assets of the space</p>	<p>considerable landscape-related significance and important compositional and scenic role of the preserved former mining facilities</p>	<p>maintaining former industrial facilities as part of cultural heritage and showcasing the preserved assets (dynamic role)</p>	<p>Göttelborn, Saar-Saarlouis (G)</p>	



As has been demonstrated in the article, the post-industrial transformations of the examined collieries often head in completely different directions, which instantly affects the current condition and role of these facilities as former mining units. The above problem may be viewed in several related aspects, relevant to the present and the future of the Saarland-Moselle region as a trans-border post-industrial space.

The results of the field research carried out by the Author in the trans-border region of Saarland-Moselle have been collected and synthetically presented in the table below (Table 1).

3.1. Degree of mining infrastructure preservation

Analysis of the degree in which the mining infrastructure has been preserved is a key component in the evaluation of the results of liquidating defunct collieries. As has been mentioned before, the evaluation basically refers to the facilities situated above ground, since liquidation of the coal mining companies has (with one exception) entailed permanent blocking and sealing off of underground workings, with no option of making these spaces accessible for any purposes.

Liquidation of numerous collieries means comprehensive and complete demolition and clearance of the aboveground mining infrastructure. Such cases may be described as an intentional and irreversible physical destruction of collieries. However, a significant part of the liquidated coal mining enterprises has survived in their physical form, preserving, to various extents, their aboveground facilities. This group comprises both collieries whose complexes of headframes are not used and the ones that have been adapted to new functions – related to coal mining or not. Where the defunct colliery has not been redeveloped, leaving the former mining facilities without giving them a new function, contributes to their progressing technical degradation and, in consequence, to inevitable destruction. Hence, it may be assumed that the ultimate result of refraining from any action with reference to the former coal mining facilities is similar to the one of their complete liquidation and, in the long-term perspective, entails total removal of the disused infrastructure. Evidence supporting the above thesis may be found in the remnants of the defunct collieries, where the abandoned shaft headframes have soon fallen into disrepair, which – in all probability – cancels any chances of modernisation and further use of these facilities.

The situation of shaft facilities, which, following the process of colliery liquidation, have been adapted to new purposes, is different. When it comes to facilities whose new function bears no relation to their original use, the technical condition of the redeveloped infrastructure is maintained at a stable and satisfactory level – according to the needs of the new users of the preserved facilities. It refers primarily to large-scale former mining buildings, usually adapted to the storage function, much less frequently to shaft headframes, which – due to their specific character and form, are difficult to adapt to any other function than the one related to mining. As it is referred to revitalised collieries – comprehensive projects of redeveloping the former coal mining facilities and areas stipulate extensive use of the preserved infrastructure, mostly for public utility purposes. The observations made in the Saarland-Moselle region clearly indicate that revitalisation of defunct collieries comprises partial restructuring of former shaft facilities, renovation and modernisation of mining infrastructure components,

including interiors of buildings, while at the same time introducing new buildings and other components of development in the open area. A characteristic feature of the reconstruction process in the revitalised areas is conservation of the original technical condition of the existing development and the pursuit to preserve their original character and décor.

Evaluation of the degree of mining infrastructure preservation in collieries currently undergoing the process of liquidation is a complex issue. Since the liquidation process requires that certain underground works still need to be done, the necessary part of the colliery infrastructure must be maintained in the condition allowing its safe use for the purposes of continuing the liquidation works. It also refers to shaft headframes, which – at the stage of the colliery liquidation – must enable communication and transportation in selected shafts. At the same time, the collieries undergoing liquidation no longer continue their mining operations, which makes a greater part of the preserved mining infrastructure useless. The analysis of the liquidated collieries in the Saarland-Moselle region gives ground for formulating the conclusion that facilities permanently barred from the mining function tend to find new users, who – through modernisation and adaptation – greatly improve the technical standard of these facilities, also by using modern materials and building technologies.

3.2. Functional significance of defunct collieries

Before we begin to discuss the present functional significance of former mining facilities in the Saarland-Moselle region, it must be emphasised that underground coal workings have been partly redeveloped for the purpose of creating a generally accessible tourist trail only in one liquidated colliery. In all the remaining cases, the evaluation of the present use of the preserved mining infrastructure refers solely to the objects situated above ground.

It is impossible to talk about any functional significance of former mining facilities with reference to the collieries, which have been completely liquidated. Degassing installations, which have their vents above the surface of the ground, are obviously important for safety considerations, yet they do not play any other role. Areas cleared of the shaft facilities usually remain unused as wasteland or are incorporated into extensive farming acreages. Occasionally, locations of the old shafts are marked by information boards, which may point out to a certain tourist significance, yet they are not linked by any trails or a theme path, and their accessibility is restricted.

A large group of facilities among the examined ones are shaft facilities, which have at least partly survived the liquidation procedure and still remain in the space of the former collieries, but they have not been adapted to any new functions. The author has no knowledge as to the reasons of this situation, yet it may be assumed that they are of economic and/or technical nature. What is more important for the present analysis are the results of the observed process, because, as has already been mentioned, permanent disuse of the preserved mining facilities contributes considerably to their technical degradation.

The functional significance of defunct collieries redeveloped after completion of the liquidation process to perform new roles must be evaluated entirely differently. The most frequent trend in functional adaptation of former mining areas and facilities in the Saarland-Moselle region is to put them to some commercial use unconnected with their original function, mostly by local



businesses, which adapt and use the preserved facilities according to their needs. Former mining infrastructure, especially large-scale buildings as well as their accompanying open areas, usually perform some commercial function – storage, warehousing or workshop, less frequently – they are used for trading or other services.

In the case of revitalised collieries, an important indicator of the revitalisation process is the reconstruction and the ultimate intended use of the defunct former industrial facilities and areas for public utility purposes – in close relation to the original function of these objects. The main trends in the functional adaptation of such collieries are: museums, culture, art, education, science and entertainment, completed with subsidiary forms of commercial activity, such as retail, gastronomic services etc. It is worth noting that revitalisation as one of the methods to utilise defunct collieries usually entails using their surrounding open areas, stipulating, among others, attractive forms of utilising the dumping grounds situated in the vicinity of former mining shafts.

Analysis of the present functional significance of collieries currently in the process of liquidation demonstrates that they are “hybrid” structures when it comes to their function. On the one hand, the mining company performing the liquidation works remains an industrial unit, and on the other – since there is no coal extraction going on at the colliery, its premises feature a lot of aboveground infrastructure, which no longer performs any function. Observations made *in situ* lead to the conclusion that the period of inutility of these facilities has been relatively short, and the process of their functional transformation is progressing smoothly, limiting the transition stage between the mining operations and the functional adaptation for new needs. As the liquidation process progresses, subsequent parts of the liquidated shaft facilities are successively given over to new users, for – among others – headquarters of external companies, which use the specific former industrial space to raise their prestige. Unusual scenery, highlighted by the shape of the shaft headframes – characteristic for underground mining industry, is an environment readily chosen to locate conference and training facilities, business centres, fairs and exhibitions.

3.3. Landscape-related role of former mining facilities

Another important role of former collieries, irrespective of their technical condition and present functional significance, is their landscape-related function, especially the role that these facilities play in different visual relations and in shaping the urban composition of towns in the Saarland-Moselle region.

Visual and compositional significance of former mining facilities in the landscape depends on the degree of their preservation and the mode of use. For obvious reasons, the shaft facilities of defunct collieries that have been completely cleared are absent from the region's landscape. Even if locations of these facilities are marked by information boards or installations serving the purpose of degassing the cut-off underground workings, the sites are not displayed in any way and are only visible from a close distance.

Collieries, which have preserved their aboveground infrastructure, at least in part, in the greatest majority of cases composed of large-scale and high-rise buildings, play a significantly larger role in the landscape of the region. It may be observed, on the basis of the performed field analysis, that facilities, which have not been subject to functional adaptation, are less

clearly defined in space – mostly because of the impervious screen of high greenery, which – over time – overgrows and hides the preserved, though unused, remains of the colliery.

Shaft infrastructure redeveloped for new functions is more clearly visible in the landscape and it plays a significant compositional and visual role, regardless of whether the adaptation is in any way related to its original function. It stems mainly from the fact that the buildings are maintained in a good technical condition and the areas around the facilities tend to be kept clear of high greenery or they feature a restricted amount of high trees, which promotes visual exposure of former shafts and ensures their good visibility, even from large distances. A particularly important landscape-related function is performed by steel structures of shaft headframes in vivid colours and fairly varied shapes and heights, towering over the remaining shaft infrastructure. The structures are not only characteristic compositional dominants, but also orientation points in the area. Collieries currently in liquidation, which still operate as mining companies, while at the same time undergoing dynamic transformation, also have high visual and compositional significance. Both in the case of such facilities and in the case of revitalised collieries, the traditional mining landscape has become the basic component of building the visual appeal of the space, also serving marketing purposes.

An important feature of the revitalised collieries as well as the facilities now at the stage of liquidation is highlighting the landscape-related role of redeveloped dumping grounds. These features are clearly different from natural topographic forms of terrain and from dumping grounds transformed into wooded areas. Moreover, dumping grounds made accessible to the public are convenient viewing points offering wide and distant panoramas.

3.4. Influence of colliery liquidation on the culture-related value of former industrial facilities

The links between the Saarland-Moselle region and the mining industry are strongly accentuated and treated as an important factor of its contemporary appeal created on the basis of the cultural heritage of the industry represented by coal mining and its accompanying sectors, including steel metallurgy³ and conventional power generation industry. At the time of the region's functional transformation, the problem of putting this specific heritage to adequate use acquires a special importance in the context of developing such functions as tourism and recreation. Another important issue is the need to preserve the local identity, rooted in mining, now becoming a thing of the past. For this reason, evaluation of the influence of the liquidation of collieries on their culture-related value is an important part of this research.

Liquidation of a colliery resulting in complete disassembly and clearance of the aboveground mining infrastructure is equivalent to losing the culture-related value of the removed components. As has been mentioned earlier, locations of former shafts marked by information boards are not incorporated into the regional tourist infrastructure of cycling, hiking or horse riding trails. Similarly, the closed mining shafts equipped with installations degassing underground workings

³ One of the most important components of Saarland-Moselle cultural heritage is the former steelworks in Völklingen (Weltkulturerbe Völklinger Hütte) – legally protected and entered on the UNESCO World Heritage List. The facility is now a centre of culture, science and art and, at the same time, a modern museum of steel metallurgy.



are of negligible significance, though the facilities may seem interesting from the culture-related point of view, since they illustrate the method of securing sealed off workings as one of the stages of land regeneration following termination of coal extraction in an underground colliery.

In defunct collieries with partly preserved but unused shaft infrastructure, prolonged disuse of former mining facilities brings about their degradation and subsequently their complete ruin, thus leading to the loss of culture-related value. The final effect of this liquidation mode for the culture-related aspect is then similar to the one when the infrastructure is completely cleared off, the only difference being that it is slightly postponed.

Collieries, which have prolonged their existence beyond the moment of coal mining termination by functional adaptation to new purposes, are of special significance for cultural heritage. With reference to facilities used in a way that is unrelated to their original industrial function, we may talk about their *static* cultural role. They contribute to the region's material stock that has some culture-related relevance, yet the specific character of the preserved assets is not emphasised. The colliery infrastructure is used and maintained in a relatively good technical condition, but the mining past of these facilities is largely irrelevant. Therefore, the culture-related value of these facilities is not a factor determining their use.

The situation of revitalised collieries is entirely different. In all examined cases, the culture-related value of the facilities subjected to revitalisation was the main reason for their redevelopment for the purposes of public utility functions closely related to the mining history and tradition. The revitalisation process may be seen as striving to maintain a variety of culture-related elements, but also as intentionally showcasing the existing assets, which, on the one hand, ensures effective protection of the mining heritage and, on the other, clearly improves the quality of the space and attracts new users. Thus, thanks to revitalisation, defunct collieries acquire a totally new culture-related significance, playing the *dynamic* role in this aspect, based on the preserved material and non-material assets.

The analysis of the influence of colliery liquidation on the sphere of culture is particularly interesting with reference to enterprises still carrying on liquidation works. It would seem that the culture-related role of such collieries must be limited. Meanwhile, the research has clearly demonstrated the tendency to smoothly incorporate the infrastructure undergoing liquidation into the cultural heritage stock of the region. Their unique value rests in the fact that they offer unrestricted access to facilities that are still at the stage of liquidation, thus providing a chance to directly observe actual mining works, e.g. forming dumping grounds, which would be very difficult, if not entirely impossible, in normal circumstances. Thus, it is not only rich history, but also the present mining activities that are integrally connected to culture, and the colliery itself may be compared to a venue staging an unusual spectacle.

4. Summary and conclusions

The trans-border former mining region comprising the Saar Basin in Germany and the Moselle region in France is undoubtedly a region of intensive changes taking place in close relation with liquidation of coal mining as a traditional sector of the industry, present in this

area for several centuries. The ongoing transformation of the region has – once and for all – put an end to the existence of numerous collieries located on both sides of the German-French border. Referring back to the title of this article, it could be said that all these facilities have been *faced with death*, both in the material and culture-related dimension, yet their fates in the post-industrial era are not always the same.

The field research carried out by the Author has demonstrated that the defunct collieries are by no means uniform in character – they differ in many things: the current stage of the liquidation process and the most important characteristics: the condition of the aboveground mining infrastructure, the scope of its use and the type of functional adaptation, landscape-related, scenic and compositional role as well as the significance for the region's cultural heritage.

It has been found in the course of the research that many of the liquidated collieries have been totally annihilated, in other words – they *died*. Some have survived, but have fallen into disuse and are now slowly *coming to the end of their lives*; others have *been born again* acquiring an entirely new function. However, the key question that must be taken into account in the considerations on the *life and death* of former collieries is the rationale and the real possibility of preserving mining facilities permanently excluded from industrial operation. The decisions on a complete liquidation or further transformations of the closed-down collieries were certainly taken after a careful scrutiny in which numerous arguments were taken into consideration. The prevailing ones, it would seem, were the economic factors – redeveloping a closed-down colliery generates enormous cost. The research results show that numerous collieries in the Saarland-Moselle region have undergone effective rebuilding and functional adaptation following termination of their mining activities, which proves that prolonging the life of such facilities is at times feasible. In the cases of defunct shaft infrastructure now used in the function that is not related to their mining past, redeveloping the former industrial facilities must have made sense from the economic perspective, both for the enterprise managing the preserved infrastructure of the colliery and for the new tenants, who use them for the purposes of their business activity. In the case of revitalised collieries, the economic factor may be of secondary importance. The implemented revitalisation programmes and projects stipulate functional adaptation of the former mining facilities mainly for public utility purposes, with commercial activity viewed as supplementary. In such a situation, the overall economic balance of the facility may be negative and the current functioning of the revitalised colliery may require financial support. Yet, it is their unquestionable culture-related value that determines the feasibility of keeping such collieries alive. Moreover, facilities subjected to revitalisation are characterised by a significant compositional and visual role in the landscape and they are attractive from the point of view of utility, especially in the context of the ongoing functional transformation of the region aiming at developing tourism, science, culture, high technology industry and business.

The above observation leads to the conclusion that revitalisation of a colliery is the best way of prolonging its life into the post-industrial stage, or – more precisely – of its rebirth in an entirely new role, at the same time safeguarding full protection of former mining facilities as an important part of the specific cultural heritage. Revitalisation of all, very numerous, collieries in the region would be impossible for obvious reasons. Factors determining the fates of collieries



destined for liquidation remain outside the scope of this research. However, it is understood that the following factors – among others – must be taken into account when considering the option of revitalisation: the condition of the former industrial infrastructure and its diversity, technical possibilities of adaptation, the size of the area for revitalisation as well as its accessibility, spatial and transportation connections with its surroundings, especially with large cities of the region.

Defunct collieries, which – for a variety of reasons – are not intended for revitalisation, may escape death by functional adaptation for purposes unrelated to their original mining operations. The Author's research shows that such transformation does not entail an attractive form of use, but it supports the landscape-related function of former mining facilities and prolongs their relative protection, at least as long as the colliery is still used.

The mining history, identity and cultural continuity of the Saarland-Moselle region would be best emphasised, it seems, by creating a culture theme trail connecting all the former locations of collieries – both those that have been preserved and those that have completely wiped out from the surface. Such a project may contribute to strengthening of the tourist appeal of the region; it may also help to showcase these former mining facilities, which are only accessible with difficulty and are thus marginalised.

All the considerations presented in this article refer directly to a specific area, i.e. the trans-border region of Saarland-Moselle. The research results are, however, a good starting point for evaluating similar phenomena and processes going on in other places related to underground coal mining. They may also be true for Polish mining areas, *inter alia* for Upper Silesia, Zagłębie Dąbrowskie (Dąbrowa Basin) or the Lower Silesia Coal Basin, where transformation of mining as a traditional industrial sector has already commenced or will be initiated in the near future.

References

- [1] Gawlik L., *Węgiel kamienny energetyczny. Perspektywy rozwoju w świetle priorytetów środowiskowych*, raport Polskiego Komitetu Światowej Rady Energetycznej, Kraków 2011.
- [2] Jones L., Woods M., *Case study contextual report 5. Saarland*, DERREG (Developing Europe's Rural Regions in the Era of Globalization).
- [3] Dörrenbächer P., Bierbrauer F., Brücher W., *The External and Internal Influences on Coal Mining and Steel Industry in the Saarland/FRG*, [in:] *Zeitschrift für Wirtschaftsgeographie*, Vol. 32, Issue 1, 209–221.
- [4] Fabian G., *Globalny rynek węgla – jaki był?*, „Biuletyn górniczy”, 2015, 34–36.
- [5] Fabian G., *Niemieckie górnictwo węgla kamiennego w 2012 roku*, „Biuletyn górniczy”, 2012.
- [6] Lorenz U., Ozga-Blaschke U., Stala-Szlugaj K., Grudziński Z., Olkusiński T., *Wpływ katastrofy w Fukushima na światowy popyt na węgiel energetyczny*, [in:] *Zeszyty Naukowe Instytutu Gospodarki Surowcami Mineralnymi i Energią Polskiej Akademii Nauk*, No. 82, 2012, 57–70.
- [7] Malko J., *Energiewinde. Niemiecka transformacja energetyczna*, „Polityka energetyczna – Energy Policy Journal”, 2014, Vol. 17, No. 2.
- [8] www.dw.com, *Niemcy: Koniec kopalń węgla kamiennego*, 19.12.2015 (access: 08.02.2017).
- [9] www.m.nettg.pl, *Zwrot energetyczny w Niemczech*, 30.11.2012 (access: 21.01.2017).

Wojciech Kujawski (wk.kujawski@gmail.com)

RAIC, LEED AP, iiSBE – Principal at Integrative Solutions Group Inc., at INPOL Consulting, lecturer at Building Science and Eco-Design at Algonquin College, Ottawa, Canada

NEW ROLE OF BUILDINGS AS CONTRIBUTORS TO THE INFRASTRUCTURE

NOWA ROLA BUDYNKÓW JAKO ELEMENTÓW WSPÓŁTWORZĄCYCH INFRASTRUKTURĘ

Abstract

Buildings can create a sense of community and add to the character of neighborhoods and cities. They can also support communities by either directly contributing to the infrastructure requirements of their neighbors, or by reducing their own demands and/or creating their own supply and treatment systems to create capacity for others in, for example, community energy and water systems. Buildings can also reduce wastage with its environmental and economic burdens by recapturing heat being lost through inefficient systems and by using municipal waste, especially bio-waste, as a fuel source. Building energy demands are a significant part of the challenge to reduce dependence on fossil fuels, save on resources, to cut emissions and mitigate the effects of climate change, while also representing opportunities to reduce the negative impacts on municipal infrastructure. This paper explains how buildings can mitigate such impacts while also acting as elements of infrastructure.

Keywords: energy, infrastructure, energy efficiency, environment, community, neighborhood

Streszczenie

Budynki mogą tworzyć poczucie wspólnoty i dodawać do charakteru dzielnic i miast. Mogą też wspierać społeczności poprzez bezpośredni wkład w wymagania infrastrukturalne sąsiadów lub poprzez zmniejszenie własnych potrzeb oraz/lub tworzenie systemów zaopatrzenia i oczyszczania w celu zwiększenia pojemności systemów, na przykład w odniesieniu do energii i wody. Budynki mogą również zmniejszyć marnotrawstwo w środowisku i obciążeniach ekonomicznych, odzyskując ciepło utracone przez nieefektywne systemy i wykorzystując odpady komunalne, zwłaszcza bioodpady, jako źródło paliwa. Zapotrzebowanie na energię w budynkach stanowi znaczną część wyzwania, aby zmniejszyć uzależnienie od paliw kopalnych, oszczędzać zasoby, zmniejszyć emisję i złagodzić skutki zmian klimatycznych, a jednocześnie przedstawiać możliwości zmniejszenia negatywnego wpływu na infrastrukturę komunalną. Niniejszy artykuł wyjaśnia, jak budynki mogą złagodzić takie oddziaływania, a jednocześnie działać jako elementy infrastruktury.

Słowa kluczowe: energia, infrastruktura, energooszczędność, środowisko, społeczność, ekologia, sąsiedztwo

1. Introduction

Buildings, besides their traditional roles as shelters and providers of services, can not only mitigate their impacts on surrounding infrastructure, be it neighbourhood, community or city itself, but also contribute to it by producing energy, clean water, food and converting waste to resources. Building energy demands were always a significant part of the challenge to reduce dependence on fossil fuels, to cut emissions, and save on natural resources, all the while representing potential opportunities to reduce the impacts on municipal infrastructure if properly designed. An integration of buildings and infrastructure represents a major change in coexistence of urban form, which is actually created by buildings, then neighborhoods, then communities; however, none of these entities can function well without an efficient infrastructure. Improving building performance by any degree would move the city system model closer to the sustainable community model.

“(…) Infrastructure matters because it represents the major capital outlay for the developer and a key accounting element in pricing the buildings, after land. (…) to be competitive, infrastructure costs have to be equal to or lower than what conventionally has been achieved in previous developments or by the industry at large” [2].

This paper describes the benefits of buildings as strategic contributors [1] to the city systems helping understand:

- ▶ The design implications of buildings as components of community infrastructure,
- ▶ Development, design and construction issues,
- ▶ Certain aspects of costs and savings incurred in sustainable buildings and communities in relation to infrastructure.

Building can be classified into well known “green”, “sustainable”, “living” or “regenerative”. The very basic features for Green Buildings became a starting point from which the designers can measure their progress.

Table 1. Characteristics of Green Buildings [1]

Issue within	Related systems/features
Location	Not on fragile landscapes Doesn't contribute to urban sprawl Close to mass transit systems
Site	Focuses on surface water management and retention (holding ponds, porous paving) Xeriscaping Minimal or zero impact on local ecology Increased green space
Exterior	Renewable energy systems (geothermal, wind, solar, etc.) Window canopies or light shelves Green roofs Active transportation infrastructure (bicycle parking, etc.) Efficient, targeted exterior lighting, mitigation /elimination of light pollution

Interior	Minimal use of materials (e.g., leaving exposed structures, where possible and/or appropriate) Flexible layouts (movable walls, raised floors for services) Occupant controls of heat and light (as opposed to large zone thermostats or light switches) Abundant natural light and access to views Air quality better than in conventional buildings Low-flow water fixtures Supports sustainable practices (such as built-in recycling and composting bins)
Hidden features or attributes	High-performance building envelopes Materials selected to meet building goals (minimal environmental effects, low VOCs) High-efficiency mechanical systems integrated with electrical, structural, and architectural elements Energy-efficient lighting systems The use of maintenance materials (e.g., detergents) that also meet sustainability goals Continued monitoring and optimization of system performance over time.

The terms “green,” “sustainable,” “living” and “regenerative” can be confusing as they are often used interchangeably when, in fact, there are substantial differences.

- ▶ **Green buildings** follow a pre-design, design, construction and commissioning, and operations model, and performance is measured based on energy and resource consumption, environmental loading and indoor environmental quality.
- ▶ **Sustainable buildings** follow the same principles but with added economic, social and cultural aspects.
- ▶ **Living buildings** add to the urban environment by acting like ecosystems, maximizing the health of animals, plants and people. Like an ecosystem, methods of creating a living building are specific to the area where it is built.
- ▶ **Regenerative building** projects repair damaged ecosystems, replace agricultural opportunities, add to community energy and water supplies, etc., and, in essence, become critical components of community infrastructure. They are basically Energy Positive buildings (producing, on top of the energy for their own needs, a surplus energy that is used by other buildings or sold to the grid) that free up capacity within local utilities, reduce or eliminate impacts to water, road and energy infrastructure, treat water and wastewater on site, produce some food, while providing greenspaces and other community social areas, giving people opportunities to drive less and to walk, cycle or take public transit more often.

Sustainable buildings can incorporate high performance water conservation techniques (apart from water-efficient fixtures), such as on-site water and wastewater treatment, rainwater collection, xeriscaping and green roofs, can reduce the impact to municipal water, wastewater and stormwater systems. However, if a building treats local wastewater, it would be considered a regenerative building (with other criteria fulfilled as well).

The Integrative Design Collaborative of Arlington, Massachusetts helps builders understand the connections between buildings, the environment and people by employing a “regenerative design” model, as shown (Fig. 1).



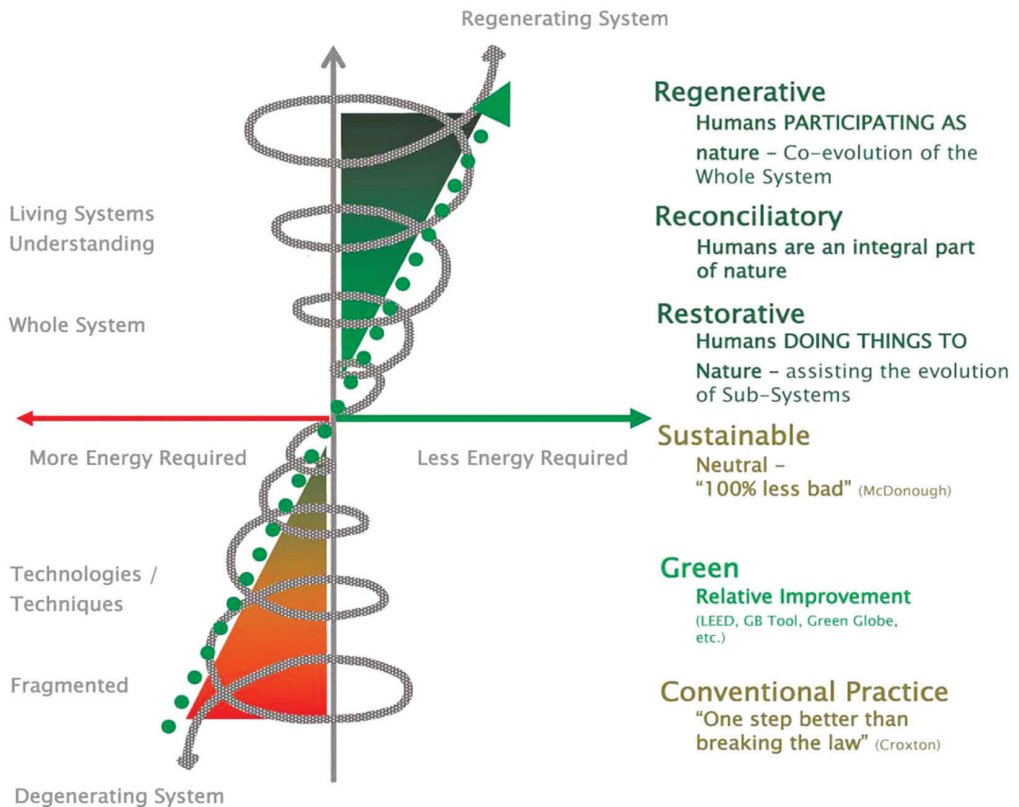


Fig. 1. Regenerative Design Model. Courtesy of the Integrative Design Collaborative

In both the developed and developing worlds the possible solutions lie in a mitigation of the infrastructure construction and its expansion [3]; however, only the most obvious aspects of building’s contributions are shown in a more detailed way in this paper. Some are only mentioned; all should give a reader the idea that we are at the brink of a new vision of how we should prepare ourselves for the future.

2. Eco-industrial networks

So called eco-industrial networks (EIN) and eco-industrial parks [13] are structured around both energy and waste sharing between producers and consumers (Fig. 2) and while networks usually supply entire communities, the parks, generally, share within themselves, and then almost nothing is wasted and everything is used.

A good, but quite old, example of such EIN is Kalundborg (Fig. 3) in Denmark (a city first settled in 1167). It started their network in 1961 with a single power station project and have expanded it over time into a cluster of companies that rely on each other for material inputs and supply of energy to the entire community while reducing waste and improving

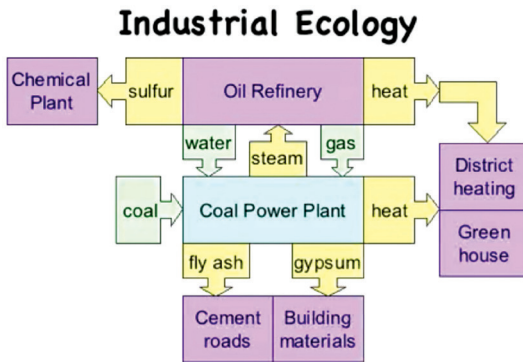


Fig. 2. Idea of EIN (source: [14])



Fig. 3. View of Kalundborg (source: [15])

its economics and environment. They do it for mutual benefit, on the basis that by-products from one business can be used as low-cost inputs by the others [4].

For example, treated wastewater from one place is used as cooling water by the adjacent power station. Others purchase ‘waste’ process steam from the power station for their operations. Surplus heat from the power station is used for heating adjacent homes, and warm a local fish farm. Other by-product, such as fly ash, is used in cement work and roadbuilding and to obtain gypsum; such purchases meet almost two-thirds of needs. Surplus gas from the refinery, a low-cost energy source, instead of being flared off, is delivered to others. The use for household heating of the excess heat from its producer has eliminated about 3,500 oil-burning domestic heating systems [16].

Original motivation behind the clustering of “park stakeholders” was to reduce costs by using unwanted by-products; but soon it was complemented by a vision of environmental benefits shared by everybody.

Larsson et al [3] synthesized two important ideas: **Smart Grids** – optimization of supply and demand of electrical power at a regional level, and a **Synergy Zone** dealing with the interaction of other issues such as:

- ▶ Thermal energy for space heating or cooling;
- ▶ Domestic hot water;
- ▶ Grey water;
- ▶ DC power at the zone and building level;
- ▶ Solid waste generated by building operations.

Each of these urban sub-systems could benefit from appropriate storage systems, methodology for optimization of supply and demand, and distribution networks.

Tillie et al. [5] developed an inventory of a wide range of buildings, with different cooling/heating needs patterns changing throughout the day and the year. With an appropriate mix of buildings (a heat/cold ratio close to one) and heat/cold storage facilities at the neighborhood scale, the waste streams could be reused, thus this process could theoretically lead to almost 50% reduction in energy consumption for heating and cooling: as all the heat usually wasted by cooling systems is reused, heating could be “free”.

Such strategies could be implemented to building, neighborhood, district/community and even the whole city itself while reducing energy consumption, applying reuse and exchange of waste energy and production of renewable energy (Fig. 4).

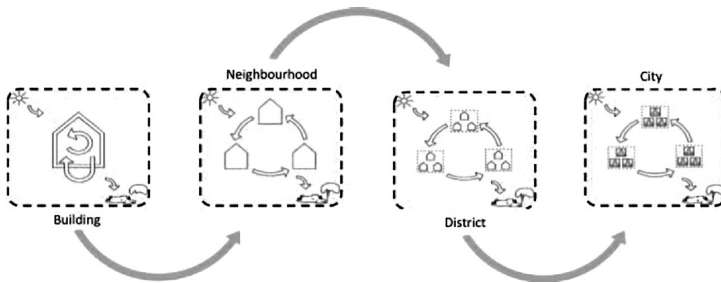


Fig. 4. Knotting the flows at every scale (adapted from [5])

Since heat is a natural byproduct of many manufacturing processes, some developers preferred to locate residential, office or other types of buildings close to industrial or manufacturing plants to take advantage of all potential benefits possible within, district heating including.

Buildings that supply their own energy and produce it also for others nearby, are often the most cost-effective. Combined Heat and Power (CHP) systems achieve peak efficiency when they run continuously on full time loads in their own neighbourhood or a community. Having also its own water treatment facility, and greenhouses etc. they can remain functional even in times of emergency.

Scaling from the building up determines if energy can be exchanged or stored especially between buildings in the neighborhood where the diversity of uses and configurations affect the efficiencies of most systems. They usually work much better on a neighbourhood, than a single building, scale, thus came the logical necessity of a creation of community as a system, rather than a community of separate buildings. The benefits available through different building sites go beyond the traditional infrastructure and now, even a food production of a scale, can be considered.

With the advances in renewable energy technologies such as photovoltaics (PVs), geothermal and in heating and cooling systems, combined heat and power (CHP), the viability of local energy production has improved significantly. Local and individual production can also reduce the peak energy demand and stresses it gives into a community system. When individual buildings take on this role, then retrofitting and expansion of existing grids is avoided. That is the main reason for strong push from utilities for energy efficiency, which could be seen as against their interest, until the cost of a new infrastructure comes to the light.

Also many communities became stronger and more resilient by implementing decentralized systems in which neighbourhoods could still remain functional during and after an event, be it climatic, weather related, natural disaster etc. Table 1 and Fig. 5 show the range of building supported infrastructure features.

Table 2. What types of infrastructure can buildings support? [1]

Infrastructure Component	Sustainable Building Element(s)	Potential Benefits to the developer, occupants, municipality, and/or the community
Energy (heating, cooling, electricity, ventilation, humidification)	<ul style="list-style-type: none"> ▶ District heating (renewable or fossil fuels) ▶ Renewable energy (wind, micro-hydro, solar thermal, PV, geothermal) ▶ High-performance building envelope ▶ use of thermal mass (passive solar design) ▶ Natural light (solar, light tubes, etc.) ▶ Energy-efficient lighting ▶ Controls (sensors, timers, etc.) ▶ Natural, no- or low-VOC finishes (related to indoor air quality) 	<ul style="list-style-type: none"> ▶ Reduced energy demands on municipal or provincial utilities ▶ Reduced equipment sizing requirements ▶ Improved indoor and outdoor air quality ▶ Reduced GHG emissions through energy efficiency and reduction of fossil fuel use ▶ Reduced operating and maintenance costs for owners and occupants ▶ Growth of renewable energy and sustainable building technology sectors ▶ Revenue opportunities to sell surplus energy or carbon credits
Roads & Transportation	<ul style="list-style-type: none"> ▶ Optimal street design (e.g., fused grid) ▶ Transit-oriented development ▶ Limited parking spaces ▶ Active transportation infrastructure, (bike paths, racks and storage, sidewalks, etc.) 	<ul style="list-style-type: none"> ▶ Reduced urban heat island effect ▶ Reduced GHG emissions and improvement of air quality with fewer cars on roads ▶ Reduced costs to developers with fewer parking spaces and freed up land
Water/ Wastewater/ Storm water	<ul style="list-style-type: none"> ▶ Permeable surfaces ▶ On-site water reuse ▶ Stormwater management techniques ▶ Green roofs ▶ Rain capture systems ▶ Water efficient appliances (low-flow fixtures, etc.) 	<ul style="list-style-type: none"> ▶ Reduced impacts, size and cost to municipal water, wastewater and stormwater systems ▶ Reduced stormwater runoff ▶ Reduced water costs for occupants ▶ Green roofs may reduce cooling requirements and the urban heat island effect
Waste (garbage, recycling, composting)	<ul style="list-style-type: none"> ▶ On-site composting and/or recycling facilities ▶ Reusable/recycled/recyclable building materials ▶ On-site waste reduction during construction and demolition 	<ul style="list-style-type: none"> ▶ Extended lifespan of municipal landfill sites ▶ Reduced GHG emissions from landfills (methane = 20x the global warming of CO₂) ▶ Reduced landfill tipping costs by limiting waste during construction and creating revenue from selling useable construction materials
Greenspace	<ul style="list-style-type: none"> ▶ Site location ▶ Community gardening spaces (including green walls and roofs) 	<ul style="list-style-type: none"> ▶ Avoidance of disturbing sensitive natural areas ▶ Increased native or drought-resistant flora ▶ Reduced maintenance and remediation costs ▶ Provision of social, recreation and fitness opportunities for residents



Energy	Parking	Landscape and Water	Waste Management
<ul style="list-style-type: none"> • Meet an overall energy performance baseline (equal to two LEED energy points) • Specify energy-efficient appliances and occupancy sensors • Utilize the neighbourhood energy utility (district heating system) 	<ul style="list-style-type: none"> • Provide preferred parking for co-op and car-share vehicles • Relax minimum quota for parking stalls • "Unbundle" parking from the sale of a residential unit (the purchaser has the option to opt in or out of ownership of a parking space) 	<ul style="list-style-type: none"> • Specify low flow toilets, faucets and showerheads • Use drought resistant and/or native plant species (goal of zero potable water use in irrigation) • Install green roofs on 50 per cent of roof area • Create space for urban agriculture in landscaped areas • Implement on-site stormwater management practices 	<ul style="list-style-type: none"> • Provide space for three streams of waste collection: garbage, recycling and organics • Implement composting capacity in gardens and landscaped areas • Divert 75 per cent of construction waste from landfill 

Fig. 5. Courtesy of R. Bailey, 2010, Vancouver

3. Buildings at Work

Many of the building developments, while acting as infrastructure, can either reduce their impact on community infrastructure, or eliminate entirely the need to connect to its elements such as electricity grids or municipal, waste and storm water systems.

Brownfield Redevelopments

Building on brownfields can often be challenging due to the need for very costly site remediation. However, it can easily be outbalanced by potential benefits such as prime location, usually the urban core, and reduced construction and operating costs, because most of the infrastructure is already in place.

BO01, Malmö, Sweden. Well known project that contributes to the municipal infrastructure capacity by, among other features, producing on-site renewable energy and reducing stormwater runoff.

BO01 ("Living 2001") is a mixed-use development on a brownfield site in Malmö, Sweden (Fig. 6) with close to 10,000 residents – one of the most important and already symbolic examples, because it works on a big scale while contributing to most of the infrastructure elements.

Built on a former industrial site, taller buildings were located on the edges of the development to shelter smaller blocks and courtyards from winds coming off the Baltic Sea. A nearby 2 MW wind facility, supplemented by photovoltaics (PVs) provides almost all electricity needs; however, a part of energy for homes and cars is provided by a methane from household waste, captured through vacuum garbage collection system. All garbage, organic waste and recyclables are connected to the underground pipeline system sucking material to a central storage area where it is picked up by municipal trucks, reducing GHG



Fig. 6. Aerial view of BO01. Courtesy of the City of Malmö

emissions and the traffic areas. Energy for water heating comes from seawater and solar and the heat is distributed through municipal sewage and waste infrastructure. Green roofs were installed on most buildings to absorb rainwater, cool the buildings, mitigate heat island effects and provide gardening space for residents. The roofs also delay stormwater runoff, lowering the risk of sewer overflows and overloads at the municipal treatment plant.

Southeast False Creek, Vancouver, British Columbia, Canada

This project contributes to the municipal infrastructure capacity by using a district heating system with sewer heat recovery [17] and providing space for urban agriculture.

Historically, Southeast False Creek (SEFC) was used for industrial and commercial purposes. In 1991, the City of Vancouver decided to transform the site into a model sustainable development.

This residential development, which was also home to the 2010 Winter Olympics Village, includes space for wildlife habitat, playgrounds and urban agriculture. At the heart of it is the city-owned Neighbourhood Energy Utility (NEU), a community energy system (Fig. 7) that provides space heating and domestic hot water.

The system uses several sources for heating, including waste heat from the municipal sewer system and rooftop solar thermal modules.

A Seniors Residency, designed as NetZero building, had waste heat planned to be delivered to its occupants from refrigeration equipment in retail spaces. Interestingly, the new equipment was so energy efficient that there was not enough waste heat, the possibility unthinkable only few years earlier.



SEFC Neighbourhood Energy Utility Schematic

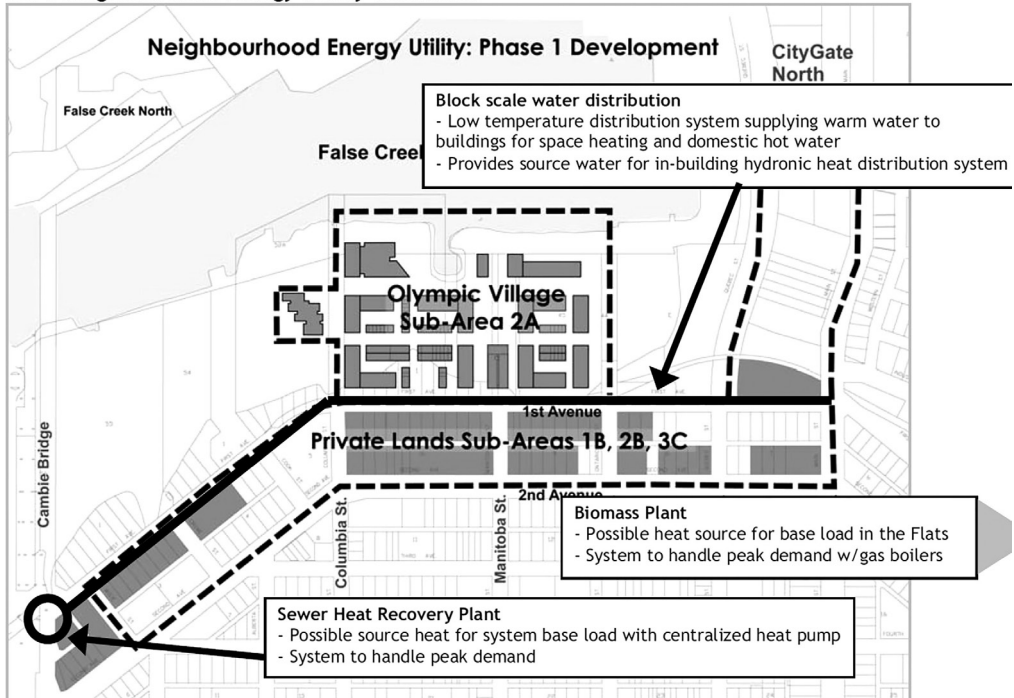


Fig. 7. SEFC Site Plan and Neighbourhood Utility. Graphic courtesy of the City of Vancouver



Fig. 8. SEFC – view. Courtesy of the City of Vancouver

The Currents, Ottawa, Ontario, Canada

This building project uses a passive solar heating system and reduces the impact to municipal water systems by reusing water.

The Currents tower (Fig. 9) was the first mixed-use facility in Canada to achieve a LEED Gold rating. The 44-unit condominium was built on a remediated brownfield and incorporates several different technologies and building construction methods that help support infrastructure systems. The southern façade is dominated by a SolarWall installation that gets heat from the sun during the winter months to preheat incoming air used then to heat and ventilate the residential units.

Retrofits

Existing buildings that were designed with a 50–100-year life expectancy (mainly institutional, hospitals, schools, etc.) usually are good candidates for retrofits such as re-glazing and installation of PVs or geothermal.

The Willis Tower, Chicago, Illinois, USA

This building project saves enough energy to supply one new hotel and adds capacity to the municipal grid.

Replacement of its 16,000 windows, installation of new gas boilers using fuel cell to generate electricity, solar panels to heat water for toilets, smart lighting and control systems combined with upgrade of elevators and escalators and conservation practices led to reduction of annual electricity consumption by 34 percent. The building saves 40% of water each year, or the equivalent of 156,448 full bathtubs, by relying on low water-flow fixtures [19] (Fig. 10). An adjacent 50-storey energy-efficient hotel uses renewable energy systems to fulfill its energy demand. This new building uses less energy than that saved in the renovation of the Willis Tower, thus the entire project is a net contributor to Chicago's infrastructure capacity.



Fig. 9. The Currents, Ottawa (source: [18])



Fig. 10. The Willis Tower, Chicago (source: [20])

District heating systems, well known and used in Europe can be economically feasible when applied to high- density developments, especially with a low-cost energy source. If cogeneration is added, the waste heat from a district heating plant can also be used to generate electrical power for the neighbourhood; or heat from municipal sewage systems can be transferred back to the heating plant.

Dockside Green, Victoria, British Columbia, Canada [21]

Project reduces municipal waste by using energy heating from biomass and reduces infrastructure loads with on-site water treatment systems.

The mixed-use development (Fig. 11) is supposed to produce its own heat (including hot water heating) converting wood waste into gas, eliminating fossil fuels and simply using a landfilled waste product. The sewage is treated on-site and reused (blackwater is filtered for reuse as greywater for flushing toilets and for irrigation).



Fig. 11. Dockside Green phases. Source: Windmill Developments



Fig. 12. Greenway

A communal greenway serves as both a public greenspace and a vital part of the wastewater and stormwater management system, in which stormwater flowing to the greenway [22] (Fig. 12) is filtered and added for reuse for toilets and irrigation.

Water-saving appliances and fixtures are a standard issue reducing the need to draw potable water from municipal supplies. The 2008 crisis has stopped the development (Fig. 13) for several years at

22% of expected density (Fig. 14) and it restarted only in January 2017 with a modified plan, which calls for another 100,000 m² of development and 1,000 residential units in buildings that go up rather than spread out, preserving; however, most of the environmental features planned in their original version.



Fig. 13. Phase 1 Design
(source: Windmill Developments)



Fig. 14. Phase 1 in 2016 (source: [23])

4. Design Reality check

Regent Park, Toronto, Ontario, Canada [24, 25]

This project adds to the municipal infrastructure capacity by using a district heating plant. It also has the potential to generate electricity from renewable sources in future.

Regent Park – Canada’s largest and oldest publicly funded community, the complete redevelopment of a 50 acre site in the centre of Toronto. The site was previously a rundown area with low rise apartments plagued by all kinds of social problems. Today it’s a mixed use development of social and market housing, with cultural, religious, educational and



Figs 15 & 16. Regent Park’s 22 – story building with district heating plant (inset). Courtesy of Doug Pollard



Fig. 17. Regent Park’s today. Courtesy of CMHC

commercial uses (Fig. 17). The mixture of uses, with their differing peak loads, is important for maintaining a required constant load demand for the CHP system. Each building in this project is/will be built to LEED Gold standard certification.

Reconstruction included a natural gas-fired district heating plant in the centre of the development integrated into the first 22-story residential tower, which is situated next to the central greenspace (Fig. 15 & 16). The plant produces high-efficiency heating and cooling for all of the residential and commercial properties (around 12,000 people) and has the potential to generate electricity using renewable energy source such as geothermal and/or solar [26].

5. Renewable Energy

Buildings as Energy Providers

The most obvious role buildings can assume as infrastructure components is as energy producers with the help of renewable sources such as wind, geothermal and solar to heat, cool and power. Using such sources can reduce GHG emissions and direct energy costs, and provide backup power during both power outages and peak energy demand when renewable energy supplied into the grid can alleviate the need to build new power plants thus element of infrastructure.

The Centre for Interactive Research on Sustainability (CIRS) Building, Vancouver, British Columbia, Canada

This building reduces the impact to municipal infrastructure systems by use of a geothermal heating system and PVs to generate electricity.

The CIRS [27] is located at the University of British Columbia (UBC) in Vancouver and is dedicated to research collaboration and outreach on urban sustainability. Its vision is to be the most innovative high performance building in North America and an internationally recognized leader in accelerating the adoption of sustainable building and urban practices.

CIRS key features (Fig. 18) significantly mitigate the infrastructure needs and improve the environment by:

- ▶ 600 tons of carbon dioxide sequestered in the structure,
- ▶ Campus energy consumption reduced by 275 megawatt-hours per year,
- ▶ Water 100% supplied by rainwater,
- ▶ Campus carbon dioxide emissions reduced by 150 tons each year.

The building uses waste heat generated by an adjacent building as well as a geothermal heating system.

The Solar Aquatics System™ duplicates, under controlled conditions, the natural purification process of fresh water streams, meadows and wetlands (Fig. 19). Using greenhouses to enhance the growth of algae, plants, bacteria and aquatic animals, sewage flows through a series of aerated, plant covered, tanks and constructed wetlands where contaminants are eliminated typically in less than three days [28]. Besides saving energy, buildings can produce some or all of it, depending on weather conditions with photovoltaics integrated into facades (Fig. 20).

CIRS Sustainable Design Goals

DESIGN PROCESS

1. Paperless 3D virtual design
2. Lifecycle Assessment (LCA) on whole building design

SITE DESIGN

3. Neutralize ecological impact
4. Sustainable contributions to local community

ENERGY

5. Sustainable and renewable energy sources, net annual power generation and GHG neutral
6. Passive design strategies and very low energy requirements
7. 100% day-lighting illumination during the day

WATER

8. On-site collection of rainwater to meet 100% of potable water requirements
9. All wastewater will be collected and treated on site
10. All storm water will be controlled, re-used and discharged on site

RESOURCE CONSERVATION

11. Minimize resource consumption and GHG impact of building construction by maximizing life, flexibility and recycling potential of the building
12. All solid waste generated to be reused or recycled
13. Maximize hours of operation and density of use

OCCUPANT HEALTH

14. Workspaces will be 100% day-lit
15. Very pure indoor air quality and user control over comfort conditions
16. CIRS will oxygenate indoor and exterior environments
17. Design of workspaces based on healthy body and mind principles

BUILDING OPERATION AND MAINTENANCE

18. Seamless integration of design and ongoing operations

CIRS OUTREACH

19. Provide the building infrastructure and resources required to advance the knowledge of sustainable design strategies, in partnership with manufacturers, policy makers and CIRS researchers
20. "Living lab" for CIRS researchers and software companies to develop and test predictive software for energy efficiency, energy distribution, thermal mass, ventilation models, IAQ, acoustics, and day-lighting effectiveness
21. Minimize external and community environmental impacts of CIRS's staff and visitors
22. CIRS will disseminate sustainable design practices, knowledge and experience

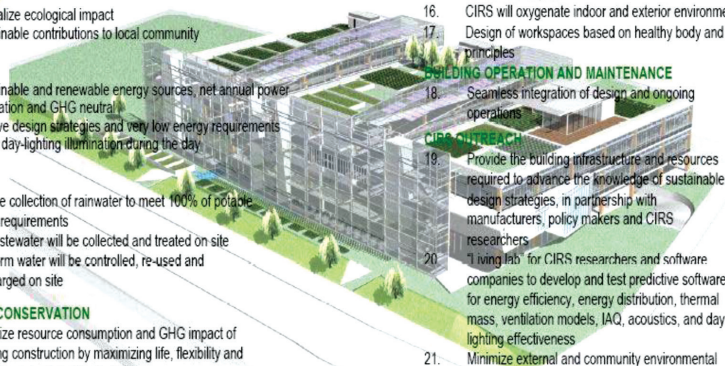


Fig. 18. Graphic courtesy of the International Initiative for a Sustainable Built Environment

Supplying 100% of the facility's water needs, CIRS collects and treats rainwater for potable use and purifies wastewater on-site in a solar aquatics biofiltration system.

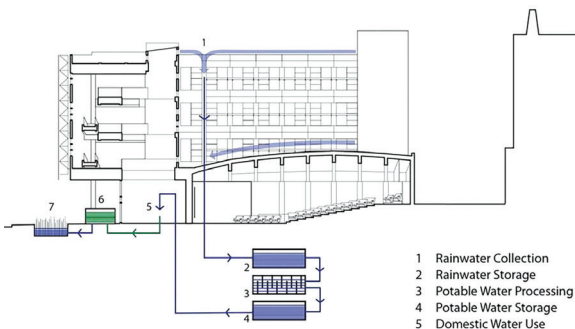


Fig. 19. Graphic courtesy of the Perkins+Will



Fig. 20. CIRS Photo courtesy of blogs.ubc.ca

Bahrain World Trade Center (WTC), Manama, Bahrain [29]

This project uses wind energy to generate a portion of the electricity demand of the buildings.

Completed in 2008, the WTC is a complex with two 240-metre high towers. Three 29-metre wind turbines were installed on bridges between the towers which funnel and accelerate wind velocity (Fig. 21). Each tower has a slightly different sail-like shape helping reduce pressure differences between the bridges. Combined with increased wind speed at high levels, this provides an equal velocity between the turbines and promotes greater efficiency. The three wind turbines operate approximately 50% of the time, providing between 10–15% of the electricity for both towers.



Fig. 21. The Bahrain WTC building has three 29-metre high wind turbines. Image courtesy of Wikipedia (By Fred Hsu [30, 31])

Greywater Reuse

Greywater reuse systems, used in new and existing buildings, capture water from laundry, showers and sinks, then treat and reuse it for toilet flushing or irrigation. They conserve potable municipal water and can also reduce the wastewater infrastructure thus reducing water and sewage costs for owners and infrastructure costs to municipalities; however, some Canadian projects show that systems' costs can often outweigh the savings (problems with training and maintenance).

BedZED, London, UK

Beddington Zero (fossil) Energy Development or BedZED, is targeting low energy and renewable fuel, including biomass CHP and PVs, zero net carbon emissions, water conservation strategies, and biodiversity measures.

BedZED combines both functions: capturing rainwater for reuse and processing blackwater on site to serve residential and office space. BedZED also produces its own energy in a CHP system, produces electricity with PVs integrated in the glazing, has green roofs and other sustainable strategies to eliminate the need for municipal infrastructure [32] (Fig. 23). It contributes to the transportation system by supplying shared electric vehicles (powered by windows' PVs) and eliminating commuting by integrating work spaces nearby (Fig. 22).

Equilibrium™ Communities [34] project – Station Pointe Greens [35], Edmonton, Alberta, Canada

Project based on Passive Design principles will include, if built as planned, apartments in buildings from 6 to 18 storeys, and townhouses (Fig. 25) resulting in a transit-supportive 250 units per hectare. SPG will have all amenities on-site and a biological wastewater

treatment facility (Fig. 24) to treat 100% of the wastewater to be re-used for toilets flushing and irrigation. The design includes reduction of stormwater run-off through green roofs over 50% of the site and bioretention cells. All those features combined with the light rail station and bus terminal, contribute to a very significant potential reduction of the infrastructure.

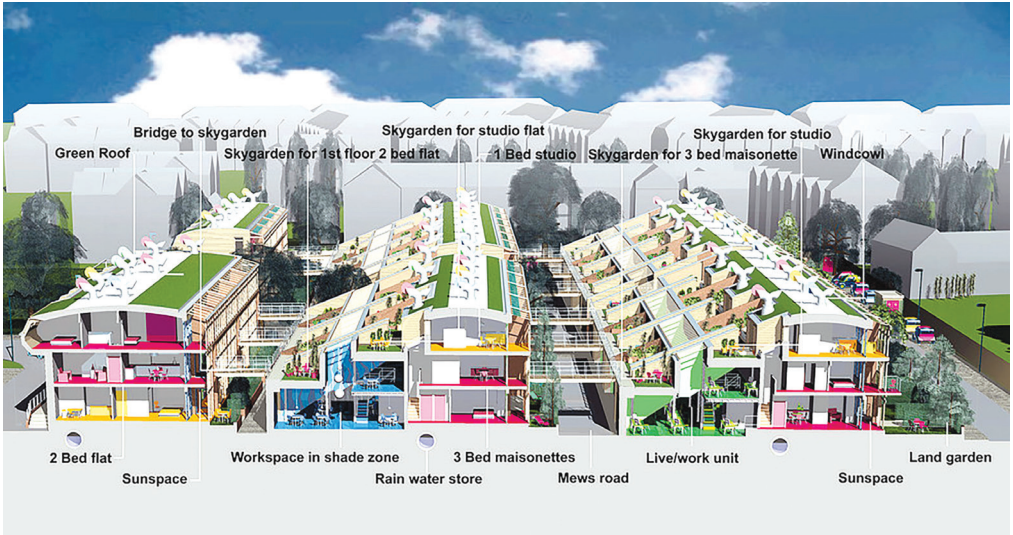


Fig. 22. Sectional perspective. Courtesy of zedfactory (source: [33])

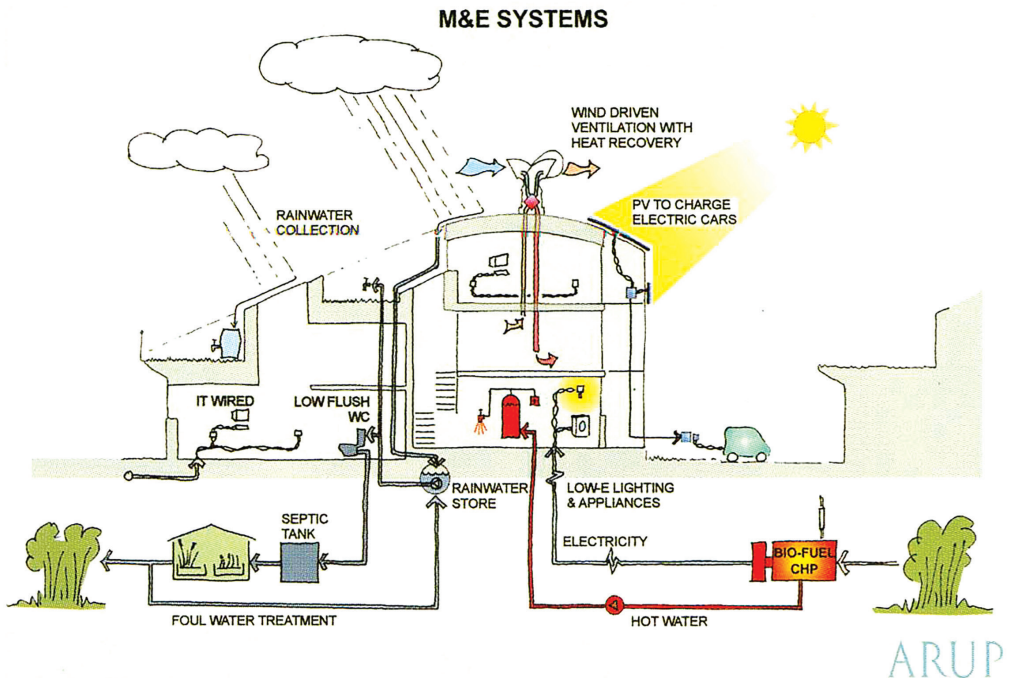


Fig. 24. BedZed, courtesy of ARUP

6. Challenges & Design Considerations

Changes can be difficult and usually are. Some in the development community believe ideas used are too expensive or complicated. Following are some of the challenges.

Cost

A number of studies show that there are no significant differences in average costs between sustainable buildings and conventional ones. While there can be additional costs, they are typically not as high as perceived by the development industry.. This is primarily because operational savings are often found through measures such as lower heating and cooling loads, revenue from construction waste, the sale of surplus energy, higher market values, etc. These long-term savings can offset increased capital cost as shown in Table 3 below.



Fig. 24. Wastewater treatment facility



Fig. 25. Aerial view. Courtesy of Hartwig Architects

Table 3. Cost of measures and related benefits [1]

Capital and operating costs	Reduced energy demand optimizes capital and operating costs by reduced equipment size (e.g., heating, ventilation or cooling systems, etc.) [8]
Density bonuses	Offered by municipalities to developers in exchange for the provision of certain amenities that benefit the community as a whole
Building envelope	The high performance envelope can reduce the costs of mechanical systems
Renewable energy	Reduces the need for fossil fueled energy, creates a potential source of income
Energy efficiency	Combined with reduced GHG emissions allows developers to sell carbon credits or reduce operating costs (long-term savings can be included in higher building sale prices)
Daylight, high efficiency lighting	Properly designed, located and shaded buildings (to avoid overheating) and use of LEDs reduce the energy requirements
Transit-oriented development	Proximity of transit can substantially reduce the requirements for parking spaces and their cost [9]

Active transportation amenities	Secure bicycle parking or better pedestrian areas, can reduce the amount of parking required and make streets safer [10]
Green roofs	Green roofs reduce stormwater runoff and provide additional insulation, which can reduce heating, cooling requirements [11]
Xeriscaping	Planting native and/or drought-tolerant plants can reduce water consumption and landscaping maintenance costs
Rainwater capture	Reduces the cost of water required for irrigation
Incentive programs	Many levels of government and utilities offer incentive programs for green buildings or for energy-efficiency retrofits
Preferential financing	Some financial institutions offer preferential financing for green buildings
Preferential insurance rates	Some companies offer credits for firms that incorporate renewable energy [12]

However, from a developer’s perspective, first costs are the most important factors and long-term savings are rarely considered, unless developer owns and operates such buildings.

Street Patterns with building as urban component and infrastructure contributor

Main road network within any community is created by local streets and usually big part of its infrastructure budget is used there over lifetime. Paved/ impermeable streets increase stormwater systems and contribute to the urban heat island effect, which in turn increase the demand for cooling. Well-designed streets, however, can mitigate traffic, enable active transportation, reduce the transportation energy and related GHG emissions. Several CMHC [36] studies show how even minor adjustments to street patterns can create opportunities to build higher density developments and reduce the impacts to municipal infrastructure. One such road pattern is the “fused grid” that combines conventional and grid-based layouts, optimizes use of land, requires less hard surfaces, allows for higher densities and more open space, and is more cost effective to service and maintain (Fig. 26).

Table 4 [2]

Fused grid elements	Potential Benefits
Traffic calming and control	Reduced noise and air pollution Fewer cars can reduce wear and tear on roads
Street design	Pedestrian and cyclist safety Reduced noise and air pollution Better stormwater management and permeable surfaces
Greenspace and water retention	Promotes better water quality Improves local air quality Provides habitat for plants and animals and local flora



Table 4 cont.

<p>Optimal development density and mixed use</p>	<p>Encourages active transportation and discourages car trips Higher density can create a higher tax base for the municipality and greater revenues for developers Supports mass transit systems</p>
<p>Active transportation infrastructure (cycling lanes, sidewalks, etc.)</p>	<p>Encourages active transportation Promotes greater physical activity among residents</p>

Fused grid neighbourhoods encourage greenspaces throughout a development that can provide connections between neighbourhood elements and food production locations, function as storm and wastewater management components, make higher density more acceptable when developed in conjunction with open space, and more viable for locating co-generation and shared energy systems [2].

Streets may now be used as stormwater collection routes, if not built as permeable, greywater gardens, and linear, vegetated parks that cool and improve air, stormwater quality and provide habitat and pleasure. The sheltered courtyards are ideal for food production, rainwater storage, grey water purification etc. and some of them may function as greenhouses.

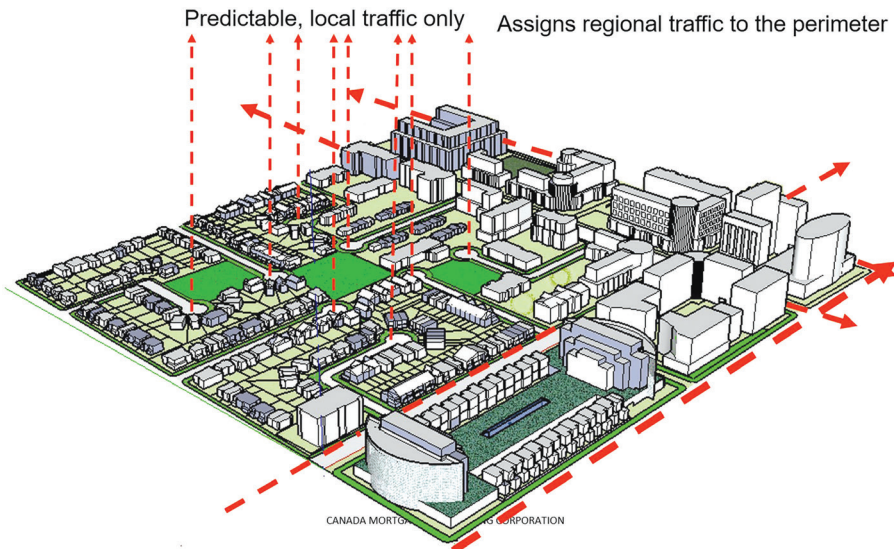


Fig. 26. Modelling fused grid. Courtesy of F.Grammenos

7. Fused Grid in Works

Saddleton, Calgary, Alberta, Canada

By using a fused-grid model, the project reduces the additional road space that can then be used for on-site stormwater storage and treatment.

The fused grid was implemented for the Saddleton, a site with the density between 25 and 30 units/ha, 50% higher than conventional. Heavy traffic was shifted to major perimeter roads and smaller collector streets were introduced. High density buildings are along light rail corridors (Fig. 27). Green spaces are used instead of hard surfaces. When compared to the conventional suburban design, the fused grid pattern, as applied in Saddleton, cuts road space by about 2.2 hectares, making it available as habitat, recreational space, food production, stormwater treatment areas (Fig. 28).



Fig. 27. Saddleton street network and land use pla

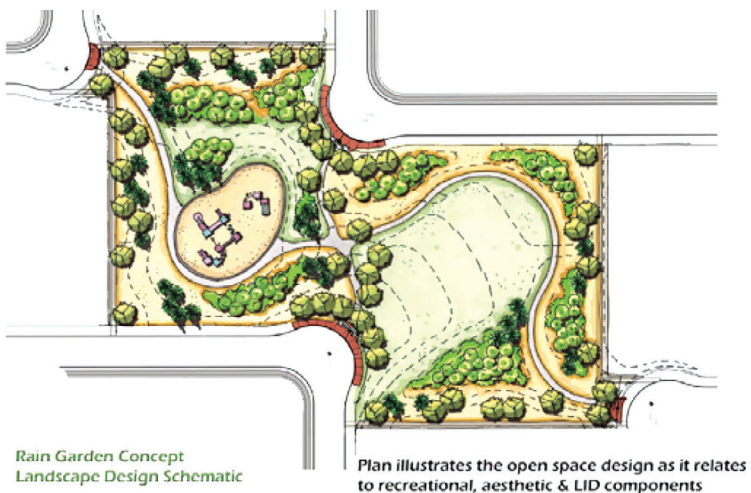


Fig. 28. The rainwater garden space – recreation, pathway node and rainwater filtration. Courtesy of CMHC

8. Conclusions

Infrastructure matters because it represents the major capital outlay for the developer and a key accounting element in pricing, after land. (...) to be competitive infrastructure costs have to be equal to or lower than what conventionally has been achieved in previous developments or by the industry at large [2].

The infrastructure can be significantly improved and reduced by including buildings as direct contributors to it that should:

- ▶ Be designed as a part of community design with the efficient road and infrastructure grids,
- ▶ Be a net-zero/positive energy producers to minimize the need for new energy plants,
- ▶ Include systems that treat and manage water, wastewater or stormwater, reducing/eliminating the need to be connected to municipal water systems,
- ▶ Use less energy, cut GHG emissions, air pollution and reduce their dependence on fossil fuels [4].

Once buildings are identified with their potential roles, the next step is to analyse the neighbourhood capacity and needs in terms of energy, greywater, blackwater, heat (including sewer/waste heat). Then the analysis would show what to do with buildings to make them the best contributors. For example, improvements made to building envelope would increase the energy performance. Almost all roofs, part of the envelope, may become candidates for roles such as to mitigate rain water impact, heat losses and gains, air quality improvement, food production as well as installation of solar collection/energy production systems.

Other buildings would also be analysed in regards to the feasibility of upgrading their performance and reducing their needs in the future. Even recent buildings may have a potential there, especially those built to the basic code requirements, or with only a profit in mind.

There are many existing tools, a lot of data, experience and expertise to learn from and the next step to make buildings as contributors to a community infrastructure can be relatively easy and no matter what reasons are behind the actions, when buildings act as such, the benefits can spread to everybody from the owner to the greater community.

Bibliography

- [1] Kujawski W., Pollard D. – some case studies, Grammenos F. – Fused Grid. Boddy S. – writer Contracted by CMHC, *Buildings as Infrastructure Contributors*, Article for Ontario Association of Architects – OAA, CMHC, 2009.
- [2] Grammenos F., Lovegrove G.R. *Remaking the City Street Grid. A Model for Urban and Suburban Development*, 2015.
- [3] Larsson N., Salat S. *Performance Synergies in Small Urban Zones*, 2013.
- [4] Pollard D., *Corelation of Infrastructure and Nature*, Article for American Institute of Architects, 2016.

- [5] Tillie N. et al. 2009a. *REAP: Towards CO₂ neutral urban planning*, 45th ISOCARP Congress 2009.
- [6] Tillie N. et al. 2009b. *REAP Rotterdam Energy Approach and Planning, Towards CO₂ – neutral urban Development*, Rotterdam.
- [7] Pratt R.G. et al., *The Smart Grid: An Estimation of the Energy and CO₂ Benefits*, U.S. Department of Energy Revision 1, 2010.
- [8] BioRegional Development Group, *Beddington Zero Energy Development*, 2002.
- [9] Canada Green Building Council, *Green Building in Canada: Overview and Summary of Case Studies*, 2006.
- [10] City of Ottawa, *Cash in Lieu of Parking Review*.
- [11] Transport Canada. Urban Transportation Showcase Program, *Complete Streets: Making Canada's roads safer for all*, http://publications.gc.ca/collections/collection_2012/tc/T41-1-72-eng.pdf (access: March 2017).
- [12] CMHC, *Green Roofs: A Resource Manual for Municipal Policy Makers*, 2006, <https://www03.cmhc-schl.gc.ca/catalog/productDetail.cfm?lang=en&cat=123&itm=73&sere=2&start=1&stfl=green%20roof&fr=1495130589887> (access: March 2017).
- [13] Ceres, *From Risk to Opportunity: Insurer Responses to Climate Change*, 2009, <http://insurance.lbl.gov/opportunities/risk-to-opportunity-2008.pdf> (access: March 2017).
- [14] https://en.wikipedia.org/wiki/Eco-industrial_park (access: March 2017).
- [15] <https://www.youtube.com/watch?v=bYs9DFGQxHg> (access: March 2017).
- [16] https://en.wikipedia.org/wiki/Kalundborg_Eco-industrial_Park (access: March 2017).
- [17] <https://www.iisd.org/business/viewcasestudy.aspx?id=77> (access: March 2017).
- [18] <http://vancouver.ca/home-property-development/southeast-false-creek-neighborhood-energy-utility.aspx> (access: March 2017).
- [19] <http://korbanltd.com/portfolio/the-currents-wellington-street-ottawa> (access: March 2017).
- [20] <http://www.willistower.com/building-information/sustainability> (access: March 2017).
- [21] <https://traveldigg.com/willis-tower-the-chicagos-skyscraper> (access: March 2017).
- [22] <http://www.timescolonist.com/life/islander/new-beginning-for-dockside-green-project-in-vic-west-1.9377150> (access: March 2017).
- [23] http://www.solaripedia.com/13/247/2607/dockside_green_water_feature.html (access: March 2017).
- [24] www.googleearth.pl (access: March 2017).
- [25] <http://urbantoronto.ca/news/2015/05/scale-model-regent-park-gives-insight-future> (access: March 2017).
- [26] https://www1.toronto.ca/city_of_toronto/city_planning/community_planning/files/pdf/regentpark_planning-rationale.pdf (access: March 2017).
- [27] <http://www.fvbenergy.com/projects/regent-park-community-energy-system> (access: March 2017).
- [28] https://en.wikipedia.org/wiki/Centre_for_Interactive_Research_on_Sustainability (access: March 2017).



- [29] http://www.ecotek.ca/ECO-TEK_Ecological_Technologies/Home.html (access: March 2017).
- [30] https://en.wikipedia.org/wiki/Bahrain_World_Trade_Center (access: March 2017).
- [31] <https://www.flickr.com/photos/fhsu/4486351029> (access: March 2017).
- [32] <https://commons.wikimedia.org/w/index.php?curid=46532306> (access: March 2017).
- [33] <http://www.bioregional.com/beddington-zero-energy-development-case-study-report> (access: March 2017).
- [34] <https://goo.gl/images/yADkxz> (access: March 2017).
- [35] https://www.cmhc-schl.gc.ca/en/inpr/su/eqsucoin/eqsucoin_003.cfm (access: March 2017).
- [36] <https://www.cmhc-schl.gc.ca/odpub/pdf/67063.pdf> (access: March 2017).
- [37] <https://www.cmhc-schl.gc.ca/odpub/pdf/66071.pdf> (access: March 2017).
- [38] <https://www.cmhc-schl.gc.ca/odpub/pdf/63760.pdf> (access: March 2017).
- [39] http://www.cscd.gov.bc.ca/lgd/greencommunities/sustainable_development.html (access: March 2017).

Magdalena Rogalska

Faculty of Civil Engineering and Architecture, Lublin University of Technology

Zdzisław Hejducki (zdzislaw.hejducki@pwr.edu.pl)

Faculty of Civil Engineering, Wrocław University of Technology

THE APPLICATION OF TIME COUPLING METHODS IN THE ENGINEERING OF CONSTRUCTION PROJECTS

ZASTOSOWANIE METOD SPRZĘŻEŃ CZASOWYCH W INŻYNIERII PRZEDSIĘWZIĘĆ

Abstract

This paper summarises methods of scheduling construction processes with the use of artificial intelligence methods. Rules used for the calculation are characterised taking into account the implementation of priorities and resource constraints.

Keywords: scheduling, time coupling method, artificial intelligence

Streszczenie

W artykule przedstawiono metody harmonogramowanie procesów budowlanych z wykorzystaniem metod sztucznej inteligencji. Scharakteryzowano zasady stosowania obliczeń z uwzględnieniem priorytetów wykonawczych i ograniczeń zasobów.

Słowa kluczowe: harmonogramowanie, metody sprzężeń czasowych, sztuczna inteligencja

1. Introduction

Time coupling methods (TCM) allow the performing of schedules which take into account the technological and organisational limitations. These methods include: TCM I – continuity of work on the working plots of land; TCM II – continuity of work of the construction brigades; TCM III – minimising the duration of the project implementation; TCM IV, V & VI – continuity of the construction processes with the use of catty-cornered couplings, reverse catty-cornered couplings, sites of works and implementation resources. TCM is based on algorithmic notation which enables the automation of calculations and the introduction of numerous limitations. Traditional methods of scheduling do not provide the possibility to automatically prioritise tasks. In these methods, tasks are prioritised intuitively based on engineering knowledge. The research is focused on modelling construction projects, taking into account the tools of artificial intelligence as an optimisation calculation device. The research covers issues such as perfecting time coupling methods using metaheuristic algorithms, optimisation of duration, and cost correlation with the use of artificial intelligence methods (evolutionary algorithms, Tabu Search etc.), scheduling of construction projects with fuzzy duration of completing the tasks, planning construction projects with the dependencies between the duration, cost and resources, using genetic algorithms and a hybrid evolutionary algorithm. TCM was devised and developed by Professors V. Afanasjew, (1980, 1985, 1988, 1994), J. Mrozowicz (1982, 1997), and Z. Hejducki (2000, 2004, 2004). Specific methods of flow nature are involved in TCM application. The continuation of developing these methods has been undertaken. Issues pertaining to the scheduling of construction processes with the use of artificial intelligence methods are displayed in Fig. 1.

2. Systematising Time Coupling Methods TCM I, TCM II, TCM III, TCM IV, TCM V, TCM VI

While covering *subject matter 1*, TCM methods from I to VI were systematised. Various applications of each of the six time coupling methods were explained in a simple manner in publications [3–5, 19–21]. Previous scientific on TCM were denied wide recognition because of their extremely complicated mathematical notation. The methods were described according to the nomenclature and symbols used in international literature. The most important premisses of particular methods were presented for comparative purposes and schedules for every method were developed using the same database – this made presenting the research results possible in foreign journals. The most remarkable achievement of this stage was the publishing of a monograph [5] entitled *Time Couplings Methods: Construction Scheduling and Time/Cost Optimization*.

The effects of covering *Subject matter 1* include systematising the TCM methods, introducing international symbols, and indicating directions for the further development of TCM.

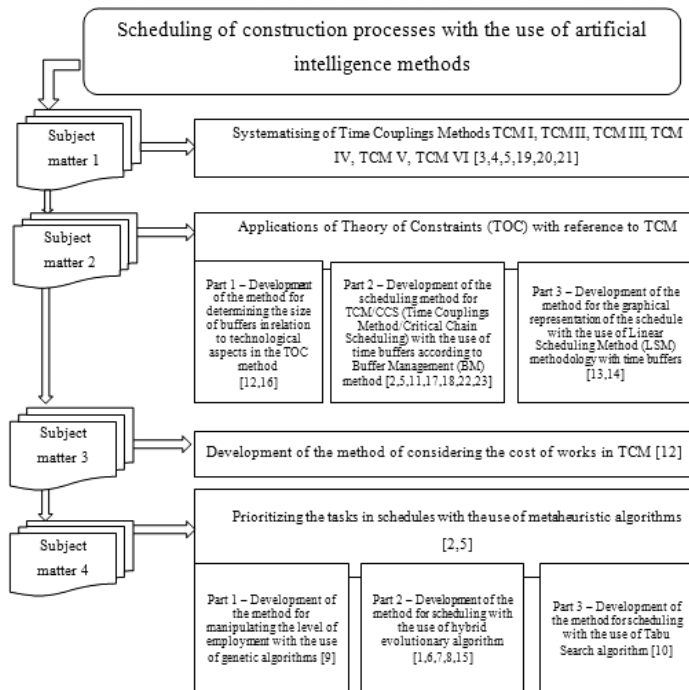


Fig. 1. Scheduling construction processes with the use of artificial intelligence methods

3. Applications of Theory of Constraints (TOC) with reference to TCM

Subject matter 2 consists of introducing the premisses of Goldratt's theory of constraints (TOC) into the time coupling method (TCM) – the research results are presented in publications [2, 5, 11, 13, 14, 17, 18, 22, 23]. In TOC, project buffers (PB) and feeding buffers (FB) are introduced into the schedule in order to secure a contractor and project manager from the delay in the date of completing the works. In theory, the size of the time buffers constitute 25% of an allotted critical path. In papers [12, 16], the influence of choosing a critical path and also the influence of the system of project and feeding buffers on the overall duration of the project was analysed. The performed analysis and calculations indicate that shortening the duration of particular processes by 25% does not result in shortening the overall duration of the whole project by the same value. The duration of completing the whole project depends on the choice of the particular elements in the critical chain. While analysing graphical models (cycle graphs built in accordance with the methodology of linear scheduling model [LSM]) – it can be observed that adopting the critical chain which is closest to the right edge of the graph results in the most substantial shortening of the duration of the project. Furthermore, in cycle graphs it is necessary to treat feeding buffers (FB) as separate processes – this is due to the need to preserve the continuity of work of the construction teams and to avoid financial losses connected with unnecessary stoppages. The method of calculating the size of time buffers, different from the value proposed by Goldratt (25%), was introduced. The newly proposed

solution takes into consideration aspects such as the level of risk in completing a particular process, as well as technological limitations resulting from techniques of manufacturing. The proposed solution also takes into consideration opportunities to accelerate the process completion and the necessity to preserve technological breaks. The elements of scientific novelty in this doesn't work, consider using something like 'characteristics of' *Subject matter 2* are as follows:

- ▶ introducing TOC into the TCM method;
- ▶ determining the method of producing cycle graphs according to LSM in the TOC/TCM method and introducing international symbols;
- ▶ developing the methodology for calculations in TOC/TCM in accordance with Goldratt's premisses and considering the risk factors and technological factors of the influence, such as changes in the size of feeding buffers and a project buffer
- ▶ performing the analysis of choosing the critical path from the available critical chains in the aspect of minimising the duration of completing the project.

4. Development of the method of considering the cost of works in TCM

In *subject matter 3*, the second criterion of optimisation, namely the cost minimisation, is introduced into TCM [12]. Methodology for calculating the correlation between cost and duration in the TOC/TCM method while planning and completing construction projects is proposed. The developed method assumes three stages of creating schedules. The first stage is the output schedule, which is formed in a traditional way. The schedule of the second stage considers estimation of the risk connected with the duration and cost of completing the works. It is assumed that the risk can be estimated using all the available methods, including the Delphi method, fuzzy sets, automatic neural networks, the Monte Carlo method (Risk 4.0), and the method of construction risk assessment (MOCRA) etc. As a result of the conducted analysis, the level of risk for particular processes is estimated and the second schedule is created – usually with a longer project duration – which considers the risk connected with the duration and cost of completing the project. The third stage assumes the reduction of risk by introducing levelling factors, such as insurance, changes in the logistics system, in the involvement of resources, work organisation etc., as well as introducing feeding buffers and a project buffer, adequate for the opportunity to reduce the works. As the result of the changes made individually for every process, the third schedule is created and modified by reducing the influence of risk factors and by introducing time buffers. The correlation between the duration and cost of the project is estimated again, whereas the extra time and financial resources are left as security for completing the task. The schedules of the particular stages are presented in the following way – the 1st stage for the investor, the 2nd stage for the contractor and the 3rd stage for project manager.

The elements of scientific novelty in *subject matter 3* are as follows:

- ▶ developing the concept of introducing two criteria for optimisation of the duration and cost into the TCM method;

- ▶ developing the methodology of the 3-stage scheduling, considering risk factors and reducing the risks through technological and organisational changes and by introducing the TOC/TCM method;
- ▶ displaying the functional correlation between the size of buffers and the value of variance of the process duration with the value of variance resulting from the risk analysis.

5. Prioritising the tasks in schedules with the use of metaheuristic algorithms

In *Subject matter 4*, resources were introduced into the TCM method as the third criterion of optimisation. The methodology was developed to apply metaheuristic algorithms in order to prioritise the tasks in TCM, whilst considering duration, cost and use of resources [2, 5, 9]. There is a premise adopted in which a schedule is the equivalent of a chromosome. New modified schedules are obtained by mutation, crossing and selection. Limitations, which ensure the logical construction of the estimated schedule and correct decoding of chromosomes, are introduced. Hard limitations, namely those which can never be omitted, are connected with the order of completing the tasks – these are taken into account in the objective function. For instance, the objective function was determined so as to get a regular level of employment of the construction site employees. Genetic algorithms, hybrid evolutionary algorithms and the Tabu Search algorithm were used for calculations.

In *Part 1 of Subject matter 4*, traditional evolutionary algorithms were used for calculations because of their high usefulness for finding the range containing the optimal goal function value. The calculations result in an approximation of the value (a so-called suboptimal solution).

In *Part 2 of Subject matter 4*, hybrid evolutionary algorithms (memetic algorithms) were used for calculations [1, 6, 7, 8, 15]. The activity of an algorithm starts with creating the initial population, which might be created in a random manner. The best member of the initial population is assumed to be the suboptimal solution. A new population is generated in the following manner – a set of local minima is established and certain elements are determined, considering these population members which appear on the same positions in local minima, forming a set of determined elements and positions. Every permutation of a new population has certain elements at the determined positions. Permutations of finite sets can be identified with set population members of a set in a certain order. The algorithms finishes after generating a predetermined number of generations – usually, this is between 10,000 and 100,000. The calculations are considered to be correct when, after increasing the number of generations by, for instance 1000, a better result was not obtained. The results of numerical experiments connected with using a hybrid evolutionary algorithm for scheduling the construction project are presented in the papers. Optimal planning of the course of construction works are taken into account while adopting a criterion for measuring the regularity in the demand for resources, i.e. the level of employment of workers. Moreover, the limitations connected with applying the methodology of the critical chain (CSS/BM) were accepted. A classical genetic algorithm and a modified hybrid evolutionary algorithm were used for optimisation calculations.

Applying the Tabu Search (TS) procedure constitutes *Part 3 of Subject matter 4* [10]. This procedure was used for obtaining optimal solutions or solutions not far from being optimal. The basic idea of the algorithm is searching the space including all the possible solutions, using a sequence of movements. In the sequence of movements, there are movements which are not allowed – these are called tabu movements. The algorithm avoids oscillating around the local minimum as it is storing the information about the already checked solutions in the form of the tabu list (TL). Fuzzy numbers, used for the calculations, were generated from the average time in such a way that a time shorter than the average time by 16.6% was adopted as the minimum, whereas a time longer than the average by 33.3% was adopted as the maximum. The aim of the calculations was not to determine the value of fuzzy numbers of the duration of processes, but to check the possibility of using the Tabu Search algorithm for searching for the optimal solution – the minimum duration of the construction project. The obtained results were compared with the calculations made using the TS method and deterministic data. The average approximation errors of algorithms [%] were used for measuring the accuracy of calculations. The average approximation errors were 18.4% for the deterministic TS and 7.5% for the fuzzy TS. Thus, it might be assumed that when the priority of tasks is determined by using an algorithm with fuzzy parameters, the value of the objective function is changed to a much smaller extent while the duration of completing the tasks is disturbed.

The elements of scientific novelty in *subject matter 4* are as follows:

- ▶ development of the method of scheduling with the use of the Tabu Search algorithm;
- ▶ replacement of deterministic data with fuzzy data, according to the accepted rule, with the aim of obtaining the result with a smaller approximation error.

6. Summary

The research topic discussed in this paper has a specific character as it relates to the unique accomplishments of the authors. There is no possibility to cite other researchers' work. The work schedule is an essential part of the construction process, it is important to take into account the constraints of resources and working methods. Due to the algorithmic nature of the calculations, there is the possible application of many new solutions to the TCM as application of controlled buffers depending on technological and organizational conditions or using of probabilistic values of execution times of construction processes.

References

- [1] Bożejko W., Hejducki Z., Rogalska M., Wodecki M., *Analiza szczególnej zależności typu czas/koszt z zastosowaniem metod sztucznej inteligencji, Problemy naukowo-badawcze budownictwa, Zagadnienia materiałowo-technologiczne infrastruktury i budownictwa – monografia (rozdział)*, Wydawnictwo Politechniki Białostockiej, Białystok 2008.

- [2] Bożejko W., Hejducki Z., Rogalska M., Wodecki M., *Scheduling of construction projects with a hybrid evolutionary algorithm's application*, [in:] *Evolutionary algorithms*, ed. Eisuke Kita, InTech, Rijeka 2011, 295–308.
- [3] Hejducki Z., Rogalska M., *Metody sprzężeń czasowych TCM*, „Przegląd Budowlany”, 2/2005.
- [4] Hejducki Z., Rogalska M., *Zasady stosowania TCM*, „Przegląd Budowlany”, 3/2005.
- [5] Hejducki Z., Rogalska M., *Time coupling methods: construction scheduling and time/cost optimization*, Oficyna Wydawnicza Politechniki Wrocławskiej, Wrocław 2011.
- [6] Rogalska M., Bożejko W., Hejducki Z., *Harmonogramowanie przedsięwzięć budowlanych z zastosowaniem algorytmów ewolucyjnych*, „Przegląd Budowlany”, 9/2007.
- [7] Rogalska M., Bożejko W., Hejducki Z., *Time/cost optimization using hybrid evolutionary algorithm in construction project scheduling*, *Automation in Construction* 18, 2008, 24–31.
- [8] Rogalska M., Bożejko W., Hejducki Z., *Harmonogramowanie przedsięwzięć budowlanych z zastosowaniem hybrydowego algorytmu ewolucyjnego*, „Prace Naukowe Instytutu Budownictwa Politechniki Wrocławskiej”, 87/2006.
- [9] Rogalska M., Bożejko W., Hejducki Z., *Sterowanie poziomem zatrudnienia z zastosowaniem algorytmów genetycznych*, LI Konferencja Naukowa, Krynica 2005.
- [10] Rogalska M., Hejducki Z., *Analiza porównawcza prognozowania produkcji budowlanej z zastosowaniem metod regresji krokowej, sieci neuronowych i ARIMA*, Zeszyty naukowe WSOWL 3(157), 2010.
- [11] Rogalska M., Hejducki Z., *Skracanie czasu realizacji przedsięwzięć budowlanych z zastosowaniem Teorii Ograniczeń TOC i metody CCS/BM*, L Konferencja Naukowa KIL i W PAN KN i PZITB, Krynica 2004.
- [12] Rogalska M., Hejducki Z., *Time and Cost Contingency of Buildings Reconstruction*, International Conference Reconstruction, Sankt-Petersburg 2005.
- [13] Rogalska M., Hejducki Z., *Algorytmy synchronizacji procesów budowlanych*, „Przegląd Budowlany” 9/2004.
- [14] Rogalska M., Hejducki Z., *Harmonogramowanie robót budowlanych z zastosowaniem metodyki LSM/BM*, Konferencja naukowo-techniczna, Gdańsk 9–11.06.2005.
- [15] Rogalska M., Hejducki Z., Wodecki M., *Development of time couplings method using evolutionary algorithms*, The 25th International Symposium on Automation and Robotics in Construction ISARC-2008 June 26–29, 2008 Vilnius, 638–643.
- [16] Rogalska M., Hejducki Z., *Zastosowanie buforów czasu w harmonogramowaniu procesów budowlanych*, „Przegląd Budowlany”, 6/2005.
- [17] Rogalska M., Hejducki Z., *Modelowanie przedsięwzięć budowlanych z zastosowaniem metody sprzężeń czasowych Część I – TCM I*, Abstract, VII Ogólnopolska Konferencja Naukowa Modelowanie Preferencji a Rzyzko, 11, Ustroń 3–5.04.2011.
- [18] Rogalska M., Hejducki Z., *Shortening the realisation time of building project with application of theory of constraints and critical chain scheduling*, „Journal of Civil Engineering and Management”, 2004, vol. X, supp. 2.
- [19] Rogalska M., Hejducki Z., Łodożyński Ł., *Harmonogramowanie liniowych procesów budowlanych z uwzględnieniem metody Branch & Bound*, [in:] *Organizacja przedsięwzięć*

- budownictwa drogowego*, ed. Z. Tokarski, Zarząd Oddziału Stowarzyszenia Inżynierów i Techników Komunikacji RP: Rekrpol, Bydgoszcz: 2011, 107–118.
- [20] Rogalska M., Hejducki Z., *Modelowanie przedsięwzięć budowlanych z zastosowaniem metody sprzężeń czasowych. Cz. 2, Model TCM II*, [in:] *Organizacja przedsięwzięć budownictwa drogowego*, ed. Z. Tokarski, Zarząd Oddziału Stowarzyszenia Inżynierów i Techników Komunikacji RP: Rekrpol, Bydgoszcz: 2011, 119–130.
- [21] Rogalska M., Hejducki Z., Wodecki M., *Development of time couplings method*, Peterburgska Škola Potočnoj Organizacii Stroitel'stva: material'y mieždunarodnoi naučnoj konferencii posvāsennoj pamāti professora Viktora Alekseevica Afanas'eva, 20–21 fievralā 2014, Sankt-Petersburg 2014, 90–93.
- [22] Rogalska M., Hejducki Z., *Time buffers in construction process scheduling*, "Journal of Civil Engineering and Management", 2007, Vol. 13, No. 2, 143–148.
- [23] Afanasejv V.A., *Algoritmy formirovania rascieta i optimizacii metod organizacii rabot*, Učiebnoje pasobije, Leningrad 1980.
- [24] Afanasev V.A., *Učiet zatrat wremieni na perieboizirovanije stroitelnych organizacii pri formirovani i optimalizacii kompleksov potokov*, Aktualnyje problemy sovietskowo stroitel'stwa, Sankt-Petersburg 1994.
- [25] Afanasev V.A., Afanasev A.V., *Projektirowanije organizacii stroitel'stva, organizacii i proizvodstva rabot*, LISI, Leningrad 1988.
- [26] Afanasev V.A., Afanasev A.V., *Paralelno – potočnaja organizacija stroitel'stva*, LISI, Leningrad 1985.
- [27] Mrozowicz J., *Metody potokowe organizacii procesow budowlanych o charakterze deterministycznym*, Seria: Monografie 14, Wydawnictwo Politechniki Wrocławskiej, Wrocław 1982.
- [28] Mrozowicz J., *Metody organizacii procesow budowlanych uwzględniające sprzężenia czasowe*, Dolnośląskie Wydawnictwo Edukacyjne, Wrocław 1997.
- [29] Hejducki Z., *Sprzężenia czasowe w metodach organizacii złożonych procesow budowlanych*, Seria: Monografie 34, Wydawnictwo Politechniki Wrocławskiej, Wrocław 2000.
- [30] Hejducki Z., *Zarządzanie czasem w procesach budowlanych z zastosowaniem modeli macierzowych*, Wydawnictwo Politechniki Wrocławskiej, Wrocław 2004.
- [31] Hejducki Z., *Sequencing problems in methods of organising construction processes*, "Engineering Construction and Architectural Management", 2004, Vol. 11, No. 1, 20–32.

Janusz Kogut (jkogut@pk.edu.pl)

Jakub Zięba

Faculty of Civil Engineering, Cracow University of Technology

THE MODIFICATION OF THE DYNAMIC PROPERTIES OF COHESIVE SOIL RESULTING FROM TRIAXIAL CONSOLIDATION

ZMIANA PARAMETRÓW DYNAMICZNYCH GRUNTU PODDANEGO KONSOLIDACJI W APARACIE TRÓJOSIOWEGO ŚCISKANIA

Abstract

This paper describes the laboratory examination of the dynamic parameters of cohesive soil together with an analysis of these parameters using artificial intelligence. The analysis yielded the propagation velocity of shear wave V_s and the dynamic Kirchhoff modulus G obtained during the soil tests in the triaxial stress apparatus. The investigation was conducted using *bender* elements. The artificial neural networks trained on data obtained from the test were used for the further analysis.

Keywords: dynamics, soil parameters, wave propagation

Streszczenie

Artykuł łączy ze sobą badania laboratoryjne parametrów dynamicznych gruntu spoistego wraz z ich analizą z użyciem metod sztucznej inteligencji. Rezultatami analizy są wartości prędkości propagacji fali ścinającej V_s oraz dynamicznego modułu Kirchhoffa G uzyskane podczas badania gruntu w aparacie trójosiowego ściskania. Do otrzymania tych parametrów posłużyło wykorzystanie elementów *bender*. Do analizy użyto sztucznych sieci neuronowych uczonych na danych pozyskanych z badań.

Słowa kluczowe: dynamika, parametry gruntu, propagacja fal

1. Introduction

This paper presents a project aimed at verifying the effect of various parameters on the state and quality of soil under complex states of stresses. In the study, soil samples dug from a depth of approximately 5–6 m were utilized. They were underlying directly on a layer of clay, which, in the past, was a source of material for a brickyard in Zesławice, near Nowa Huta. Triaxial stress apparatus was used in this experiment.

By exploiting the porous quality of the soil, one may study its physical properties. When using the soil material for construction purposes, the parameters relating to strength are a significant issue. By studying the stresses in the soil, one may assess the friction between the soil particles and the liquid that make up the soil. This friction is an internal friction and in a number of soil constitutive models, it is defined as the internal friction angle. This level of friction is a function of number of soil parameters (e.g. size, shape, degree of roundness or angularity of particles, mineral composition, and the geological origin or history of the loading in the soil deposits).

As far as modelling of the soil behaviour is concerned, two parameters are particularly important: the internal friction angle and the cohesion. The internal friction angle depends on the porosity, water content and the water pressure in the pores. The cohesion may be in the form of soil resistance to external forces dependent on the forces attracting the particles and the liquid component accumulated in the soil. The quantity of liquid is important mainly in cohesive soils, and may depend on particle size, water content, and the origin of mineral composites. If the water content of soil decreases, the cohesive forces in the soil become larger; the strongest cohesive forces are found in soil that is in a dry and hard state. However, the degree of internal friction and cohesion also depends on the state of soil and how the soil structure acts when the pores are filled with water. It is commonly known that the in-situ conditions are different depending on whether the zones are aerated or saturated. In the aeration zone, soil is a mixture of particles (mineral and/or organic), gases (air) and liquid (mostly water) confined in the pores. It is therefore a three-phase mixture which may be partially saturated – this occurs in the case of soil located above the water table. It is natural to assume that soil below the water table would be completely saturated. In such conditions, one assumes that the soil becomes a two-phase mixture, i.e. it is composed of mineral and/or organic particles and liquid which is primarily water, completely filling the pores of the soil.

2. Laboratory tests of soil

Laboratory test methods for basic static soil parameters, where the relationship between the stress and strain is determined, are based on the equipment and procedures recommended by European and ISO standards e.g. PN EN ISO TS 17892:

- ▶ direct and residual shear machine (total value of Φ_c and c_c);
- ▶ oedometer (oedometric modulus of compressibility);
- ▶ cone penetrometer (shear strength – C_u);

- ▶ triaxial stress apparatus (depending on the methodology: total value of Φ_c and c_c or effective value of Φ' and c').

Dynamic testing may be conducted with appropriately equipped triaxial stress apparatus. This type of apparatus may be supplemented with additional elements such as a resonant column or, as was used in this study, bender element test equipment.

The research conducted with the use of the triaxial stress apparatus may be performed in various ways. In fact, one may distinguish between three basic test methods depending upon how excess water is drained from the soil sample:

- ▶ unconsolidated undrained (UU) method – the shear strength of the sample is received with respect to total stress without a preliminary soil consolidation. During basic research, the pore pressure of water in the sample is not usually measured and the test is performed without draining the water from the sample. Tests using this method are performed when the investigated soil will carry the loading from the building for which the live load has to account for over 70% of the total loading. From these studies, the strength parameters are determined on the basis of the total stress (Φ_{uu} and c_{uu}).
- ▶ consolidated (isotropic) undrained (CU, CIU) method – soil samples are initially consolidated. During fundamental testing, the measurement of pore pressure of water in the sample is carried out and the test is performed without draining the water from the sample. The effective stress is then calculated as the difference between the total stress and the pore pressure. This method is used when the loading imposed on the building varies from 30% to 70% of the total loading; such conditions may occur when after the construction of a building, the operational loading is anticipated in a relatively short period of time. Therefore, on the basis of this test, one may determine total and effective strength parameters (Φ_{cu} and c_{cu} or Φ'_{cu} and c'_{cu}).
- ▶ consolidated (isotropic) drained (CD, CID) method – this test method is similar to the CU test; it is performed very slowly and shear samples are subjected to a pre-consolidation procedure. During basic investigation, followed by a continuous flow of water from the sample, the test speed is adjusted so that the value of pore pressure measured in the sample is at a constant level. This method is used in cases where the anticipated operational load of the building does not exceed 30% of the total load, and the construction time is long enough to develop full consolidation of the substrate. Therefore, on the basis of this test, one may determine the effective strength parameters (Φ'_{cd} and c'_{cd}).

The significant difference between the parameters achieved by diverse testing methods is shown in Fig. 1 [1, 2]. You can see a distinct change in the position of the Mohr's circles, when considering different types of stress.

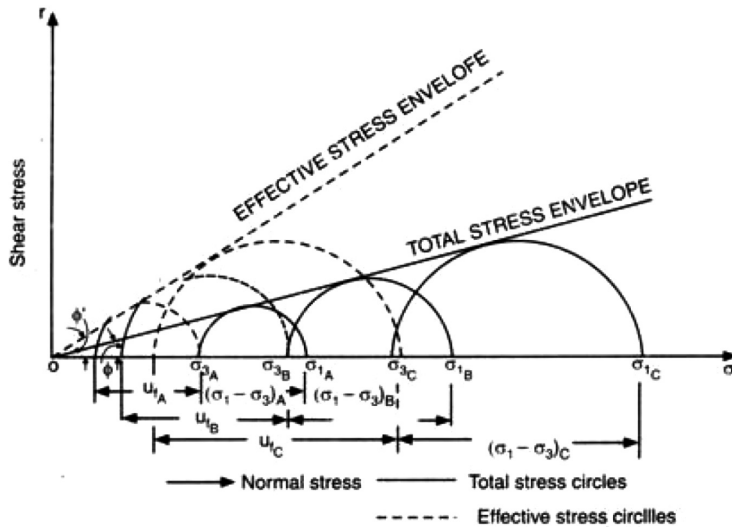


Fig. 1. Mohr's circles obtained for various types of tests in the triaxial stress apparatus for the cohesionless soil

3. The application of bender elements in the chamber of the triaxial stress apparatus

The study of dynamic stiffness or wave propagation in soil by bender elements has been in use since the 1970s. This method is carried out due to its ease of execution and accurate results for small deformations in the soil. Bender elements are made of piezoelectric ceramic material and are used to measure the propagation of the longitudinal wave and the transverse (shear) wave of a soil sample under laboratory conditions. This test involves inserting two piezoelectric elements, i.e. transmitter and receiver, into the soil and applying tension of the excitation wave in transmitter and measurement of wave propagation by the receiver. Piezoelectric bender elements are shown in Fig. 2.

The methodology for bender element tests is based on several simplifying assumptions that underlie all laboratory testing methods of wave propagation in porous medium [6]:

- ▶ the deformation induced in the soil by the transmitter is very small; therefore, the response to dynamic excitation of soil is in the elastic range;
- ▶ the wave induced by the transmitter in the soil sample is a shear wave – this means that only the transverse wave travels at shear wave velocity and the course of the shear wave is equal to the distance between the transmitter and receiver;
- ▶ the soil sample is an infinite body in a given configuration, i.e. all the reflected waves in the sample arrive later than the wave coming directly from the transmitter; the soil sample is treated as a homogeneous and isotropic medium.

Fig. 3a shows the bender elements mounted to the soil sample and the set located on the base of the triaxial stress apparatus; Fig. 3b shows the polycarbonate chamber of the triaxial stress apparatus and instrumentation during the test. The pore pressure gauge is visible in the front.

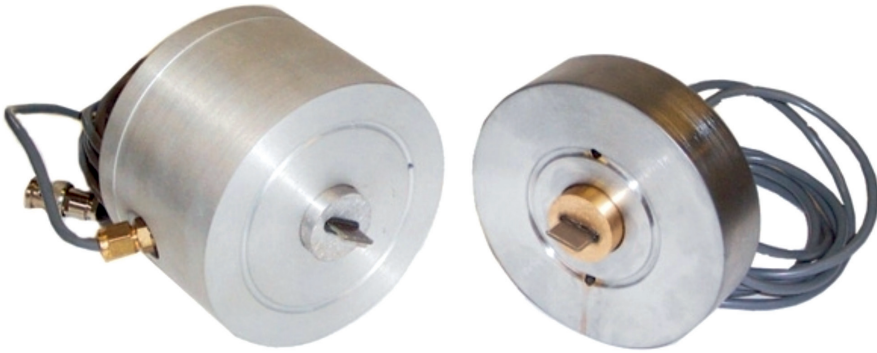


Fig. 2. Cylinders with visible piezoelectric elements used to study wave propagation under laboratory conditions in triaxial stress apparatus

a)



b)



Fig. 3. Bender elements, mounted on the base of the apparatus (a) and located directly in the polycarbonate chamber during triaxial stress testing (b), used for the testing of wave propagation under laboratory conditions

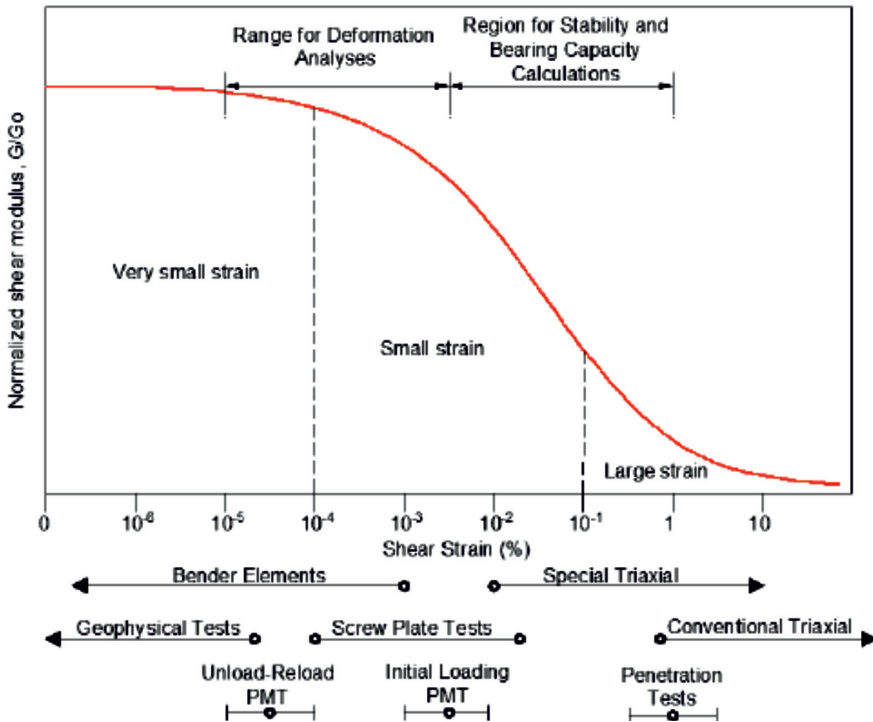


Fig. 4. The ranges of the Kirchhoff modulus obtained using different testing methods [7]

Fig. 4 shows dynamic Kirchhoff module range obtained with the application of various laboratory test methods. Bender elements allow one to obtain reliable results in the range of deformations less than 0.001%; therefore, the method is particularly appropriate for small elastic deformation of soil. In Fig. 4, laboratory methods are supplemented by applying other methods for the field investigation of dynamic soil parameters. These types of tests take place in perspective investment areas or areas of seismic or paraseismic wave action [3–5].

As far as the propagation of the transverse wave is concerned, a *peak to peak* method is applied in which running times of vibration displacements are obtained from the excitation waveforms and the waveform registered at the receiver. Assuming that the medium is an elastic body, one may use the basic relationship between the velocity of propagation of shear wave and shear module G as:

$$G = \rho V_s^2 \quad (1)$$

where:

- ρ – soil density [kg/m^3],
- V_s – shear wave velocity [m/s].

Fig. 5 shows what the waveforms induced in the source and recorded by the receiver look like. The *peak to peak* method allows you to find the duration of the waveform and the known height of the sample allows us to obtain the value of velocity of the propagation of transverse wave V_s .

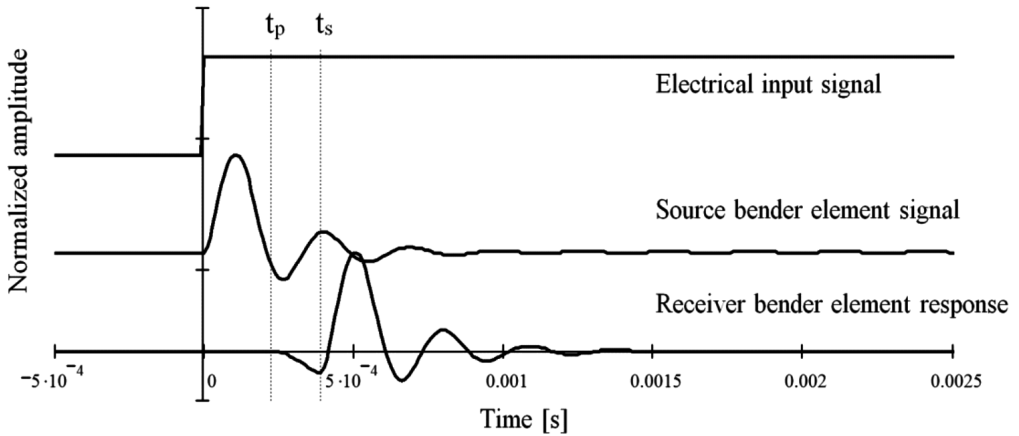


Fig. 5. Example of time history of wave propagation registered during bender element test

4. Results of the laboratory tests

Under laboratory conditions, a cohesive soil sample obtained *in-situ* from the former brickyard in Zesławice, near Nowa Huta was analysed with triaxial stress apparatus using bender elements. The soil bulk density was $\rho = 2300 \text{ kg/m}^3$, and the average water content was $w_n = 15.5\%$. The sample was subjected to a consolidation process in the triaxial stress apparatus with different paths of consolidating isotropic stress values in the range of $[0, 300] \text{ kPa}$. The studies were carried out at different soil consolidation times. During the tests, neither drainage water from the sample nor pore water pressure measurement was possible.

There were three phases of action that could be distinguished as follows:

Phase 1 – type UU conditions: during this phase, the soil underwent a regular isotropic consolidation process from 0 to 150 kPa. Over a short period of time, tension increased with an increment of $\delta = 25 \text{ kPa}$. Simultaneously, shear wave propagation V_s and Kirchhoff modulus G were determined. After reaching a consolidation stress level equal to 150 kPa, the soil was left for 96 hours to consolidate.

Phase 2 – it was assumed that CU (CIU) conditions were present. Therefore, it made further study of shear wave propagation V_s and Kirchhoff modulus G with value of consolidation stresses increasing by $\delta = 50 \text{ kPa}$ up to 300 kPa. Again, the soil was allowed to fully consolidate, this time for another 48 hours.

Phase 3 – unloading phase, during this phase, the rate of the over-consolidation ratio (OCR) changes, isotropic stress consolidation was reduced to 150 kPa. Thus, the OCR changed from 1 to 2.

Fig. 6 presents the actual time history of wave propagation. It is obtained by the propagation in the soil sinusoidal wave with a frequency of 1 kHz at voltage of 5 V. The soil was consolidated with the stress of 25 kPa. The results obtained during the experiment are shown in Table 1.

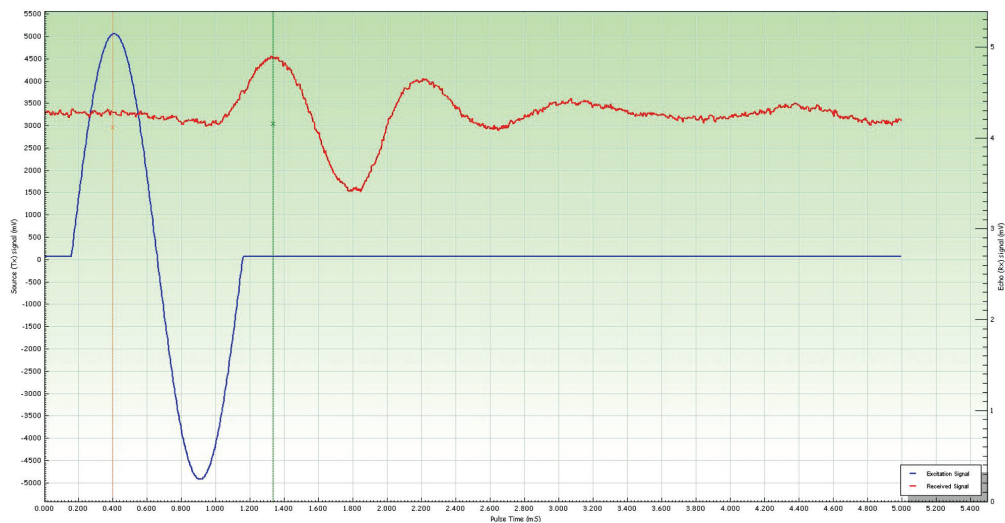


Fig. 6. Actual time history of propagation of transversal waves received during the measurements of the soil with the isotropic consolidation of 25 kPa

Table 1. The velocity of transversal waves and shear module G obtained in laboratory tests of soil

Time of consolidation [hrs.]	Consolidation stress [kPa]	Vs [m/s]	OCR [-]	G [MPa]
0	0	80	1	14.7
1	25	100	1	23.0
1	50	120	1	33.1
1	75	140	1	45.1
1	100	152	1	53.1
1	125	170	1	66.5
1	150	185	1	78.8
96	150	220	1	111.3
96	200	240	1	132.5
96	250	250	1	143.8
96	300	255	1	149.6
144	300	270	1	167.7
144	250	255	1.2	149.6
144	150	245	2	138.1

Fig. 7 presents a graph of modulus G as a function of the consolidation stress in phase 1, i.e. under normal consolidation. The increase of the consolidation stress follows a significant

rise of the dynamic Kirchhoff modulus G . However, this increase is non-linear. With a six-fold increase of consolidating stresses (from 25 kPa to 150 kPa), modulus G increased by a factor of approximately 3.5.

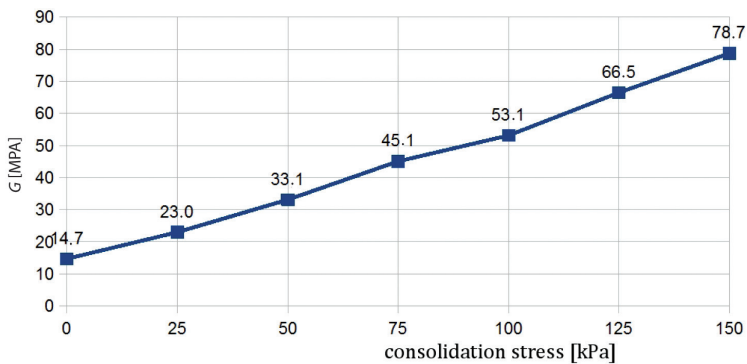


Fig. 7. Modification of the dynamic Kirchhoff modulus during normal soil consolidation (UU)

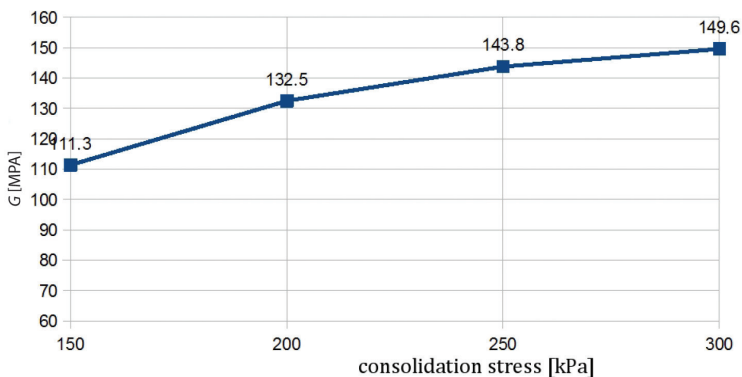


Fig. 8. Modification of the dynamic Kirchhoff modulus during normal soil consolidation (CU)

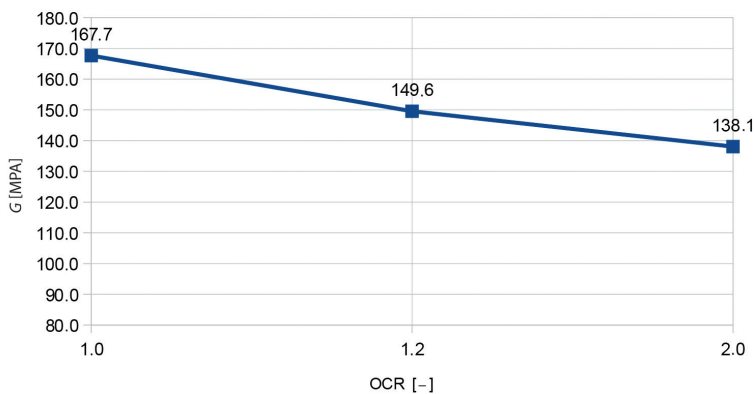


Fig. 9. Modification of the dynamic Kirchhoff modulus of over-consolidated soil during the unloading phase

Fig. 8 presents the behaviour of the Kirchhoff modulus after 96 hours of isotropic soil consolidation under 150 kPa of stress. In the remaining steps, the consolidation stress increased and both the velocity of the transverse wave and the dynamic modulus G were measured until the level of the stress reached 300 kPa. In this phase of the experiment, the consolidation stress increased by a factor of two, while the shear modulus G only increased by about 35%. A clear change that is non-linear is visible from the figure. Fig. 9 shows the change in the dynamic modulus G during the unloading phase when the soil was over-consolidated with a stress level of 300 kPa. OCR changed twice, while the shear modulus was reduced by approximately 18 percent. Fig. 10 shows the results obtained under different consolidation conditions for a stress level of 150 kPa. One may notice from the figure that the history of the load affects the dynamic Kirchhoff modulus. It may vary, according to the values obtained in this study, it even nearly doubles. This is particularly important when dealing with shallow layers of soil. In such situations, the process of modelling dynamic behaviour results from, for example, the interaction between a vehicle and the road, the substrate becomes very complex.

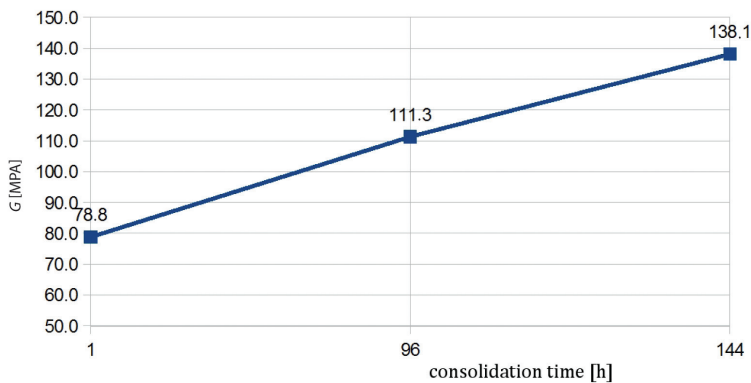


Fig. 10. Modification of the dynamic Kirchhoff modulus for soil consolidated with a stress level of 150 kPa

5. Analysing the data using artificial neural networks

Artificial neural networks (ANNs) were applied for the analysis of experimental results. During the study, different networks have been tested, that are learned on the data by the method of error backpropagation [8, 9]. The main objective of the application of this tool was to obtain the possibility of complete fit of the learning outcomes of the research results. Unfortunately, this objective was not met using the methods of convergence of results using several different gradient methods. Both, the method of Polak-Ribière with algorithm of conjugate gradient and quasi-Newton BFGS method, which requires storage of Hessian matrix [10] did not give proper convergence. Briefly, in both cases, the solution got stuck in a local minimum of error despite the use of different variants of the network topology

and number of neurons. The best method proved to be the resilient backpropagation (rpop) method [11] as it managed to obtain an expected convergence (Fig. 11). The data used for analysis is shown in Table 1.

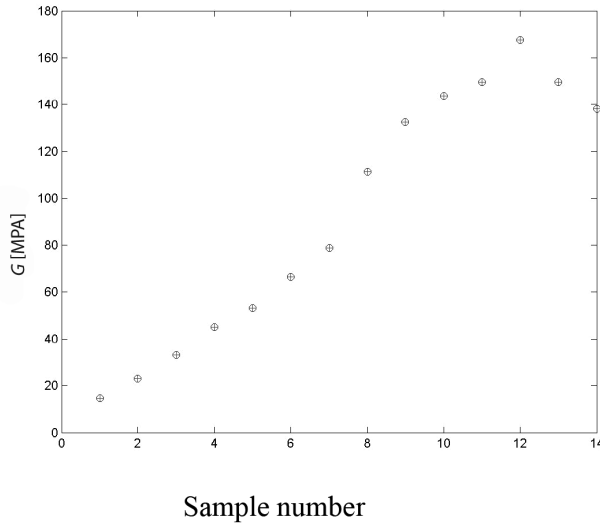


Fig. 11. Comparison of the results of network training (rpop) with the experimental data ('o' experimental results, '+' ANN results)

There are three parameters which are inputs to the network: the time of consolidation; the level of consolidation; the OCR ratio. The output data is the result describing the propagation velocity of shear wave V_s and the dynamic Kirchhoff modulus G . Both values are linked; therefore, the network also has the ability to assess the correlation between them according to formula (1). The network consisted of two layers of hidden neurons. In the present case, namely 61 and 31 neurons with arc-tangent activation function were applied.

6. Tests and ANN simulations results

Subsequently, ANN is applied in order to simulate the behaviour of the soil under different load conditions and variable coefficients of OCR. Table 2 shows the results obtained for the simulations of the cohesive soil behaviour under isotropic stress consolidation of 150 kPa. The results of further simulations are also shown in a graph of shear modulus as a function of the OCR coefficient. Fig. 12 presents a change in the dynamic modulus G during the unloading phase in cases where the soil is over-consolidated. For stress levels of 150 kPa, when the OCR coefficient increases, the dynamic Kirchhoff module at first increases and then decreases. The difference is minimal.

Table 2. SSN test results for soil consolidated stress of 150 kPa and various parameters of OCR

Time of consolidation [hrs.]	Consolidation stress [kPa]	Vs [m/s]	OCR [-]	G [MPa]
144	150	247.3	1.0	140.8
144	150	247.9	1.2	141.7
144	150	249.9	1.7	143.1
144	150	246.4	1.9	139.8
144	150	245.0	2.0*	138.1

* refers to outputs obtained from measurements and reproduced by ANN (Fig. 11)

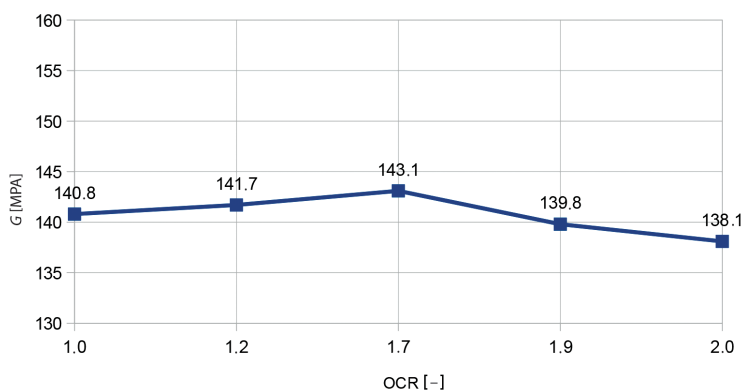


Fig. 12. Modification of the Kirchhoff dynamic modulus for soil consolidated stress of 150 kPa and various OCR

Table 3. The results of SSN for soil consolidated stress of 250 kPa and various OCR

Time of consolidation [hrs.]	Consolidation stress [kPa]	Vs [m/s]	OCR [-]	G [MPa]
144	250	256.3	1.0	151.2
144	250	255.0	1.2*	149.6
144	250	244.2	1.7	136.5
144	250	243.0	1.9	135.0

* refers to outputs obtained from measurements and reproduced by ANN (Fig. 11)

Table 3 presents the results obtained for the stress consolidation of 250 kPa. Fig. 13 exhibits a change in the dynamic modulus G during the unloading phase, in cases where the soil is over-consolidated. For stress levels of 250 kPa when the OCR coefficient increases, Kirchhoff modulus G decreases significantly. The difference of Kirchhoff modulus G in this range of OCR is about 12% in comparison to the initial value.

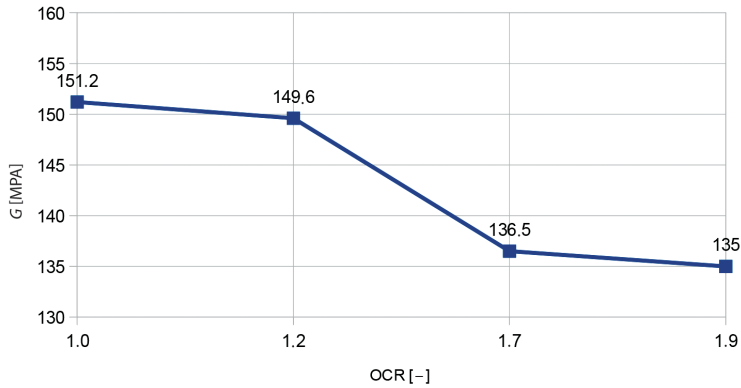


Fig. 13. Modification of Kirchhoff dynamic modulus for soil consolidated stress of 250 kPa and various OCR

Table 4 shows the results obtained for the consolidation stress at 180 kPa. Such stress is not taken into account in training samples; therefore, the results are entirely dependent on the quality of the generalisation of the neural network.

Table 4. The results of ANN generalisation for soil consolidated stress of 180 kPa and various OCR ratios

Time of consolidation [hrs.]	Consolidation stress [kPa]	Vs [m/s]	OCR [-]	G [MPa]
144	180	247.7	1.0	141.3
144	180	248.3	1.2	142.0
144	180	251.5	1.5	145.9
144	180	249.2	1.7	142.6
144	180	245.9	1.9	138.3

Fig. 14 presents changes in the dynamic modulus G during the unloading phase when the soil is over-consolidated with a stress level of 180 kPa. In this case, the OCR increases, while the Kirchhoff modulus first increases and then decreases. Fluctuations are limited to a very short range. The process of the function describing the nature of the changes is similar to that which was previously shown for stress levels of 150 kPa.

Table 5 shows the behaviour of the network for completely unknown values of consolidation stress and OCR ratios. The results of ANN generalisation are very good – in this case, the neural network, despite the low amount of the training data, does not display unrealistic values of shear wave propagation velocity V_s and Kirchhoff dynamic modulus G .

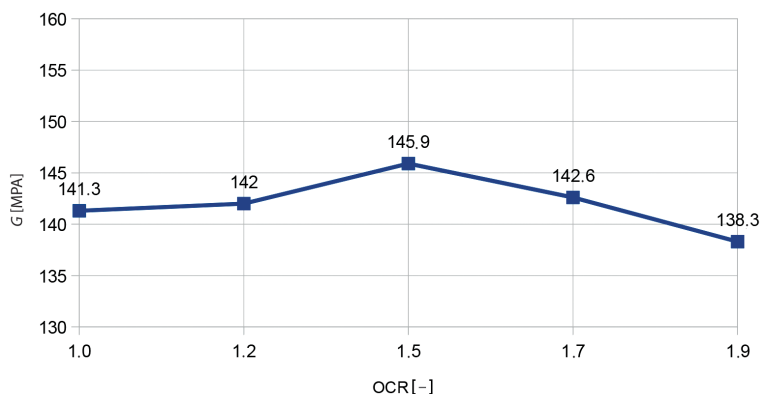


Fig. 14. Modification of Kirchhoff dynamic modulus for soil consolidated stress of 180 kPa and various OCR

Table 5. The results of ANN generalisation for the cohesive soil consolidated with different stresses and different OCR

Time of consolidation [hrs.]	Consolidation stress [kPa]	V_s [m/s]	OCR [-]	G [MPa]
144	180	251.5	1.5	145.9
144	220	245.9	1.7	138.5
144	240	243.2	1.9	135.2

7. Final remarks

This work brings together the laboratory examination of the dynamic parameters of cohesive soil together with an analysis using an artificial intelligence method. The results of the analysis are the propagation velocity of shear wave V_s and the dynamic Kirchhoff modulus G obtained during the soil tests in the triaxial stress apparatus. These results are obtained using bender elements. The artificial neural network trained on data obtained from the test was used for further analysis. The ANN is very well trained and it reproduced the output results accurately. Then the network is used to simulate other states of soil. Despite the small database of results collected from the experiment, ANN simulates appropriately dynamic soil parameters. The *in-situ* tests (i.e. SCPT, SASW, CSWS) complement and verify the dynamic parameters obtained during the laboratory tests and broaden their range in various states of stress and strain. In the future, it is planned to further study soil behaviour in terms of undrained and drained consolidation and take into account other soil parameters from the measurements (e.g. pore pressure) in the other soil types.

References

- [1] Head K.H., *Manual of Soil Testing*, Vol. 3, Effective stress test, Wiley, New York 1998.
- [2] Godlewski T., Kacprzak G., Witowski M., *Praktyczna ocena parametrów geotechnicznych podłoża do projektowania ścian szczelinowych posadowionych w ilach „plioceńskich”* Warszawy, „Budownictwo i Inżynieria Środowiska”, 4/2013, 13–19.
- [3] Kogut J., *Wyznaczanie parametrów dynamicznych podłoża gruntowego na podstawie badań doświadczalnych*, „Czasopismo Techniczne”, 1-Ś/2007, 45–53.
- [4] Kogut J., *Oszacowanie parametrów dynamicznych podłoża gruntowego*, „Czasopismo Techniczne”, 2-B/2007, 55–63.
- [5] Kogut J., *Dynamic soil profile determination with the use of a neural network*, CAMES – Computer Assisted Mechanics and Engineering Sciences, 2007, (14) 2, 209–217.
- [6] Jovičić V., *The measurement and interpretation of small strain stiffness of soils*, PhD thesis, The City University, London 1997.
- [7] Gryczmański M., *Wprowadzenie do opisu sprężysto-plastycznych modeli gruntu*, IPPT PAN, Warszawa 1995.
- [8] Osowski St., *Sieci neuronowe w ujęciu algorytmicznym*, WNT, Warszawa 1996.
- [9] Masters T., *Sieci neuronowe w praktyce. Programowanie w C++*, WNT, Warszawa 1996.
- [10] Hertz J., Krogh A., Palmer R., *Wstęp do obliczeń neuronowych*, WNT, Warszawa 1993.
- [11] Demuth H., Beale M., *Neural Network Toolbox*, “The MathWorks”, Inc., Natick, Ma, 2000.

Maria Kośmiejka (maria.kosmiejka@put.poznan.pl)

Jerzy Pasławski (jerzy.paslowski@put.poznan.pl)

Institute of Structural Engineering, Faculty of Civil and Environmental Engineering,
Poznan University of Technology

A FLEXIBLE APPROACH TO THE EVALUATION OF THE COST EFFECTIVENESS OF INVESTMENT PROJECTS

OCENA EFEKTYWNOŚCI FINANSOWEJ PRZEDSIĘWZIĘĆ INWESTYCYJNYCH. PODEJŚCIE ELASTYCZNE

Abstract

This article presents basic ideas for flexible design in construction investments through the presentation of methods used for assessing the financial effectiveness of investments. The **classification** of these methods based on two main factors, time and risk, is shown. The authors propose an algorithm for the analysis of the economic efficiency of projects implemented in a flexible manner.

Keywords: economic efficiency, flexibility, risk

Streszczenie

W artykule przedstawiono podstawowe idee elastycznego projektowania w budownictwie. Omówiono metody oceny efektywności finansowej przedsięwzięć inwestycyjnych. Pokazano podział tych metod ze względu na dwa najważniejsze czynniki: czas i ryzyko. Zaproponowano algorytm postępowania podczas analiz efektywności ekonomicznej przedsięwzięć realizowanych w sposób elastyczny.

Słowa kluczowe: efektywność ekonomiczna, elastyczność, ryzyko

1. Introduction

Today's accelerating rhythm of life causes pervasive changes in the world around us, including demography, migration, conflicts, complex interaction of systems. The consequence of such phenomena of rapid technological and material progress and globalisation is the disorder of traditional market structures. Future events are becoming more difficult to predict, even in the case of the fairly near future.

Therefore, strategies taken by companies should be flexible so that they will be able to follow the changes in the environment and allow taking advantage of the appearing opportunities in an uncertain environment.

The traditional approach to project planning is becoming obsolete due to it being based on assumptions of analytical thinking and the evaluation of the probability of an event – this is insufficient when the future becomes more and more unpredictable.

Therefore, this justifies the introduction of a new approach based on flexibility understood as the possibility (but not a necessity) to introduce some options assuming change of the configuration parameters of the system or its components over time [7].

The purpose of research is demonstrating the profitability of the application a flexibilities in the engineering planning on the example of construction investments. Moreover, analysis of a few differing cases is supposed to enable the development of a procedure which allows the assessment of the possibilities of applying various flexible options. Apart from the typical economic criterion (taking into account e.g. NPV, IRR) also should be possible to taking into account conditioning associated with different criteria (e.g. technical specifications, quality and ecology).

The purpose of this article is to review the specifics of the situation in the analysis and provide an evaluation of the possibility of introducing a flexible approach when planning infrastructure investments and to propose an algorithm or set of procedures of conduct in this field based on the method of scenarios. The following scheme (Fig. 1) shows a sequence of operations for introducing the flexibility of an investment. To begin with, we are checking whether in the project, the flexibility can be led, we are assessing the risk, tactics and appropriate strategies in this way in order to identify elements that will enable the elimination of risk. Generating three scenarios, different from each other in sizes of individual essential parameters is next action (e.g. traffic loading, the height of users or the fall in this parameter). Next, after performing appropriate simulations, we receive the best plan of action for the given investment.

Classical methods for the financial evaluation of economic efficiency, which are based on updated cash flows, have become inadequate for the proper assessment of projects, which are based on flexibility, understood as the ability to modify investments during the entire life. These methods are also not able to correctly assess opportunities that may open up in the future, before undertaking a result of taking a particular action. This is happening this way, because the traditional methods require that during planning of the investment project and assuming its course companies predict the future (which in many cases impossible), and on that basis irreversible decisions about the future shape of the project are made [3] In addition,

during the definition of an investment project and the calculation of its effectiveness, future changes and modifications are not presumed which may happened during the realisation [1].

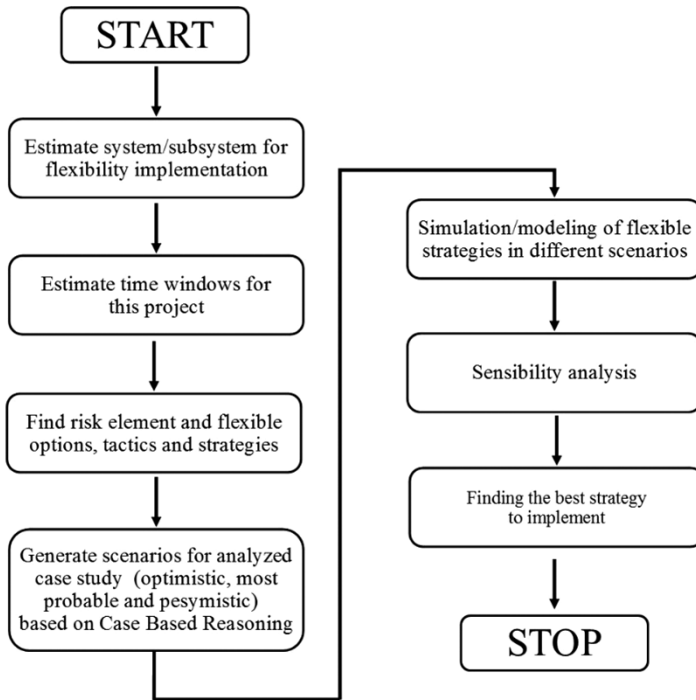


Fig. 1. Algorithm/procedures for introducing a flexible approach when planning infrastructure investments

Some reviews of the literature say that predicting the future is burdened with considerable uncertainty, in which case, the method of updated cash flows that are currently considered the best methods for assessing economic efficiency are only secondary tools, this is because they do not allow exploited opportunities or protect against the risk of following strategy. In fact, during the analysis of the traditionally used methods of assessing the effectiveness of investment, it is hard not to notice that these methods ignore the possibility of introducing flexibility in the project and are not able to take into account or properly assess options that can follow when determining the appropriate strategy.

2. Traditional methods of assessing the effectiveness of investments

In practice, there are many traditional techniques for calculating the financial viability of a project, starting from the most simple and intuitive and ending with some very complex methods. In the nineteen-thirties, I. Fisher developed the basis for the efficiency assessment

methods used today [6]; thus, today they are called 'traditional' as over the decades, they have gained widespread acceptance and have entered into business practice.

Unquestionably, the most important methods of assessing financial performance are widely described in literature – these two methods are based on the updated time value of money, they include the method of net present value (NPV) and the internal rate of return (IRR); however, simple, static methods are also widely used.

In an article which was reviewed by the methods for assessing the economic efficiency can be differentiated on the basis of two main parameters which must be taken into account when calculating the profitability of projects, namely, time and risk. These two factors are key because when making investment decisions, there is firstly a need to prepare the bill of financial benefits – these must take into account the change in the time value of money, and secondly, to expect that the assumed effects may occur but not necessarily.

2.1. Time factor approach

The first criterion for the classification methods is the time factor and more specifically, changes in the value of money over time. Thus, these methods can be divided into two groups – 'simple' (static) which do not include changes in the value of money and 'discount' (dynamic) [12], which take this factor into account.

2.1.1. Statistical methods

Statistical methods are a group of intuitive, simple methods used to get an overview about the economical investment. They are used mainly in the early stages of the investment process and their application enables their simplicity and clarity [1].

The first statistical method, which is fairly common in investment processes for reconstructions and modernisations, is the bill of comparative costs. The result presents an opportunity to choose the best investment option from all the variants which are characterised by the same advantages but differ with regard to the total financial expenditure incurred by the investor. Under these conditions, the decision criterion of optimisation is to minimise the cost [11].

The second method, commonly used as a comparative account of profitability, though there are the many variations and names, is the so-called accounting rate of return. This is expressed as a percentage and it is the ratio of the accounting profit from investments and involved capital [8] – the investment is deemed acceptable if it reaches the minimum threshold set by the investor.

The main advantage of this method is its simplicity and ease of use, since it is based on data included in the financial statements. Unfortunately, this is also its drawback as the actual cash flows are used. Indeed, basing the decision on book values, e.g. the net profit, should be considered as one of the major errors of investment planning [5].

The third static method most commonly used in practice is the method of payback period. This is based on the time period after which the proceeds of the investment project equal the expenses incurred for this project, of course, the shorter the time, the better. The

most important advantage of this method is the fact that the result is given in years – this is readable and understandable for the potential investor. However, the drawback is the lack of information about the profitability of the project and the difficulty of applying method because the expenditures are incurred also during the investment operation [10].

2.1.2. Dynamic methods

The basic feature of these methods is the inclusion of the time factor, specifically, changes in the value of money over time and the timing of receipts and payments related to the preparation, implementation and operation of investment [3].

The literature highlights the two most important dynamic methods, known collectively as methods of discounted cash flow DCF.

2.1.2.1. The method of net present value NPV

This method is based on the ratio of expense flows to the present value of the future investment income which is defined as the difference between the sum of the discounted cash flow achieved during the life of the investment and the amount discounted for the same year of investment for the implementation of the investment project [10].

The basic criterion for the decision is a positive NPV account value. This is a very flexible economic instrument because its formula may be adjusted and converted according to the specifications of a particular investment environment [1].

2.1.2.2. Internal rate of return IRR

During calculations of the net present value, it is necessary to determine the discount rate assumed by the investor. On the other hand, when the investor is interested in ensuring at which discount rate the investment outlays in a given period returns, he can use a tool which is the method of Internal Rate of Return.

To put it simply it can be said that the internal rate of return is the discount rate at which the NPV of the investment project is equal to zero. Therefore, the IRR is equivalent to the discount rate at which, during the analysis of the updated value of financial income is equal to the discounted value of the investment. In other words, the capital outlay pay for itself.

2.2. Recognition of risk factor

As previously mentioned, any investment involves risk; therefore, risk should be taken into account during the analysis of the economic efficiency of each project.

2.2.1. Direct risk factor recognition

The method of equivalent of certainty CE states that the expected cash flows are modified to reflect the risks associated with [9]. Thus, the flows that have a greater risk are reduced – this is due to the need to recognise a ‘non-risk equivalent’ [9] of risky funds invested in the project.



During calculations, classical equation NPV is modified in risky cash flows and they are replaced with equivalents.

This method is extremely advantageous when the cash flows of the project for different periods have different degrees of risk – this is a common phenomenon, because the cash flow is subjected to a greater risk the further the project progresses.

The second method of evaluating the economic efficiency, which in its calculation takes into account the risk method is Risk Adjusted Rate RADR. Like the previous method, this also introduces a risk factor for the calculation of NPV.

The basic principle of this method is based on the assumption that investment projects burdened with bigger risk should have a higher discount rate than projects with less risk. What means that with an increase in the risk the discount rate is increasing as well as the investor rate of return on a risky investment.

2.2.2. Indirectly included risk

The methods of directly taking into account the risk analysis are based on calculations of NPV ratio. By contrast, the literature describes methods for the subject which are used in practice and indirectly take risk into account. The results of these methods include the measured standard deviation risk *and* information about possible changes in factors affecting the NPV [2].

Sensitivity analysis is an analysis in which on the understanding that changes in different variables (e.g. price, expenses, cash flow) included in the calculations show the profitability of the investment project. The basic premise of this method is characterised by the fact that the future is so unpredictable that the actual values of the variables will be at the turn of time deflecting from the goals. As a result of this, it can be determined which variables have a real impact on the economic value of the investment project – this eliminates variables that are characterised by mean volatility but have a negligible impact on the final profitability of the investment.

Another discussed method is scenario analysis – this takes into account the effect of several variables at once on the value of the project during the calculations. Usually, three scenarios that contain different combinations of parameters affecting the value of the project are factored in (optimistic, pessimistic, and most likely) during the calculations.

The third type of these methods are simulation methods – these are a group which include the Monte Carlo method, which takes into account multiple combination design parameters that have influence on the final value of the investment. The Monte Carlo method is the most common method within this group. This method is subject to a simulation formula of NPV or IRR in the following manner [4]: a) the selection of the parameters considered at risk; b) determine the probability of individual variables and the relationships between them; c) random selection of variables; d) the calculation of the net cash flows for each year and then the NPV of the project; e) repeat calculations 'c)' and 'd)' several hundred times; f) the result is obtained in the form of the probability distribution of NPV.

The final method among the indirect risk-based methods is decision tree analysis DTA. This method graphically shows possible investment decisions that can be taken at different times during the project. At the same time, it shows the relationship between decisions and give each of them amount of probability. Each variant that is entered onto decision tree is multiplied by the gain from the project and shows the distribution of benefits relating to individual decisions.

3. Conclusions

The implementation of investment projects with the rapid pace of changes in the conditions of the project is extremely difficult. Hence, it even becomes indispensable creation and implementation of investments in idea of the flexibility. Flexible approach in this situation is characterized by the formation of the initial action plan, that adapts to changing market conditions, evolving course of the project in such a way as to limit expansion, deferment during implementation, change parameters or in extreme cases withdraw from the investment.

In current assessments of the costs of investment through the life cycle of a project (starting from the design stage through the construction stage and finishing with exploitation) was assuming at most a changeability of rate of returns on investment. However, the accepted period for analyses amounts to around 30 years, and consequently arbitrarily attempting to assess the level of costs can be a process that is riddled with errors. An alternative solution could be to include in calculation cost the risk factors what could have an impact on cost values in every stage of investment. The authors of the present article, however, propose introducing flexibility i.e. the consideration of different scenarios which anticipate changes in the configuration of parameters of the object in the cycle of its life. Next proposal is using a multi-criteria approach, which enables calculating quantitative and qualitative criteria influencing the size of life cycle costs at final selecting variant.

Traditional methods for assessing economic efficiency capture investment flows in a very static manner. Even if a few forecasts of development of the project are considered, there are still assumed predetermined values of financial flows in them. Therefore, they cannot be used in the analysis of investments using flexible tools, as when having to deal with different elastic options, the size of future cash flows is closely dependent upon what decisions that will be taken in the future.

Due to the variety and various features of methods discussed above of investment analysis using the tool of flexibility should not be limited to just one, instead, a few should be used as this would provide a full picture of the situation of the project under assessment. In addition, at each stage of the project, from analysis through to implementation and operation, these methods should be used to protect projects from the risk and to enable the investor to seize opportunities that arise in an uncertain future.

In examinations of authors of the article are basing on the scenario analysis expanded on simulation method. The assessment of these methods are made by joining the discounted cash flows NPV and IRR.

References

- [1] Dziworska K., *Decyzje inwestycyjne przedsiębiorstw*, Uniwersytet Gdański, Gdańsk 2000.
- [2] Pluta W., *Budżetowanie kapitałów*, Polskie Wydawnictwo Ekonomiczne, Warszawa 2000.
- [3] Ziarkowski R., *Opcje rzeczowe oraz ich zastosowanie w formułowaniu i ocenie projektów inwestycyjnych*, PRACE NAUKOWE Akademii Ekonomicznej im. Karola Adamieckiego w Katowicach, Katowice 2004.
- [4] Copland T.E, Keenan P.T., *How Much is Flexibility Worth?*, The McKinsey Quarterly No. 2, 1998, 38–49.
- [5] Dimkoff G., *Avoid Major Mistakes In Capital Budgeting*, Facilities Design & Mangement, February 1994.
- [6] Fisher I., *The Theory of Interest*, Macmillan, New York 1930.
- [7] Gajzler M, Kośmiejka M, Pasławski J., *Elastic designing the road infrastructure in example*, Czasopismo Techniczne, 2-B/2014.
- [8] Lumby S., *Investment Appraisal and Financing Decision*, Chapman&Hall, London 1991.
- [9] Malinowski A., Tarapata Z., *Ocena projektów gospodarczych*, Defin, Warszawa 2001.
- [10] Marcinek K., *Finansowa ocena przedsięwzięć inwestycyjnych przedsiębiorstw*, Akademia Ekonomiczna, Katowice 2001.
- [11] Czechowski L., Dziworska K., Gostrzowska-Drzewicka T., Górczyńska A., Ostrowska E., *Projekty inwestycyjne*, ODDK, Gdańsk 1999.
- [12] Nowak E., Pielichaty E., Poszwa M., *Rachunek opłacalności inwestowania*, PWN, Warszawa 1999.

Dorota Olszewska (dolszewska@igf.edu.pl)
Institute of Geophysics, Polish Academy of Sciences, Warsaw

THE ACCELERATION RESPONSE SPECTRA FOR LEGNICA-GLOGOW COPPER DISTRICT

PRZYSPIESZENIOWE SPEKTRA ODPOWIEDZI DLA REJONU LEGNICKO-GŁOGOWSKIEGO OKRĘGU MIEDZIOWEGO

Abstract

This paper presents average normalised acceleration response spectra calculated for mining induced seismic events which were recorded by twenty-one stations located in the area of Legnica-Glogow Copper District (LGCD). In this paper, 5246 ground motion signals with peak ground acceleration (PGA) over 0.03 m/s^2 were analysed. The ground motions were caused by 1886 mining events with M_L greater than 2 (energy $> 10^5 \text{ J}$), which occurred from 2004 to 2015. The design response spectra were estimated based on average normalised acceleration response spectra. Further analysis of results shows that the shape and amplitude of response spectra are strongly dependent on the event magnitude, the epicentral distance and the location of the stations. The obtained response spectra could be used for computing seismic forces which have impact on buildings response to ground motions caused by mining events in LGCD.

Keywords: Response spectra, induced seismicity, local amplification

Streszczenie

W pracy wyznaczono średnie znormalizowane przyspieszeniowe spektra odpowiedzi na podstawie zapisów drgań wstrząsów górniczych, zarejestrowanych przez 21 stanowisk akcelerometrycznych znajdujących się, na terenie Legnicko Głogowskiego Okręgu Miedziowego (LGOM). Do analizy wykorzystano 5246 rejestracje drgań gruntu o wartościach szczytowych powyżej 0.03 m/s^2 , wywołane 1886 wstrząsami górniczymi, o M_L powyżej 2 (energia od 10^5 J), które miały miejsce od 2004 do 2015 roku. Na podstawie wyznaczonych znormalizowanych przyspieszeniowych spektrów odpowiedzi wyznaczono wzorcowe spektrum odpowiedzi dla tego rejonu. Pokazano także, że kształt i amplituda spektrów odpowiedzi zależy od wielkości zjawiska, odległości epicentralnej oraz od miejsca. Otrzymane wzorcowe spektrum odpowiedzi może być wykorzystywane do obliczania sił sejsmicznych oddziałujących na budowle w wyniku drgań podłoża wywołanych wstrząsami górniczymi w tym rejonie.

Słowa kluczowe: Spektra odpowiedzi, sejsmiczność indukowana, lokalna amplifikacja

1. Introduction

Earthquakes and anthropogenic-induced seismic events (e.g. mining events, seismicity connected with oil and gas exploitation, water reservoirs impoundment) are sources of ground motions, which could have considerable impacts on the Earth's surface, particularly on buildings. The infrastructures affected by these strong forces may be damaged or even destroyed. The areas which are subjected to the influence of seismic events are monitored in order to assess the influence of ground motions on the structural buildings properties. The results of those measurements are interpreted and ground motion parameters are estimated. Consequently, special norms for observing, forecasting and modelling seismic impact in regions where tectonic earthquakes occur is needed. Therefore, seismic hazard studies are one of the fundamental methods of seismic risk analysis providing seismic hazard maps, showing e.g. the 10% PGA exceedance probability in 50 years at particular sites. (e.g. <http://www.share-eu.org> [Europe], <https://earthquake.usgs.gov/hazards/hazmaps/> [USA] and the references therein). Engineers use these maps and associated tools for earthquake resistant design of buildings and other infrastructures. Special rules and regulations in this field are covered by, among others, European Standard 'Eurocode 8: Design of structures for earthquake resistance (Part1)'.

Induced seismicity areas are characterised with lower intensity shocks than natural ones, however, the magnitudes of such anthropogenic events are often large enough ($M > 5.0$ and up to 7.9, [4, p. 171–185] and references therein) to provoke hazard and cause local or regional devastation [e.g. 5; 25, p. 4–19]. The issues related to induced seismicity are known and remain valid [7; 17, p. 385–396 and the references therein]; therefore, a wide range of specialised analyses [e.g. 24, p. 1766–782; 22, p. 1011–1026; 12, p. 2592–2608; 13, p. 7085–7101; 2, p. 158–173; 11, p. 5–15; 28, p. 1517–1537] have been conducted on such areas, in particular, Probabilistic Seismic Hazard Analysis (PSHA) [e.g. 30, p. 105–121; 15, p. 28–37]. Recently, the impact of induced seismicity has been a source of rising scientific and public concern, taking into account the growing needs to develop new methods for the exploration and exploitation of georesources, e.g. Shale Gas. These activities are often carried out on so far aseismic, yet populated areas. As expected, the infrastructure of aseismic areas is not adequately prepared for even relatively weak seismic effects. Because these areas are not affected by tectonic earthquakes, the expected PGA values, based on seismic hazard maps, are too low to have an impact on the infrastructure. This situation changes significantly if exploration of resources starts on the close vicinity of such areas, e.g. in the USA [8, p. 618–626]. Therefore, it is necessary to develop appropriate analyses for such areas in order to be able to assess the effects of seismic impact and to provide adequate resistance measures against them. Thus, the recent US Seismic Hazard Maps has been updated to include areas exposed to induced seismicity [23, p. 772–783]. The design response spectra proposed by the European Seismic Code, Eurocode 8, are inadequate for low intensity induced seismicity; however, due to its apparent impact, the spectra should be adapted to take these conditions into account [1; 33, p. 81–90]. This is especially true when the suitable database of ground motion catalogue is available.

The growing importance of seismic-induced issues is also evident by the development of research infrastructures (RI) for the purpose of addressing them. An example of such RI is the Thematic Core Service – Anthropogenic Hazard (TCS-AH) is being developed by fourteen European research institutions in the framework of the work package WP14 of the EPOS IP infrastructural project (H2020-EU.1.4.1.1. in the years 2016–2019), and will be integrated with other thematic core services by EPOS Integrated Core Services (ICS). The main TCS-AH service is the IS-EPOS platform which contains special data sets related to induced seismicity – episodes, dedicated applications, and a rich document repository (tcs.ah-epos.eu). The platform is open to accommodate data integrated with other research projects and it is continuously being updated and improved through both the enhancement of current features and the implementation of new features.

In terms of buildings resilience, the amplitudes of the ground motions are less important than the oscillations caused by the abovementioned events. It can be assumed that the oscillations of buildings may be approximated by the movement of the oscillator with a single degree of freedom. Therefore, it is essential to identify the distribution of the maximum amplitudes of the oscillator with known damping and natural frequencies in response to ground motions – this distribution is called “response spectra” [10, p. 1097–1125]. On the basis of the estimated response spectra, the frequency band for the expected largest influences can be assessed – this corresponds to the dominant frequencies of the ground motions. Additionally, the response spectra are closely related to the local conditions; thus, the response spectra are assessed in relation to the ground type [9] – this is because the local amplification of ground motions varies with different ground types; this has connotations for the effects of the events observed on the surface. The response spectra are used in construction to assess seismic forces acting on the structures of the building which are caused by seismic events followed by ground motions [e.g. 3].

The knowledge of parameters of potential ground motions and their possible influence on the construction of building is useful at the stage of project works. Based on previous observations of ground motions and spectral amplitudes, ground motion prediction equations can be estimated – this enables the assessment of ground motion amplitudes induced by hypothetical earthquakes [e.g. 6, p. 43–104]. The average response spectra, representing rockburst seismic loading, are also useful for these kinds of analyses as they allow the dynamic verification of existing buildings and help in the designing of new objects [26].

Legnica-Glogow Copper District (LGCD), as an area where seismicity is induced by the mining exploitation of copper ore, is one of the regions of Poland where seismicity is relatively substantial. Thus, various researches have been conducted to assess the influence of ground motions on this area and on the surrounding building infrastructures. Examples of such research are: the estimation of the ground motion prediction equations (GMPE) for peak ground acceleration [e.g 19; 14, p. 1130–1155]; peak ground velocity and spectral amplitudes [19]; Probabilistic Seismic Hazard Assessment [15, p. 28–37]. A site effect which has an important impact on the value of the peak ground motion is also examined. The area is considered to have a uniform ground type because the actual area of the mine activity is rather small and the velocity wave in the surface layer is relatively uniform [18; 21]. Nevertheless,



the analysis of the HVSR (Horizontal to Vertical Spectral Ratio) curves [20] and also the residuals of the GMPE [19; 14, p. 1130–115] indicate that the local effect depends on location. The analysis of the ground motion shows also that there are two types of events in this area [31, p. 11–23].

- ▶ Records of type I occur rather often (return period of 3–6 months) with very short durations (1–2 s) and Fourier spectra shifted to higher frequencies (about 20–40 Hz). Despite this fact, these records have high values of peak ground accelerations ($PGA = 1.5\text{--}2 \text{ m/s}^2$) characterised by their low intensity in reference to the buildings and low peak ground velocity ($PGV < 2\text{--}3 \text{ cm/s}$).
- ▶ Records of type II occur rarely (return period 1-2 years) with longer durations than type I (about 5 s or more) and with the dominant part of the Fourier spectra below 5 Hz – similar to recordings of a weak, shallow earthquake. These records are characterised by their higher values of peak ground velocity ($PGV = 6\text{--}18 \text{ cm/s}$) and their significant, unfavourable influence on building infrastructure.

Type I ground motion has high PGA which corresponds to higher dominant frequencies (about 20–40 Hz); thus, its impact on the building is negligible – this is because, the frequency bands of the natural oscillations of the buildings is up to 10 Hz [29]. Therefore, the standard procedure for processing ground motion data from that area is parametrizes registration in frequency range of up to 10 Hz. This results in PGA which could have a significant impact on buildings by eliminating the influence of higher frequencies of type I ground motions. So this is ‘standardisation’ of PGA for the engineering purposes in that area. More detailed analyses of the impact of ground motion on building infrastructure are also prepared for that area [e.g. 32, p. 1403–1416; 27, p. 442–458; 16, p. 1769–1791; 33, p. 81–90]. One of them is the calculation of the average response spectra representing seismic rockburst loading for that region [26; 19; 32, p. 1403–1416] and also estimation of the design spectra for various ground types according to Eurocode 8 [33, p. 81–90]. Nevertheless, the latest proposed design spectra are based only on eighteen registration-intensive, type II ground recordings (with lower dominant frequencies) caused by two events.

The paper proposes new response spectra for horizontal and vertical components for LGCD area; thus, a seismic load can be defined for civil engineering purposes. The main advantages of these spectra are greater accuracy and unification in the frequency domain. These were achieved by using a large amount of data (5.246 ground motion records) and by avoiding negligible high frequencies, from structural point of view, which only concerns a part of the ground motion (10 Hz low pass filtration of input data). Further studies of the obtained spectra, possibly due to the substantial amount of available data, included analysis in relation to the scale of the event, the distance between epicentre and the stations and the division of response spectra due to the nature of the spectral curve.

2. Characteristics of the LGCD mining region

In Poland, induced seismicity is mainly related to mining activities. LGCD, located in north-central part of the Lower Silesia voivodeship, is an area where seismicity induced by underground mining is relatively substantial. There are three copper mines in the area – Lubin, Polkowice-Sieroszowice and Rudna; all of these are part of KGHM Polska Miedź S.A.

Strongground motions caused by underground mining operations have a negative influence on the surface and might even damage the nearby infrastructure. Considering the importance of the building infrastructure in the area, mines and local communities conduct continuous monitoring of ground motions caused by seismic events, which provides a wide range of data for scientific research. Seismic networks belonging to the Polkowice commune and KGHM Polska Miedź S.A and seismic network LUMINEOS (LUBin Mining INduced Earthquake Observation System) belonging to the Institute of Geophysics Polish Academy of Science (IG PAS) provided the data for further analysis. All the data are stored in a seismometric database, which is owned and governed by IG PAS. All stations within the above mentioned networks have 3 component sensors measuring ground motion acceleration. Currently, about 20.000 accelerograms, registered since January 2000 by a total number of 51 stations, are stored in this database. All records have explicitly assigned parameters of events that triggered ground motions as energy or local magnitude, event coordinates, epicentral distance to stations (if event was located by seismic network).

Ground motion recordings with peak ground acceleration of at least 0.03 m/s^2 for any component, caused by events with $M_L \geq 2$ (energy $\geq 10^5 \text{ J}$), were chosen for further analysis; these recordings were restricted to those made from 2004 to the end of 2015.

Table 1. The basic parameters of measured units selected for analysis

No. of unit	Stations	Coordinates		Amount of data	Period of time	
		X2000	Y2000		Start	End
1	2	3	4	5	6	7
20	3-go Maja	5 708 549	5 574 411	458	Jan. 2004	Dec. 2015
21	Akacyjowa	5 707 965	5 574 751	317	Jan. 2004	Dec. 2015
22	Biedzychowa	5 705 205	5 576 367	572	Jan. 2004	Oct. 2015
23	Fiołkowa	5 708 265	5 573 378	150	Aug. 2005	Dec. 2015
24	Miedziana	5 708 285	5 574 628	357	Jan. 2004	Dec. 2015
25	Moskorzyn	5 712 545	5 575 201	321	Jan. 2004	Jan. 2015
26	Pieszkowice	5 705 930	5 579 069	87	Sep. 2004-wrz	Jul. 2015
27	Sosnowa	5 707 950	5 575 589	461	Jan. 2004	Aug. 2015
28	Żuków	5 712 765	5 579 667	146	May 2006	Dec. 2014
29	Guzice	5 711 184	5 576 599	334	Jan. 2004	Aug. 2014
30	Trzebcz 31	5 710 090	5 577 152	91	Jan. 2004	Jul. 2005
32	Trzebcz	5 710 160	5 577 259	275	Aug. 2005	Nov. 2014

Table 1 cont.

1	2	3	4	5	6	7
33	Guzice_n	5 711 164	5 576 590	52	Oct. 2014	Dec. 2015
42	Tarnówek	5 709 620	5 580 770	82	Apr. 2010	Jun. 2014
50	Grodowiec	5 712 811	5 581 318	170	Jan. 2004	Dec. 2015
51	Komorniki	5 710 871	5 579 539	329	Jan. 2004	Dec. 2015
80	Hotel	5 707 919	5 574 388	226	Jan. 2004	Jan. 2015
81	Spółdzielnia	5 708 289	5 574 818	275	Jan. 2004	Dec. 2015
82	Tarnówek-gmina	5 709 719	5 580 918	39	Apr. 2010	Feb. 2014
83	Skalników	5 708 859	5 574 548	350	Jan. 2004	Dec. 2015
84	Polkowice Dolne	5 708 199	5 573 438	154	Nov. 2004	Mar. 2014

Very weak events and recordings at the noise level were eliminated from the analysed data due to the aforementioned criteria. Stations located on the Żelazny Most repository embankment and Stations with less than thirty-five records were also discarded from the analysis. After the selection process, 5,246 ground motion records remained – these were recorded by twenty-one stations. Table 1 presents basic information about all chosen data: number; full name and coordinates of stations; total number of ground motion record for each station; period of registration.

The selected records are associated with 1,886 seismic events. The surface distribution of these events along with locations of measurement stations is presented in Fig. 1.

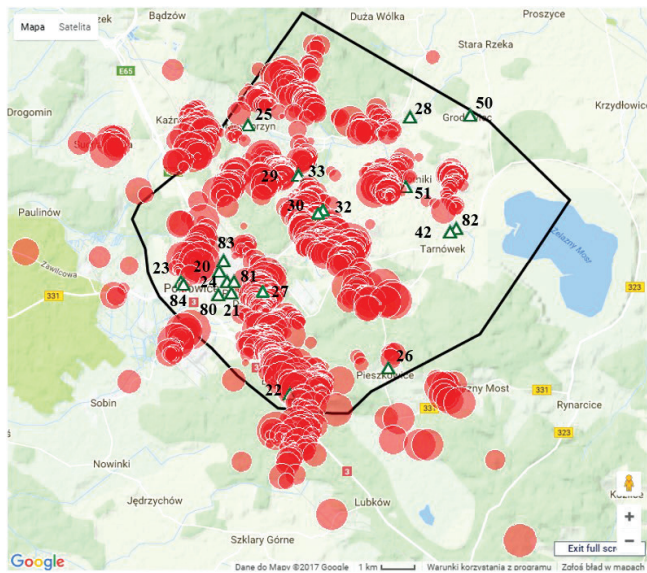


Fig. 1. Locations of stations and seismic events, Green triangles are the seismic stations and red circles are the seismic events

3. The average normalised response spectra

Oscillators with a single-degree of dynamic freedom and subjected to kinematic forces as a result of ground motions, have maximum amplitudes of oscillations related to their own known damping and natural frequencies – these relationships are called response spectra. Response spectra have a wide range of applications in regions which have notable seismicity [10, p. 1097–1125].

The movement of an oscillator with known damping, D , and natural angular frequency of oscillations, ω , forced by ground motions, can be described by the following formula:

$$\ddot{x} + 2D\omega\dot{x} + \omega^2 x = -a(t) \quad (1)$$

where:

- x – mass displacement in relation to the surface;
- D – fraction of critical damping;
- ω – angular frequency of oscillator;
- $a(t)$ – ground motion (accelerations).

The solution to this equation is Duhamel's integral:

$$x(t, \omega, D) = \frac{-1}{\omega\sqrt{1-D^2}} \int_0^{t_{end}} a(\tau) e^{-\omega D(t-\tau)} \sin\omega\sqrt{1-D^2}(t-\tau) d\tau \quad (2)$$

This equation describes the convolution of the seismometric signal with sinusoidal and exponential functions. The solution of equation (1) for discrete signals is given by the convolution of series; this is a time series connected with angular frequency (ω) and damping (D). Angular frequency ($\omega = 2\pi f$ or $\omega = 2\pi/T$) can be easily calculated to frequency f (Hz) or period T (s); thus, the solution to equation (1) is presented as a function of one of these parameters. Response spectra corresponds to maximum amplitudes of oscillator in the function of natural period of oscillation, considering constant damping factor (e.g. $D = 0.05$). Spectral acceleration, SA, is relevant to maximum absolute accelerations of masses within oscillators, which have the same values of damping, in the function of natural period of oscillations (which are response to ground motions).

$$SA(\omega, D) = \max_{t \in [0, t_k]} |\ddot{x}(t, \omega, D) + a(t)| \quad (3)$$

If the natural frequency of oscillations is close to zero, then the acceleration response spectra will also have values close to zero; however, when the natural frequency of oscillations is heading to infinity, the acceleration response spectra reaches peak values of ground acceleration. Normalised acceleration response spectra is useful tool for comparing the acceleration response spectra of various signals. The calculated values of spectral amplitudes are divided by the peak ground acceleration; thus, the amplitude for the maximum natural frequency of oscillations is equal to 1. The normalised response spectra are non-dimensional and show how many times the vibration of the oscillator are larger than the ground vibrations amplitudes.

For all considered signals, acceleration response spectra were calculated for damping at a level of 5% and a natural frequency of oscillations between 1 and 100 Hz. The larger of x and y components was chosen as horizontal component for further calculations. As was mentioned before, the rockburst-induced ground motion for that area can be divided into two groups [31, p. 11–23]. Briefly, the first group is characterised by high PGA which corresponds to dominant frequencies over 20 Hz and the second group relates to dominant frequencies of about 5 Hz. The impact of the type I ground recording on the building is negligible but the impact of the type II ground recording could be significant taking into account interesting frequency band in respect to the natural building oscillation (up to 10 Hz). Therefore, the analysis of ground motion measurement in the frequency band of up to 10 Hz is the standard procedure for that area. Thus, the response spectra were also calculated for records in the frequency band of up to 10 Hz. Next, a case study was conducted to explain the advantages of such a solution. Weak events ($M < 3$), occurring in the vicinity (within 1–2 km) of the stations, have weak records but with a large contribution of high frequencies. These frequencies are dominant in the spectra; however, their influence on the infrastructure is minor. As a result of this, response spectra estimated for signals before and after filtration were compared. This comparison was particularly important in the case of records with dominant frequencies over 10 Hz (Fig. 2). Acceleration response spectra and normalised response spectra, calculated from the filtered signal (Fig. 3a, b; green curve), do not have local maximum for frequencies of above 12 Hz. They were removed from the signal as a result of the process of low-pass filtration. The response spectra before and after filtration have rather similar shapes (Fig. 3a) for frequency ranges up to 10 Hz; however, local maximum amplitudes of normalised spectra before and after filtration differ significantly (Fig. 3b). The value of response spectra for 9 Hz is 1.7 in the case of spectra obtained with signals without frequency modification, and 2.6 in the case of spectra obtained for signals in frequency ranges up to 10 Hz. This difference is an effect of calculating normalised response spectra through dividing spectral amplitudes by appropriate values of peak ground accelerations – these are 0.117 m/s^2 and 0.057 m/s^2 . According to this, if we calculate response spectra for single ground records, there is no significant difference between assessing oscillator response based on record across the full range of frequencies or in selected frequency bands. When comparing multiple curves of normalised response spectra, calculated for ground motions with various dominant frequencies (especially in the frequency band interesting from our point of view), the situation is more complicated. The average estimated from normalised response spectra would be reduced in f band important for us (e.g. up to 10 Hz) if there will be much more records with dominant frequencies beyond the interest f band (e.g. $> 10 \text{ Hz}$) (Fig. 3). Considering the fact that the majority of analysed ground motion records are caused by weak events (which obviously occur more frequently), there is a necessity to narrow the frequency band of ground motions down to 10 Hz, before calculating normalised response spectra. As was mentioned before, such a type of low-pass filtering is commonly used for ground motion analysis in LGCD area, as ‘standardisation’ of PGA for engineering purposes in that area. After the application of a low-pass filter with a frequency range of up to 10 Hz, records were unified in the frequency domain. This was done to demonstrate the impact of seismic loading on the buildings in the frequency band

essential for infrastructure. This can be also done by only choosing intensive, type II ground recordings which have dominant frequencies of around 5 Hz for analysis. Zembaty *et al.* [33, p. 81–90] select only eighteen, intensive, type II ground records from that area and based on them calculated an average response spectra representing rockburst seismic loading. There are two weaknesses to this approach – suitable records have to be chosen and the average values are biased due to a lack of data.

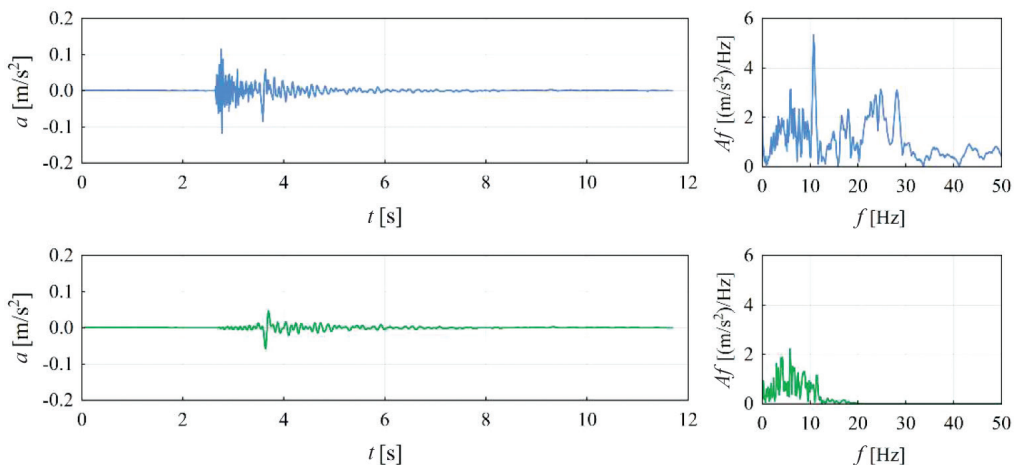


Fig. 2. An example registration of the ground motion x component with an amplitude FFT spectrum of the LGCD region (station 21) (blue curve), and in the frequency range of up to 10 Hz (green curve)

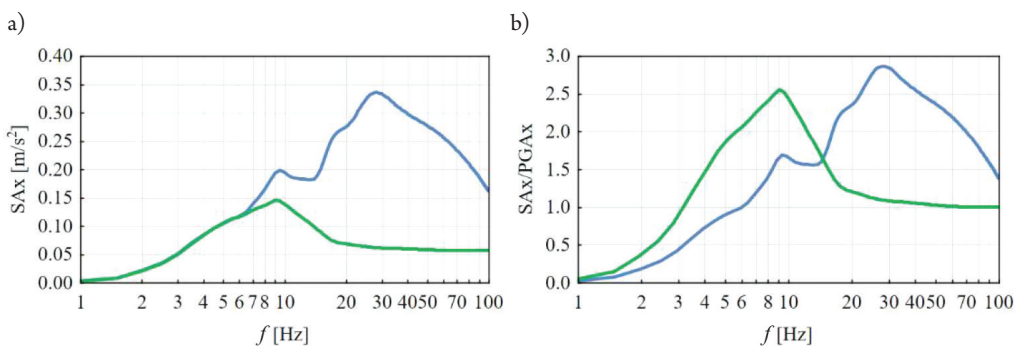


Fig. 3. x component of acceleration response spectra for the example registration across the whole frequency range (blue curve) and in the frequency range of up to 10 Hz (green curve); a) normalised acceleration response spectra, b) normalised acceleration response spectra

Fig. 4. Averages of normalised acceleration response spectra for station 21 based on ground motion across the whole frequency range (blue curve) and in the frequency range of up to 10 Hz (green curve); dashed lines show standard deviation of mean

In the next step, the average normalised acceleration response spectra for the horizontal and vertical components of each station were calculated (Figs. 7 & 8). Larger events possess lower dominant frequencies (~ 4 – 5 Hz); therefore, the average normalised response spectra

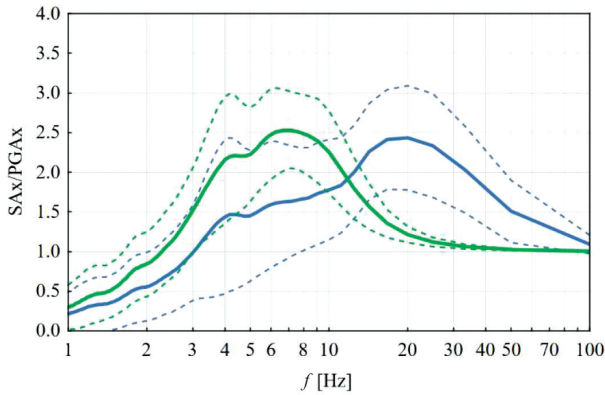


Fig. 4. Average normalised acceleration response spectra dependent upon the local magnitude of events which caused the analysed ground motion at station 21

were calculated according to the values of magnitude and the epicentral distance (Figs. 5 & 6 – example spectra for station no. 21). Those figures show that magnitudes and epicentral distances are factors that affect the values of spectral amplitudes and dominant frequencies of oscillators, for which the largest amplification of ground motions occurs. The larger the magnitude and epicentral distance, the lower the dominant frequency of oscillator (for which the largest amplification of ground motions occurs). Moreover, spectral amplitudes are slightly larger when these two parameters increase. As previously mentioned, weak events ($M < 3$) possess higher dominant frequencies than stronger events. The distributions of spectral amplitudes in the function of epicentral distances and in the function of magnitudes are similar due to the fact that the distribution of events according to the above mentioned parameters are correlated. Recorded signals caused by events occurring at distances greater than 2 km from the station (Fig. 6, red and orange curves) are also caused by events with $M > 3$ (67% of analysed data in the mentioned range of epicentral distances). Recorded signals, caused by events occurring in a distance smaller than 2 km from the station (Fig. 6, green and blue curves), are at the same time caused by events with $M < 3$ in 84% of cases.

The design average response spectra were estimated based on the averaged normalised acceleration response spectra for the horizontal and vertical components of each station. Firstly, the weighted arithmetic mean was calculated from the averages of spectra for each station and for both component separately. Smoothing of the averaged acceleration response spectra was then performed [26], resulting in the design acceleration response spectra for the vertical and horizontal components (Fig. 7):

$$SAh(f) = \begin{cases} -0.24 + 0.5 \cdot f, & f \in [1, 6] \\ 3.00, & f \in [6, 9] \\ 0.95 + \frac{10.40}{f - 5.0}, & f > 10.1 \end{cases} \quad (4)$$

$$SAv(f) = \begin{cases} -0.19 + 0.41 \cdot f, & f \in [1, 7.8] \\ 3.00, & f \in (7.8, 10.1] \\ 0.95 + \frac{10.40}{f - 5.00}, & f > 10.1 \end{cases} \quad (5)$$

The new design response spectra for the horizontal component, in comparison to the previous one made by the author, differ in the value of the constant spectral branch and with range of them. The new spectra has a higher value of the constant part and the upper frequency limit is smaller, it does not contain frequencies higher than 10 Hz. This is the effect of calculating response spectra for records in the frequency range of up to 10 Hz. The response spectra proposed by Tataru [26] has lower the constant branch with an even more narrow range of frequencies. This probably depends on input data, but there is not enough detailed information about the used recordings for calculating response spectra in the Tataru [26] monography. The significant differences are in relation to the response spectra estimated by Zembaty *et al.* [33, p. 81–90]. The response spectra for the different ground types are estimated using fully stochastic ground response analysis and for overall eighteen signals were used as a input data. The frequency ranges of the constant branch of the Zembaty response spectra are wider and also comprise frequencies below 5 Hz. Only individual response

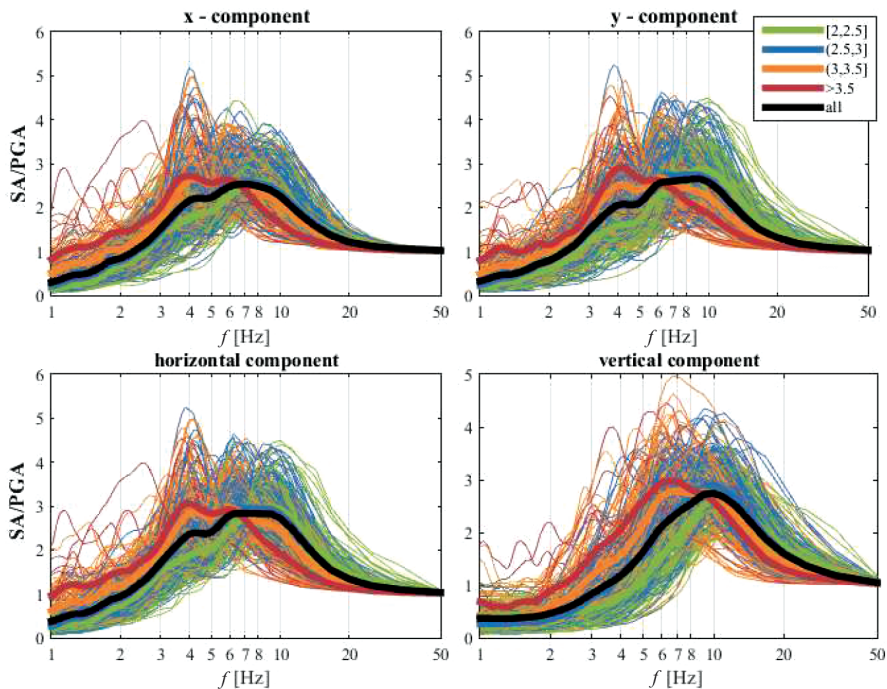


Fig. 5. Average normalised acceleration response spectra dependent upon the epicentral distance of events which caused the analysed ground motion at station 21

spectra have local maximum in that range of frequencies (Fig. 5). Thus, such high values of response spectra are probably biased by data input. Zembaty *et al.* [33, p. 81–90] used only one of the most intensive seismic events in that area which was really rare and unique. This is why a thorough comparison of response spectra should be done for different ground class separately and for representative input data. Therefore, because of the overall number of pieces of data, the new average response spectra can be treated as global for that area and should definitely be estimated according to different ground types in the future.

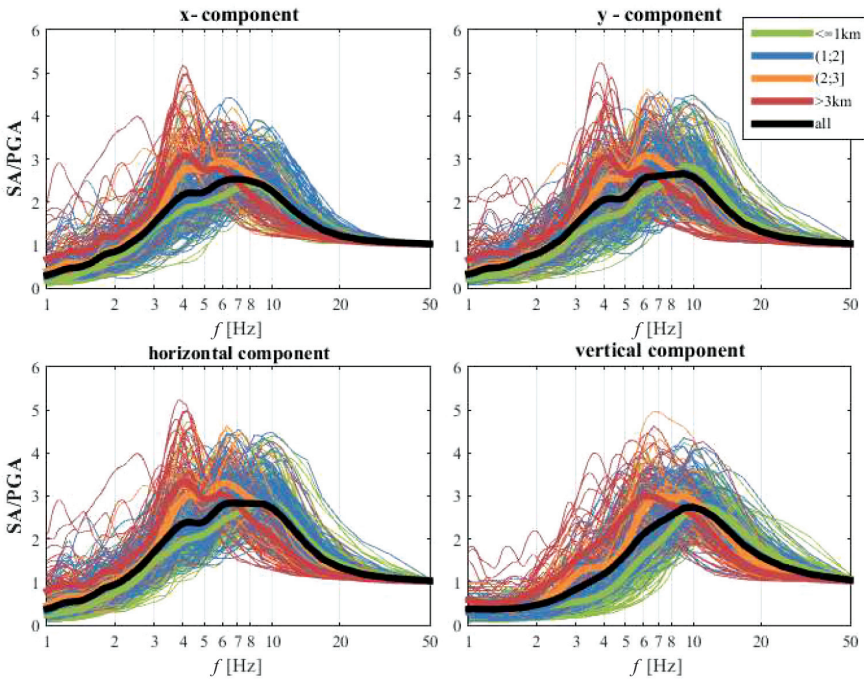


Fig. 6. Comparison of average response spectra for the horizontal component prepared for the LGCD area

The average response spectra for all stations and for both components were compared with adequate design response spectra. Three groups were separated according locations of local maximum of the stations response spectra and design spectra (Fig. 8, Fig. 9). For the horizontal component, the division of the three groups was performed in the manner stated below:

- ▶ the first group consisted of averaged spectra which had maximum in the lower frequencies than the frequency of the design spectra, that is to 5 Hz (Fig. 8a),
- ▶ the second group comprised averaged spectra which had maximum in a similar frequency band to the design spectra (6–9 Hz); however, their curves are slightly higher than the design spectra in frequency range of up to 6 Hz (Fig. 8b),
- ▶ the third group consisted of average spectra which had maximum located in the design spectra frequency band or higher (> 7 Hz), and their spectral amplitudes are mostly equal to amplitudes of the design spectra in the frequency range up to 6 Hz (Fig. 8c).

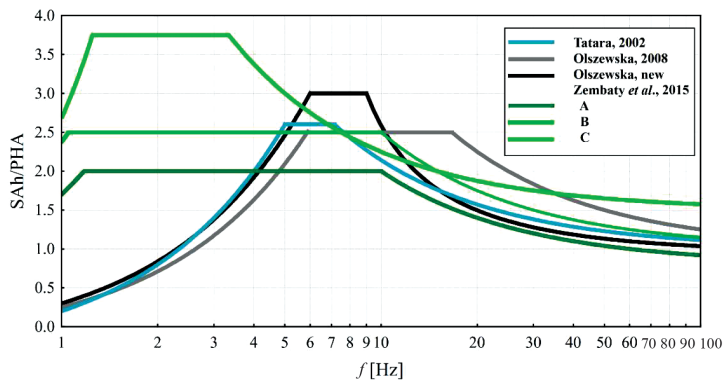


Fig. 7. Average normalised acceleration response spectra of horizontal component for the stations from the LGCD region with the design response spectra (black line)

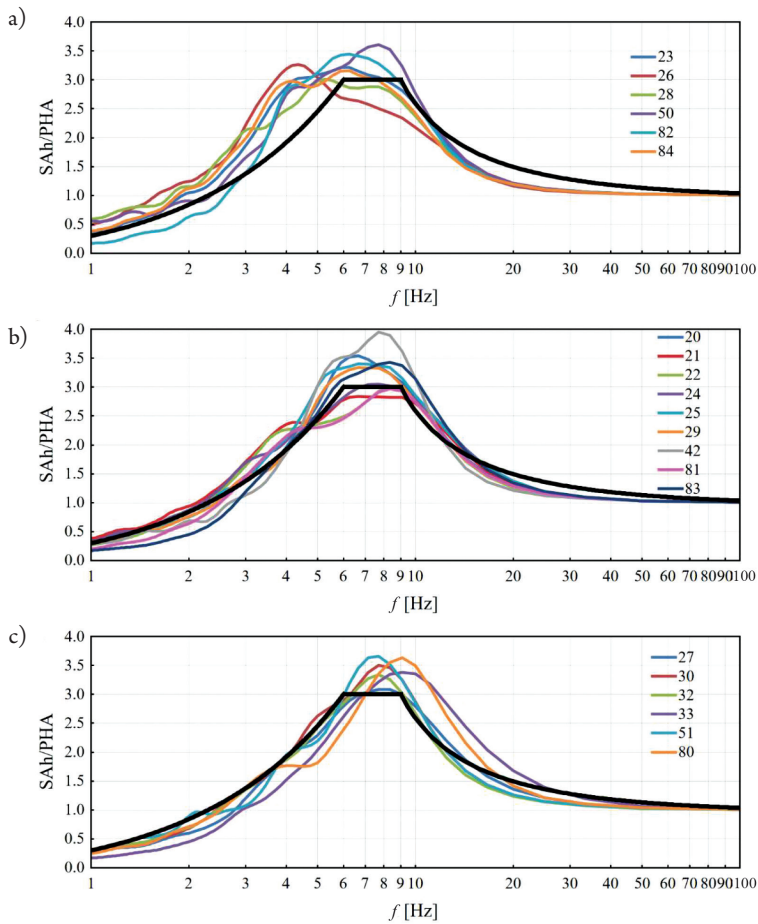


Fig. 8. Average normalised acceleration response spectra of the vertical component for the stations from the LGCD region with the design response spectra (black line)

For the vertical component, the classification of averaged spectra for the three subgroups was similar, with two small differences – the frequency band for the first group was up to 6 Hz (Fig. 9a) and the frequency band for the third group was above 8 Hz (Fig. 9c). Variations of average acceleration response spectra are *closely related* to the underlying ground conditions at the site of measurement (Eurocode-8). The lower the type of ground, the higher the amplification of the ground motions that occur; thus, ground motions are amplified and the maximal spectral amplitudes occur for lower frequencies. According to this, the aforementioned classification of the response spectra generally allows to distinguish local ground conditions at the LGCD area, as has been shown by Olszewska [19].

If the shape of the averaged response spectra is related to the local geological conditions and the ground motions amplifications, then the average normalised acceleration response spectra should have a compatible shape for areas with similar geological conditions and amplifications.

Further research will investigate this problem to a more detailed level. At present, it can be assumed that for close distances (100–200 m), local conditions should be similar to *each other*. Therefore, the average acceleration response spectra for nearby stations should have comparable shapes, or at least be in the same subgroup. This situation can be observed for the average response spectra for stations 23 and 84 (Fig. 8a – blue and orange curve) and for stations 21 and 81 (Fig. 8b – red and magenta curve). However, for some stations, despite being in very close proximity to each other (e.g. 22 m), the averages of response spectra differ enough for them to be classified into separate subgroups; this is the case for stations 29 and 33. This difference might be the a result of unique local conditions in that area. Factors concerning the manner of installing the sensor on the site may also be the reason for this difference.

4. Summary and conclusions

In this paper, the design acceleration response spectra for horizontal and vertical components were calculated for ground motions recorded by selected stations located in the LGCD area in order to enable seismic load to be defined for civil engineering purposes.

It was shown that for ground motions with different ranges of dominant frequencies, the average normalised response spectra should be calculated in the chosen frequency range. Thus, for the analysed area, the average normalised acceleration response spectra and the design response spectra for each station were evaluated from signals which were filtered to a frequency range of up to 10 Hz. As a consequence of this, the recordings were unified in the frequency domain – this is needed because of great part of type II recording with dominant frequencies is higher than for engineering purpose. Thus, the selection of only intensive, type II ground recording it is not necessary and uncertainties of obtain design response spectra is lower thanks to suitable number of data.

Moreover, the relationship between the response spectra and factors such as magnitude and epicentral distance has been presented. Maximal spectral amplitudes of strong events (with dominant lower frequencies) are in the lower band (~ 5–6 Hz).

Response spectra are strongly dependent upon the measurement site and the underlying ground conditions. The analysed area is rather small and previous research shows that ground type is uniform for that area. Nevertheless, the average response spectra have been divided into subgroups on the basis of their shapes; hence the assumption that stations were classified regarding the similarity of local ground conditions. However, this classification requires further studies.

As a result of this paper, the design acceleration response spectra for the vertical and horizontal components of the LGCD area have been estimated [equations (5) and (6)]. These response spectra can be used for analysis of ground motion influences on building infrastructure in the LGCD area and can help with the estimation of the local ground condition.

This work was supported within statutory activities of IG PAS No3841/E-41/S/2017 of Ministry of Science and Higher Education of Poland.

References

- [1] Arup (2015), NEN-NPR *Topic 2: Site Classes and Design Response Spectra*, Doc. Ref. 229746_033.0_NOT1002.
- [2] Bommer J.J., Dost B., Edwards B., Stafford P. J., van Elk J., Doornhof D., Ntinalexis M., *Developing an Application-Specific Ground-Motion Model for Induced Seismicity*. Bulletin of the Seismological Society of America, 106 (1)/2015, 158–173. DOI: 10.1785/0120150184.
- [3] Chmielewski T., Zembaty Z., *Dynamika budowli*, Politechnika Opolska, Opole 1997.
- [4] Davies R., Foulger G., Bindley A., Styles P., *Induced seismicity and hydraulic fracturing for the recovery of hydrocarbons*, Mar. Petrol. Geol., 45/2013, 171–185.
- [5] Di Manna, P., Guerrieri L., Piccardi L., Vittori E., Castaldini D., Berlusconi A., Bonadeo L., Comerci V., Ferrario F., Gambillara R., Livio F., Lucarini M., Michetti A. M. *Ground effects induced by the 2012 seismic sequence in Emilia: implications for seismic hazard assessment in the Po Plain*. Annals of Geophysics, 55 (4)/2012, DOI: 10.4401/ag-6143.
- [6] Douglas J., *Earthquake ground motion estimation using strong-motion records: a review of equations for the estimation of peak ground acceleration and response spectra*, Earth-Science Reviews 61/2003, 43–104.
- [7] Ellsworth W.L., *Injection-Induced Earthquakes*, Science, 341 (6142)/2013, 1225942. DOI: 10.1126/science.1225942.
- [8] Ellsworth W.L., Llenos A.L., McGarr A.F., Michael A.J., Rubinstein J.L., Mueller C.S., Petersen M.D., Calais E., *Increasing seismicity in the U.S. midcontinent: Implications for earthquake hazard*, The Leading Edge, 34 (6)/2015, 618–626, DOI: 10.1190/tle34060618.1
- [9] Eurocode-8: Design of structures for earthquake resistance – the European Standard. ENV 1998-1-3: 1995.



- [10] Jennings P.C., *An introduction to the Earthquake Response Spectra*, [in:] *International Handbook of Earthquake Engineering Seismology*, Vol. 18B, W.H.K. Lee, H. Kanamori, P.C. Jennings, C. Kisslinger, (ed.) Academic, Amsterdam 2003, 1097–1125.
- [11] Kozłowska M., Orlecka-Sikora B., Rudziński Ł., Cielesta S., Mutke G., *A typical evolution of seismicity patterns resulting from the coupled natural, human-induced and coseismic stresses in a longwall coal mining environment*, *International Journal of Rock Mechanics and Mining Sciences*, 86/2016, 5–15. DOI: 10.1016/j.ijrmmms.2016.03.024.
- [12] Kwiatek, G., Plenkers K., Dresen G., *Source Parameters of Picoseismicity Recorded at Mponeng Deep Gold Mine, South Africa: Implications for Scaling Relations*, *Bulletin of the Seismological Society of America*, 101 (6)/2011, 2592–2608, DOI: 10.1785/0120110094.
- [13] Kwiatek G., Martinez-Garzon P., Dresen G., Bohnhoff M., Sone H., Hartline C., *Effects of long-term fluid injection on induced seismicity parameters and maximum magnitude in northwestern part of The Geysers geothermal field*, *Journal of Geophysical Research: Solid Earth*, 120 (10)/2015, 7085–7101, DOI: 10.1002/2015JB012362.
- [14] Lasocki S., *Site Specific Prediction Equations for Peak Acceleration of Ground Motion Due to Earthquakes Induced by Underground Mining in Legnica-Głogów Copper District in Poland*, *Acta Geoph. 61 (5)/2013*, 1130–1155.
- [15] Lasocki S., Orlecka-Sikora B., *Seismic hazard assessment under complex source size distribution of mining-induced seismicity*, *Tectonophysics*, 456 (1–2)/2008, 28–37.
- [16] Maciąg E., Kuźniar K., Tatara T., *Response spectra of the ground motion and building foundation vibrations excited by rockbursts in the LGC region*, *Earthq Spectra* 32(3)/2016, 1769–1791, DOI:10.1193/020515EQS022M.
- [17] McGarr A.F., Simpson D., *A broad look at induced and triggered seismicity*, [in:] *Rockburst and seismicity in mines*. Balkema, Rotterdam 1977, 385–396.
- [18] Mutke G., Muszyński L., Lurka A., Siata R., Logiewa H., Musiał M., Byrczek B., *Assessment of correctness of measurements of ground vibrations for ZG Rudna mine rockbursts (in Polish)*, GIG report number 42162719-123, April 2000.
- [19] Olszewska D., *Analysis of site effects and spectrum of signals in order to improve the accuracy of the prognosis of ground motion caused by mining-induced seismic events in Legnica-Głogów Copper District*, Ph.D. Thesis, AGH University of Science and Technology, Kraków 2008.
- [20] Olszewska D., Lasocki S., *Application of the horizontal to vertical spectral ratio technique for estimating the site characteristics of ground motion caused by mining induced seismic events*, *Acta Geophys. Pol*, Vol. 52, No. 3/2004, 301–318.
- [21] Olszewska D., Kula D., *Preliminary site-effects characterization by inversion of HVSR data in mining area*, ESC General Assembly 2016, Trieste, Italy 2016, Abstracts.
- [22] Oye V., Bungum H., Roth M., *Source Parameters and Scaling Relations for Mining-Related Seismicity within the Pyhasalmi Ore Mine, Finland*, *Bulletin of the Seismological Society of America*, 95 (3)/2005, 1011–1026, DOI: 10.1785/0120040170,
- [23] Petersen M.D., Mueller C.S., Moschetti M.P., et al., 2017 *One-Year Seismic-Hazard Forecast for the Central and Eastern United States from Induced and Natural*

Earthquakes, Seismological Research letters, Vol. 88, No. 3/2017, 772–783, DOI: 10.1785/0220170005.

- [24] Richardson E., Jordan T.H., *Seismicity in Deep Gold Mines of South Africa: Implications for Tectonic Earthquakes*, Bulletin of the Seismological Society of America, 92 (5)/2002, 1766–1782, DOI: 10.1785/0120000226.
- [25] Soeder D.J., Sharma S., Pekney N., Hopkinson L., Dilmore R., Kutcho B., Stewart B., Carter K., Hakala A., Capo R., *An approach for assessing engineering risk from shale gas wells in the United States*, International Journal of Coal Geology, 126/2014, 4–19, DOI: 10.1016/j.coal.2014.01.004.
- [26] Tataro T., *Działanie drgań powierzchniowych wywołanych wstrząsami górniczymi na niską tradycyjną zabudowę mieszkalną*, Zeszyty Naukowe Politechniki Krakowskiej, seria: Inżynieria Łądowa, Kraków 2002.
- [27] Tataro T., Pachla F., *Uszkodzenia w obiektach budowlanych w warunkach wstrząsów górniczych*, [in:] Pilecka E (ed.) Mat. XIV Warsztaty Górnicze „Zagrożenia naturalne w górnictwie”, [in:] Mat. XIV Warsztaty Górnicze „Zagrożenia naturalne w górnictwie”, Pilecka E (ed.), Wyd. JGSMiE PAN, Kraków, 2012, 442–458.
- [28] Urban P., Lasocki S., Blascheck P., do Nascimento A.F., Van Giang N., Kwiatek G., *Violations of Gutenberg–Richter Relation in Anthropogenic Seismicity*, Pure and Applied Geophysics, 173 (5)/2016, 1517–1537, DOI: 10.1007/s00024-015-1188-5.
- [29] Wodyński A., *Zużycie Techniczne Budynków na Terenach Górniczych*, Wydawnictwa AGH, Kraków 2007.
- [30] Van Eck T., Goutbeek F., Haak H., Dost B., *Seismic hazard due to small-magnitude, shallow-source, induced earthquakes in The Netherlands*, Engineering Geology, 87 (12)/2006, 105–121, DOI: 10.1016/j.enggeo.2006.06.005.
- [31] Zembaty Z., *Rockburst induced ground motion – a comparative study*, Soil Dyn Earthq Eng 24/2004, 11–23, DOI: 10.1016/j.solidyn.2003.10.001.
- [32] Zembaty Z., *How to model rockburst seismic loads for civil engineering purposes?*, Bull Earthq Eng 9/2011, 1403–1416, DOI:10.1007/s10518-011-9269-z.
- [33] Zembaty Z., Kokot S., Bozzoni F., Scandella L., Lai C.G., Kuś J., Bobra P., *A system to mitigate deep mine tremor effects in the design of civil infrastructure*, International Journal of Rock Mechanics and Mining Sciences, Vol. 74/2015, 81–90, DOI: 10.1016/j.ijrmmms.2015.01.004.

Dariusz Skorupka

Artur Duchaczek

Agnieszka Waniewska (a.waniewska@wso.wroc.pl)

Faculty of Management, The General Tadeusz Kosciuszko Military Academy of Land Forces

OPTIMISATION OF THE CHOICE OF UAV INTENDED TO CONTROL
THE IMPLEMENTATION OF CONSTRUCTION PROJECTS AND WORKS USING
THE AHP METHOD

OPTIMALIZACJA WYBÓRU BSL PRZEZNACZONEGO DO KONTROLI
REALIZACJI PRZEDSIĘWZIĘĆ I ROBÓT BUDOWLANYCH
PRZY WYKORZYSTANIU METODY AHP

Abstract

Modern technologies, which may include unmanned aerial vehicles (UAV, Polish abbreviation BSL), potentially have a very wide range of applications. Research has been conducted on the possibility of using UAVs to control the execution of construction works by the authors of the article among other researchers. The technical parameters of the applied measurement instruments are of great significance. This paper presents a possibility for the optimal choice of unmanned aerial vehicles using the AHP method. The popularity of this method results not only from its effectiveness in solving complex decision problems, but also from its transparency and ease of application. The decision-making analysis adopts the criteria that are essential with regard to the supervision of construction works which they may support.

Keywords: unmanned aerial vehicles, multi-criteria optimization, making decisions, decision models

Streszczenie

Nowe technologie, do których można zaliczyć bezzałogowe statki latające (BSL), mają potencjalnie bardzo szerokie zastosowanie. Prowadzone są badania, także przez autorów artykułu, nad możliwością wykorzystania BSL do kontroli wykonania robót budowlanych. Istotne znaczenie mają parametry techniczne zastosowanych urządzeń pomiarowych. W pracy zaprezentowano możliwość optymalnego wyboru bezzałogowych statków latających przy zastosowaniu metody AHP. Popularność tej metody wynika nie tylko ze skuteczności w rozwiązywaniu złożonych problemów decyzyjnych, ale również przejrzystości i łatwości stosowania. W analizie decyzyjnej przyjęto kryteria mające kluczowe znaczenie ze względu na nadzór robót budowlanych, który mogą wspomagać.

Słowa kluczowe: bezzałogowe statki latające, optymalizacja wielokryterialna, podejmowanie decyzji, modele decyzyjne

1. Introduction

The availability of unmanned aerial vehicles (UAV) affects the increase in popularity of such systems. Currently, the area of potential applications of this type of technology is constantly growing [1]. The aim of this article is to present the parameters and specifications of selected unmanned aircraft and present the possibility of choosing an optimal model UAV for use in the process of monitoring the implementation of linear building objects using the AHP method. The authors have identified criteria which may be of crucial importance as a result of the specific examination of selected construction projects. According to the authors of this study, the selection of the optimal UAV will improve the efficiency of identifying potential hazards that may occur during the implementation of the project.

UVAs coupled with appropriate cameras and sensors allows data of interest to be recorded. The advantage of this method is primarily economic efficiency, accuracy and measuring speed [2]. The authors have also carried out studies on the use of UVAs in other areas of construction engineering, these are described, inter alia, in the work [3]. In recent years, the use of unmanned aircraft has become an innovative method of taking measurements. Unmanned aerial vehicles equipped with high resolution cameras are able to inspect construction objects precisely [2]. Furthermore, the lack of negative impact in the use of UAVs on the environment and the low risk of damage in the event of a vehicle failure make it possible to conduct flights over facilities in urban areas [4]. In literature, one can find a wide range of possible applications of UVAs described both in quantitative and qualitative research.

2. Possible applications of unmanned aerial vehicles in construction engineering

In attempting to choose the optimal UAV, the authors identified criteria which are essential in the process of monitoring the implementation of linear building objects (see also [3]). The first criterion is the speed of flight, which often translates into flight range. The flight speed is crucial for the professional supervision of a large area. In general, the more professional the equipment, the longer the flight and operation time. Another criterion enabling the operation of the device in an open space is the range of the remote control device, this is usually around 2 km. In the event of loss of communication between the transmitter and the receiver, an unmanned vehicle has the function for self-return to a pre-designated location. In the case of executing longer observations, it is worth purchasing equipment capable of operating in the air up within a maximising the time that the UAV can operate [5].

The maximum flight distance is one of the most important criteria when measurements are made over a wide area. UAV operation time in the air depends on the weight of a model, the batteries and other components [3]. Thus, weight is a significant parameter which relies mainly on the dimensions and material from which a UAV is produced. It should be emphasised that during long-distance cruises, it is important that a UAV is made of a suitable material in order to meet monitoring requirements, for example, concerning flight distance. It is the weight of a UAV that determines whether a vehicle is characterised by stability and

strength when in the air. The analysis assumes that heavier UAVs should offer the possibility of hanging off heavier measurement equipment. The fifth criterion identified by the authors is the maximum flight altitude.

When flying at a certain altitude, a shot from directly above can be obtained of virtually the entire construction site, especially in hard-to-reach places. A UAV's ability to rise to the desired altitude enables the creation of 3D models of selected objects or simply the photographing of certain areas and the subsequent creation of maps. The last criterion is the possibility of connecting sensors and detectors which are included in UAV equipment. Unmanned aircraft can be equipped with a range of sensors that provide data to the operator. The most frequently used sensors are: an accelerometer; a gyroscope; an ultrasonic sensor; a pressure sensor; a vertical camera measuring the velocity over ground. The nature of the conducted study makes it necessary to assess not only whether a UAV meets certain criteria, but also to what extent they are met. Not all criteria are equally relevant for a decision maker. The fundamental issue is, therefore, the specification of the criteria that are essential and will allow decision-makers to choose the optimal UAV which should support the execution and supervision of construction works [6].

3. Principles of the AHP method

The AHP method was used to choose the optimal UAV – this is one of methods of multi-criteria analysis. The AHP method was developed and described by T. L. Saaty [7, 8]. Based on works [9] and [10], with this (as is the case with works [11–13]), the authors presented only the most important theoretical assumptions of the AHP.

In principle, this method should help to make optimal choices in the case of multi-criteria optimisation due to their reduction to a series of pairwise comparisons [9]. Since the characteristic feature of the method is the fact that elements in pairs are compared with each other, the rating scales applied as standards are generally of very limited use. For this reason, a new nine-point grading scale has been introduced [8].

In order to evaluate the elements at particular levels of the analysed structure a matrix of comparisons A with elements a_{ij} ($i, j = 1, 2, \dots, n$) was constructed, in which the order n is the number of elements being compared, wherein, if the criterion K_i is equivalent to the criterion K_j , then $a_{ij} = 1$ and $a_{ji} = 1$. In other cases, if $a_{ij} = z$, then $a_{ji} = 1/z$ for $z \neq 0$ [9].

All elements of the model under analysis are organised by importance of priority vectors $W = w_1, \dots, w_n$. To make a calculation of a priority vector W , the matrix A must first be normalised by dividing each of its elements by the sum of the elements of the column in which it is situated (then the matrix B is created) [9]:

$$b_{ij} = \frac{a_{ij}}{\sum_{i=1}^n a_{ij}} \quad (1)$$

Thereafter, the average values are determined for each matrix row, being elements w_i of the priority vector W [9]:



$$w_i = \frac{\sum_{j=1}^n b_{ij}}{n} \quad (2)$$

where $i, j = 1, \dots, n$, wherein $\sum_{i=1}^n w_i = 1$. The symbol k_i is applied in the case of the priority vector of the analysed criteria, while the symbol o_{ij} is used for the priority vector of the i^{th} object according to the criterion j^{th} .

The value of the coefficient AHP marked h_i is determined based on the relation [12]:

$$h_i = \sum_{i=1}^n (k_i o_{ij}), \quad (3)$$

where k_i is the value of the element of the priority vector for the i^{th} criterion (the so-called i^{th} criterion weight), while o_{ij} is the value of the element of the priority vector for the j^{th} object with respect to the i^{th} criterion, wherein $\sum_{i=1}^n h_i = 1$.

Therefore, it can be stated that particular criteria and analysed variants are compared through determining the degree of superiority of one element over another. These operations are quite subjective; therefore, they can be characterised by a lack of consistency in the assessment.

In the AHP method, the reliability of results is verified primarily by determining the consequence ratio CR calculated according to the formula [9]:

$$CR = \frac{CI}{RI} 100\%, \quad (4)$$

wherein RI is a random index dependent on the matrix order n (e.g. if $n = 6$, then $RI = 1.24$) [9]. The consequence index CI is determined from the relation [9]:

$$CI = \frac{(\lambda_{\max} - n)}{(n-1)}, \quad (5)$$

where λ_{\max} is the maximum eigenvalue of the matrix, which is always greater than or equal to the matrix order n .

The approximate maximum eigenvalue of the matrix λ_{\max} can be calculated as the sum of products of the average row values of standardised weights and column sums corresponding to the individual criteria, which can be written with the expression [10]:

$$\lambda_{\max} = \sum_{i=1}^n \left(w_i \sum_{j=1}^n a_{ij} \right). \quad (6)$$

It was assumed that if the value of the consequence ratio CR exceeds 10%, then the whole process of assessment should be repeated [9].

4. The application of the AHP method in the process of the optimal choice of UAV

The main objective of the performed analyses was to choose the most optimal UAV, taking into account the established criteria. Six variants of solutions to this problem were adopted for the analyses, as shown in Table 1. In the example under consideration, six criteria were assumed, these include: the flight speed (K1); the maximum flight distance (K2); the range of the controller (K3); the weight (K4); the maximum flight altitude (K5); the number of detectors and sensors belonging to UAV equipment (K6).

Table 1. Data of unmanned aerial vehicles selected for the analysis

Name of the selected model		The selected criteria					
		K1	K2	K3	K4	K5	K6
		[m/s]	[min.]	[km]	[kg]	[km]	[no.]
DJI Inspire 1 PRO	W1	22.00	18.00	2.00	2.90	4.50	0.00
ParrotAR.Drone 2.0	W2	16.00	15.00	0.05	0.44	0.10	4.00
DJI Phantom 3 Standard	W3	16.00	25.00	1.00	1.22	0.50	4.00
Tornado H920	W4	21.00	24.00	2.00	5.00	1.00	5.00
Yuneec Typhoon H	W5	10.00	22.00	1.00	0.19	0.12	2.00
Quadcopter Matrice 100 DJI	W6	22.00	22.00	2.00	0.24	0.17	3.00

Formula (2) was used to specify the values of the priority vector k_i for the adopted criteria – these are presented in Table 2 as the importance coefficients (i.e. weights) of these criteria. The subjective assessment expressed by the priority value k_i showed that the most important criterion in the selection process is the range of the controller (K3), while the least significant criterion – the flight speed (K1).

Table 2. Weights of criteria adopted for analyses

Specification		K1	K2	K3	K4	K5	K6	The priority vector k_i
flight speed	K1	1.000	0.200	0.167	0.250	0.502	0.334	0.048
maximum flight distance	K2	5.000	1.000	0.833	1.249	2.502	1.666	0.238
range of a controller	K3	5.988	1.200	1.000	1.499	3.003	2.000	0.286
weight	K4	4.000	0.801	0.667	1.000	2.003	1.334	0.191
maximum flight altitude	K5	1.992	0.400	0.333	0.499	1.000	0.666	0.095
number of detectors and sensors	K6	2.994	0.600	0.500	0.750	1.502	1.000	0.143
The value of the consequence ratio CR = 0.00%								

Table 3 presents the evaluation of particular variants (types of UAVs) in accordance with the six adopted criteria. In this case, the table also shows the values of the priority vector o_{ij} for each of the variants obtained using formula (2).

Table 3 presents the values of the consequence ratio CR defined by formula (4). Having performed the analysis of the value of this ratio, it can be stated that the assessment of individual variants were very consistent, since the value of CR was far below 10%.

Table 4 presents the final results of the calculations performed according to formula (3). The results unequivocally prove that the *Tornado H920* (W4) is the optimal UAV in the considered computational conditions. Obviously, these conclusions can also be reached intuitively however, using the AHP method, numerical values are obtained that can be used for further analysis.

Table 3. Assessment of individual variants according to the established criteria

Assessment of the variants according to criteria K1									
Specification		W1	W2	W3	W4	W5	W6	Priority vector o_{ii}	Consequence ratio CR
DJI Inspire 1 PRO	W1	1.000	1.370	1.370	1.050	2.220	1.000	0.206	0.00
Parrot AR. Drone 2.0	W2	0.730	1.000	1.000	0.770	1.620	0.730	0.150	
DJI Phantom 3 Standard	W3	0.730	1.000	1.000	0.770	1.620	0.730	0.150	
Tornado H920	W4	0.952	1.299	1.299	1.000	2.110	0.950	0.195	
Yuneec Typhoon H	W5	0.450	0.617	0.617	0.474	1.000	0.450	0.093	
Quadrocopter Matrice 100 DJI	W6	1.000	1.370	1.370	1.053	2.222	1.000	0.206	
Assessment of the variants according to criteria K2									
DJI Inspire 1 PRO	W1	1.000	1.200	0.720	0.750	0.820	0.820	0.142	0.41
Parrot AR. Drone 2.0	W2	0.833	1.000	0.600	0.625	0.680	0.680	0.118	
DJI Phantom 3 Standard	W3	1.389	1.667	1.000	1.670	1.140	1.140	0.215	
Tornado H920	W4	1.333	1.600	0.599	1.000	1.090	1.090	0.177	
Yuneec Typhoon H	W5	1.220	1.471	0.877	0.917	1.000	1.000	0.174	
Quadrocopter Matrice 100 DJI	W6	1.220	1.471	0.877	0.917	1.000	1.000	0.174	
Assessment of the variants according to criteria K3									
DJI Inspire 1 PRO	W1	1.000	33.330	2.000	1.000	2.000	1.000	0.248	0.00
Parrot AR. Drone 2.0	W2	0.030	1.000	0.060	0.030	0.060	0.030	0.007	
DJI Phantom 3 Standard	W3	0.500	16.667	1.000	0.500	1.000	0.500	0.124	
Tornado H920	W4	1.000	33.333	2.000	1.000	2.000	1.000	0.248	
Yuneec Typhoon H	W5	0.500	16.667	1.000	0.500	1.000	0.500	0.124	
Quadrocopter Matrice 100 DJI	W6	1.000	33.333	2.000	1.000	2.000	1.000	0.248	
Assessment of the variants according to criteria K4									

DJI Inspire 1 PRO	W1	1.000	6.440	2.420	0.580	14.500	11.600	0.290	0.00
Parrot AR. Drone 2.0	W2	0.155	1.000	0.375	0.090	2.250	1.800	0.045	
DJI Phantom 3 Standard	W3	0.413	2.667	1.000	0.240	6.000	4.800	0.120	
Tornado H920	W4	1.724	11.111	4.167	1.000	25.000	20.000	0.500	
Yuneec Typhoon H	W5	0.069	0.444	0.167	0.040	1.00	0.800	0.020	
Quadrocopter Matrice 100 DJI	W6	0.086	0.556	0.208	0.050	1.250	1.000	0.025	
Assessment of the variants according to criteria K5									
DJI Inspire 1 PRO	W1	1.000	50.000	9.090	4.550	33.330	25.000	0.704	0.00
Parrot AR. Drone 2.0	W2	0.020	1.000	0.180	0.090	0.670	0.500	0.014	
DJI Phantom 3 Standard	W3	0.110	5.556	1.000	0.500	3.670	2.750	0.078	
Tornado H920	W4	0.220	11.111	2.000	1.000	7.330	5.500	0.155	
Yuneec Typhoon H	W5	0.030	1.493	0.272	0.136	1.000	0.750	0.021	
Quadrocopter Matrice 100 DJI	W6	0.040	2.000	0.364	0.182	1.333	1.000	0.028	
Assessment of the variants according to criteria K6									
DJI Inspire 1 PRO	W1	1.000	0.003	0.003	0.002	0.005	0.003	0.001	0.02
Parrot AR. Drone 2.0	W2	400.000	1.000	1.000	0.800	2.000	1.330	0.221	
DJI Phantom 3 Standard	W3	400.000	1.000	1.000	0.800	2.000	1.330	0.221	
Tornado H920	W4	500.000	1.250	1.250	1.000	2.500	1.667	0.277	
Yuneec Typhoon H	W5	200.000	0.500	0.500	0.400	1.000	0.667	0.111	
Quadrocopter Matrice 100 DJI	W6	333.333	0.752	0.752	0.600	1.499	1.000	0.169	

Table 4. Results of calculations by the AHP method

Variants	Name of the selected model	The value of the AHP ratio – h_i
W1	DJI Inspire 1 PRO	0.200
W2	Parrot AR. Drone 2.0	0.095
W3	DJI Phantom 3 Standard	0.160
W4	Tornado H920	0.283
W5	Yuneec Typhoon H	0.100
W6	Quadrocopter Matrice 100 DJI	0.162

5. Conclusion

Unmanned aerial vehicles have highly diversified technical features, which determines the need to select specific criteria for their assessment. The correctness of carried out analyzes is dependent on these criteria. The presented issues based on the method of multi-criteria optimisation is possible to be used in the broadly understood civil engineering, particularly in the context of the supervision of construction works and monitoring the progress of work

on a construction site [14–18]. Due to the application of the AHP method, the obtained numerical values clearly show that the best-suited device for this type of projects is the *Tornado H920*.

In the AHP method, the rating scale for quantitative criteria is actually difficult to implement. In this paper, the rates received during the pairwise comparisons of individual decision variants were expressed as the ratio of values of individual criteria. The overall conclusion is that the adopted AHP method is an option for choosing the optimal UAV, but not an option that is recommended. It seems more reasonable to take advantage of methods directly using the values of individual criteria for the comparison process, for example, the Bellinger methods, as presented in paper [3].

References

- [1] Cavoukian A., *Privacy and Drones: Unmanned Aerial Vehicles*, Information and Privacy Commissioner of Ontario, Canada 2012.
- [2] Kowalski P., Bielecki K., *Zastosowanie termowizji z wykorzystaniem dronów w budownictwie*, <http://www.inzynierbudownictwa.pl> (access: 07.03.2016).
- [3] Skorupka D., Duchaczek A., Waniewska A., Kowacka M., *Optimization of the choice of unmanned aerial vehicles used to monitor the implementation of selected construction projects*, Proceedings of the International Conference on Numerical Analysis and Applied Mathematics 2016, ICNAAM-2016, Simos T.E., Tsitouras C. (eds.), Numerical Analysis and Applied Mathematics, Rhodes, Greece, 19.09–25.09.2016.
- [4] Sobolewski J., *Wykorzystanie dronów do oblotu sieci elektroenergetycznych*, <http://www.rynek-gazu.cire.pl/pliki/2/wykorzystaniedronowdooblotusiecielekroenergetycznych.pdf> (access: 07.03.2016).
- [5] <http://www.dji.com/product/phantom-4> (access: 07.03.2016).
- [6] Audronis T., *Drony. Wprowadzenie*, HELION, Gliwice 2015.
- [7] Saaty T.L., *Some Mathematical Concepts of the Analytic Hierarchy Process*, *Behaviormetrika*, 29, 1991, 1–9.
- [8] Saaty T.L., Vargas L., *Models, Methods, Concepts and Applications of the Analytic Hierarchy Process*, Kluwer Academic Publishing, Boston 2001.
- [9] Ostrega A., *Sposoby zagospodarowania wyrobisk i terenów po eksploatacji złóż surowców węglanowych na przykładzie Krzemionek Podgórskich w Krakowie*, Ph.D. thesis, Faculty of Mining and Geoengineering, AGH University of Science and Technology, Kraków 2004.
- [10] Teknomo K., *Analytic Hierarchy Process. Kardi Teknomo's Homepage*, <http://people.revoledu.com/karti/tutorial/AHP/AHP.htm> (access: 07.03.2016).
- [11] Duchaczek A., Skorupka D., *Evaluation of probability of bridge damage as a result of terrorist attack*, *Archives of Civil Engineering*, 2013, 59(2), 215–227.
- [12] Skorupka D., Duchaczek A., *Metoda oceny ryzyka uszkodzeń obiektów komunikacyjnych w warunkach kryzysowych (Damage risk assessment method of bridge objects in conditions*

- of crisis), [in:] *Inżynieria przedsięwzięć budowlanych: rekomendowane metody i techniki*, Kasprowicz T. (ed.), Warsaw University and Technology, Publishing House: Section of Engineering Projects Construction KILiW PAN: Polish Chamber of Civil Engineers, 2015, 209–228.
- [13] Duchaczek A., Skorupka D., *A Risk Assessment Method of Bridge Facilities Damage in the Aspect of Potential Terrorist Attacks*, *Periodica Polytechnica Civil Engineering*, 2016, 60(2), 189–198.
- [14] Kapliński O., Janusz L., *Three phases of multifactor modelling of construction processes*, *Journal of Civil Engineering and Management*, 2006, 12(2), 127–134.
- [15] Kasprowicz T., *Cost-time scheduling of construction works execution*, *J. Infrastructure Planning and Management*, 2000, 660 (IV–49).
- [16] Połośki M., *The analysis of the reliability of realization cost and investments, time-limits in Warsaw*, *Electronic Journal of Polish Agricultural Universities Topic Civil Engineering*, 2006, 9(4), #10.
- [17] Sobotka A., Czarnigowska A., *Analysis of supply system models for planning construction project logistics*, *Journal of Civil Engineering and Management*, 2005, 11(1), 73–82.
- [18] Plebankiewicz E., Leśniak A., *Overhead costs and profit calculation by Polish contractors*, *Technological and Economic Development of Economy*, 2013, 19.1, 141–161.



Andrzej Więckowski (awiecko@agh.edu.pl)

Department of Geomechanics, Civil Engineering and Geotechnics, Faculty of Mining and Geoengineering, AGH University of Science and Technology

MODELLING THE DELIVERY AND LAYING OF CONCRETE MIX

MODELOWANIE DOSTAW I WBUDOWANIA MIESZANKI BETONOWEJ

Abstract

The aim of this paper is to indicate solutions which fulfil the conditions for laying concrete mix before it starts setting. Using models $M/M/N/-/N$, for organization I for the so-called delivery directly after unloading, with automatic transfer of information using the RFID system, and $M/M/1/FIFO/N/F$, for organisation II with transportation units working in closed cycle. Of example, organisation I, with RFID system is more advisable as it is characterised by a shorter waiting time on construction sites; and longer at the concrete-mixing plant. At the same time, it increases the efficiency of working units compared with organisation II which has self-regulating transportation units running in closed cycle.

Keywords: queueing theory, construction, production organisation

Streszczenie

Celem artykułu jest badanie zmienności, gwarantowanych czasów urabiania mieszanki betonowej wraz ze wskazaniem rozwiązań spełniających warunek ukończenia wbudowywania każdej porcji, jeszcze przed chwilą początku wiązania cementu. Zastosowano modele teorii kolejek: $M/M/N/-/N$ – organizacja I, dla przypadku „realizacji dostaw bezpośrednio po rozładunkach” przy automatycznym przesyłaniu informacji z budowy do betonowni systemem *RFID* oraz $M/M/1/FIFO/N/F$ – organizacja II, z funkcjonowaniem jednostek transportowych w „cyklu zamkniętym” i samoregulacją ich pracy. W przykładzie betonowania przeszła estakady, przy zastosowaniu organizacji I, wskazano mniejsze czasy oczekiwania samochodów z mieszanką na budowie, a większe oczekiwania pojazdów niezaladowanych w betonowni, jak też większą wydajność zespołów wbudowujących mieszankę, w porównaniu z organizacją II.

Słowa kluczowe: teoria kolejek, budownictwo, organizacja produkcji

1. Introduction

Large distances between concrete plants and construction sites, as well as distortions in traffic of concrete mixers, cause variability in the transportation time of concrete mix. Furthermore, the time of unloading/pumping and laying the mix is not constant. Therefore, the required waiting time, both on the part of the concrete laying team operating the pump for transport of the mix, and on the part of vehicles queuing for the unloading procedure, [4, 11, 12, 16–18]. In the case of concrete laying, in the case of each of the connected mix batches, the condition must be met that concrete laying and its monolithic connection with the surrounding mix (laid earlier or later) should occur still before the beginning of cement setting [10, 17].

Standard analyses operate with site units (namely brigades or their selected parts, smaller teams, or even operators with the equipment) which, in the case of resignation from inter-operational storage, directly cooperate with the transport units, [1, 2, 14, 15]. These are, for example, excavation crews removing soil with heavy construction equipment, or gangs working with cranes erecting prefabricated elements which are continuously transported to the site [5, 6]. Usually, optimisation is oriented towards minimising the cost of the works. In the case of works involving concrete, there is a need to lay and connect the mix portion still before cement starts setting. Therefore, an important element of the analysis involves determining the time taken from mixing the cement with water at the concrete plant until such times as it is laid and along with other batches of mix on site [17, 19].

2. Typical systems in the queuing theory

The work of construction crews and transportation can be described using queuing theory models. In such models, the queuing system represents the functioning of an object rendering a service, e.g. the operation of a computer processor performing consecutive calculations, or on a construction site, the work of a concrete laying crew with a pump for the transfer of a concrete mix from vehicle-mounted concrete mixers.

Rich literature on the subject, e.g. [3, 7–9, 13], includes the analyses of many queuing systems, ‘open’ systems with an infinite source of customers, and with a source limited to N units circulating within a closed system. The processes of arrivals and servicing can be described with both typical theoretical distributions and with random distributions. There are systems with one or many parallel channels, with unlimited queues, or with ‘impatient customers’ who do not join queues that are too long or resign from service in the event of too long a waiting time.

In the case of cooperation between site teams (e.g. a crew with equipment) with transport units functioning in a closed cycle, which immediately leave and carry out the next delivery after unloading at the site, or in the case of loading material (e.g. soil) and immediately removing it and returning for another load to be removed, the $M/M/m/FIFO/N/F$ queuing system is applied. According to the notation by Kendall and Lee [8], such a model means

a queuing system with Markov process related to the circulation time (corresponding to the time where the customer remains outside the system, that is time interval from the customer's leaving the system until his return to the system), and also with Markov process related to the servicing time, with the station featuring m service channels, queue according to the FIFO model (where customers are serviced in the order of arrival), and with N units functioning in a closed cycle F . The model, therefore, assumes that the processes of circulation and servicing meet the conditions of being stationary, memoryless and independent [7–9].

Furthermore, it was adopted that the intensity of the stream of customers amounts to $\lambda = \frac{1}{\bar{t}}$, where \bar{t} refers to the average time that customers remaining outside the system, and μ refers to the intensity of the servicing stream, and where $\rho = \frac{\lambda}{\mu}$, $\rho < 1$.

According to [8], the probability of the service apparatus being idle amounts to:

The probability p_i and p_k of having i and k customers in the system amounts to [35]:

$$p_0 = \left(\sum_{i=0}^m \frac{N!}{i!(N-i)!} \rho^i + \sum_{k=m+1}^N \frac{N!}{m!(N-k)!m^{k-m}} \rho^k \right)^{-1} \quad (1)$$

$$p_i = \frac{N!}{i!(N-i)!} \rho^i p_0, \quad i=1, \dots, m, \quad (2)$$

$$p_k = \frac{N!}{m!m^{k-m}(N-k)!} \rho^k p_0, \quad k=m+1, \dots, N, \quad (3)$$

In cases where $I = 0$, the service apparatus is idle, and there is no customer in the system, while in the case of $1 \leq i \leq m$, i customers are being serviced while the queue status still equals 0. It is only in the case of $m+1 \leq k \leq N$ that m customers are serviced, while $k-m$ wait in the queue.

The average number of customers q waiting in the queue is calculated according to the following formula [3, 7–9]:

$$q = \sum_{j=0}^{N-m} j p_{m+j} = \frac{N!}{m!} p_0 \sum_{j=0}^{N-m} \frac{j}{m^j (N-m-j)} \rho^{m+j}. \quad (4)$$

3. The queuing model for orders directly after unloading

When analysing the supply and unloading of concrete mix at a building site, apart from the organisation where N concrete mixers circulate in a closed cycle, other solutions can be applied with 'ordering deliveries directly after unloading'. In order to describe the organisation with 'ordering deliveries...', one can apply the $M/M/N/-/N$ queuing system.

Let us assume that we have N transport units (concrete mixer trucks), while the time of loading the mix, transportation to the site, and unloading/pumping are independent random

variables with exponential distributions and with average values of $\frac{1}{\lambda}$ and $\frac{1}{\mu}$, respectively, whereas $\rho = \frac{\lambda}{\mu}$, $\rho < 1$.

Assume $p_j(t)$ is the probability of a situation where at time t , there is a 'surplus' of i concrete mixers ahead of the pump. Directly after unloading each delivery, another delivery is ordered, with the immediate loading of another concrete mixer at the production plant and its transport to the site. Therefore, the sum of transport units at the site and those ordered equals the maximum number N .

When analysing the graph of transitions presenting the evolution of the number of concrete mixers at the site, three characteristic cases can be observed (Fig. 1), [8, 9]:

- ▶ no surplus, 0 transport units to be unloaded, $i = 0$;
- ▶ the number of units ahead of the pump amounts to i , $i = 1, \dots, N - 1$;
- ▶ the number of units amounts to N , $i = N$.

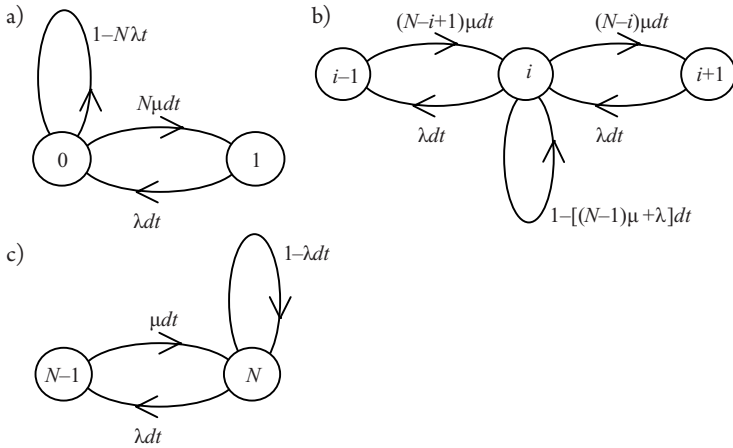


Fig. 1. Characteristic states of inventories: a – for $i = 0$; b – for $i = 1, \dots, N - 1$; c – for $i = N$, [8]

If the number of ongoing orders substitutes the surplus volume, the order of status numbering is reversed and we receive the $M/M/N/-/N$ model, namely for $m = N$ [8].

In such case, in the steady state, probability of service apparatus idle state amounts to the following:

$$p_0 = \lim_{t \rightarrow \infty} p_0(t) = \frac{\rho^N}{\sum_{j=0}^N \rho^j} \tag{5}$$

The average number of concrete mixers unloaded within a time unit amounts to:

$$Q = \lambda(1 - p_0), \tag{6}$$

while the average number of transport units at the site amounts to:

$$\bar{n} = \sum_{j=1}^N j p_j, \quad (7)$$

whereas the average number of orders (loading commencements) in a time unit can be determined on the basis of the following relation:

$$\mu(N - \bar{n}) = \lambda(1 - p_o). \quad (8)$$

4. Guaranteed delivery and pumping time and direct costs

In the analysed systems, $M/M/m/FIFO/N/F$ and $M/M/N/-/N$, the operation of concrete mixer trucks and pumps is interpreted with Markov processes referring to arrivals and servicing. Furthermore, the exit process complies with exponential distribution:

$$f(t) = \lambda e^{-\lambda t}, \quad t \geq 0, \quad (9)$$

with the cumulative distribution function:

$$F(t) = 1 - e^{-\lambda t}, \quad t \geq 0. \quad (10)$$

After transformation and taking logs, the following is obtained:

$$\lambda t = \ln \frac{1}{1 - F(t)}. \quad (11)$$

Value t – the longest duration of delivery/pumping τ_{dp} can be calculated after substitution of the cumulative distribution function $F(t)$ with the required probability level to be guaranteed to observe t , and of $\frac{1}{\lambda}$ with the average number Q of concrete mixers unloaded by the pump at the site.

The most favourable number of transport units (N) for the concrete laying team with the pump can be determined by minimising the total direct costs resulting from the operation of the servicing system, and additionally, from the increase of the unit cost of the concrete mix with the increased time of the start of setting τ_{pw} (required to meet the terms of high guarantee).

The sum of the direct costs of system operation and the increased cost of the mix per load amounts to:

$$K_b = \frac{K_{bp} + \bar{n}K_b + k_m(t)}{Q}, \quad (12)$$

where, according to [16–18]:

- K_{bp} – cost per machine hour of mix pump operation, $K_{bp} = €57 / \text{h}$;
- K_{bm} – cost per machine hour of concrete mix rental, $K_{bm} = €36 / \text{h}$;
- \bar{n} – average number of customers in the system, according to (7);
- $k_m(t)$ – additional unit cost due to application of the mix with increased time of commenced setting, $t < \tau_{pw}$, $k_m(0 < t \leq 3) = 0$, $k_m(3 < t \leq 12) = (\text{€}2,22 \text{ per commenced } 0.5 \text{ hour})$,
- Q – average number of unloading procedures per hour of team operation, according to (3.4).

5. Exemplary results of calculations according to M/M/N/-/N and M/M/1/FIFO/N/F models

The example uses data acquired from the empirical measurements of concrete laying for the span of the trestle at the crossing of Wielicka and Powstańców Śląskich i Wielkopolskich Streets in Krakow, where 1057 m^3 concrete mix was used – this was delivered through the city streets in concrete mixer trucks with a nominal capacity of 8 m^3 from a plant situated 7.5 km away from the site. The following average time values were determined [16]:

- ▶ loading at the concrete plant and transport of mix to the site (31 minutes, 53 seconds), $\frac{1}{\lambda} = 0.531389 \text{ h}$;
- ▶ circulation' (according to section 2, including the passage of the vehicle for the mix, its loading and return to the site – 50 minutes, 20 seconds) $\frac{1}{\lambda^*} = 0.838885 \text{ h}$;
- ▶ pumping of the mix from each delivery (16 minutes, 44 seconds), $\frac{1}{\mu} = 0.278833 \text{ h}$.

Two solutions are analysed below:

- ▶ organization I, described by model $M/M/N/-/N$, with 'deliveries directly after unloading', where loading of the next transport unit at the plant begins immediately after completion of the unloading of the concrete mixer at the site, after automatic sending of such information, for example, using *RFID* system;
- ▶ organization II, described by model $M/M/1/FIFO/N/F$, using N transport units circulating in a closed circuit (in a 'self-regulating circuit').

5.1. Results of calculations in the case of deliveries directly after completion of unloading

For the above data: $\lambda = 3.586372$; $\mu = 1.881861$; $\rho = 1.905758$; and for $N = 1, \dots, 10$, when applying the $M/M/N/-/N$ model, according to formulas (5-7), probability was calculated of idleness of the service apparatus p_0 , average numbers of transport units at the site \bar{n} and average numbers of concrete mixers unloaded in time unit Q have been presented in Fig. 2 According to (11, 12), average values were calculated for delivery/pumping times $\bar{\tau}_{dp}$, as

well as the greatest (limit) durations $\tau_{dp,90\%}$, $\tau_{dp,95\%}$, $\tau_{dp,99\%}$ and direct costs $K_{b,90\%}$, $K_{b,95\%}$, $K_{b,99\%}$, which were not exceeded at the levels of probability of 90%, 95%, 99%, respectively.

When analysing the calculation results, the lowest direct costs (considering the cost related to increase in the time of cement setting commencement) of using three concrete mixers are recorded for the solution. In this case, the cost is minimal and amounts to $K_{b,95\%} = \text{€}38.08$ per delivery/unloading. This is with a 95% guarantee of not exceeding the duration of delivery/pumping amounting to $\tau_{dp,95\%} = 2.06$ hours (from when the cement is mixed with water at the concrete plant until the end of pumping the mix at the site). The probability of pump idleness in such a case amounts to $p_o = 0.1963$, while the average length of the queue is $q = 0.66$.

In the case of using a greater number of transport units, the probability of pump idleness intensely decreases, for example, at $N = 4$ transport units, the probability of pump idleness amounts to $p_o = 0.085$. The application of four concrete mixer trucks, however, is related to the prolongation of concrete mixer trucks waiting for unloading by, on average, 0.17 h, and to the unfavourable share of long servicing, e.g. greater than $\tau_{dp,95\%} = 2.59$ h, which then occur with the probability of 5%.

Therefore, in the existing conditions, the most favourable solution is the solution using $N = 3$ concrete mixers.

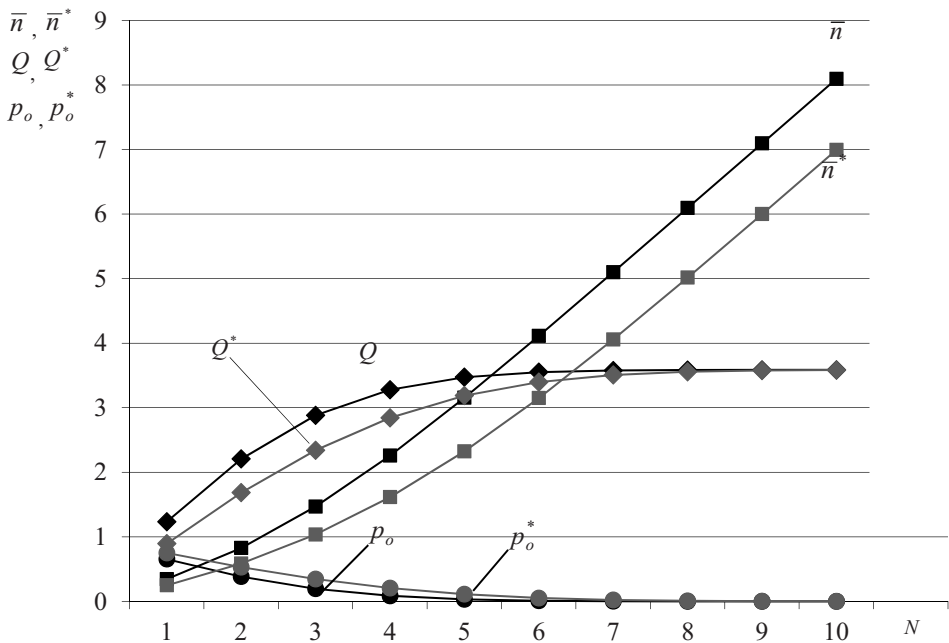


Fig. 2. Variability: p_o , p_o^* – of probabilities of pump idleness; \bar{n} , \bar{n}^* – average numbers of transport units at the site; Q , Q^* – average numbers of concrete mixers unloaded during a time unit; respectively according to models $M/M/N/-/N$ and $M/M/1/FIFO/N/F$, depending on the number N of transport units (own study)

5.2. Results relating to concrete mixer vehicles operating in closed circuits

When creating large monoliths, solutions are often applied in which N concrete mixers operate in a closed circuit – immediately after unloading, each unit drives to the concrete plant where the mix is loaded and it then returns to the site. This is an operational scheme that can be described with typical a queuing system: $M/M/1/FIFO/N/F$. In this case, for the data as above $\lambda^* = 1.192058$, $\mu^* = 3.586372$, $\rho^* = 0.332385$; the characteristics of the model were calculated according to formulas (1–4) have been presented in Fig. 4.

Calculated according to $M/M/N/-/N$ and $M/M/1/FIFO/N/F$, particular model characteristics reveal very clear differences, mainly at small N values. In the case of the most favourable solution with the application of the $M/M/N/-/N$ model (with delivery ordering directly after unloading) at $N = 3$ concrete mixers, efficiency Q has much greater values, with smaller values of pump idleness probability p_0 and lower direct costs of system operation K_b , than the values of Q^* , p_0^* , and K_b^* obtained in the model $M/M/1/FIFO/N/F$. Therefore, it is determined that in the case of creating large monoliths using concrete mixers, it is more favourable to apply the solution with deliveries directly after unloading, namely in the case of functioning according to the $M/M/N/-/N$ model, rather than applying the organisation with N transport units operating (without control) in the closed cycle, according to the $M/M/1/FIFO/N/F$ model.

6. Conclusions

The application of the queuing theory allows for analyses that consider the random variability of the duration of particular processes, in particular, modelling and analysing the cooperation of different groups of workers with transport units, in order to determine the following:

- ▶ guaranteed durations of deliveries/pumping with the assumed probabilities of their observance, as is necessary when planning the execution of concrete works where different batches of the mix must be cast on top of ('or alongside') each other before the cement starts setting.

On the basis of studies of the concrete-laying crew with a pump cooperating with concrete mixers (supplying the mix to the site via municipal roads from the concrete plant situated 7.5 km away), the following conclusions can be reached:

- ▶ it is more favourable to implement the organisation with 'deliveries directly after unloading' (where loading of the next transport unit at the plant begins immediately after completion of unloading of the concrete mixer at the site, after the automatic sending of such information, e.g. using *RFID* system), rather than the organisation using N transport units circulating in the closed circuit (in the 'self-regulating circuit');
- ▶ in such cases, the efficiency of cooperating site and transport units is greater, while the probability of pump idleness is smaller, and the direct costs of building production are lower as a result of the shorter waiting time for the unloading of vehicles with the mix at the site and the longer waiting time of unloaded concrete mixers at the plant.

References

- [1] Abdelhamid T.S., El-Gafy M., Salem O., *Lean Construction: Fundamentals And Principles*, American Professional Constructor Journal 2008.
- [2] Akhavian R., Behzadan A.H., *Evaluation of queuing systems for knowledge-based simulation of construction processes*, Automation in Construction, 7/2014, 37–49.
- [3] Asmussen S., *Applied Probability and Queues*, Springer-Verlag, New York-Berlin Heidelberg 2010.
- [4] Belniak S. et al., *Zastosowanie metod matematycznych w wybranych problemach zarządzania w budownictwie*, Wydawnictwo Politechniki Krakowskiej, Kraków 2015.
- [5] Carmichael D.G., *Shovel-truck queues: a reconciliation of theory and practice*, Construction Management and Economics, 4(2) 1986, 161–177.
- [6] Farid F., Koning T.L., *Simulation Verifies Queuing Program for Selecting Loader-Truck Fleets*, Journal of Construction Engineering and Management, 120(2) 1994, 386–404.
- [7] Filipowicz B., Dzikowska K., *Systemy i sieci kolejkowe w przykładach i zadaniach*, Wydawnictwo ABART, Kraków 2008.
- [8] Filipowicz B., *Modele stochastyczne w badaniach operacyjnych*, Wydawnictwa Naukowo-Techniczne, Warszawa 1996.
- [9] Gross D., Shortle J.F., Thompson J.M., Harris C.M., *Fundamentals of Queuing Theory*, John Wiley & Sons Inc., Hoboken, New Jersey 2008.
- [10] Jamróży Z., *Beton i jego technologie*, Wydawnictwo Naukowe PWN, Warszawa 2015.
- [11] Jaworski K., *Metodologia projektowania realizacji budowy*, Państwowe Wydawnictwo Naukowe, Warszawa 2009.
- [12] Lu M., Shen X., Chen W., *Automated Collection of Mixer Truck Operations Data in Highly Dense Urban Areas*, Journal of Construction Engineering and Management, 135(1) 2009, 17–23.
- [13] Sadeghi N., Robinson F.A., Gerami S.N., *Queue performance measures in construction simulation models containing subjective uncertainty*, Automation in Construction, 60/2015, 1–11.
- [14] Więckowski A., *Sozjoekonomiczny model realizacji procesów cyklu obiektu budowlanego*, Monografia 246, Politechnika Krakowska, Kraków 1999.
- [15] Więckowski A., *Principles of the NNM method applied in the analysis of process realisation*, Automation in Construction, Elsevier Science BV, 11(4) 2002, 409–420.
- [16] Więckowski A., *System bezmagazynowej pracy jednostek budowy i transportu*, Politechnika Krakowska, Monografia 375, Kraków 2010.
- [17] Więckowski A., *Transport mieszanek betonowej*, Wydawnictwo Politechniki Krakowskiej, Kraków 2013.
- [18] Więckowski A., *The analysis of the concrete mix delivery organisation to the construction site*, Creative Construction Conference, Budapest, Hungary 2013, 472–481.
- [19] Więckowski A., Skibniewski M., *Errors of Calculations in M/M/1/FIFO/N/F Model with Limited Duration of Shift*, The 25th International Symposium on Automation and Robotics in Construction, Vilnius 2008, 708–716.

Maciej Knapik (maciek.knapik@gmail)

Institute of Water Supply and Environmental Protection, Faculty of Environmental Engineering, Cracow University of Technology

ANALYSIS OF INFLUENCE OF LEED CERTIFICATION PROCESS TO ACHIEVE THE PASSIVE HOUSE STANDARD

ANALIZA WPŁYWU PROCESU CERTYFIKACJI LEED NA UZYSKANIE STANDARDU BUDYNKU PASYWNEGO

Abstract

The article presents an analysis of influence of the LEED certification process to achieve the passive house standard of the building. The purpose of LEED certification is to reduce building energy consumption, water consumption and to reduce building impact on the environment. The passive building is characterized by low energy demand of 15 kWh/(m²*year). Passive buildings are the result of introducing new ideas in the design process of buildings. This article presents the results of the analysis based on example objects. The results show that the LEED certification significantly influences the achievement of the passive building standard.

Keywords: LEED certification, energy consumption of the building, passive house

Streszczenie

Artykuł przedstawia analizę wpływu procesu certyfikacji LEED na osiągnięcie przez budynek standardu budynku pasywnego. Celem certyfikacji LEED jest zmniejszenie energochłonności obiektu, zużycia wody oraz zmniejszenie jego wpływu na otoczenie. Budynek pasywny charakteryzuje się niskim zapotrzebowaniem na energię wynoszącym 15 kWh/(m²*rok). Budynki pasywne są wynikiem wprowadzenia nowych idei w procesie projektowania budynków. Artykuł przedstawia wyniki analizy na podstawie przykładowych obiektów. Wyniki pokazują, że certyfikat LEED w znaczny sposób wpływa na uzyskanie standardu budynku pasywnego.

Słowa kluczowe: certyfikat LEED, energochłonność budynku, budynek pasywny

1. Introduction

The passive house standard has been set by Dr. Wolfgang Feist from the Institute of Passive Houses, Passivhaus Institut in Darmstadt. Dr. Feist said that a passive house is a building with a very low energy demand for interior heating like $15 \text{ kWh}/(\text{m}^2 \cdot \text{year})$, in which thermal comfort is ensured by passive heat sources (like residents, electrical devices, solar heat, heat recovered from the ventilation), so that the building does not need a separate active heating system. Heating demand is realized by heat recovery and reheating the air ventilating the building [1].

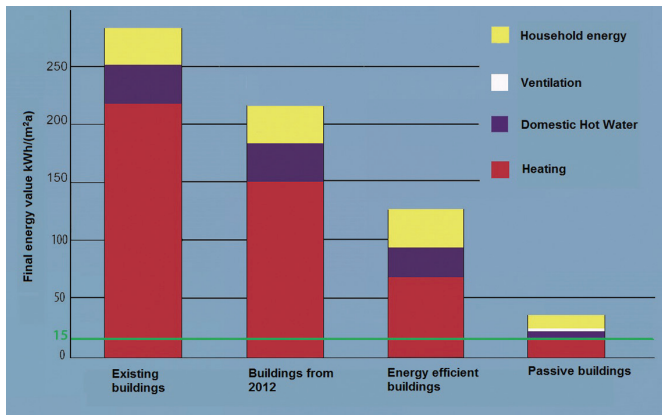


Fig. 1. Energy demands for buildings (source: [2])

By definition passive houses are environmentally friendly. Other buildings can also be environmentally friendly in case of pro-ecological certification, for example, such as LEED certification.

LEED certification – Leadership in Energy and Environmental Design is a rating system devised by the United States Green Building Council (USGBC) to evaluate the environmental performance of a building and encourage market transformation towards sustainable design, which is based on ASHRAE Standard 90.1–2010 [3]. The system is credit-based, allowing projects to earn points for environmentally friendly actions taken during construction and use of a building [4].

Of all the available types of LEED certification, we can specify LEED for Homes. LEED for Homes – is a standard for the design and construction of high performance “green” homes. A green home uses less energy, water, and natural resources; creates less waste; and is healthier and more comfortable for the occupants. The process of the LEED for Homes Rating System, available in the USA, Canada and Sweden is significantly different from the LEED New Constructions rating system. LEED for Homes projects are low rise residential and are required to work with either an American Provider Organization or a Canadian Provider Organization and a Green Rater. Green Raters are individuals that conduct the two mandatory LEED for Homes site inspections: the Thermal Bypass Inspection and the Final Inspection [5, 6].

2. Passive constructions

Passive constructions are characterized by low energy demand for heating purposes. Lower energy demand is a result of better parameters of the building envelopes. For example, heat losses can be reduced through the use of appropriate technology wall insulation, where the heat transfer coefficient U for the exterior wall of the passive building should be less than $0.15 \text{ W}/(\text{m}^2 \cdot \text{K})$.

Passive building is also characterized by better standards of thermal comfort. As noted, the measured temperature difference in different room locations are not higher than $0.8 \text{ }^\circ\text{C}$ and the difference in temperature distribution between the head and the feet of the sitting person does not exceed $2 \text{ }^\circ\text{C}$.

An important aspect of thermal comfort is the ventilation. Effective ventilation provides a feeling of comfort in the winter and allows cooling the incoming fresh air during the summer.

As a result of the lower energy demand, passive buildings are characterized by lower consumption of fossil fuels, which reduces the environmental impact.

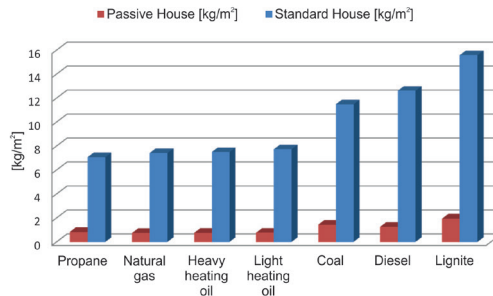


Fig. 2. Comparison of fuel requirements for passive and house, built in 2012 (own study)

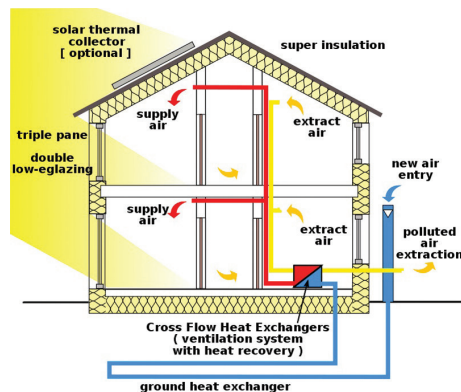


Fig. 3. The use of solar energy (source: [8])

Passive buildings try to use the heat gains from the sun in the maximum way. One of the ways to use heat gains from the sun is heating the ventilation air.

First of all, fresh air is heated up in a ground heat exchanger, afterwards this air is heated up in a heat exchanger in the air handling unit. The air supply from the air handling unit is

supplied to the rooms from the southern part of the building, where this air is heated up the air is heated up by the sun's rays passing through the triple-glazed windows. The heated air is transported to rooms on the north side of building and from there extracted through the heat exchanger and it is removed outside [7].

3. Sample of single family house – basic heat losses calculations

For analysis purposes basic calculations of the heat losses and energy demand for a standard single-family building from 2012 have been prepared. All calculations were performed in the program OZC to the heat loss calculations based on PN-EN 12831 [9].

Table 1. Basic results of heat losses and annual heat demand for heating calculations (own study)

Basic heat losses calculations		
Heated area of the building A_h :	174.8	m^2
Design heat load of the building Φ_{HL} :	13 598	W
Indicators and coefficients heat losses:		
Indicator Φ_{HL} related to area ϕ_{HL}, A :	77.8	W/m^2
Indicator Φ_{HL} related to cubature ϕ_{HL}, V :	28.5	W/m^3
The results of calculations of seasonal demand for energy E:		
Weather station:	Kraków	
Annual heat demand for heating Q_h :	71	$kWh/(m^2 \cdot year)$

According to the calculations of the annual energy demand for heating, the building is in the scope of energy efficient building, but this is already the upper limit. In order to achieve the passive house standard, the designer should introduce some innovations that will reduce the demand for heat.

It should be remembered that the above calculations relate to the building in the design phase, because the LEED certification process starts with the design phase, when it should make some decisions regarding the further design development. It should also be remembered that the start of the LEED certification process after the design phase does not close the way to receive a certificate, but significantly reduces the possibility of obtaining a higher point result.

In the design phase important decisions are made regarding future investments, improvements or innovations in the scope of LEED certification. Also in this phase the main goal – what kind of certificate will be achieved – is established.

4. LEED for Homes Scoreboard [4]

Scoring in the LEED certification process is divided into several sections. Each section focuses on a different scope, but each of them has the same goal –making the building more environmentally friendly.

The maximum number of points in the LEED certification process is 110, as shown in Table 3. In order to bring the building to the passive house standard, the highest number of points from the section Energy&Atmosphere should be achieved.

In the simple statistics, compared to the other sections Energy & Atmosphere section is the most expensive for investments, which will be significant in the further analysis.

The main task of **Integrative Processes** is to maximize opportunities for cost-effective adoption of integrative green design and construction strategies. This can be achieved easily and cheaply by hiring the appropriate team and organizing the appropriate workshops to integrate green strategies across all aspects of design.

Points in the Location and Transportation section depend on the location of the building and whether the building has access to public transportation or public buildings. A well-located facility will be able to obtain LEED points easily.

Sustainable Sites are focused on design solutions for limitation of the heat island effect, rainwater management or reduction of activity of pests. There are also known inexpensive ways to obtain LEED points in this section.

The **Water Efficiency** section is focused on reducing water consumption. There are many reasonably priced solutions reducing water consumption, such as electromagnetic valves or the appropriate metering of water supply points.

The main task of Materials and Resources are to make building more environmentally friendly by using materials important for sustainable homebuilding because of the extraction, processing, and transportation they require. An important aspect of this section is the construction waste management during the construction to find another use for this waste, for example in another construction. Environmentally friendly materials are more expensive, but still not as expensive as investments related to section Energy&Atmosphere.

Indoor Environmental Quality applies to comfort in the broad sense. Comfort means here an increased ventilation and supply of fresh air, control of air quality, proper management of heating and cooling or garages protection against air pollution with increased ventilation to remove these contaminants.

Innovation and **Regional Priority** relate to the introduction of innovative design solutions and use of materials from local producers.

5. LEED Energy&Atmosphere [4]

The Energy & Atmosphere section applies to all aspects in order to reduce the energy consumption in the building.



Table 2. Energy & Atmosphere Scoreboard (source: [4])

ENERGY & ATMOSPHERE		POSSIBLE: 38
Prereq	Minimum energy performance	REQUIRED
Prereq	Energy metering	REQUIRED
Prereq	Education of homeowner, tenant, or building manager	REQUIRED
Prereq	Home size	REQUIRED
Credit	Annual energy use	29
Credit	Efficient hot water distribution system	5
Credit	Advanced utility tracking	2
Credit	Active solar-ready design	1
Credit	HVAC Start-up credentialing	1
Credit	Building orientation for passive solar	3
Credit	Air infiltration	2
Credit	Envelope Insulation	2
Credit	Windows	3
Credit	Space heating and cooling equipment	4
Credit	Heating and cooling distribution systems	3
Credit	Efficient domestic hot water equipment	3
Credit	Lighting	2
Credit	High-efficiency appliances	2
Credit	Renewable energy	4

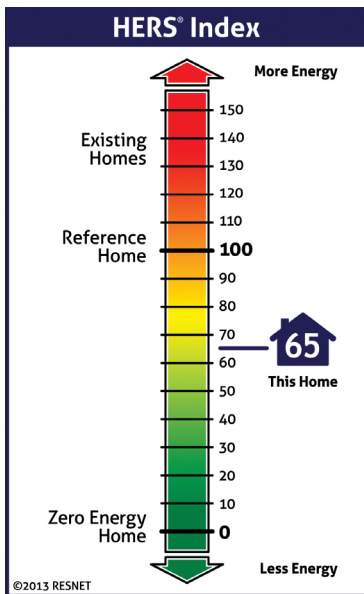


Fig. 4. HERS index (source: [19])

This section has two paths: Performance path and Prescriptive path. The Performance path is less specific and is based on the energy performance of the building. In the case of LEED certification it is a HERS [10, 11] index.

From the other side, the Prescriptive path is more detailed and more accurately describes what LEED points can be awarded for. This method gives specific guidance on how to proceed in the design phase. However, the Performance path is more easy to execute because it does not impose design solutions. It focuses on the final result of energy performance. A crucial indicator is the above mentioned HERS index.

How to understand the HERS index? This can be described with a simple example house whose index is 70. This means that the building is 30% more energy efficient than the reference building RESNET. For the building whose HERS index is 130, it is less energy efficient than the reference building RESNET by 30%. (RESNET – Residential Energy Services Network) [11].

If a sample family house, for which calculations have been made, will be considered as the reference home with the received results of the annual heat demand for heating which amounts $71 \text{ kWh}/(\text{m}^2 \cdot \text{year})$, in order to achieve the passive house standard, design solutions should allow a HERS index of 20 to be achieved. Each 1-point decrease in the HERS Index corresponds to a 1% reduction in energy consumption compared to the HERS Reference

Home. In order to achieve the passive standard ($15 \text{ kWh}/(\text{m}^2 \cdot \text{year})$), annual heat demand for heating in the analysed case should be reduced by 80%. Reduction of annual heat demand for heating from 71 to $15 \text{ kWh}/(\text{m}^2 \cdot \text{year})$, amounts to 80%. The number of LEED points depending on the achieved HERS index is shown in Figure 5. The first points can be obtained for an index value of 70, and the maximum number of points, that is 29, for a HERS index of 0.

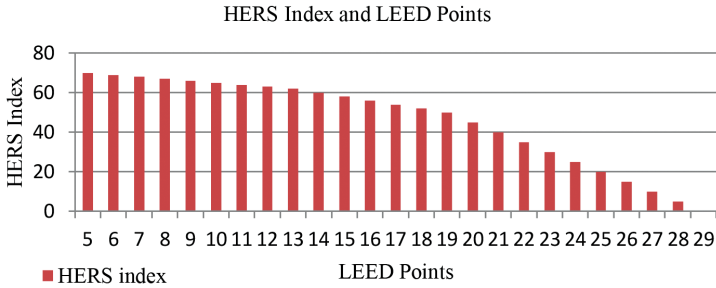


Fig. 5. HERS Index & LEED points (own study)

6. Design solutions

What should be implemented to make a building more energy efficient [12]? First of all, a highly efficient mechanical ventilation with heat recovery and the use of heat gains from the sun should be designed. In order to illustrate the scheme of mechanical ventilation in the passive building, please refer to illustration 1. The design of mechanical ventilation reduces energy demand for heating by 20–30%.

The use of high quality insulation and triple glazed windows reduces the energy demand for heating by 10 to 15% counting from the existing state. The main goal of this is to minimize the heat transfer coefficient U for each building envelope. The more this coefficient is reduced the better this effect will be. Figure 6 shows a cross section through a typical external wall of a passive building [7].

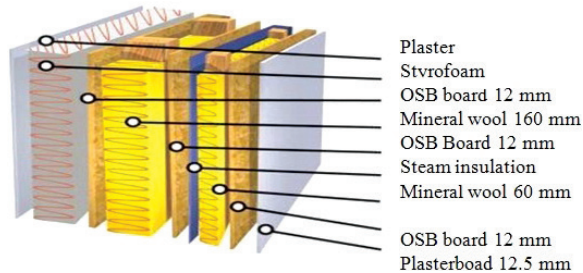


Fig. 6. Typical external wall cross section for passive building (source: [20])

Another important aspect of the improvement of energy performance of the building is to minimize the effect of thermal bridges. A thermal bridge, also called a cold bridge or heat

bridge, is an area of an object (frequently a building) which has a significantly higher heat transfer than the surrounding materials resulting in an overall reduction in thermal insulation of the object or building [13]. Thermal bridges occur in three ways, through: materials with higher thermal conductivity than the surrounding materials [14], penetrations of the thermal envelope, and discontinuities or gaps in the insulation material.

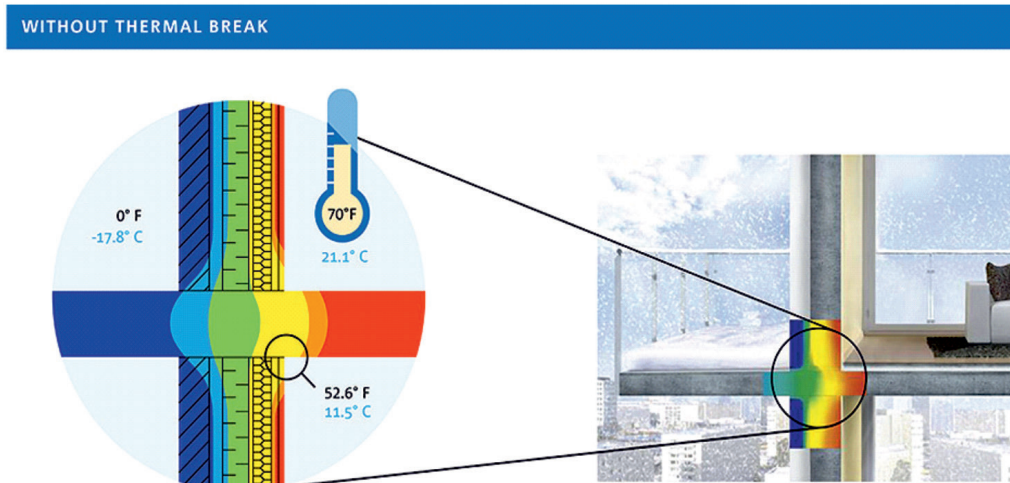


Fig. 7. Influence of thermal bridges at room temperature (source: [15])

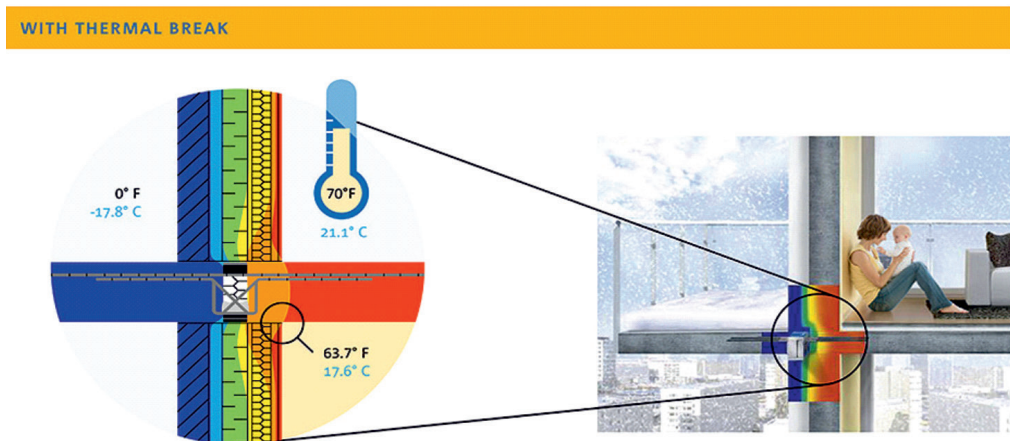


Fig. 8. Influence of thermal bridges at room temperature after use of thermal breaks (source: [15])

Designers in order to limit the influence of thermal bridges should design Thermal breaks. A thermal break is an element of low thermal conductivity placed in an assembly to reduce or prevent the flow of thermal energy between conductive materials [16].

As shown in Figure 1, in passive and energy efficient buildings, can be seen an increased energy demand for domestic hot water in relation to the energy needed for heating. In this

case, the designer needs to provide solutions to reduce the energy demand for domestic hot water through the use of renewable energy sources. An example of the use of renewable sources of energy is the cooperation of the small wind turbines and photovoltaic cells. This system is mono energetic, it means that there is only one source of energy, electricity, which is converted into thermal energy by warmer in the domestic hot water tank. In the months in which the energy production exceeds the demand, energy can be partly stored in batteries or used to power fans of mechanical ventilation. For example using water solar collectors do not have the possibility of a longer heat storage in summer and there is an increased risk of overheating the water in the water tank. A system based on electricity is more preferable. It should also be noted that the production of energy from wind turbines and photovoltaic cells is determined by the weather. In the winter months it is windier, but the winter months are characterized by lower solar radiation, thus the wind turbines produces more power compared to the photovoltaic cells. In the summer months it is the opposite. There is no wind, and the solar radiation is the highest throughout the year.

In this case, in the summer months, the production of energy from photovoltaic cells is much higher than the production of energy from wind turbines.

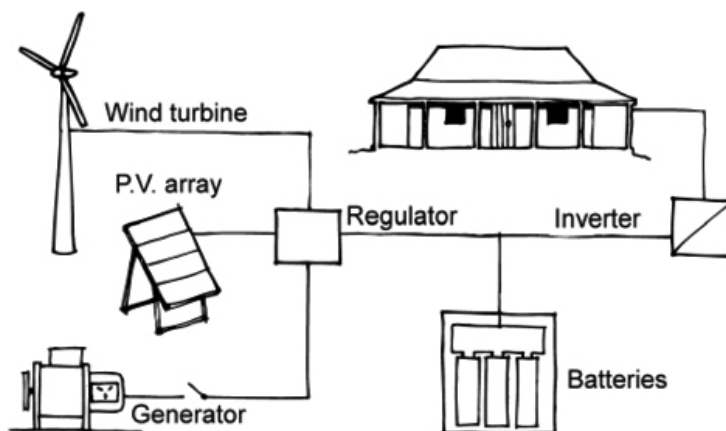


Fig. 9. Example of system generating electricity using a wind turbine and a photovoltaic cell (source: [17])

An important element in energy saving is the BMS –Building Management System, which is the central nervous system of the energy efficient building. The BMS is a fully automatic system, which controls energy consumption in the building. The tasks of the BMS are the optimization of all systems so that energy consumption is adequate for current needs. For example, BMS controls the lighting so that the lighting intensity is adjusted to current external conditions and in rooms using motion sensors. Mechanical ventilation is based on CO₂ sensors, so that if there are no users in the home, the ventilation is running at a minimum level or is completely switched off. Energy from renewable energy sources is stored, used for hot water needs or household appliances, all depending on building needs will be controlled by the BMS, which will optimize the use of energy.



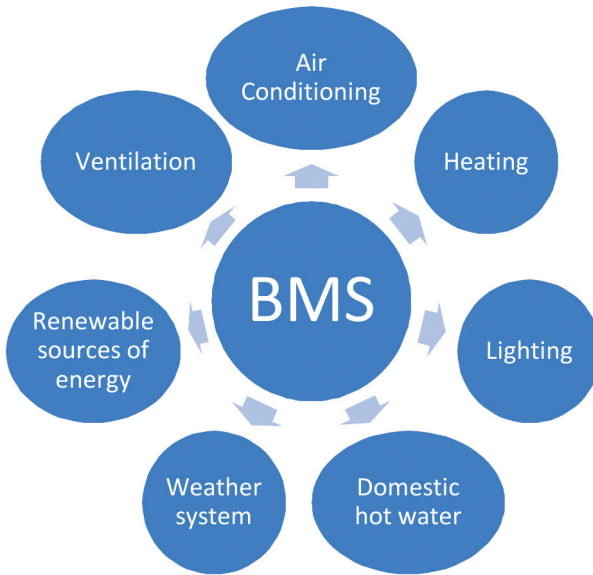


Fig. 10. BMS controls all building systems (own study)

7. LEED implementation costs

All environmentally friendly solutions are associated with higher investment costs, but in the long term investment brings tangible benefits to our environment.

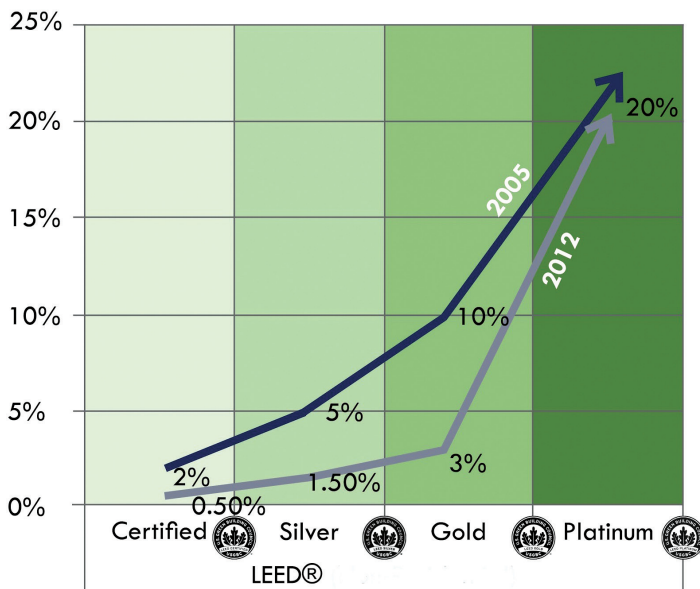


Fig. 11. The increase in investment costs, depending on the LEED certification, in 2005 and 2012 (source: [18])

On the example of LEED certification and analysis of the costs of execution of several projects, a chart was prepared that shows how much on average the basic cost of the project increases without innovation, depending on the introduced certificate.

Figure 10 applies only to small residential buildings (LEED for Homes), this does not relate to larger developments like offices or other commercial buildings, because the costs of LEED implementation in other buildings than homes is relatively higher. Investing about 20% more, we have a chance to receive LEED Platinum, and also increase your chances of achieving the passive house standard. The most expensive section of LEED for Homes is the above-mentioned section Energy & Atmosphere. Building can be of course certified by LEED Platinum without major investment in this section, but then it will significantly limit the ability to achieve the passive house standard.

Analysis of the influence of the Energy & Atmosphere section (and in total LEED certification process) to achieve passive house standard will be presented in the next section.

8. Analysis of influence of LEED certification process in achieving the passive house standard

Table 3. LEED for Homes Scoreboard (source: [4])

Credit		Points
Integrative Process		2
Location and Transportation		15
Sustainable Sites		7
Water Efficiency		12
Energy and Atmosphere		38
Materials and Resources		10
Indoor Environmental Quality		16
Innovation		6
Regional Priority		4
TOTAL	Possible Points:	110
Certified: 40 to 49 points, Silver: 50 to 59 points, Gold: 60 to 79 points, Platinum: 80 to 110		

The point of the baseline analysis was to determine the probability of obtaining a point in the section. The probability of obtaining a point was created on the basis of several projects that have received LEED certification. The probability changes depending on the kind of LEED certificate. The results obtained are summarized in table 4. To clarify – **Prob.** means the probability of obtaining a point (It depends on the design, the investment costs, materials used, the project execution phase and the type of certificate. The probability increases with the type of certificate because it requires more complex design solutions, which will reduce



energy consumption). **P.** represents the probable amount of LEED points obtained in each Section and **HERS** is a HERS Index, which shows much energy efficient the building is.

Table 4. Probability of obtaining a LEED points (own study)

Prob.	P.	HERS	Prob.	P.	HERS	Prob.	P.	HERS	Prob.	P.	HERS
1	2	30 % More energy efficient building	1	2	31 % More energy efficient building	1	2	35 % More energy efficient building	1	2	70 % More energy efficient building
0.33	5		0.5	8		0.6	9		0.7	11	
0.33	3		0.55	4		0.6	5		0.7	5	
0.33	4		0.55	7		0.6	8		0.7	9	
0.13	5		0.15	6		0.25	10		0.6	23	
0.5	5		0.55	6		0.6	6		0.75	8	
0.33	6		0.4	7		0.6	10		0.7	12	
1	6		1	6		1	6		1	6	
1	4		1	4		1	4		1	4	
LEED Certified	40		LEED Silver	50		LEED Gold	60		LEED Platinum	80	
40		50		60		80					

As shown in the table, the lowest probability is characterized by section Energy & Atmosphere due to higher investment costs. How do the results impact on achieving the passive building standard?

The results of the probable amount of points obtained from the section Energy & Atmosphere and using the HERS Index allow to determine the probable chance of receiving passive house standard, comparing the amount of obtained LEED points to the maximum number of points from the Performance Path.

The results of probability of obtaining passive house standard, depending on the type of LEED are presented in Figure 11.

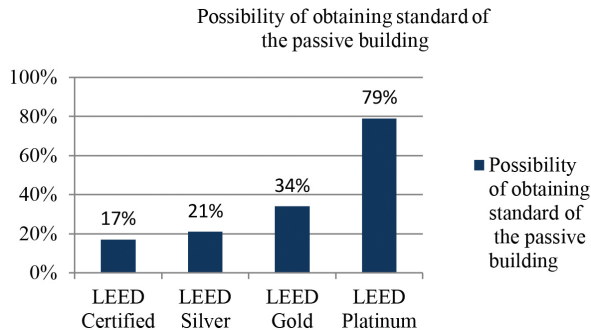


Fig. 12. Probability of obtaining passive house standard (own study)

9. Summary and Conclusions

Passive and low energy buildings are characterized by a lower consumption of fossil fuels, which causes lower emissions to the environment. These buildings are friendlier for the environment by using for example renewable sources of energy and heat gains from the sun. However, the standard of these buildings could not easily be achieved without proper funding. The incentive for this type of investment is LEED certification.

LEED certification significantly helps new constructions, to become more environmentally friendly. LEED certification is responsible for the reduction of energy consumption which is submitted that the building could become the passive building.

The type of certificate which a building will receive depends on the investor and his financial investment, because as demonstrated by the analysis of costs, the basic investment costs could increase by 20%.

Increased investment costs primarily come from the section Energy & Atmosphere, and it is this section that has the largest impact on reducing energy consumption and passivity of the building.

The small demand for points in this section has been confirmed by probability of obtaining LEED points during the certification.

The reasons for increase in investment costs are better insulating properties of partitions, installation of mechanical ventilation, and a complex BMS.

The analysis also showed that the better the kind of certificate, the higher the probability that the building will achieve the passive house standard.

The passive standard of the building depends on many variables, even LEED Platinum certificate does not guarantee passive standard, but it definitely helps to achieve this standard.

The analysis shows that the minimum level to achieve a LEED Platinum, give the probability of obtaining the standard of the passive house at 79%, where the LEED certified probability is 17%.

Even without achieving a passive building standard LEED certification makes the building more environmentally friendly, the more so the higher the certificate type awarded, and it should be also noted that a LEED certificate promotes renewable sources of energy and Building Management Systems, reducing energy consumption.

References

- [1] Feist W., Münzenberg U., Thumulla J., *Podstawy budownictwa pasywnego*, PIBP, Gdańsk 2009.
- [2] *Energy demands for buildings*, <http://www.pibp.pl> (access: 03.04.2016).
- [3] ANSI/ASHRAE/IES Standard 90.1-2016 – Energy Standard for Buildings Except Low-Rise Residential Buildings.
- [4] *What is LEED?, LEED v4 for Homes LEED, solutions*, www.usgbc.org (access: 03.04.2016).



- [5] Reposa J.H. Jr., *Comparison of USGBC LEED for Homes and the NAHB National Green Building Program*, International Journal of Construction Education and Research, Vol. 5, 2009, Issue 2, 108–120.
- [6] Beauregard S.J., Berkland S., Hoque S., *Ever green: A post-occupancy building performance analysis of LEED certified homes in New England*, Journal of Green Building, Vol. 6, Issue 4, 138–145.
- [7] Rylewski E., *Energia własna*, TINTA, Warszawa 2002.
- [8] *The use of solar energy, wall insulation*, <http://www.passiv.de> (access: 03.04.2016).
- [9] PN-EN 12831 – Instalacje ogrzewcze w budynkach. Metoda obliczania projektowego obciążenia cieplnego.
- [10] Fumo N., *A review on the basics of building energy estimation*, Renewable and Sustainable Energy Reviews, Vol. 31, March 2014, 53–60.
- [11] *Residential Energy Services Network (RESNET)*, <http://www.resnet.us> (access: 03.04.2016).
- [12] Knapik M., *Budownictwo proekologiczne*, [in:] OSA, Odpady, Środowisko, Atmosfera, Materiały pokonferencyjne. Referaty. Prezentacje, Müller J. (ed.), Wydawnictwo PK, Kraków 2014, 87–92.
- [13] Gorse Ch.A., Johnston D., *Thermal bridge*, Oxford Dictionary of Construction, Surveying, and Civil Engineering, 3rd ed. Oxford UP, 2012, 440–441.
- [14] Binggeli C., *Building Systems for Interior Designers*, Hoboken, John Wiley & Sons, New York.
- [15] *Solutions to Thermal Bridging. Sustainable Comfort and Efficiency*, www.shock-us.com (access: 03.04.2016).
- [16] Hua G., McClung V.R., Zhang S., *Impact of balcony thermal bridges on the overall thermal performance of multi-unit residential buildings: a case study*, Energy and Buildings, 60, 2013, 163–173.
- [17] *Your Home: Australia's guide to environmentally sustainable home, Batteries and Inventers*, <http://www.yourhome.gov.au> (access: 03.04.2016).
- [18] *What is the Cost of Building Green*, blog.rkinsley.com (access: 03.04.2016).
- [19] Resnet HERS Index, hersindex.com (access: 03.04.2016).
- [20] Proinvest, proinvest.poznan.pl (access: 03.04.2016).

Ludwik Byszewski (lbyszews@pk.edu.pl)

Institute of Mathematics, Faculty of Physics, Mathematics and Computer Science,
Cracow University of Technology

CONTINUOUS DEPENDENCE OF MILD SOLUTIONS, ON INITIAL
NONLOCAL DATA, OF THE NONLOCAL SEMILINEAR EVOLUTION
CAUCHY PROBLEMS

CIĄGŁA ZALEŻNOŚĆ CAŁKOWYCH ROZWIĄZAŃ OD NIELOKALNYCH
WARUNKÓW POCZĄTKOWYCH, NIELOKALNYCH SEMILINIOWYCH
ZAGADNIEŃ CAUCHY'EGO

Abstract

The aim of the paper is to prove two theorems on continuous dependence of mild solutions, on initial nonlocal data, of the nonlocal semilinear evolution Cauchy problems. For this purpose, the method of semigroups and the theory of cosine family in Banach spaces are applied. The paper is based on publications [1–6] and is a generalization of paper [3].

Keywords: semilinear evolution Cauchy problems, continuous dependence of solutions, nonlocal conditions

Streszczenie

W artykule udowodniono dwa twierdzenia o ciągłej zależności rozwiązań całkowych od nielokalnych warunków początkowych, semiliniowych nielokalnych zagadnień Cauchy'ego. W tym celu zastosowano metodę półgrup i teorię rodziny cosinus w przestrzeniach Banacha. Artykuł bazuje na publikacjach [1–6] i jest pewnym uogólnieniem publikacji [3].

Słowa kluczowe: semiliniowe ewolucyjne zagadnienia Cauchy'ego, ciągła zależność rozwiązań, warunki nielokalne

Part I

Continuous dependence of mild solutions, on initial nonlocal data, of the nonlocal Cauchy problem of the first order

1. Introduction to Part I

In this part of the paper, we assume that E is a Banach space with norm $\|\cdot\|$ and $-A$ is the infinitesimal generator of a C_0 semigroup $\{T(t)\}_{t \geq 0}$ on E .

Throughout this part of the paper, we use the notation:

$$I = [0, a], \text{ where } a > 0,$$

$$M = \sup\{\|T(t)\|, t \in I\}$$

and

$$X = C(I, E).$$

Let p be a positive integer and t_1, \dots, t_p be given real numbers such that $0 < t_1 < \dots < t_p \leq a$. Moreover, let C_i ($i=1, \dots, p$) be given real numbers and

$$K := \sum_{i=1}^p |C_i|.$$

Consider the nonlocal Cauchy problem of the first order

$$u'(t) + Au(t) = f(t, u(t)), \quad t \in I \setminus \{0\}, \quad (1.1)$$

$$u(0) + \sum_{i=1}^p C_i u(t_i) = x_0, \quad (1.2)$$

where $f: I \rightarrow E$ and $x_0 \in E$.

In this part of the paper, we shall study a continuous dependence of a mild solution, on initial nonlocal data (1.2), of the nonlocal semilinear evolution Cauchy problem (1.1)–(1.2). The definition of this solution will be given in the next section.

This part of the paper is based on publications [1, 3–6] and generalizes some results from [3] in this sense that, now, we consider semilinear problems in contrast to [3], where linear problems were considered.

2. Theorem about a mild solution of the nonlocal Cauchy problem of the first order

A function u belonging to X and satisfying the integral equation:

$$u(t) = T(t)x_0 - T(t) \left(\sum_{i=1}^p C_i u(t_i) \right) + \int_0^t T(t-s) f(s, u(s)) ds, \quad t \in I, \quad (2.1)$$

is said to be a mild solution of the nonlocal Cauchy problem (1.1)–(1.2).

Theorem 2.1. Assume that:

- (i) $f: I \times E \rightarrow E$ is continuous with respect to the first variable on I and there exists constant $L > 0$ such that

$$\|f(s, z) - f(s, \tilde{z})\| \leq L \|z - \tilde{z}\| \quad \text{for } s \in I, z, \tilde{z} \in E. \quad (2.2)$$

- (ii) $M(aL + K) < 1$.

- (iii) $x_0 \in E$.

Then, the nonlocal Cauchy problem (1.1)–(1.2) has a unique mild solution.

Proof. See [1], Theorem 3.1 and page 28.

3. Continuous dependence of a mild solution, on initial nonlocal data (1.2), of the nonlocal Cauchy problem (1.1)–(1.2)

In this section, there is the main result of Part I.

Theorem 3.1. Let all the assumptions of Theorem 2.1 be satisfied. Suppose that u is the mild solution (satisfying (2.1)) from Theorem 2.1. Moreover, let $v \in X$, satisfying the equation:

$$v(t) = T(t)y_0 - T(t) \left(\sum_{i=1}^p C_i v(t_i) \right) + \int_0^t T(t-s) f(s, v(s)) ds, \quad t \in I, \quad (3.1)$$

be the mild solution to the nonlocal problem:

$$v'(t) + Av(t) = f(t, v(t)), \quad t \in I \setminus \{0\},$$

$$v(0) + \sum_{i=1}^p C_i v(t_i) = y_0,$$

where $y_0 \in I$.

Then, for an arbitrary $\varepsilon > 0$ there is $\delta > 0$ such that if:

$$\|x_0 - y_0\| < \delta \quad (3.2)$$

then:

$$\|u-v\|_X < \varepsilon. \quad (3.3)$$

Proof. Let ε be a positive number and let:

$$\delta := \frac{1 - MK - aML}{M} \varepsilon. \quad (3.4)$$

Observe that, from (2.1) and (3.1),

$$\begin{aligned} u(t) - v(t) &= T(t)(x_0 - y_0) - T(t) \left(\sum_{i=1}^p C_i(u(t_i) - v(t_i)) \right) + \\ &+ \int_0^t T(t-s) (f(s, u(s)) - f(s, v(s))) ds, \quad t \in I. \end{aligned} \quad (3.5)$$

Consequently, by (3.5) and (2.2),

$$\|u-v\|_X \leq M \|x_0 - y_0\| + MK \|u-v\|_X + aML \|u-v\|_X.$$

From the above inequality:

$$(1 - MK - aML) \|u-v\|_X \leq M \|x_0 - y_0\|. \quad (3.6)$$

By (3.6), (3.2) and (3.4),

$$\|u-v\|_X \leq \frac{M}{1 - MK - aML} \|x_0 - y_0\| < \frac{M}{1 - MK - aML} \delta = \varepsilon.$$

Therefore, (3.3) holds. It means that the mild solution of the nonlocal Cauchy problem (1.1)–(1.2) is continuously dependent on the initial nonlocal data (1.2).

The proof of Theorem 3.1 is complete.

Part II

Continuous dependence of mild solutions, on initial nonlocal data, of the nonlocal Cauchy problem of the second order

4. Introduction to Part II

In the second part of the paper, we consider the nonlocal Cauchy problem of the second order:

$$u''(t) = Au(t) + f(t, u(t)), \quad t \in I \setminus \{0\}, \quad (4.1)$$

$$u(0) = x_0, \quad (4.2)$$

$$u'(0) + \sum_{i=1}^p C_i u(t_i) = x_1, \quad (4.3)$$

where A is the infinitesimal generator of a strongly continuous cosine family $\{C(t): t \in \mathbb{R}\}$ of bounded linear operators from the Banach space E (with norm $\|\cdot\|$) into itself, $u: I \rightarrow E$, $f: I \times E \rightarrow E$, $I = [0, a]$, $a > 0$, $x_0, x_1 \in E$, $C_i \in \mathbb{R}$ ($i=1, \dots, p$) and t_1, \dots, t_p are as in Part I.

We will use the set:

$$\tilde{E} := \{x \in E: C(t)x \text{ is of class } C^1 \text{ with respect to } t\}$$

and the sine family $\{S(t): t \in \mathbb{R}\}$ defined by the formula

$$S(t)x := \int_0^t C(s)x ds, \quad x \in E, \quad t \in \mathbb{R}.$$

In this part of the paper, we shall study a continuous dependence of a mild solution, on initial nonlocal data (4.2)–(4.3), of the nonlocal Cauchy problem (4.1)–(4.3). The definition of this solution will be given in the next section.

The second part of the paper is based on publications [2, 3, 5] and generalizes some results from [3] in this sense that, now, we consider semilinear problems in contrast to [3], where linear problems were considered.

5. Theorem about a mild solution of the nonlocal Cauchy problem of the second order

A function u belonging to $C^1(I, E)$ and satisfying the integral equation:

$$u(t) = C(t)x_0 + S(t)x_1 - S(t) \left(\sum_{i=1}^p C_i u(t_i) \right) + \int_0^t S(t-s) f(s, u(s)) ds, \quad t \in I, \quad (5.1)$$

is said to be a mild solution of the nonlocal Cauchy problem (4.1)–(4.3).

Theorem 5.1. Assume that:

- (i) $f: I \times E \rightarrow E$ is continuous with respect to the first variable $t \in I$ and there exists a positive constant $L > 0$ such that:

$$\|f(s, z) - f(s, \tilde{z})\| \leq L \|z - \tilde{z}\| \quad \text{for } s \in I, \quad z, \tilde{z} \in E, \quad (5.2)$$

- (ii) $C(aL + K) < 1$, where:

$$C := \sup\{\|C(t)\| + \|S(t)\| + \|S'(t)\| : t \in I\} \quad \text{and} \quad K := \sum_{i=1}^p |C_i|,$$

(iii) $x_0 \in \tilde{E}$ and $x_1 \in E$.

Then, the nonlocal Cauchy problem (4.1)–(4.3) has a unique mild solution.

Proof. See [2], Theorem 2.1 and page 77.

6. Continuous dependence of a mild solution, on initial nonlocal data (4.2)–(4.3), of the nonlocal Cauchy problem (4.1)–(4.3)

In this section, there is the main result of Part II.

Theorem 6.1. Let all the assumptions of Theorem 5.1 be satisfied. Suppose that u is the mild solution (satisfying (5.1)) from Theorem 5.1. Moreover, let v satisfying the equation:

$$v(t) = C(t)y_0 + S(t)y_1 - S(t) \left(\sum_{i=1}^p C_i v(t_i) \right) + \int_0^t S(t-s) f(s, v(s)) ds, \quad t \in I, \quad (6.1)$$

be the mild solution of the nonlocal problem:

$$v''(t) = Av(t) + f(t, v(t)), \quad t \in I \setminus \{0\},$$

$$v(0) = y_0,$$

$$v'(0) + \sum_{i=1}^p C_i v(t_i) = y_1,$$

where $y_0 \in \tilde{E}$ and $y_1 \in E$.

Then, for an arbitrary $\varepsilon > 0$, there is $\delta > 0$ such that if:

$$\|x_0 - y_0\| < \delta, \quad \|x_1 - y_1\| < \delta \quad (6.2)$$

then:

$$\|u - v\|_X < \varepsilon,$$

where $X = C(I, E)$.

Proof. Let ε be a positive number and let:

$$\delta := \frac{1 - CK - aCL}{2C} \varepsilon. \quad (6.4)$$

Observe that, from (5.1) and (6.1),

$$u(t) - v(t) = C(t)(x_0 - y_0) + S(t)(x_1 - y_1) - S(t) \left(\sum_{i=1}^p C_i(u(t_i) - v(t_i)) \right) + \int_0^t S(t-s)(f(s, u(s)) - f(s, v(s))) ds, \quad t \in I. \quad (6.5)$$

Consequently, by (6.5) and (5.2),

$$\|u - v\|_X \leq C\|x_0 - y_0\| + C\|x_1 - y_1\| + CK\|u - v\|_X + aCL\|u - v\|_X.$$

From the above inequality:

$$(1 - CK - aCL)\|u - v\|_X \leq C(\|x_0 - y_0\| + \|x_1 - y_1\|). \quad (6.6)$$

By (6.6), (6.2) and (6.4),

$$\|u - v\|_X \leq \frac{C}{1 - CK - aCL} (\|x_0 - y_0\| + \|x_1 - y_1\|) < \frac{C}{1 - CK - aCL} \cdot 2\delta = \varepsilon.$$

Therefore, (6.3) holds. It means that the mild solution of the nonlocal Cauchy problem (4.1)–(4.3) is continuously dependent on the initial nonlocal data (4.2)–(4.3).

The proof of Theorem 6.1 is complete.

Remark

The nonlocal problems considered in the paper have physical interpretation. For this purpose, see the monograph: L. Byszewski, *Selected problems of differential and functional-differential equations and inequalities together with nonlocal conditions*, Monograph 505, Cracow University of Technology, Kraków 2015 (in Polish).

References

- [1] Byszewski L., *Existence and uniqueness of mild and classical solutions of semilinear functional-differential evolution nonlocal Cauchy problem*, *Selected Problems of Mathematics*, Cracow University of Technology, Anniversary Issue 6, 1995, 25–33.
- [2] Byszewski L., Winiarska T., *An abstract nonlocal second order evolution problem*, *Opuscula Mathematica* 32.1, 2012, 75–82.
- [3] Byszewski L., Winiarska T., *Continuous dependence of mild solutions, on initial nonlocal data, of the nonlocal evolution Cauchy problems*, *Technical Transactions*, 1-NP/2013, 27–32.

- [4] Pazy A., *Semigroups of Linear Operators and Applications to Partial Differential Equations*, Springer-Verlag, New York, Berlin, Heidelberg, Tokyo 1983.
- [5] Szarski J., *Differential Inequalities*, Polish Scientific Publishers, Warszawa 1967.
- [6] Winiarska T., *Differential Equations with Parameters*, Monograph 68, Cracow University of Technology, Kraków 1988.

Mariusz Domagała (domagala@mech.pk.edu.pl)

Institute of Applied Informatics, Faculty of Mechanical Engineering, Cracow University of Technology

Hassan Momeni

Department of Mechanical and Marine Engineering, Western Norway University of Applied Sciences

CFD SIMULATION OF CAVITATION OVER WATER TURBINE HYDROFOILS

SYMULACJE CFD ZJAWISKA KAWITACJI PRZY OPLYWIE PROFILI TURBIN PŁYWÓW MORSKICH

Abstract

Tidal turbines are gaining more and more interest as a source of renewable energy. Energy from tidal currents may be extracted in a similar way as wind energy but tidal turbines have to meet much higher requirements. Cavitation phenomena, which are difficult to predict, have great influence on hydrodynamic efficiency. This paper presents the use of CFD simulation for prediction of cavitation during flow over typical NACA airfoils.

Keywords: CFD, cavitation

Streszczenie

Turbiny wykorzystujące pływy morskie są coraz częściej wykorzystywane jako źródła czystej energii. Energię pływów morskich można uzyskać w podobny sposób jak w przypadku energii wiatrowej, ale turbiny wykorzystujące pływy morskie muszą spełnić znacznie bardziej rygorystyczne wymagania. Jednym z czynników mających wpływ na efektywność hydrodynamiczną turbin jest zjawisko kawitacji. Artykuł przedstawia wykorzystanie metod CFD do symulacji zjawiska kawitacji przy opływie typowych profili lotniczych.

Słowa kluczowe: CFD, kawitacja

1. Introduction

Renewable energy is becoming a real alternative to traditional energy sources. Tidal energy looks very promising due to its predictability and high energy density. Extracting power from tidal flow can be made in a very similar way to extracting wind energy, using turbines with horizontal or vertical axis. Commercial applications of tidal turbine are already available. Contrary to wind energy, tidal turbines have to meet much higher requirements. Moreover, one of the most important issues for extracting tidal energy is a proper selection of hydrofoil, which may be a typical airfoil or tailor made. One of the most important problems for tidal turbine is cavitation, which is very difficult to predict, and which may have significant influence on turbine efficiency or even cause turbine blade damages. The nature of cavitation cause sudden phase change, which disturbs flow and may cause blades wear. Cavitation is a complex problem investigated from many years, whose fundamental physics is presented in studies [1, 2]. The basic principle of cavitation is a sudden pressure drop below the saturation pressure at given temperature. Other studies show that also contaminations and liquid aeration may have influence on nucleation formation. Despite the rapid development of simulation tools, including Computational Fluid Dynamics (CFD), cavitation modeling is still a complex task. This paper presents an attempt to predict cavitation during flow over typical hydrofoils (NACA 4418, 4416 and 4412) with the use of Ansys CFX and a CFD code.

2. Mathematical model of cavitation

Mathematical description of cavitation has been a subject of studies for many years. Generally, the tendency of flow to bubbles formation may be expressed as the following cavitation number:

$$c_a = \frac{p - p_v}{0.5\rho U^2} \quad (1)$$

The Rayleigh-Plesset Formula is a common approach which describes bubble dynamics:

$$R_b \frac{d^2 R_b}{dt^2} + \frac{3}{2} \left(\frac{dR_b}{dt} \right)^2 + \frac{2\sigma}{\rho R_b} = \frac{p_v - p}{\rho} \quad (2)$$

After neglecting surface tension and the term of second order, the above eq. has the following form:

$$\frac{dR_b}{dt} = \sqrt{\frac{2}{3} \left(\frac{p_v - p}{\rho} \right)} \quad (3)$$

The rate of changes of bubble volume is as follows:

$$\frac{dV_b}{dt} = 4\pi R_b^2 \sqrt{\frac{2}{3} \left(\frac{p_v - p}{\rho} \right)} \quad (4)$$

The rate of changes of bubble mass is as follows:

$$\frac{dm_g}{dt} = 4\pi R_b^2 \rho_g \sqrt{\left(\frac{2}{3} \frac{p_v - p}{\rho}\right)} \quad (5)$$

The number of bubbles N_b per unit volume r_g is expressed by:

$$r_g = \frac{4}{3} \pi R_b^2 N_b \quad (6)$$

The total interphase mass transfer per unit volume is as follows:

$$\dot{m}_{fg} = 3 \frac{r_g \rho_g}{R_b} \sqrt{\frac{2}{3} \frac{p_v - p}{p_f}} \quad (7)$$

After including condensation, the above expression has the following form:

$$\dot{m}_{fg} = 3F \frac{r_g \rho_g}{R_b} \sqrt{\frac{2}{3} \frac{|p_v - p|}{p_f} \text{sgn}(p_v - p)} \quad (8)$$

And finally, the vapor transport equation has the form of:

$$\frac{\partial}{\partial t} (\alpha \rho_v) + \nabla \cdot (\alpha \rho_v \mathbf{V}) = R_e - R_c \quad (9)$$

where:

- R_b – bubble radius,
- p_v – vapor pressure,
- p – pressure of liquid surrounding the bubble,
- ρ – liquid density,
- ρ_g – vapor density,
- σ – surface tension,
- U – liquid velocity,
- α – vapor volume fraction,
- n – bubble number,
- R – phase change rate,
- f_v – vapor mass fraction,
- f_g – non-condensable gases.

3. CFD simulation

Flow simulations of hydrofoils were conducted for 2D models for 0 degree of angle of attack. Geometry of hydrofoils were created using a 3D CAD Creo Parametric system and a set of points with coordinates [3]. Models of three profiles: NACA 4418, 4416 and 4412 were created. An example of NACA 4418 is presented in Fig. 1.



Fig. 1. Set of points used for creating geometry of NACA 4418

Grids for simulation were used using quadrilateral cells with edges aligned to create a profile. Figures 2 and 3 show the grid used in simulations. To avoid problems with the influence of boundary conditions on the flow over the foil, rules for creating computational domains for external flow were used.

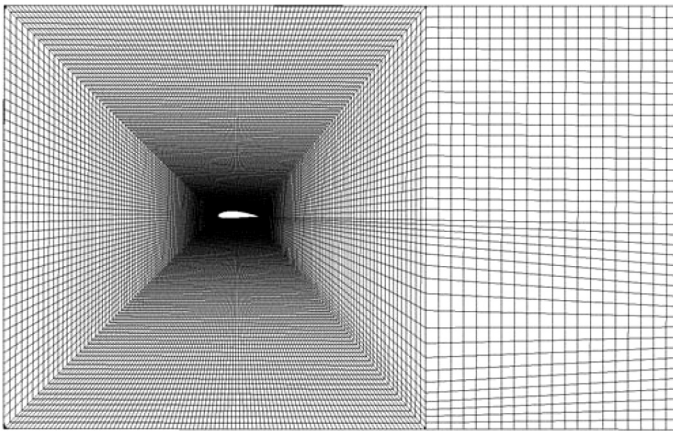


Fig. 2. Grid for NACA 4418 foil

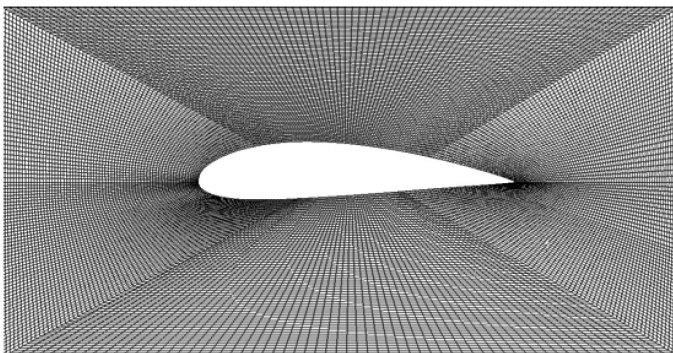


Fig. 3. Grid at the vicinity of foil

CFD simulations were conducted in the Ansys CFX code as two phase flows (water and water vapor) without interphase heat exchange for conditions corresponding to 5 m water depth and two water velocities of 5 m/s and 8 m/s. Cavitation and turbulent flow is random

by nature, but for simplification simulations were conducted for steady state conditions with constant water properties for typical sea water. Calculations were conducted for the same conditions for all foils. It was also assumed that both phases are homogenous and no solid or air (vapor or air) particles are presented.

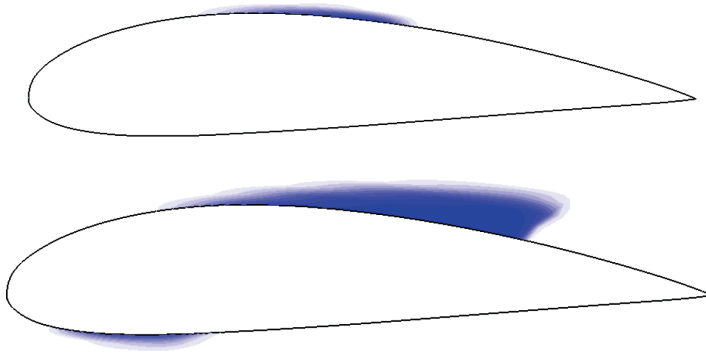


Fig. 4. NACA 4418 vapor volume fraction for 5 m/s and 8 m/s water flow

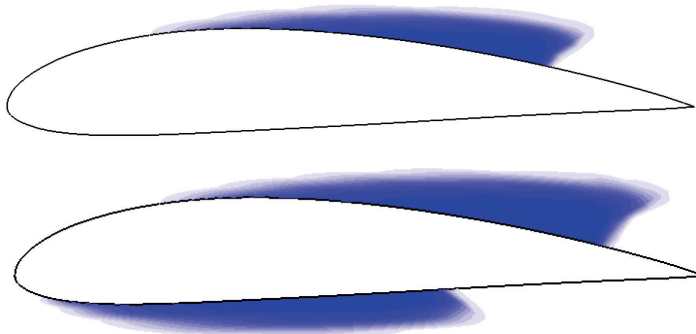


Fig. 5. NACA 4416 vapor volume fraction for 5 m/s and 8 m/s water flow

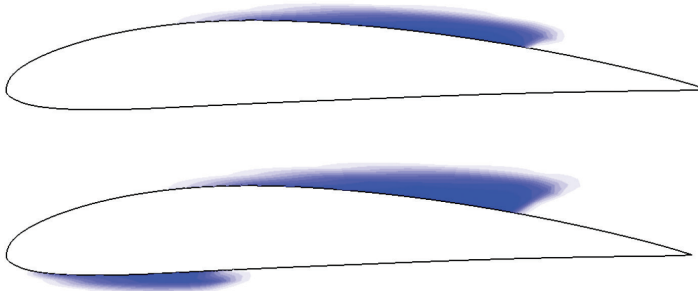


Fig. 6. NACA 4412 vapor volume fraction for 5 m/s and 8 m/s water flow



The results presented above for the selected foils show that nucleation forms in the areas with the highest velocity, which was to be expected. Simulation shows that foil shape has significant influence on the formulation of cavitation. Among three investigated foils, NACA 4418 has a much lower tendency for formulation cavitation.

4. Conclusions

Cavitation is a key issue for designing tidal turbines which describes hydrodynamics efficiency. It is difficult to predict, but by using CFD methods it is possible to reduce the probability of its appearance. Therefore, CFD methods may be treated as a very effective tool for designing tidal turbines.

References

- [1] Brennen C.E., *Cavitation and bubble dynamics*, Oxford University Press, 1995.
- [2] Szkodo M., *Mathematical description and evaluation of cavitation erosion resistance of materials*, Journal of Materials Processing Technology, 2005.
- [3] <http://airfoiltools.com> (access: 24.02.2017).
- [4] Bahaj A.S., Batten W.M.J., Chaplina J.R., *Experimental verifications of numerical predictions for the hydrodynamic performance of horizontal axis marine current turbines*, Renewable Energy 32, 2007, 2479–2490.
- [5] Mehmood N., Liang Z., Khan J., *Diffuser Augmented Horizontal Axis Tidal Current Turbines*, Research Journal of Applied Sciences, Engineering and Technology 4(18), 2012, 3522–3532.
- [6] *CFD for Wind and Tidal Offshore Turbines*, E. Ferrer, A. Montlaur (eds.), Springer Tracts in Mechanical Engineering, ISSN 2195-9870 (electronic), Springer 2015.
- [7] Bir G.S., Lawson M.J., Li Y., *Structural Design of a Horizontal-Axis Tidal Current Turbine Composite Blade*, ASME 30th International Conference on Ocean, Offshore, and Arctic Engineering Rotterdam, Netherlands, June 19–24, 2011.
- [8] Zeiner-Gundersen D.H., *Turbine design and field development concepts for tidal, ocean, and river applications*, Energy Science and Engineering 2015, 3(1): 27–42.
- [9] Domagała M., *Simulation of cavitation in jet pumps*, Technical Transactions, 1-M/2013.
- [10] Domagała M., Momeni H., *Proceedings of the 8th International Conference on Business and Technology Transfer (ICBTT 2016)*, Magdeburg, Germany.

Joanna Fabiś-Domagala (fabis@mech.pk.edu.pl)
Institute of Applied Informatics, Faculty of Mechanical Engineering,
Cracow University of Technology

QUALITY FUNCTION DEPLOYMENT METHOD FOR SELECTED WEBSITE
USABILITY ANALYSIS

METODA ROZWINIĘCIA FUNKCJI JAKOŚCI W ANALIE UŻYTECZNOŚCI
WYBRANEGO SERWISU INTERNETOWEGO

Abstract

The paper presents an analysis of the usability of a selected web site using the QFD quality method. User requirements and related technical parameters used for creating diagrams of similarities and dependencies have been identified. Diagrams showing user and technical benchmarking as well as graphs of target values evaluated for user requirements and technical parameters were created.

Keywords: QFD method, usability analysis, internet service

Streszczenie

W pracy przedstawiono analizę użyteczności wybranego serwisu internetowego przy wykorzystaniu jakościowej metody QFD. Zidentyfikowano wymagania użytkowników oraz związane z nimi parametry techniczne tworząc diagramy podobieństw i zależności. Opracowano zarówno wykresy przedstawiające wyniki benchmarkingu użytkownika oraz benchmarkingu technicznego, jak i wykresy wartości docelowych obliczone dla wymagań użytkownika i parametrów technicznych.

Słowa kluczowe: metoda QFD, analiza użyteczności, serwis internetowy

1. Introduction

Due to the rapid development of on-line applications, appropriate methods of creating such services have to be used. Until recently, Internet systems played purely informational role, delivering just relevant information. At present, on-line services are rapidly growing and extending areas of application. This requires from websites provision of such services in reasonable time and in a friendly, attractive and competitive form in a highly demanding market. Therefore, the analysis of usability of web-based services which investigate the intuitiveness of navigation, browsing information or providing appropriate information becomes a necessity. Such analysis allows web services to fulfill user requirements and expectations and eliminate the most common errors. Various methods are used in practice, tools and techniques for the evaluation of usefulness of websites. One of them is the qualitative QFD method (Quality Function Deployment), which is a method of identifying user requirements and matching them to technical specifications of Internet services.

2. QFD principles

The QFD method was used for the first time in 1972 at the Kobe shipyard in Japan. Since the 1980s, it has been used in the automotive and electrical industries. Nowadays, when the quality of services is a major customer requirement, quality management tools are also implemented for on-line services. Diagrams linked together which have the structure of a house are the basic tool of the QFD method. Therefore, this method is also recognized as a “quality house” that shows the relationship between the identified user requirements (matrix rows) and the technical parameters of the website (matrix columns). The sequence of the diagrams in the QFD method [1, 2] is as follows: 01 – user requirements, 02 – user requirements importance, 03 – benchmarking of user, 04 – evaluation of relative user requirements importance (Ei), 05 – technical parameters of the service, 06 – diagram dependency of technical parameters, 07 – diagram of dependency user requirements and technical parameter, 08 – determination of technical parameters (Fi), 09 – technical parameter target, 10-technical benchmarking. The number of diagrams may vary depending on the needs and complexity of the website which is investigated. Figure 1 shows the relationships between diagrams in the QFD method.

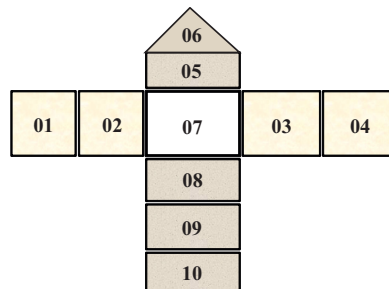


Fig. 1. Diagrams in QFD method

3. QFD usability analysis

QFD usability analysis was performed for the website of the Eye Hospital in Cracow [3]. The analysis was carried out in two stages. The first step was a horizontal analysis of marketing information: user requirements, competitive comparisons and user quality objectives. The second step was a vertical analysis which included technical information: identification of technical parameters, dependence between user requirements and technical parameters as well as determination of user quality objectives from the web designer point of view. At the first stage of the QFD qualitative analysis, user requirements were identified, then selected and grouped into relevant thematic categories (01-similarity diagrams). User requirements have various importance value. Therefore, the importance of user requirements was evaluated (02) by questionnaires. A scale from 1 to 5 was used, where 1-minor requirement, 5- the most important requirement for the user.

Table 1. Similarity diagram and user requirements importance

		01 User requirements	02 Requirements importance
Thematic Categories	I. website esthetics	1. Graphics	3
		2. Colors	3
		3. Clarity	4
		4. Advertisements	3
	II. Easiness of use	5. Information quality	5
		6. Ability to find	3
		7. Browsing	4
		8. Website launch	3
		9. Intuitiveness for elderly people	5
	III. contact	10. Ways of contact	5
		11. Location	4
		12. On-line registration	3
	IV. services	13. News	3
		14. Services	4
		15. Opinions	2

A user benchmark was conducted (03) to evaluate the investigated website (N) against two competitors [4, 5]: Retina (X) and Clinical Eye Hospital (Y) in Warsaw. The evaluation was scored on a scale ranging from 1 to 5, where 1 – requirement completely unfulfilled, 5 –requirement completely met. The fulfillment of user requirements by websites was

presented in the form of graphs in Fig. 2. This allows for observation in which areas the analyzed website is better than competition and which improvement measures need to be taken. In the next step, the priority (relative importance) of each identified requirement was determined. For that purpose, a benchmarking index (04) was elaborated. The following formula for the relative value E_i [6] was used:

$$E_i = \frac{D_i}{\sum_{(i=1)}^n D_i} \quad (1)$$

where:

- E_i – relative importance for i requirements,
- n – number of user requirements,
- D_i – weighted value for i requirements evaluated from the formula [6]:

$$D_i = A_i \cdot B_i \cdot C_i \quad (2)$$

where:

- A_i – rank of importance of i user requirements,
- C_i – degree of fulfillment of i requirements,
- B_i – indicator of the degree of improvement of the fulfillment of i requirements calculated according to the formula [6]:

$$B_i = \frac{P_i}{N_i} \quad (3)$$

where:

- P_i – targeted level of fulfillment of i requirements,
- N_i – state of fulfillment of i requirements.

A benchmarking chart (particularly the values in the E_i column) was used for determining the objectives of usability quality (from the user's point of view) to improve the analyzed website. The values in the E_i column were given in percentages. At the second stage of the qualitative QFD method (vertical analysis), technical parameters were identified to satisfy user requirements and grouped into thematic categories (05) (Table 2).

At the next step, the direction of improvement (KD) was determined to meet requirements:

- 1: the greater the parameter is, the better the website will meet user requirements,
- 1: the smaller the parameter is, the better the service will meet user requirements,
- 0: the given parameter must have a specified nominal value to meet user requirements best.

According to the QFD usability analysis, technical parameters are often interrelated, which affects not only on the quality of technical solutions but also user requirements and expectations. Therefore, in the next step of the analysis, the relationships between parameters (06) were determined using the following rules:

- ▶ (-) if incrementing one parameter causes the decrease of the second parameter,
- ▶ (+) if incrementing one parameter results in the increase of the second parameter,
- ▶ if there is no relationship between the parameters, the cell is empty.

Table 2. Similarity diagram for technical parameters of the website

05					
Thematic Categories					
		A. Navigation	B. Graphics and esthetics	C. Usability	D. Functions and modules
Technical parameters	1	Browser	Pictures size	Website launch	E-patient
	2	Links	Pictures quality	Advertisements	Contact form
	3	Domain	Correct reading characters	Segmentation	E-registration
	4		Consistencies	Number of advertisements	
	5		Font size		

In the next step of analysis, relations between technical parameters and user requirements (07) were determined. Dependencies were described using numerical values: 0-1-3-9. Value 0 means no dependence, 1 means weak, 3 strong and 9 very strong dependence. The relative importance of the technical parameters (08) was determined by means of the following formula [6]:

$$F_j = \frac{T_j}{\sum_{j=1}^n T_j} \quad (4)$$

where:

F_i – relative importance,

m – number of parameters included in diagrams,

T_i – coefficient of importance of technical parameters expressed as [6]:

$$T_j = \sum_{(i=1)}^n A_i \cdot Z_{ij} \quad (5)$$

where:

Z_{ij} – coefficient of correlation between i requirement and j parameter.

The value of F_j in the diagram was expressed in percentage and later it was used to create bar charts representing technical parameters. In the next step, technical values were assigned to the values at which user expectations will be met (09). However, these values must always be real and measurable in the process of improving the website and achievable within a certain timeframe. The investigated website (10) was compared with two competitors. This allows for evaluating the technical level of offered solutions within each of the listed technical parameters. Evaluation rank is numbered from 1 to 5, in a similar way as in the case of user benchmarking. Linear charts describing the status of each service were developed to identify areas for improvement.

4. Graphical presentation of the results

A graphical presentation of results for the qualitative usability analysis QFD is presented in Figure 2. It allows for indicating which user requirements have primary importance and what is the status in the analyzed website. Technical and operational requirements say that the range of offered services, on-line registration and lack of registration form are issues which need to be improved. These are three areas (III contact, IV services, and D – functions and services), where improvement efforts should be taken because they are below the competitive website. In case of the analyzed website, there is no on-line registration while competitive websites have such possibilities. In addition, none of the analyzed websites have a contact form or search engine that would allow the user to find information, which would make the website intuitive and easy to navigate.

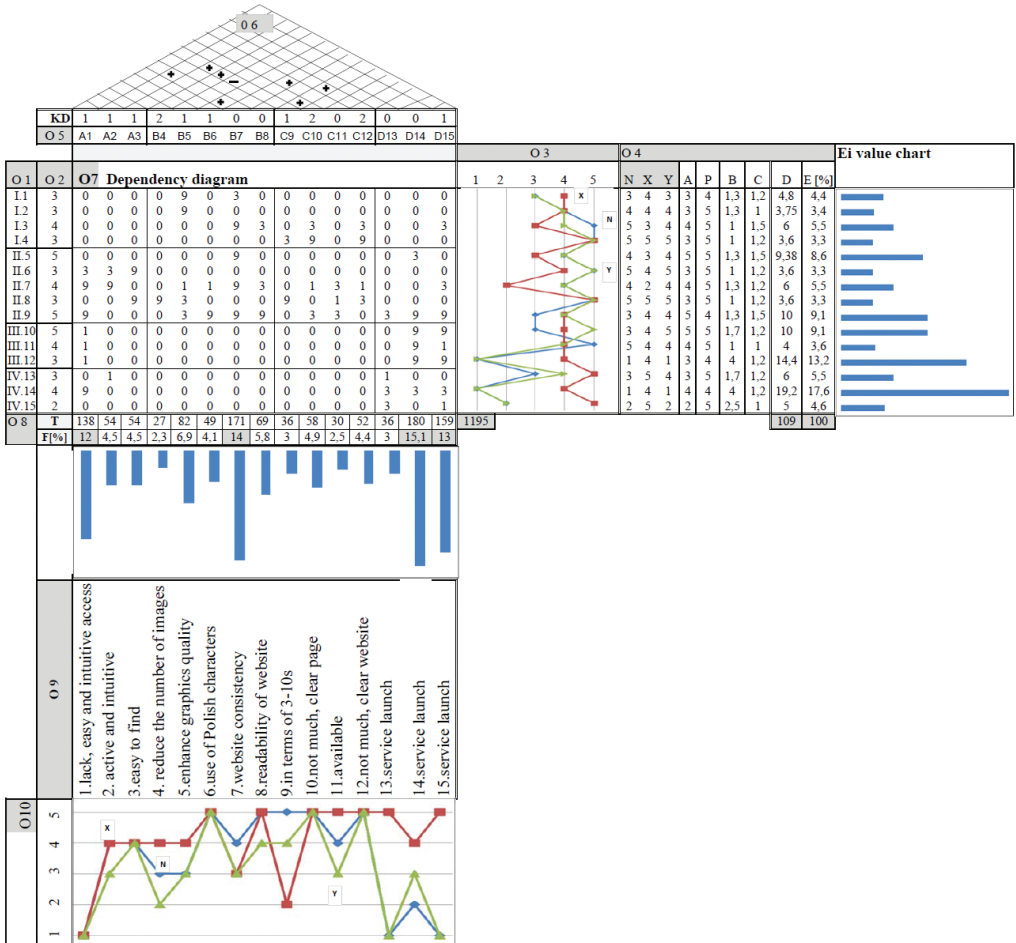


Fig. 2. House of quality, where KD-direction of improvement

5. Summary

The paper presents the application of the QFD method to evaluate the usability of a selected website. During the analysis, user requirements were defined as well as the technical parameters that have influence on these requirements. During the QFD analysis, also competitive websites were tested. After the QFD analysis, areas that require improvement were identified.

Usability analysis methods such as the QFD method can be useful tools for determining the scope of modification and upgrading of web services to meet user requirements and market demands.

References

- [1] Hamrol A., Mantura W., *Zarządzanie jakością. Teoria i praktyka*, Wydawnictwo Naukowe PWN, 2006.
- [2] *Quality Function Deployment*, <http://www.public.iastate.edu> (access: 15.01.2017).
- [3] www.retina.pl (access: 15.01.2017).
- [4] www.spkso.waw.pl (access: 31.01.2017).
- [5] Sikorski M., *Zastosowanie metody QFD do doskonalenia jakości użytkowej wybranego serwisu www*, Politechnika Gdańska, 2003.

Renata Filipowska (renata.filipowska@pk.edu.pl)
Institute of Applied Informatics, Faculty of Mechanical Engineering,
Cracow University of Technology

HOMOTOPY PERTURBATION METHOD FOR SOLVING FOURTH – ORDER
BOUNDARY VALUE PROBLEMS WITH ADDITIONAL BOUNDARY CONDITION

HOMOTOPIJNA METODA PERTURBACYJNA ZASTOSOWANA
DO ZAGADNIENIA BRZEGOWEGO CZWARTEGO RZĘDU Z DODATKOWYM
WARUNKIEM BRZEGOWYM

Abstract

This paper presents the homotopy perturbation method for solving linear and non-linear two-point boundary value problems in the form of a fourth-order differential equation and five boundary conditions. Three initial and two final conditions were taken into account. The solution of this problem is possible only when the considered equation includes an unknown parameter. The presented method has been illustrated with a numerical example.

Keywords: boundary value problem, homotopy perturbation method, system of integral equations, system of differential equations

Streszczenie

W artykule przedstawiono homotopijną metodę perturbacyjną zastosowaną do rozwiązywania zarówno liniowego, jak i nieliniowego dwupunktowego zagadnienia brzegowego składającego się z równania różniczkowego czwartego rzędu oraz pięciu warunków brzegowych. Pod uwagę wzięto trzy początkowe i dwa końcowe warunki brzegowe. Rozwiązanie tak postawionego problemu jest możliwe tylko wtedy, gdy rozpatrywane równanie zawiera nieznaną parametr. Prezentowaną metodę zilustrowano przykładem obliczeniowym.

Słowa kluczowe: zagadnienie brzegowe, homotopijna metoda perturbacyjna, układ równań całkowych, układ równań różniczkowych

1. Introduction

The boundary value problem (BVP) plays an important role in many fields, e.g. in mathematical modeling, physical and engineering sciences. Most methods of solving these problems concern the standard BVP, where the order of equation and number of boundary conditions are the same. Sometimes we have a non-standard BVP, where the number of boundary conditions is more than the order of a differential equation. In such a situation we can apply e.g. the iterative shooting method (ISM) [1], whose modification was described in [2] or a modification [3] of the variational iteration technique (VIT) [4], which is based on the variational iteration method (VIM) [5, 6].

In this paper, a different alternative method will be presented – the homotopy perturbation method (HPM) [7, 8], modified and applied for solving non-standard higher-order BVP. An example is given to illustrate this method.

2. Basic Concept of the Homotopy Perturbation Method

We will take into consideration the system of the Volterra integral equations, which is written in the matrix form [7, 9]:

$$\mathbf{F}(t) = \mathbf{G}(t) + \lambda \int_a^t \mathbf{K}(t,s) \mathbf{F}(s) ds \quad (1)$$

$$\mathbf{F}(t) = \begin{bmatrix} f_1(t) \\ \vdots \\ f_n(t) \end{bmatrix}, \quad \mathbf{G}(t) = \begin{bmatrix} g_1(t) \\ \vdots \\ g_n(t) \end{bmatrix}, \quad \mathbf{K}(t,s) = \begin{bmatrix} k_{11}(t,s) & \cdots & k_{1n}(t,s) \\ \vdots & \ddots & \vdots \\ k_{n1}(t,s) & \cdots & k_{nn}(t,s) \end{bmatrix} \quad (2)$$

To illustrate the basic idea of the HPM [10, 11] and present its application to the system (1), in the first step we consider a general equation:

$$L(u) = 0 \quad (3)$$

where L is a differential or integral operator. Next, according to the homotopy perturbation technique, we construct a homotopy operator:

$$H(u,p) = (1-p)F(u) + pL(u) = 0, \quad F(u) = L(u) - L(v_0), \quad p \in [0,1] \quad (4)$$

where:

- p – an embedding parameter,
- $F(u)$ – a functional operator,
- v_0 – an initial approximation of (3). Taking into consideration (4), we have:

$$H(u,0) = F(u), \quad H(u,1) = L(u) \quad (5)$$

The process of changing p from zero to unity shows that $H(u, p)$ changes from a starting point $H(v_0, 0)$ to a solution $H(u, 1)$. This is called deformation. The HMP uses the p s an expanding parameter [11] and in the next step we search for the solution of (4) which can be written as a power series in p :

$$u = \sum_{i=0}^{\infty} p^i u_i = u_0 + pu_1 + p^2 u_2 + \dots, \quad y = \lim_{p \rightarrow 1} u = \sum_{i=0}^{\infty} u_i \quad (6)$$

If $p \rightarrow 1$ then (4) becomes the approximate solution of (3). The convergence of series (6) was proved by He [10].

Considering (1) and (6), we have the following system:

$$y_1(t) = \sum_{i=0}^{\infty} p^i z_i, \quad y_2(t) = \sum_{i=0}^{\infty} p^i h_i, \quad y_3(t) = \sum_{i=0}^{\infty} p^i s_i, \dots \quad (7)$$

By comparing the expressions with the same powers of parameter p , we receive the solution of imposed order.

3. Homotopy Perturbation Method – BVP with additional boundary condition

We consider the non-standard BVP, which consists of the following fourth-order differential equation:

$$u^{(IV)}(x) + f(x, u(x), u'(x), u''(x), u'''(x), q_1) = 0 \quad (8)$$

and five boundary conditions:

$$u(a) = u_a, \quad u'(a) = u_{1a}, \quad u''(a) = u_{2a}, \quad u(b) = u_b, \quad u'(b) = u_{1b} \quad (9)$$

A solution of equation (8) can fulfill conditions (9) only when this equation contains one unknown parameter q_1 . By means of the following transformations:

$$\frac{du}{dx} = z(x), \quad \frac{dz}{dx} = h(x), \quad \frac{dh}{dx} = s(x) \quad (10)$$

we can convert the BVP (8) and (9) to an initial value problem (IVP), which consists of a system of four first – order differential equations:

$$\frac{du}{dx} = z(x), \quad \frac{dz}{dx} = h(x), \quad \frac{dh}{dx} = s(x), \quad \frac{ds}{dx} = f(x, u(x), z(x), h(x), s(x), q_1) \quad (11)$$

and four initial conditions, which include a subsequent unknown parameter q_2 :

$$u(a) = u_a, \quad z(a) = u_{1a}, \quad h(a) = u_{2a}, \quad s(a) = q_2 \quad (12)$$

We can rewrite system (11) as a system of four integral equations:

$$\begin{aligned} u(x) &= u(a) + \int_0^x z(t) dt, \quad z(x) = z(a) + \int_0^x h(t) dt, \quad h(x) = h(a) + \int_0^x s(t) dt \\ s(x) &= s(a) + \int_0^x f(t, u(t), z(t), h(t), s(t), q_1) dt \end{aligned} \quad (13)$$

If we use (4) and (6) for (13), we will obtain:

$$\begin{cases} u_0 + pu_1 + p^2u_2 + \dots = u(a) + p \int_0^x (z_0 + pz_1 + p^2z_2 + \dots) dt \\ z_0 + pz_1 + p^2z_2 + \dots = z(a) + p \int_0^x (h_0 + ph_1 + p^2h_2 + \dots) dt \\ h_0 + ph_1 + p^2h_2 + \dots = h(a) + p \int_0^x (s_0 + ps_1 + p^2s_2 + \dots) dt \\ s_0 + ps_1 + p^2s_2 + \dots = s(a) + p \int_0^x f(t, u(t), z(t), h(t), s(t), q_1) dt \end{cases} \quad (14)$$

Comparing the coefficient of like powers of p , we obtain subsequent approximations of $u(x)$, $z(x)$, $h(x)$, $s(x)$, which include still unknown parameters q_1 and q_2 . Using (6) and two boundary conditions (9) at the right end of the domain, we obtain an additional system of two equations:

$$u(b) = u_b, \quad u'(b) = u_{1b} \quad (15)$$

The solution of system (15) gives the values of parameters q_1 , q_2 and $u(x)$ – sought solution of equation (8) in terms of convergent series with a required expansion order, which fulfills all conditions (9).

4. Numerical Example

To apply HPM to BVP with an additional boundary condition, an example will be presented as a fourth-order differential equation which contains unknown q_1 :

$$u^{(IV)}(x) = u^2(x) - x^{10} + 4x^9 - 4x^8 - 4x^7 + 8x^6 - 4x^4 + q_1 x - 48 \quad (16)$$

and five boundary conditions:

$$u(0) = 0, \quad u'(0) = 0, \quad u''(0) = 4, \quad u(1) = 1, \quad u'(1) = 1 \quad (17)$$

We know ([4]) that for $q_1 = 120$, equation (16) has the following exact solution:

$$u(x) = x^5 - 2x^4 + 2x^2 \quad (18)$$

which fulfills all boundary conditions (17). In the first step, using (10), we rewrite the above BVP as a system of four first-order differential equations:

$$\begin{aligned} \frac{du}{dx} &= z(x), & \frac{dz}{dx} &= h(x), & \frac{dh}{dx} &= s(x), \\ \frac{ds}{dx} &= u(x) - x^{10} + 4x^9 - 4x^8 - 4x^7 + 8x^6 - 4x^4 + q_1x - 48 \end{aligned} \quad (19)$$

with four initial conditions, which include a second unknown parameter q_2 :

$$u(0) = 0, \quad z(0) = 0, \quad h(0) = 4, \quad s(0) = q_2 \quad (20)$$

Taking into consideration (14), in the next step we can rewrite the system (19) as a system of four integral equations with the embedding parameter p :

$$\begin{cases} u_0 + pu_1 + p^2u_2 + \dots = 0 + p \int_0^x (z_0 + pz_1 + p^2z_2 + \dots) dt \\ z_0 + pz_1 + p^2z_2 + \dots = 0 + p \int_0^x (h_0 + ph_1 + p^2h_2 + \dots) dt \\ h_0 + ph_1 + p^2h_2 + \dots = 4 + p \int_0^x (s_0 + ps_1 + p^2s_2 + \dots) dt \\ s_0 + ps_1 + p^2s_2 + \dots = q_2 + p \int_0^x [(u_0 + pu_1 + p^2u_2 + \dots)^2 - t^{10} + \\ \quad + 4t^9 - 4t^8 - 4t^7 + 8t^6 - 4t^4 + q_1t - 48] dt \end{cases} \quad (21)$$

The *Maple*TM program with accuracy *Digits* = 20 and order of power series in an embedding parameter $n = 20$ were used to solve this non-standard problem. Using the boundary conditions at $x = 1$, we obtain: $q_1 = 120.000004947$, $q_2 = -2.10539 \cdot 10^{-7}$, and the series solution is given by:

$$u(x) = 2x^2 - 3.52 \cdot 10^{-8} x^3 - 2x^4 + x^5 - 4.65 \cdot 10^{-11} x^9 + \dots + 6.73 \cdot 10^{-20} x^{38} \quad (22)$$

Table 1 exhibits the exact solutions (18), a comparison between the errors obtained by means of the modified HPM, VIT [3] and ISM [2], presented in this paper and used for the BVP with additional boundary conditions.

Table 1. Error estimates

x	$u_{\text{exact}}(x)$	Errors* (HPM)	Errors* (VIT)	Errors* (ISM)
0.0	0.00000	0.0000	0.0000	0.0000
0.1	0.01981	$3.4678 \cdot 10^{-11}$	$3.4279 \cdot 10^{-14}$	$9.8256 \cdot 10^{-15}$
0.2	0.07712	$2.6753 \cdot 10^{-10}$	$2.6465 \cdot 10^{-13}$	$8.0465 \cdot 10^{-14}$
0.3	0.16623	$8.4726 \cdot 10^{-10}$	$8.3881 \cdot 10^{-13}$	$8.4766 \cdot 10^{-14}$
0.4	0.27904	$1.8236 \cdot 10^{-9}$	$1.7599 \cdot 10^{-12}$	$3.4477 \cdot 10^{-14}$

Table 1. cont

0.5	0.40625	$3.0982 \cdot 10^{-9}$	$1.4173 \cdot 10^{-12}$	$1.0776 \cdot 10^{-13}$
0.6	0.53856	$4.3754 \cdot 10^{-9}$	$2.3855 \cdot 10^{-11}$	$1.0341 \cdot 10^{-13}$
0.7	0.66787	$5.1241 \cdot 10^{-9}$	$2.9626 \cdot 10^{-10}$	$4.0618 \cdot 10^{-14}$
0.8	0.78848	$4.6096 \cdot 10^{-9}$	$2.2899 \cdot 10^{-9}$	$3.4080 \cdot 10^{-14}$
0.9	0.89829	$2.3140 \cdot 10^{-9}$	$1.3479 \cdot 10^{-8}$	$5.9746 \cdot 10^{-14}$
1.0	1.00000	$2 \cdot 10^{-19}$	$6.4569 \cdot 10^{-8}$	$1.6930 \cdot 10^{-13}$

*Error = abs (exact solution – series solution (HPM), series solution (VIT) or discrete solution (ISM)).

5. Summary

Taking into consideration methods for the non-standard higher order BVP: the ISM [2], the VIT [3] and HPM described in this article, which can be successfully applied for the BVP with one or more additional conditions, we can conclude that the differential equation must contain unknown parameters, whose number must correspond to the number of excessive boundary conditions. The values of these components can be calculated by applying additional boundary conditions. Taking into consideration the HPM, like the VIT, we obtain a solution in the terms of convergent series. Higher accuracy can be obtained by increasing the expansion order in series solution, but it has impact on time consuming computational work. For example, for $n = 20$, the max error is $5.12 \cdot 10^{-9}$, whereas for $n = 30$ it is reduced to $3.74 \cdot 10^{-12}$. The HPM is easy to implement, powerful and efficient in finding analytical solutions of differential equations.

References

- [1] Sung N.Ha., *A nonlinear shooting method for two-point boundary value problems*, Comp. and Math. with Appl., 42, 2001, 1411–1420.
- [2] Filipowska R., *An iterative shooting method for the solution of higher order boundary value problems with additional boundary conditions*, Solid State Phenomena, 235, 2015, 31–36.
- [3] Filipowska R., *Variational iteration technique for solving higher order boundary value problem with additional boundary conditions*, Technical Transactions, 4- M/ 2016, 15–20.
- [4] Noor A.M., Mohyud-Din S.T., *Variational iteration technique for solving higher-order boundary value problems*, Applied Math. and Computation, 189, 2007, 1929–1942.
- [5] He J.H., Wu X.H., *Variational iteration method: New development and applications*, Comp. and Math. with Appl., 54, 2007, 881–894.
- [6] Zhang J., *The numerical solution of fifth-order boundary value problems by the variational iteration method*, Com. and Math. with Appl., 58, 2009, 2347–2350.
- [7] Noor A.M., Mohyud-Din S.T., *An efficient algorithm for solving fifth-order boundary value problems*, Math. and Comp. Modelling, 45, 2007, 954–964.

- [8] Chun Ch., Sakthivel R., *Homotopy perturbation technique for solving two-point boundary value problems—comparison with other methods*, Comp. Physics Communications, 181, 2010, 1021–1024.
- [9] Hetmaniok E., Słota D., Wróbel A., Zielonka A., *Application of the homotopy perturbation method for the systems of Volterra integral equations*, Zesz. Nauk. PŚ, Mat. Stosow., 5, 2015, 71–77.
- [10] He J.H., *Homotopy perturbation technique*, Comput. Methods Appl. Mech. Eng., 178, 1999, 257–262.
- [11] Nayfeh A.H., *Introduction to Perturbation Technique*, John Wiley and Sons, New York 1981.



Ewa Kozieln (koziene@uek.krakow.pl)

Department of Strategy Management and Organization Growth, Faculty of Economics and International Relations, Cracow University of Economics

APPLICATION OF APPROXIMATION TECHNIQUE TO ON-LINE UPDATING
OF THE ACTUAL COST CURVE IN THE EARNED VALUE METHOD

ZASTOSOWANIE METOD APROKSYMACJI DO BIEŻĄCEGO UAKTUALNIANIA
PRZEBIEGU KRZYWEJ KOSZTU RZECZYWISTEGO W METODZIE WARTOŚCI
WYPRACOWANEJ

Abstract

The Earned Value Method (EVM) is a method commonly used in the quantitative project management. The course of the actual curve is usually different from the course of the planned curve. In order to provide a reliable estimation of the time of the project implementation or its real cost, the method of on-line updating the actual cost (AC) original curve can be applied. The actual cost curve is usually of the S-curve character. The approximation method is often used in the engineering applications. In the paper, the possibility of applying the polynomial type approximation method to the on-line updating of the actual cost curve is discussed.

Keywords: Earned value method, S-curve, approximation

Streszczenie

Metoda wartości wypracowanej (EVM) jest powszechnie stosowana w ilościowym zarządzaniu projektami. Przebieg krzywej kosztów rzeczywistych jest zwykle inny niż przebieg krzywej kosztów planowanych. W celu realistycznej oceny czasu końcowego realizacji projektu bądź jego rzeczywistych kosztów może być zastosowana metoda bieżącego poprawiania przebiegu krzywej kosztów rzeczywistych. Krzywa kosztów rzeczywistych ma zwykle przebieg podobny do przebiegu krzywej S. Metody aproksymacji są często stosowane w zastosowaniach inżynierskich. W artykule dyskutowana jest możliwość zastosowania wielomianów trzeciego stopnia do bieżącego uaktualniania przebiegu krzywej kosztów bieżących.

Słowa kluczowe: metoda wartości wypracowanej, krzywa S, aproksymacja

1. Introduction

Currently, the method of the earned value analysis – EVM (Earned Value Method) – has been used in the quantitative project management and has been computer-assisted in the form of universal computer programs packages (e.g. EVMS for Project™) [3, 9, 17, 21, 23]. The Earned Value is a program management technique that makes it possible to indicate what will happen to work in the future, based on the actual time data [12]. Unique and huge projects require specially created computer packages. As a whole, it connects the incurred expenses and the time of the project realization. It also requires the accurate determination of the schedule as well as providing the time of activity completion. In the classic approach, the method allows the current estimation of the progress of the project, and to be precise, the deviation from the accepted schedule. The analysis of the deviation (working in favour or to the detriment – acceleration or delay of the project) allows monitoring the execution of the project in the current moment of its implementation. It is therefore a convenient tool for the control of the project execution. The proper interpretation of the earned value parameters poses a problem. One of the most interesting possibilities of applications, however, is the estimation of the real (revised) time of the project completion or real (revised) total cost of implementation, which may be predicted in every moment of its execution. It is a crucial problem; however, it is barely developed in the literature. The heretofore applied approaches are based on the knowledge of the on-line known values of the earned value (budgeted cost of work performed, EV, BCWP) and actual cost (actual cost of work performed, AC, ACWP) functions and the course of the planned value (budgeted cost of work scheduled, PV, BCWS) curve. Such an approach may be encumbered with a big error, especially when applying it in the intermediate stages of the project implementation. The reason for that lies in the fact that it does not allow for the scheme of the project lifetime cycle, legitimate for the majority of projects, which leads in a straight line to the so-called S-curve, incurred expenses in the function of the project implementation time. In practice, it is a problem of predicting the course of the AC function, which is the extrapolation of the course beyond the course of its definiteness. The extrapolation's limit, which has to be taken into consideration, is the real schedule – the known PV function's course.

In the paper, the author considers the possibility of applying the approximation method in the S-curves class to the on-line updating of the actual cost curve. In the future, it will make it possible for the on-line updating of the estimated time duration (ED) or estimate cost at completion (EAC) values in ways other than the ones known in literature [5, 6, 11, 14–16, 19, 20].

The originality of the analysis is the detailed analysis of advantages, disadvantages and crucial points of using the polynomial of the third range to estimate the actual S-curve. Using polynomial in approximation is a very popular and useful technique due to the simple application of the last square method in order to find the proper form of the approximate function. Therefore, the crucial part of the practical application of the proposed approximation method is using the obtained shape and values of the approximation curve beyond the range of time from the beginning of project to the actual time (AT) of its realization.

2. S-curve

2.1. S-curves in EVM

The analysis of the project implementation prompts an observation that, despite the fact that the incurred expenses vary in particular stages of the project, if presented in a cumulated form of the accrued costs incurred from the beginning of the project execution, will take the form of the known in the economics S-curve. The name of the curve originates from its waveform, which resembles the letter S, or from the first letter of the term “spending-curve”.

To be more precise, three curves, which are the functions of time, may be distinguished in the EVM method: planned value curve ($PV(t)$ or $BCWS(t)$), earned value one ($EV(t)$ or $BCWP(t)$) and actual cost one ($AC(t)$ or $ACWP(t)$). The course of all the curves refers to the S-curve form. The accepted in a project's stage course of the $PV(t)$ expenses function is of a particular course defined in the interval of the design life of the project implementation ($t \in [0, PD]$, PD-planned duration). In practice, one may usually encounter a course deviation, which results in a necessity for a regular creation of a $EV(t)$ or $AC(t)$ curve. In reality, however, the interval of the functions' definiteness is changing during the project realization and is defined after the project completion as ($t \in [0, SAC]$, SAC-schedule at completion), or is estimated on a regular basis as ($t \in [0, ED]$, ED-estimated duration).

The notion of a fast delayed start of the project implementation is one of the practical problems. In such a case, one may imagine two limit curves of the project implementation, with the assumption that the end schedule is met when the total costs and the implementation time are met. Considering the acquired shape of the area, it is sometimes called a banana curve [3].

It should be noted that the Earned Value's S-curves are not the same as those used for project cash flow analysis. This does not facilitate combined interpretation of project performance in terms of work progress, receipts and expenditures [6].

2.2. Up-dating of AC curve

In a case when there are clear differences between the planned schedule and its real implementation, a process of a specific up-dating of the original schedule may occur. The process should not be performed too often. In the relevant literature, one may find a discussion on a single and multiple up-dating of the $AC(t)$ curve's course [4, 13, 15, 16]. The approach presented under the 3 point is an alternative to the one discussed in the article.

It should be noted that the regression based methodology to interpolate characteristics of growth models are an important way to forecast project cost at completion [15]. Defining an equation for the S-curve model requires consideration of some issues relevant to nonlinear regression analysis [15].

2.3. Analytical formulas for S-curve

In the classic approach, the equation of the S curve takes a form of the so-called logistic curve in form (1) [16, 18, 24], where the defining parameters meet the following conditions: $a > 0$, $c > 0$ and $b > 1$. The course of the function has been presented in Fig. 1.

$$Y(t) = \frac{a}{1 + b \cdot e^{-c \cdot t}} \quad (1)$$

D.F. Cioffi proposed a parametrized S-curve tool for managing cost of ongoing project [4, 15] introducing a different analytic function, which implements the similar tendency in form (2) [4]. Fig.1 presents the course of the curves defined by (1) and (2) for the following parameters' value: $a = 1$, $b = 100$, $c = 10$.

$$Y(t) = a \cdot \frac{1 - e^{(-c \cdot t)}}{1 + b \cdot e^{(-c \cdot t)}} \quad (2)$$

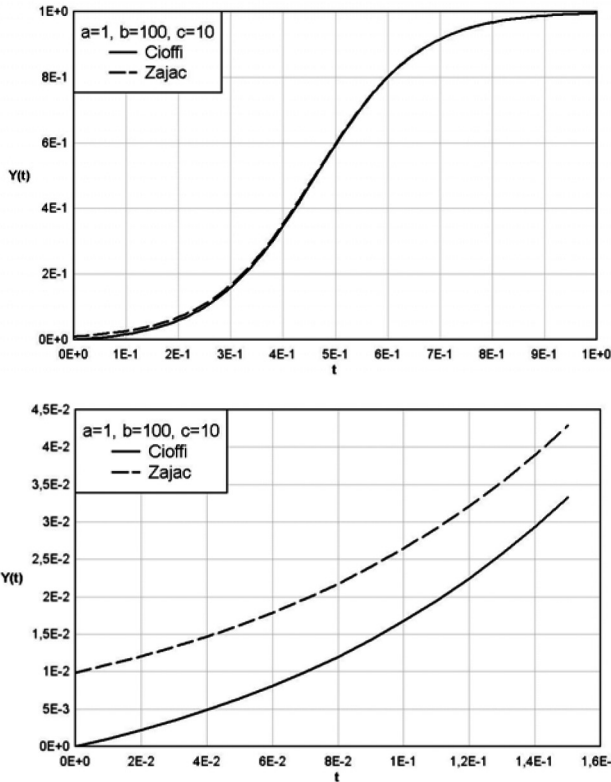


Fig. 1. Comparison of the courses of the logistic curve and D.F. Cioffi's S-curve

One may notice a clear similarity between the courses of the functions in a great time scale, which is visible in the left picture. The fundamental difference is shown around the time

value, which equals zero. Two horizontal asymptotes are the characteristics of the logistic function course, which is visible in Fig. 1. The first one for $y = 0$, the second one for $y = a$. This means that, in order to obtain zero costs for $t = 0$, one should shift the course of the function downwards. The value of the shift, however, depends on the configuration of the a , b and c parameters, whereas the course of the second function's value, by definition, is zero for $t = 0$. The behaviour of the functions for the time value near zero is shown in the right picture. The provided observation shows the analytic function, which models the S-curve, and according to D.F. Cioffi, is more convenient for the EVM applications.

The other analytical functions of exponential type, which are used in approximation of the S-curves, are reviewed by T. Narbaev and A. De Marco [16]. They are functions proposed by G.A.F. Seber and C.J. Wild [18] – the Gompertz one (3), proposed by Bass [2] (4) and proposed by W.W. Hines and D.C. Montgomery [10] – the Weibull one (5).

$$Y(t) = a \cdot e^{-e^{-b(t-c)}} \quad (3)$$

$$Y(t) = \frac{1 - e^{-(a+b)t}}{1 + \frac{b}{a} e^{-(a+b)t}} \quad (4)$$

$$Y(t) = \frac{a}{1 - e^{-\left[\left(\frac{t}{b}\right)^c\right]}} \quad (5)$$

In some of the applications to the approximation, the curve from the hyperbolic tangent family (6) may be used where the natural n value ($n \in N$) is accepted in relation to the postulated curve course (see Fig. 2 for some values of n). For $a = 1$, the course of the presented formula (7) has two horizontal asymptotes: $y = 0$ and $y = 1$ [1].

$$Y(t) = a \cdot \frac{1}{2} \cdot [1 + \tanh(nt)] \quad (6)$$

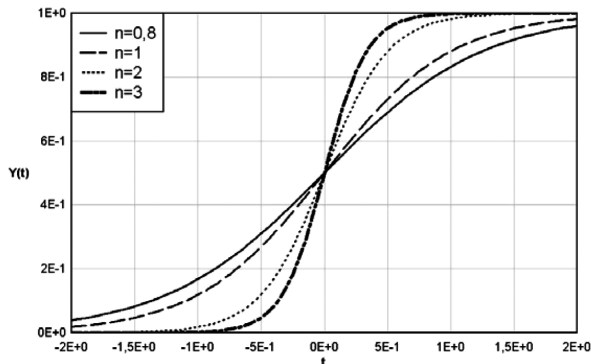


Fig. 2. Hyperbolic tangent family (n -parameter)

Let us consider the nonlinear first-order ordinary differential equation, called the logistic equation (8). Let us assume that: $a > 0, b > 0$. The solution of the equation with the original condition (9), where t_0 of the requested instant, whose value of the function is Y_0 , takes the form (10) [13]. The obtained curve is a logistic curve with horizontal asymptotes $Y = 0$ and $Y = b/a$, which is the S-curve type (see Fig. 3). The differential equation in the considered form may be used for a description of the population growth dynamics [4]. A properly calibrated curve, as a solution of the differential equation, served M.K. Hubbert as a means to predict the decrease in oil extraction in the United States of America in the 1970's [13].

$$\frac{dY(t)}{dt} - aY(t) + bY^2(t) = 0 \tag{7}$$

$$Y(t_0) = Y_0 \tag{8}$$

$$Y(t) = \frac{\frac{a}{b}}{1 + \left(\frac{a}{b} \frac{1}{Y_0} - 1\right) e^{-a(t-t_0)}} \tag{9}$$

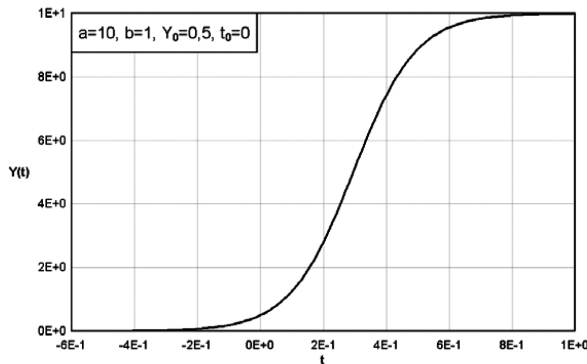


Fig. 3. The course of the curve which is the solution of the differential equation (10) for $a = 10, b = 1, Y_0 = 0.5$ and $t_0 = 0$

The S-curve can be approximated by the polynomial type families of normalized functions of the second order (11). It is visualized in Fig. 4 for $a = 0$ and $b = 1$. The values of curves are between 0 and 1. The function has its inflection point for the time variable equal to $t_{pp} = (a + b)/2$. A disadvantage of applying the second order polynomial is its definition in two sub-ranges. The advantage is its limited values of the function in the range $[0, 1]$ for normalized formulation (11).

A. Czarniogowska [6] after J. Evensmo and J.T. Karlsen [8] proposes application of the part of the third order polynomial function to the ex-post analysis of the actual cost function (12). They formulate the approximate formula for $AC(t)$ and $EV(t)$ directly taking into account values of budget at completion (BAC), estimate of completion (EAC) and the

on-line determined schedule performance index (SPI). Application of formula in general formulation (13) makes it possible to easily apply the regression analysis for approximation. In formula (13), it is assumed that project starts for $t = 0$, i.e. $Y(0) = 0$. Moreover, if we assume that for the time variable equal to t_{pp} the considered function (13) has its inflection point, the additional relationship (14) may be formulated. This relationship is useful for application of the formula to approximation of the realistic $AC(t)$ curve in the later time part of realization, when the realistic value of t_{pp} is known. A disadvantage of applying the third order polynomial is changing the S-type form of the function out of the limited range of time.

Application of the polynomial type of approximation is very useful for practical application. The least mean squares method can be used for finding the values of unknown parameters of the approximate function. In practice, there is no problem with the number of points, for which the actual cost values are known.

$$Y(t) = \begin{cases} 0 & \text{for } t < a \\ 2\left(\frac{t-a}{b-a}\right)^2 & \text{for } a \leq t \leq \frac{a+b}{2} \\ 1 - 2\left(\frac{t-b}{b-a}\right)^2 & \text{for } \frac{a+b}{2} \leq t \leq b \\ 1 & \text{for } t > b \end{cases} \quad (10)$$

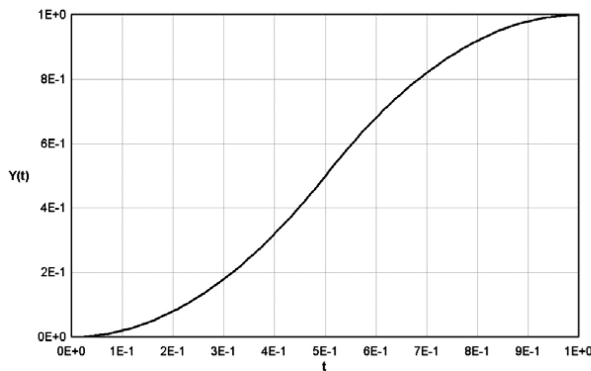


Fig. 4. Example of the polynomial second order spline function (11) for $a = 0$ and $b = 1$

$$AC(t) = \frac{EAC}{T^2} \left(3t^2 - \frac{2}{T}t^3 \right); \quad T = \frac{T}{SPI} \quad (11)$$

$$Y(t) = at^3 + bt^2 + ct \quad (12)$$

$$b = -3at_{pp} \quad (13)$$

3. Function approximation

The essence of the notion of function interpolation and approximation is creating a continuous function, which describes the course of the chosen parameter's variations in the best way possible. The values of the parameters are known in the specific point, in our case in the specific instants, namely in the discrete form. The notion of interpolation is connected with defining the function exactly going through the discrete points. The notion of approximation, however, does not contain the limit of going beyond the discrete points and set of discrete data. The considered problem of defining the real time of project implementation is a problem of approximation, in which, with data on a fragment of the project execution time, we estimate what is going to happen in the future. The notion of extrapolation is not unequivocally stated and is related to two problems: the choice of the class of the approximation function (type of the function) and the criteria of the approximation error, which, when minimized, define the notion of the best approximation for the considered problem. When the problem of nonlinear approximation is considered (e.g. the *S*-curve type approximation), the problem of selecting the chosen class of approximation curve is more important than the obtained average (discrete or integral) value of the chosen error measure – if the procedure of error minimization has been applied to the obtained values of parameters, which define the approximation curve. It also introduces the problem of interpolation and multidimensional approximation, in which the created functions depend on numerous parameters (independent variables). In the analysed case, it is a single-valued approximation, as the functions in the EVM methods are only the functions of time. It is worth pointing out that one of the approximation methods is the least squares method, and especially the linear regression in which the approximate function is a linear function with unknown coefficients subject to evaluation (it is possible to build non-linear functions by using a proper transform). The error measurement is written in the form of a quadratic function, after the variance function likeness. However, different kinds of approximation may be encountered in technology, e.g. in the Fourier series, Chebyshev, Lagrange and Legendre polynomials.

S-type function courses are essential for the EVM applications. It is crucial to choose the best values of the *a*, *b* and *c* parameters. Various possibilities of approximation, which lead to various extrapolation courses, have been presented in [1, 4, 6, 13, 15, 16, 24]. It is therefore crucial to estimate the criteria of the extrapolation, which is also connected with the criteria used in the management of a given project.

S-type function courses, discussed in the previous section, are essential for the EVM applications. It is crucial to choose the best values of the *a*, *b* and *c* parameters. Various possibilities of approximation, which lead to various extrapolation courses, have been presented in an approach determined in Fig. 5. Comments “better”, “poor” and “average” describe the quality of approximation with relation to the PV curve. It is therefore crucial to estimate the criteria of the extrapolation, which are also connected with the criteria used in management of a given project.

It is also possible to use the calculus of the probability approach for the notion of the $AC(t)$ curve approximation, starting from the actual time (AT) instant, in a way similar as

in the case of creating the $PV_i(t)$ curve family. In such an approach, the ellipse of project completions is created as well – Fig. 6. A series of simulations with the Monte Carlo method should be used for determining the ellipse in the most convenient way.

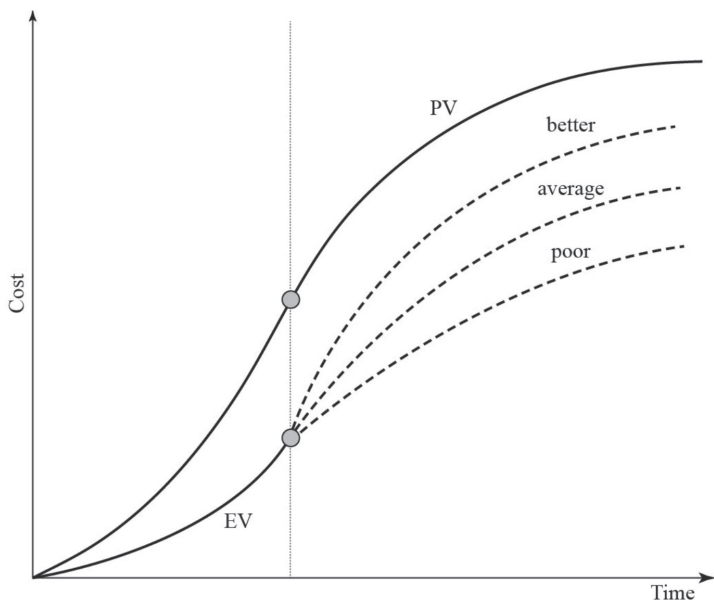


Fig. 5. Examples of various approximations of the $EV(t)$ function course in the determined approach [3]

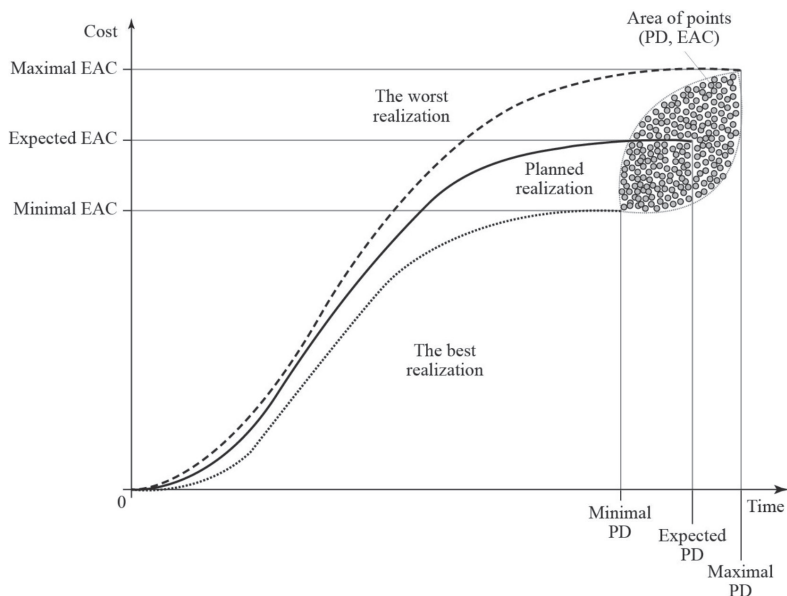


Fig. 6. The calculus of probability presentation of the $AC(t)$ curve approximation [9]

4. An exemplary analyses

4.1. General remarks

During the project implementation in the EVM method, one has at the disposal the $PV(t)$ function of the planned value and the $AC(t)$ curves of the actual cost of the performed activities, as well as the $EV(t)$ of the earned value, determined only up to the actual time (AT), $t \in [0, AT]$ instant. As has been mentioned above, usually the functions are of a character similar to the S-type function. It is therefore natural that in order to predict it, the function approximation method with the choice of approximate function class is used, taking into consideration all the above-mentioned limits to the approach. The values of some of the parameters may, or even should, at least when considering the range of their values, be selected with the $PV(t)$ function course taken into account. Next, one should subjectively choose the criteria of the best approximation. For the polynomial type of approximation, the least square method is commonly used to find the best approximation (to minimize the error of approximation).

4.2. Real investment project

In order to present the application of the estimation method, the example of a completed building and refurbishment project, described by S. Wawak [22], was taken into consideration. The $AC(t)$ curve is defined for $t \in [0, 101]$ and is presented in the Fig. 7, where time is scaled in weeks. Looking at the curve as a whole, it has a form of the S-curve, but it is not the model course of the S-curve, especially in the final part of realization of the project.

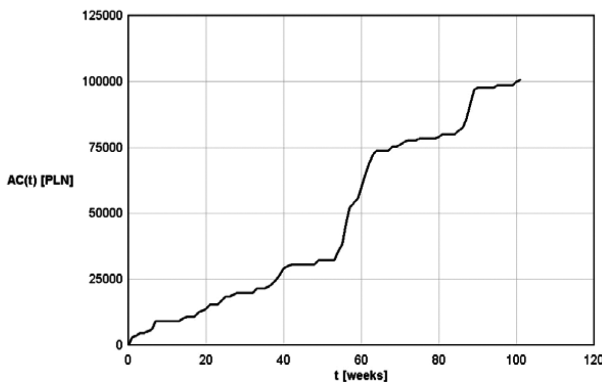


Fig. 7. The example course of the actual cost curve for the real investment project [22]

The on-line updating of the $AC(t)$ curve is tested by taking into account the only data to chosen time value t_n . More detailed $t \in [0, t_n]$, $n \in [0, 100]$. The method is applied to extrapolation of the function after its inflection point, hence $t_p = 62$, $n > 62$ and formula (14) is used for the least square method. The parameter chosen for validation of the

method is the final cost of the project t_{101} . The realistic value is equal to $t_{101} = 100\,769$. In Table 1, there are compared values of final cost obtained by the on-line type of estimation and the percentage relative error of estimation. As an example the approximation function obtained for $n = 100$ has form (15).

$$Y_{100}(t) = -\frac{1324249618837}{10921580194370}t^3 + \frac{123155214551841}{5460790097185}t^2 - \frac{1324249618837}{10921580194370}t \quad (14)$$

Table 1. Relative error of on-line estimation of the final cost

n	Final cost [tys. PLN]	Relative error [%]
Exact	100.769	–
70	109.547	8.7
80	108.668	7.8
90	105.941	5.1
100	101.641	0.9

4.3. S-curves analysed by A. Czarniogowska

A. Czarniogowska analysed the two project models, which are purely hypothetical, but were used to illustrate the discussed method in the article [6]. The actual cost functions have the form of S-curves and are defined in the period $t \in [0, 12]$. The on-line approximated functions obtained by the last mean squares method for $t = 7$ for both cases are shown in Fig. 8 together with the original functions. The assumed inflection point is $t = 6$ for both cases. The analytical formula for the approximation formula for the first case has the form (16) and is shown in Fig. 8 (top). The analytical formula for the approximation formula for the second case has the form (17) and is shown in Fig. 8 (bottom).

$$Y_7(t) = -1.174301691t^3 + 21.13743044t^2 - 1.174301691t \quad (15)$$

$$Y_7(t) = -\frac{759759}{352652}t^3 + \frac{11396385}{352652}t^2 - \frac{759759}{352652}t \quad (16)$$

The approximation function for the first case is almost the same as the analysed function (see Fig. 7 – left). For the second case, due to the position of the inflection point, the obtained approximate S-curve starts to go down before the end of the analysed range (planned duration time – PD). It can be observed when the approximation formula has the form of polynomial of the third order. In a practical application, it means that estimated time duration (ED) is shorter than planned time duration (PD). The possibility of such experience in practical realization must be verified in comparison with other parameters of project monitoring, or the other method of estimation of ED should be applied for comparison.

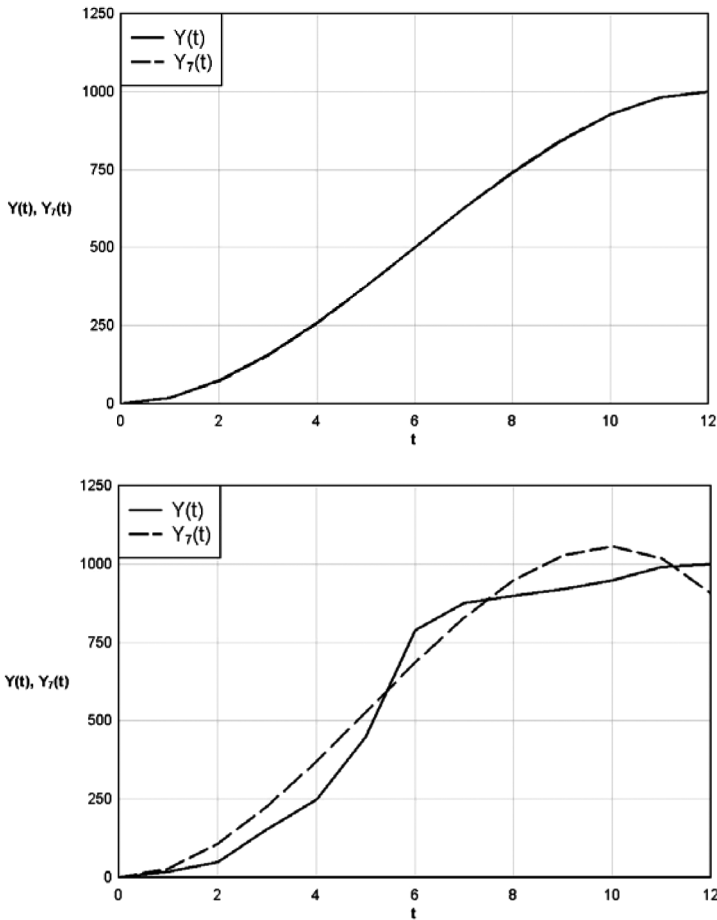


Fig. 8. The actual costs curves analysed by A.Czarniogowska [6] and their approximations

4.4. S-curve analysed by J. Dolezal

J. Dolezal [7] analysed the project described by the planned value function $PV(t)$ (see Fig. 8). Its realization is monitored by the actual cost function $AC(t)$ defined up to time equal to 6 weeks (see Fig. 8). The actual cost function is extrapolated by polynomial function of the third order by the least square method assuming the inflection point for $t = 9$ week, as it is observed for the $PV(t)$ curve (see Fig. 9). The approximation function is defined by formula (18), and is shown in Fig. 9.

$$AC_9(t) = -\frac{2747}{102444}t^3 + \frac{24723}{34148}t^2 + \frac{846584}{179277}t \quad (17)$$

The planned final cost of the project is equal to $PV(15) = 151$, and estimated by the up-dated actual cost curve is equal to $AC_9(15) = 143$. The relative error of estimation of this value is equal to 5.3%.

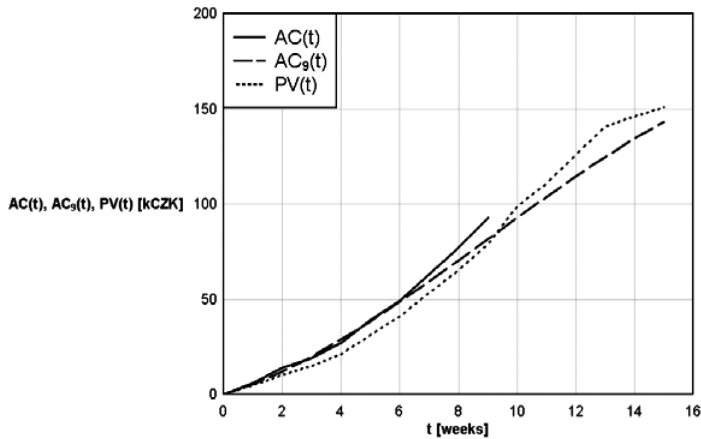


Fig. 9. The actual cost function approximation for the case analysed by J. Dolezal [7]

5. Conclusions

The proposed method of the on-line approximation of the actual cost curve shape is a flexible method with a great range of application possibilities. The essence of the presented approximation is connected with the applied family of the approximation function. It is polynomial of the third order. It makes the approximation much more convenient than the exponential type functions commonly used in literature.

The examples used in the presented article for verification of the method are taken from literature and are chosen to show the following problems of approximation:

- ▶ Irregular (non-ideal) form of the $AC(t)$ function after S. Wawak [22],
- ▶ $AC(t)$ of ideal form and shape with translated in time domain inflection point after A. Czarniogowska [6],
- ▶ $AC(t)$ function defined before it reached its inflection point after J. Dolezal [7].

The analysed examples show the possibility of applying the polynomial of the third order function for the approximation of the S-type function. For a proper approximation, the inflection point must be defined. The obtained values of estimated time duration (ED) or estimate cost at completion (EAC) for some extraordinary cases, e.g. when the obtained approximate S-curve starts to go down before the end of the planed time duration (PD), must be verified in comparison with other parameters of project monitoring, or the other method of estimation of ED should be applied for comparison.

The presented method may be used as yet another assisting tool for the project manager, whose aim is to facilitate the estimation of the real project ED time or the real project EAC cost.

References

- [1] Arfken G.B., Weber J.W., *Mathematical Models for Physicist*, Burlington MA, Harcourt/Academic Press San Diego, San Francisco, New York, Boston, London, Sydney, Toronto, Tokyo 2001.
- [2] Bass' Basement Research Institute (BBRI), *Mathematical derivation of the Bass model*, 2012, <http://www.bassbasement.org/BassModel>
- [3] Burke R., *Project Management. Planning and Control Techniques*, John Wiley & Sons Ltd, Chichester, New York, Weinheim, Brisbane, Singapore, Toronto 1999.
- [4] Cioffi D.F., *A tool for managing project: an analytic parametrization of the S-curve*, *International Journal of Project Management*, 2001, No. 23, 215–222.
- [5] Corovic R., *Why EVM is not good for schedule performance analyses (and how it could be...)*, *The Measurable News*, www.earnedschedule.com/papers, 2006–2007.
- [6] Czarnigowska A., *Earned value method as a tool for project control*, *Budownictwo i Architektura*, 2008, No. 3, 15–32.
- [7] Dolezal J., *Projektovy management. Komplexne, prakticky a podle svetovych standardu*, Grada Publishing, Praha 2016.
- [8] Evensmo J., Karlsen J.T., *Earned value based forecasts – some pitfalls*, *AACE International Transactions*, 2006.
- [9] Hillson D., *Earned value management and risk management: a practical synergy*, *PMI 2004 Global Congress Proceedings*, Anaheim, California, USA 2004.
- [10] Hines W.W., Montgomery D.C., *Probability and statistics in engineering and management science*, Wiley, New York 1990.
- [11] Lipke W., Henderson K., *Earned schedule – an emerging enhancement to EVM*, 2007, www.pmicos.org/EVMDEC07.pdf
- [12] Mahadik S.G., Bhangale P.P., *Study & analysis of construction project management with earn value management system*, *International Journal of Innovative Technology and Exploring Engineering*, 2013, Vol. 3, Iss. 4, 40–44.
- [13] Morrison F., *The Art of Modeling Dynamic Systems. Forecasting for Chaos, Randomness and Determinism*, Multiscience Press Inc., 1991.
- [14] Murmis G.M., *S curves for monitoring project progress*, *Project Manage Journal*, 1997, 29–35.
- [15] Narbaev T., De Marco A., *An earned schedule-based regression model to improve cost at completion*, *Journal of Project Management*, 2013, Vol. 32, No. 6, 1007–1018.
- [16] Narbaev T., De Marco A., *Combination of growth model and earned schedule to forecast project cost at completion*, *Journal of Construction Engineering and Management*, 2014, Vol. 140, No. 1.
- [17] Project Management Institute (PMI), *Practice standard for earned value management*, Newtown Square, PA, 2011.
- [18] Seber G.A.F., Wild C.J., *Nonlinear regression*, Wiley, New York 1989.

- [19] Vandevoorde S., Vanhoucke M., *A comparison of different project duration forecasting methods using earned value metrics*, 2006, International Journal of Project Management, Vol. 24, 289–302.
- [20] Walczak R., *Podstawy zarządzania projektami. Metody i przykłady*, Difin, Warszawa 2014.
- [21] Wanner R., *Earned Value Management. So machen Sie Ihr Projektcontrolling noch effektiver*, Demand GmbH, Norderstedt 2007.
- [22] Wawak S., *Earned Value – metoda kontroli procesu zmian na przykładzie projektu inwestycyjnego*, Management Forum 2000, K. Krzakiewicz, S. Cyfert (ed.), Wydawnictwo Akademii Ekonomicznej w Poznaniu, Poznań 2003, 268–271.
- [23] Webb A., *Using earned value. A project manager's guide*, Gower Publishing Ltd., Aldershot-Burlington 2003.
- [24] Zając K., *Zarys metod statystycznych*, PWE, Warszawa 1994.



Stanislaw Krenich (krenich@mech.pk.edu.pl)

Institute of Production Engineering, Department of Mechanical Engineering,
Cracow University of Technology

MULTI-THREAD EVOLUTIONARY COMPUTATION FOR DESIGN OPTIMIZATION

WIELOWĄTKOWE EWOLUCYJNE OBLICZENIA RÓWNOLEGŁE W OPTYMALIZACJI KONSTRUKCJI

Abstract

The paper presents multi-thread calculations using parallel evolutionary algorithms (EA) for single and multicriteria design optimization. This approach was implemented to avoid a negative influence of incorrectly chosen initial and EA's control parameters for the accuracy of generated solutions and thereby to improve the effectiveness of the EA's use. Parallel computation for single optimization problems relies just on running n threads with different randomly chosen parameters in order to find the best final solution. For multicriteria optimization problems, each thread generates a set of Pareto optimal solutions and at the end these sets are combined together, giving a real set of Pareto optimal solutions. During the run of the algorithm, random interactions between threads were applied. The experiments were carried out using ten-thread processes for different examples of single and multicriteria design optimization problems, two of which are presented in the paper.

Keywords: parallel computation, evolutionary algorithms, design optimization.

Streszczenie

W artykule przedstawiono wielowątkowe obliczenia równoległe z wykorzystaniem algorytmów ewolucyjnych (AE) dla jedno- i wielokryterialnej optymalizacji konstrukcji. Przedstawioną metodę wykorzystano w celu uniknięcia negatywnego wpływu niewłaściwie dobranych parametrów inicjujących i sterujących w algorytmie ewolucyjnym na dokładność obliczeń, a tym samym w celu poprawy efektywności działania algorytmu. Obliczenia równoległe dla optymalizacji jednokryterialnej polegają na uruchomieniu n wątków z losowo dobranymi parametrami AE z przyjętych zakresów i zbiorów dyskretnych. Dla optymalizacji wielokryterialnej każdy wątek generuje niezależny zbiór rozwiązań Pareto, a następnie na końcu zbiory te są łączone w finalny zbiór rozwiązań Pareto. W trakcie obliczeń wprowadzono losowe interakcję między wątkami. Eksperymenty przeprowadzono z wykorzystaniem 10 wątków równoległych dla wielu przykładów, dwa przedstawiono w artykule.

Słowa kluczowe: obliczenia równoległe, algorytmy ewolucyjne, optymalizacja konstrukcji

1. Introduction

Evolutionary algorithms (EA) are powerful and widely used stochastic optimization techniques which rely on analogies to natural processes. They can often outperform conventional optimization methods when applied to difficult real-world optimization problems. Many different evolutionary algorithm based strategies have been developed recently to find the optimum for nonlinear programming problems including design optimization [1, 4, 7, 8]. There are some problems which belong to the area of computational expensive tasks, where objective functions and constraints require large computing power, for example solved by means of Finite Element based Method (FEM). The only use of simple evolutionary algorithms in order to generate the optimal solution or the set of Pareto solutions is often ineffective due to long calculation time or required calculation accuracy. Moreover, results obtained while running simple evolutionary algorithms in order to solve all optimization tasks depend significantly on setting initial parameters, such as initial population, type and probability of crossover and mutation, type of reproduction mechanisms, population size etc. An incorrect choice of initial parameters for single criterion optimization problems may lead to a local optimum which can be far from the real global optimum. For multicriteria optimization problems the set of optimal solutions is very often either far away from the real set of Pareto optimal solutions or not all Pareto optimal solutions are generated. The latter case refers mainly to discrete and integer programming models. In the literature there are not scientifically proven rules how to set these parameters, however some attempts are made [2–4]. In majority of the cases described so far, these parameters are assigned experimentally during the optimization process. Thus, in the paper the parallel evolutionary algorithms have been implemented to avoid the problems discussed above.

2. Problem formulation

The approach presented in the paper was applied to design optimization but it can be used to solve any other nonlinear optimization problems formulated as follows:

Find the vector of decision variables:

$$\mathbf{x} = [x_1, x_2, \dots, x_N] \quad (1)$$

which will satisfy the K inequality constraints:

$$g_k(\mathbf{x}) \geq 0 \text{ for } k = 1, 2, \dots, K \quad (2)$$

and the M equality constraints:

$$h_m(\mathbf{x}) = 0 \text{ for } m = 1, 2, \dots, M \quad (3)$$

and minimize the vector of the objective functions $\mathbf{f}(\mathbf{x})$, where

$$\mathbf{f}(\mathbf{x}) = [f_1(\mathbf{x}), f_2(\mathbf{x}), \dots, f_l(\mathbf{x})] \quad (4)$$

The method can be used to solve the following optimization models: with continuous decision variables, with integer decision variables, with discrete decision variables, with mixed continuous – integer decision variables, with mixed continuous – discrete decision variables.

3. Multi-thread computation algorithm

Generally, there are two main ways of running parallel evolutionary computing called synchronous and non-synchronous algorithms [1, 5, 6, 9, 10]. The first one deals with a common population in the main thread, where the evolutionary process including selection, crossover and mutation operations is implemented. The sub-threads are responsible for the calculation of objective functions, constraints and additional parameters. In this case, high-speed communication between the main and sub-threads is required. The non-synchronous way of parallel computing consists of n independent threads. In each thread, an evolutionary algorithm searching selected sub-domain is implemented. It is allowed to exchange any information between all threads. For example, each thread can be run with different population of chromosomes, parameters, objective functions, constraints, etc.

In the paper, the parallel computation was applied as a non-synchronous multi-thread process, whose flow diagram is presented in Figure 1.

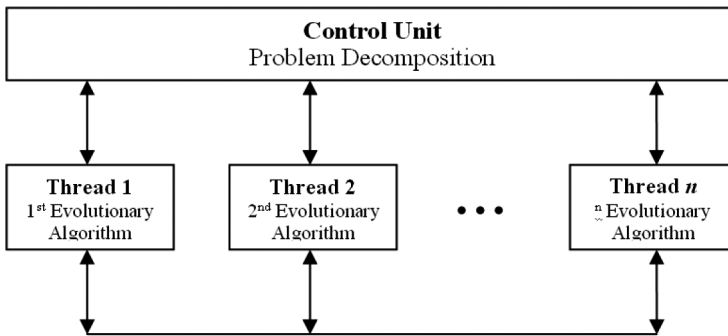


Fig. 1. Non-synchronous parallel evolutionary algorithm

The idea of parallel computations for single optimization problems consist in running n threads with different randomly chosen initial and control parameters in order to find the best final solution. For multicriteria optimization problems, each thread generates a set of Pareto optimal solutions and at the end these sets are combined together. During the parallel run of the threads, every k generations, an interaction between them is applied. This interaction is based on a random exchange of chromosomes (representing potential solution) selected from current sub-populations in different threads. The run of threads can be realized on a single computer using software or hardware decomposition to many threads or can be performed by

any computer network using the master-slave procedure. For the proper run of the proposed parallel algorithm some of parameters are required to be set. There are several parameters mentioned above which have significant influence on the effectiveness of evolutionary algorithms. The most important are selection pressure and quality of local and global search, which correspond respectively to crossover and mutation types and their settings. During all numerical experiments for these parameters, their ranges or values were assumed arbitrarily from the list of several types of evolutionary operators and for each thread were as follows:

- ▶ Range of crossover probability: $0.3 \leq RC \leq 0.8$
- ▶ Range of mutation probability: $0.0 \leq RM \leq 0.3$
- ▶ Range of initial parameter for a generator of random numbers: $1 \leq \text{seed} \leq 100$.
- ▶ List of possible selection types (refer to the selection pressure): {proportional, simple tournament, constraint tournament} [4, 7].

The remaining parameters were considered as the constant values: number of generations = 400, population size = 400, one-point crossover, uniform mutation, external penalty function with penalty parameter = 10000, numbers of threads = 10 and rate of thread exchange $k = 10$ (every k generations). The computations were carried out on the multi-core processor using C++ language.

4. Numerical Experiments

4.1. Single criteria design optimization

The problem deals with the minimum volume design of the six-step beam (Fig. 2). The results of running evolutionary algorithms for this problem while running different threads are shown in Table 1. These results show that by using the proposed approach we can avoid the influence of incorrectly chosen initial parameters and, simultaneously, we can improve the effectiveness of the use of evolutionary algorithms.

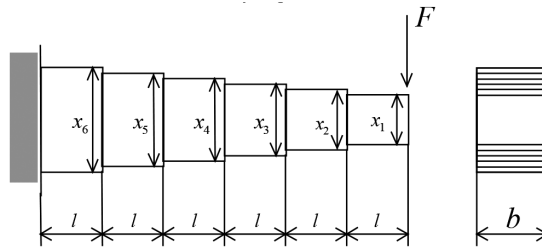


Fig. 2. Scheme of the six-step beam

The vector of decision variables is as follows:

$$X = [x_1, x_2, \dots, x_N]^T \quad (5)$$

where x_n is the thickness of the n -th part of the beam.

The objective function is the volume of the beam:

$$f(x) = bl \sum_{n=1}^N x_n \quad (6)$$

The constraints are:

► Shear stress constraints:

$$\frac{6F \times nl}{bx_n^2} \leq \sigma_g \quad \text{for } n = 1, 2, \dots, 6 \quad (7)$$

► Geometrical constraints

$$0 \leq x_1, \quad x_n \leq x_{n+1}, \quad x_N \leq d \quad \text{for } n = 1, 2, \dots, 6 \quad (8)$$

The problem was considered as a continuous programming problem and was run for the following data: $N = 6$, $l = 50$ [mm], $b = 50$ [mm], $F = 10000$ [N], $E = 2.06105$ [N/mm²], $\sigma_g = 360$ [N/mm²], $d = 32$ [mm].

All generated solutions are presented in Table 1. The calculations were carried out for randomly chosen EA's control parameters from the sets and ranges given above.

Table 1. Results of the parallel computing for the beam design problem

Thread	Objective function	Decision variables	Parameters			
	$f(x)$	$X = [x_1, x_2, x_3, x_4, x_5, x_6]$	R_c	R_m	seed ¹	Method of selection
1	371.910	[14.175, 21.698, 24.160, 27.489, 29.168, 32.073]	0.73	0.15	14	Proportional
2	349.656	[12.913, 18.262, 22.364, 25.821, 28.873, 31.628]	0.44	0.08	100	Constraint tournament
3	354.351	[13.750, 18.440, 23.120, 25.940, 28.870, 31.620]	0.65	0.05	87	Simple tournament
4	411.203	[15.120, 25.37, 288.810, 31.141, 31.984, 31.990]	0.31	0.29	28	Proportional
5	381.972	[14.540, 24.011, 24.780, 28.015, 29.460, 31.990]	0.56	0.21	3	Constraint tournament
6	406.471	[15.180, 24.810, 28.239, 30.469, 31.931, 31.970]	0.38	0.29	69	Proportional
7	359.967	[13.000, 20.130, 23.441, 26.020, 29.410, 31.980]	0.79	0.01	35	Simple tournament
8	349.595	[12.910, 18.260, 22.360, 25.820, 28.870, 31.620]	0.60	0.04	1	Constraint tournament
9	393.935	[14.300, 24.100, 26.740, 28.920, 31.520, 32.000]	0.36	0.18	43	Simple tournament
10	363.328	[13.000, 18.510, 23.440, 28.220, 30.190, 31.960]	0.53	0.13	52	Proportional
The final result	349.595	[12.910, 18.260, 22.360, 25.820, 28.870, 31.620]	0.60	0.04	1	Constraint tournament

¹ Seed decides on the initial population, R_c – crossover rate, R_m – mutation rate. All constraints satisfied

4.2. Multicriteria design optimization

Let us consider an example of the bicriterion optimization of the robot gripper mechanism presented in Fig. 3. It is assumed that all elements of the mechanism are stiff and friction forces are not considered. In order to build an optimization model, geometrical and force dependencies are calculated.

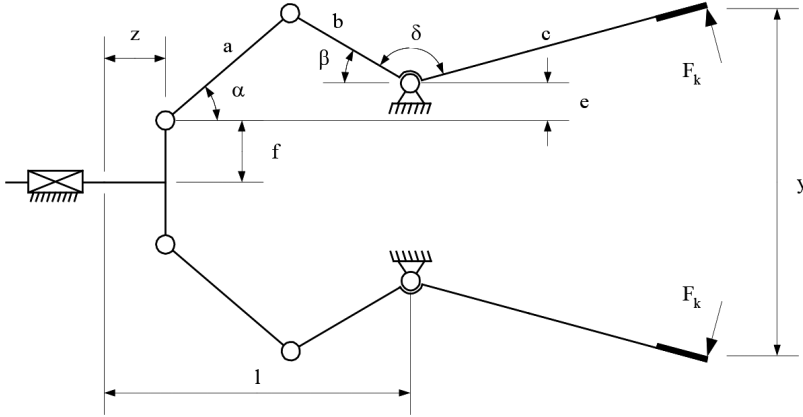


Fig. 3. Scheme of the robot gripper mechanism

The geometrical dependencies of the gripper mechanism are as follows:

$$g = \sqrt{(l-z)^2 + e^2}, \quad \varphi = \arctan\left(\frac{e}{l-z}\right) \quad (9)$$

$$\alpha = \arccos\left(\frac{a^2 + g^2 - b^2}{2 \cdot a \cdot g}\right) + \varphi, \quad \beta = \arccos\left(\frac{b^2 + g^2 - a^2}{2 \cdot b \cdot g}\right) - \varphi \quad (10)$$

$$y(\mathbf{x}, z) = 2 \cdot [e + f + c \cdot \sin(\beta + \delta)] \quad (11)$$

The force dependencies are as follows:

$$R_{AX} = \frac{P}{2}, \quad R_{AY} = \frac{P \cdot \sin(\alpha)}{2 \cdot \cos(\alpha)} \quad (12)$$

$$R_{BX} = \frac{P}{2}, \quad R_{BY} = \frac{P \cdot \sin(\alpha)}{2 \cdot \cos(\alpha)} \quad (13)$$

$$R_{CX} = \frac{P}{2} \cdot \left(1 - \frac{b \cdot \sin(\alpha + \beta) \cdot \sin(\beta + \delta)}{c \cdot \cos(\alpha)}\right) \quad (14)$$

$$R_{CY} = \frac{P}{2} \cdot \left(\frac{\sin(\alpha)}{\cos(\alpha)} + \frac{b \cdot \sin(\alpha + \beta) \cdot \cos(\beta + \delta)}{c \cdot \cos(\alpha)} \right) \quad (15)$$

$$R_A = \sqrt{\left(\frac{P}{2}\right)^2 + R_{AY}^2}, \quad R_B = \sqrt{R_{BX}^2 + R_{BY}^2}, \quad R_C = \sqrt{R_{CX}^2 + R_{CY}^2} \quad (16)$$

$$F_K = \frac{P \cdot b \cdot \sin(\alpha + \beta)}{2 \cdot c \cdot \cos(\alpha)} \quad (17)$$

For the dependencies given above, the optimization model is presented below. The vector of decision variables is as follows:

$$x = [a, b, c, e, f, l, \delta]^T \quad (18)$$

where:

a, b, c, e, f, l – dimensions of the gripper,

δ – the angle between b and c elements of the gripper.

The objective functions can be evaluated as follows:

- ▶ Maximization of minimal force transmission ratio:

$$\max f_1(\mathbf{x}, z) = \frac{\min F_k(\mathbf{x}, z)}{P}, \quad \text{for } Z_{\min} \leq z \leq Z_{\max} \quad (19)$$

- ▶ Minimization of maximal value of force reaction:

$$\min f_2(\mathbf{x}, z) = \max \{R_A(\mathbf{x}, z), R_B(\mathbf{x}, z), R_C(\mathbf{x}, z)\} \quad \text{for } Z_{\min} \leq z \leq Z_{\max} \quad (20)$$

Note that both objective functions depend on the vector of decision variables and on the displacement z . Thus, for the given vector x , values of the functions have to be evaluated for different values of z , which makes the objective functions computationally expensive and the problem becomes more complicated than a general nonlinear programming problem. From the geometry of the gripper, the following constraints can be derived:

- constraints based on the mechanism movement:

$$g_1(\mathbf{x}) = y(\mathbf{x}, z) \geq 0 \quad \text{for each } z, \text{ were } Z_{\min} \leq z \leq Z_{\max} \quad (21)$$

$$g_2(\mathbf{x}) = \alpha - \phi \geq 0 \quad \text{for each } z, \text{ were } Z_{\min} \leq z \leq Z_{\max} \quad (22)$$

$$g_3(\mathbf{x}) = \frac{\pi}{2} - \alpha \geq 0 \quad \text{for each } z, \text{ were } Z_{\min} \leq z \leq Z_{\max} \quad (23)$$

$$g_4(\mathbf{x}) = \frac{\pi}{4} - |\gamma| \geq 0 \quad \text{for each } z, \text{ were } Z_{\min} \leq z \leq Z_{\max} \quad (24)$$

$$h_1(\mathbf{x}) = z + a \cdot \cos(\alpha) + b \cdot \cos(\beta) - l = 0 \quad \text{for each } z, \text{ were } Z_{\min} \leq z \leq Z_{\max} \quad (25)$$

$$h_2(\mathbf{x}) = a \cdot \sin(\alpha) - b \cdot \sin(\beta) - e = 0 \text{ for each } z, \text{ where } Z_{\min} \leq z \leq Z_{\max} \quad (26)$$

► border constraints:

$$g_5(\mathbf{x}) = y(\mathbf{x}, Z_{\max}) - Y_{\min} \geq 0 \quad (27)$$

$$g_6(\mathbf{x}) = Y_{\max} - y(\mathbf{x}, 0) \geq 0 \quad (28)$$

$$g_7(\mathbf{x}) = l - Z_{\max} \geq 0 \quad (29)$$

where:

- $y(\mathbf{x}, z)$ – displacement of the gripper ends,
- Y_{\min} – minimal dimension of the gripping object,
- Y_{\max} – maximal dimension of the gripping object,
- Z_{\max} – maximal displacement of the gripper actuator.

Assumed values: $Y_{\min} = 0$ [mm], $Y_{\max} = 0$ [mm], $Y_{\max} = 2000$ [mm], $Z_{\max} = 50$ [mm], $P = 1$ [N]. Note that input force value P has proportional impact to functional characteristics. In order to show only the force transmission ratio of the mechanism, its value was set as equal to 1 [N]. The calculations were executed as a ten-thread run for randomly chosen EA's control parameters taken from the sets and ranges given in chapter 3. In each of the ten processes, an individual set of Pareto solutions was generated using different EA's control parameters. These sets are presented in Figure 4. At the end, these sets were combined together giving a final set of Pareto optimal solutions. This set of solutions is much more accurate than the individual sets. In this case, the front of Pareto solutions was built on the basis of threads 1, 2, 8.

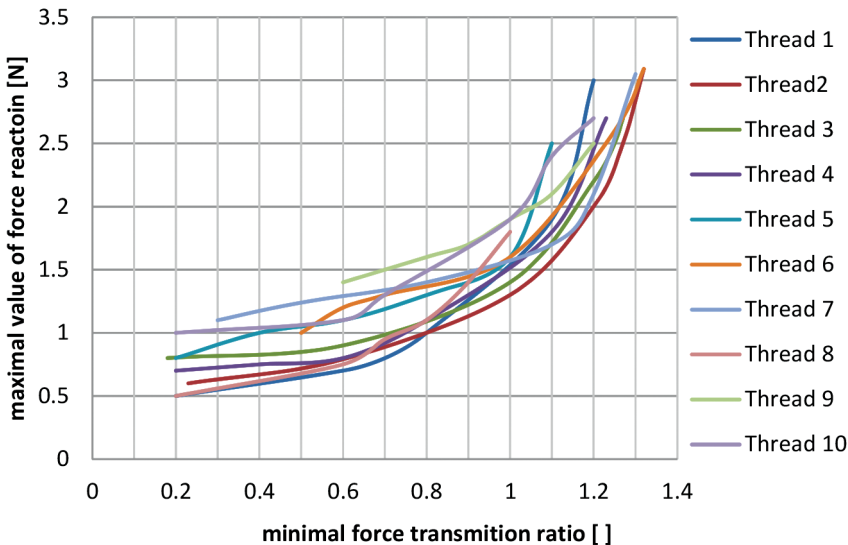


Fig. 4. Sets of Pareto optimal solutions generated while parallel computation for the gripper mechanism

Table 2. Border solutions for the gripper mechanism generated by parallel computing

Solution	Objective function	Decision variables	Control parameters			
	$f(\mathbf{x}, z) = [f_1(\mathbf{x}, z), f_2(\mathbf{x}, z)]$	$\mathbf{X} = [a, b, c, e, f, l, \delta]$	R_C	R_M	seed ^l	Method of selection
First	[0.20, 0.5]	[94.47, 70.55, 199.44, 0.37, 108.43, 100.78, 2.14]	0.58	0.12	84	constraint tournament
Last	[1.32, 3,09]	[174.32, 128.14, 150.52, 71.22, 5.17, 115.84, 2.53]	0.65	0.09	29	simple tournament

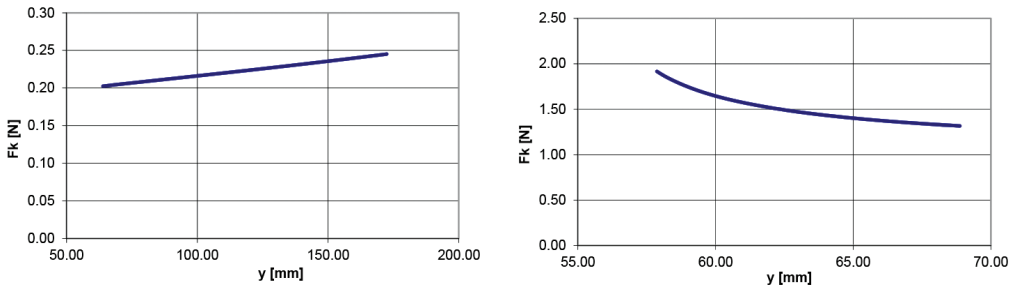


Fig. 5. Force characteristics for the border solutions (respectively the first and the last solution)

5. Conclusions

The evolutionary algorithm based on the parallel computation approach was proposed in the paper. There were many tests of single and multicriteria design optimization carried out to confirm the effectiveness of the algorithm considering its accuracy. The results obtained so far indicate that the presented method can be successfully implemented to avoid an influence of incorrectly chosen initial or control parameters of EA and, simultaneously, to improve the effectiveness of the algorithm. Interactions between different threads during the evolution of each population improved the quality of each sub-population and at the end yielded better value of the objective function or the front of Pareto solutions. But from the other point of view, the presented approach has a disadvantage. The run of the parallel algorithm requires large computation power, thus calculations on a single machine are longer. The calculation time can be improved by the use of a multi-device cluster in the local area network (LAN). Considering all properties of the method, it is clear that it provides the designer with a very effective tool for solving fairly complicated tasks. The method has a universal character and can be applied to solve a wide range of single and multicriteria design optimization problems.

References

- [1] Burczynski T., Dlugosz A., Kus W., *Parallel Evolutionary Algorithms in Shape Optimization of Heat Radiators*, Journal of Theoretical and Applied Mechanics 44, 2, Warszawa 2006, 351–366.
- [2] Grefenstette J., *Optimization of Control Parameters for Genetic Algorithms*, IEEE Transactions on Systems, Man, and Cybernetics, Vol. 16, No. 1, 1986, 122–128.
- [3] Kieś P., *Selection of genetic algorithm parameters using off-line method (In Polish)*, Instytut Naukowo-Badawczy ZTUREK, Warszawa 2000.
- [4] Krenich S., *Genetic Algorithms in Parametrical Optimization of Robot Gripper Mechanisms*, Ph.D. thesis (in Polish), Wydział Mechaniczny, Politechnika Krakowska, Kraków 2002.
- [5] Lis J., Lis M., *Self-adapting Parallel Genetic Algorithm with Dynamic Mutation Probability, Crossover Rate and Population Size*, Proceedings of the First Polish National Conference on Evolutionary Computing, J. Arabas (ed.), Politechnika Warszawska, Warszawa 1996, 324–329.
- [6] Miki M., Hiroyasu T., Hatanaka K., *Parallel Genetic Algorithms with Distributed-Environment Multiple Population Scheme*, The 3rd World Congress on Structural and Multidisciplinary Optimization, Buffalo 17–22 May, USA, 1999.
- [7] Osyczka A., *Evolutionary Algorithms for Single and Multicriteria Design Optimization*, Springer-Verlag Physica, Berlin Heidelberg, 2002.
- [8] Osyczka A., Krenich S., *Evolutionary Algorithms for Global Optimization*, [in:] *Global Optimization – Selected Case Studies*, J. Pinter (ed.), Kluwer Academic Publishers, Dordrecht/Boston/London 2007.
- [9] Osmera P., Lacko B., Peter M., *Parallel Evolutionary Algorithms*, Proceedings IEEE International Symposium on Computational Intelligence in Robotics and Automation, 2003.
- [10] Sadecki J., *Parallel algorithms for optimization and testing of their effectiveness (in Polish)*, Oficyna Wydawnicza Politechniki Opolskiej, Opole 2001.

Marek A. Książek (marek.ksiazek@pk.edu.pl)

Janusz Tarnowski

Faculty of Mechanical Engineering, Cracow University of Technology

INFLUENCE OF DUAL VIBRATIONS ON CONTROL OF PERCUSSIVE
HAND-OPERATED POWER TOOLS – EXPERIMENTAL INVESTIGATIONS

WPLYW WIBRACJI OGÓLNYCH I MIEJSCOWYCH NA STEROWANIE
NARZĘDZIEM RĘCZNYM – BADANIA DOŚWIADCZALNE

Abstract

This article presents the results of pioneer experimental research into the impact of whole body vibration (WBV) and hand arm vibration (HAV) with different amplitudes and frequencies on percussive tools which are controlled by hand. In these studies the human operator is considered as the active element of the control system. The quality of control executed by the participants of the tests was assessed by the typical parameters existing in control system engineering, such as rise time, settling time, overshoot and integral square error (ISE). The tests were performed on an especially built stand. Results are presented in the form of time histories of step reference force. Forces realized by the operator were statistically analysed and graphically presented. Local (HAV) vibration of tools and accompanying dynamic forces between the handle and the vibrating tool have a big influence on control of the tool. An increase in the frequency of the tools' vibration increases the adjustment range. The influence of platform vibrations on the adjustment range is relatively small.

Keywords: Human as manual tool control system, Influence of WBV and HAV on man's control reactions

Streszczenie

W artykule przedstawiono pionierskie wyniki badań doświadczalnych wpływu wibracji ogólnej i miejscowej o różnej amplitudzie i częstotliwości na sterowanie ręcznym narzędziem wibroudarowym. Człowiek-operator jest tu traktowany jako aktywny element układu sterowania. Jakość sterowania wykonywanego przez uczestników testów jest oceniana poprzez typowe parametry takie jak czas narastania, czas regulacji, przeregulowanie czy wskaźnik ISE. Testy były wykonywane na specjalnie zbudowanym stanowisku. Wyniki są zaprezentowane w formie przebiegów czasowych na skokowy sygnał referencyjny. Siły wywierane przez operatora zostały opracowane statystycznie i przedstawione graficznie. Wibracje miejscowe narzędzia wraz z towarzyszącymi im siłami dynamicznymi mają duży wpływ na sterowanie narzędziem. Wraz ze wzrostem częstotliwości wibracji wzrasta zakres odchyłek od wymaganej siły. Wpływ wibracji platformy na ten zakres jest relatywnie mały.

Słowa kluczowe: człowiek jako element układu sterowania narzędziem, wpływ wibracji ogólnej i miejscowej na sterowanie

1. Introduction

Human - machine interactions are one of the most interesting and difficult branches of science. The reason for this is because of the variety of the human form, physical connections between machine and operator and various other dependencies. All of these factors determine the final results of each measurement, modelling and assessment of man-machine systems. The first significant works concerning the interaction between the pilot and the control system of an aeroplane were provided by [8]. A more general approach was presented in [9]. Some aspects of the influence of whole body vibration upon human-operators' reactions and comfort were described in [2] and [10]. From the 1960s up until the time of writing this paper, many works and experiments concerning various approaches to human-machine studies have been conducted, predominantly in military laboratories.

The experimental investigations described in this paper are a continuation of a series of experiments carried out by [1, 5] showing the new effects of various factors on the manual control of hand-operated power tools.

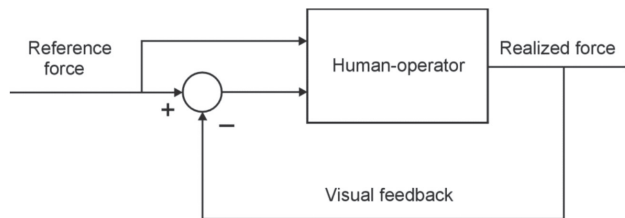


Fig. 1. General flow diagram of signals

In the tests, the human operator is treated as an element of the control-visual feedback regulator. The general scheme of the block diagram of the human – operator feedback control system is shown in Fig. 1.

2. Materials and methods

The experimental studies were conducted on the modified test bench used previously in the works of [3, 4, 7]. In the present paper, a new approach was applied and described for the human-operator subjected simultaneously to two sources of vibrations acting upon legs and hands. A schema of the used test bench with its principal components is shown in Fig. 2.

A photograph of the experimental test bench is presented in Fig. 3. The modified stand was designed as a system composed of a platform, two vertical bars and a horizontal beam placed on the piston of the electro-hydraulic Heckert SHA 140 shaker. Figure 3 shows the vertical and horizontal shakers and corresponding directions of applied excitations. As is shown in Fig. 3, the human-operator stands with one foot forward to the front of the tool on the vibrating platform holding in his hands the handle of the vibrating hand-tool whilst

watching the monitor screen. The task of the operator is to control the motion of the tool by exerting pressure on the handle in accordance with the tracking value displayed on the monitor's screen. Real-time visualisation of the two signals is realised on the front panel of a virtual instrument within LabView 7.1, shown in Fig. 4, in the form of two mobile, coloured indicators, allowing their comparison. The human-operator tool system is treated here as a typical system of control with visual feedback.

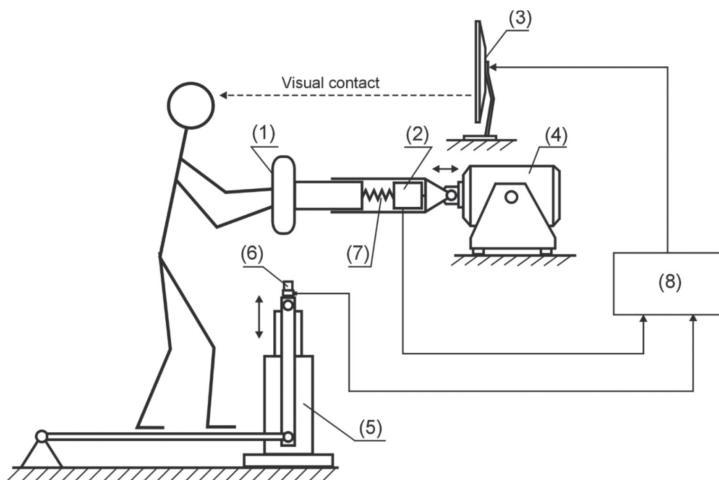


Fig. 2. Schema of the used test bench: 1 – vibrating handle of tool, 2 – vibrating tool with force sensor, 3 – monitor screen, 4 – electromagnetic shaker, 5 – electro-hydraulic shaker connected to the horizontal platform, 6 – accelerometer measuring vertical vibrations of the shaker, 7 – vibration isolation system for the handle, 8 – system of acquisition, registration and control



Fig. 3. View of experimental stand during testing

As the input signal is assigned to the monitor (a sudden step force of 80 [N]), the operator must match this value by applying pressure on the handle of the tool. The tool is connected to the other components of the test-bench through the integrated force sensor. The force exerted by the operator is continuously displayed on the monitor screen. It allows, by visual feedback and observation of state error between two signals displaced on the monitor, comparison between applied and reference forces.

Execution of the task by the operator has deliberately been made more difficult by introducing distortions coming from the vibrating platform (WBV-whole body vibration) and the vibrations of the tool (HAV-hand arm vibrations). The design of the measuring test-bench allows the introduction of different frequencies and amplitudes of vibrations submitted to the operator. The Heckert electro-hydraulic shaker vibrates the measuring platform in accordance with instructions from the controlling unit. During the tests, the shakers were controlled by sine functions with frequencies 3, 5, 10 and 15 Hz and the amplitudes corresponding to the data frequency exposure nuisance limit for standard exposures of 15 minutes. The hand tool controlled by the operator was set in oscillatory motion by the horizontal electromagnetic shaker shown in Figures 3 and 4. The frequencies generated by the shaker and the platform were assumed to be the same in order to fortify the effect of the influence of vibration disturbances on the operator.

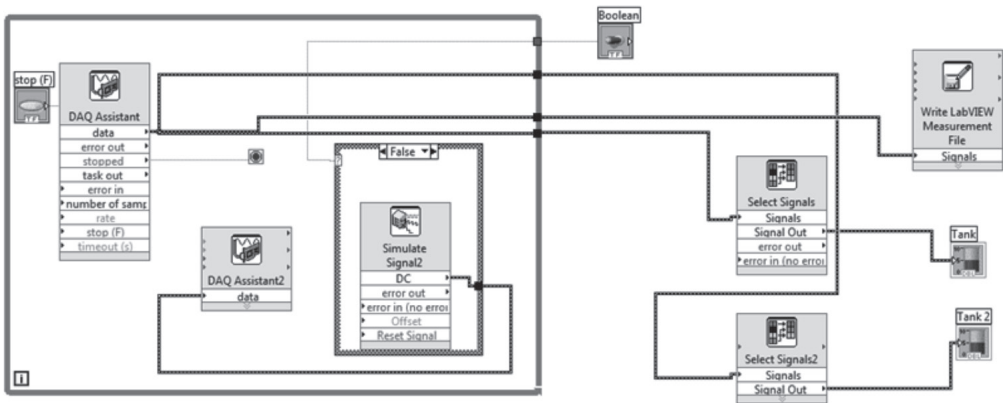


Fig. 4. Signal flow diagram

The following factors have been implemented and realized in the LabView software environment: the generation of input force; the measurement of the input force; the force exerted by the operator; the visualization and registration of both forces. Figure 5 shows the signal flow diagram of the program. The test consists of a strain gauge force sensor in the full bridge dedicated to the sensor amplifier, the strain gauge power supplier, measurement card NI DAQ 6024E together with the connections and measurement computer equipped with LabView software. A measuring track diagram is shown in Fig. 5.

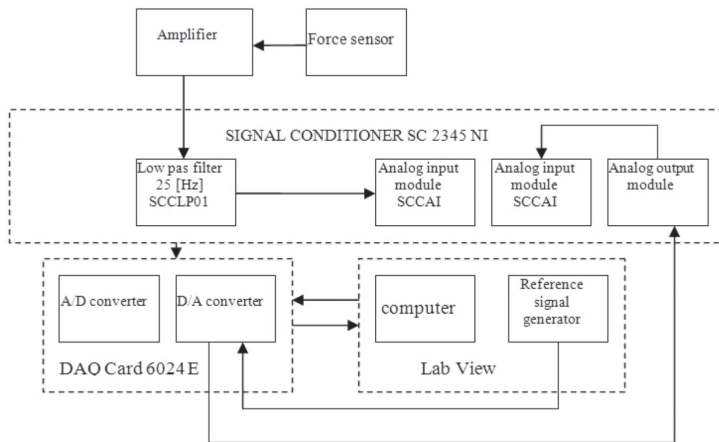


Fig. 5. Measuring track diagram

3. Results

The tests were conducted in the laboratory at the Department of Dynamics of Material Systems of Cracow University of Technology for 7 selected volunteers. Each of the participants stood on the measuring platform in a defined position under the following three conditions: 1) control of pressure force on the tool handle without whole body vibration (WBV) but with hand arm vibration (HAV); 2) control of pressure force on the tool handle with whole body vibration (WBV) only; 3) control of the realized pressure force on the tool handle with both whole body vibration (WBV) and hand arm vibration (HAV) acting simultaneously. All of the tests were carried out under the influence of vibrations with sequential frequencies 3, 5, 10, 15 Hz. Each attempt was recorded in the form of time histories of the input sudden step reference forces and the response forces exerted by the operator on the tool handle. The measured signals were sampled with a frequency of 5 kHz. Figures 6–13 show examples of typical time responses registered for different trails.

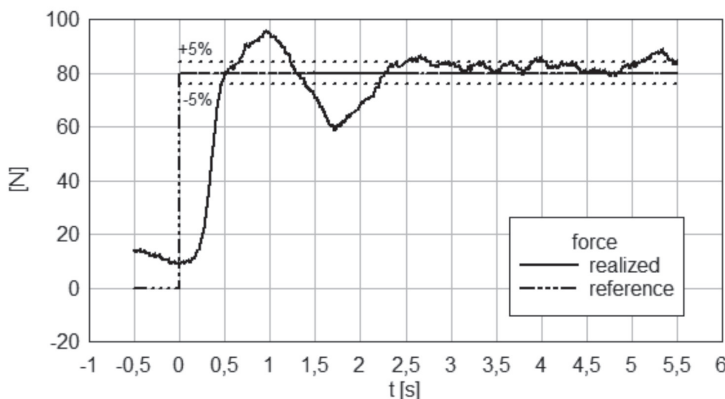


Fig. 6. The time history of the force realized by the operator subjected only to platform vibration with a frequency of 3 [Hz]

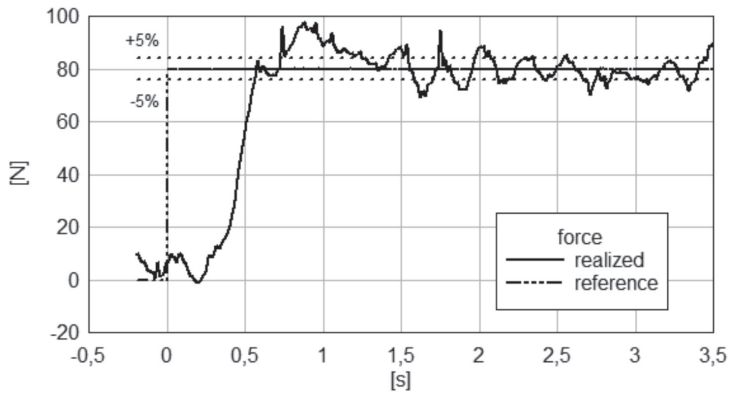


Fig. 7. The time history of the force realized by the operator subjected simultaneously to platform and tool vibration with the same frequency of 3 [Hz]

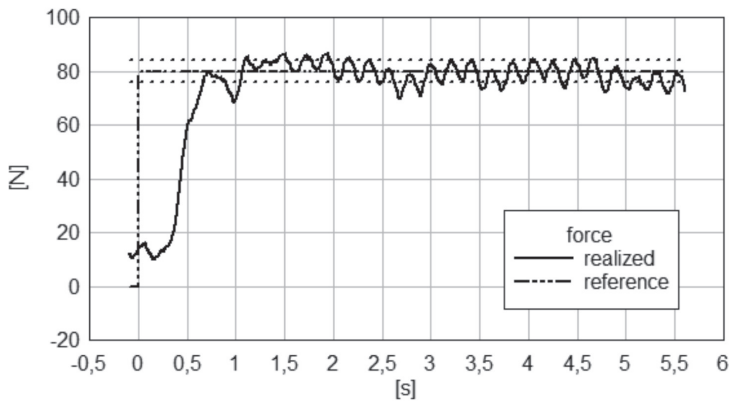


Fig. 8. The time history of the force realized by the operator only subjected to platform vibration with a frequency of 5 [Hz]

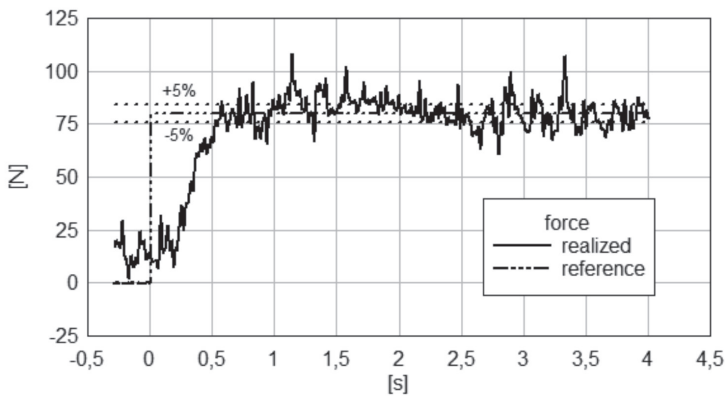


Fig. 9. The time history of the force realized by the operator subjected to platform and tool vibration simultaneously with the same frequency of 5 [Hz]

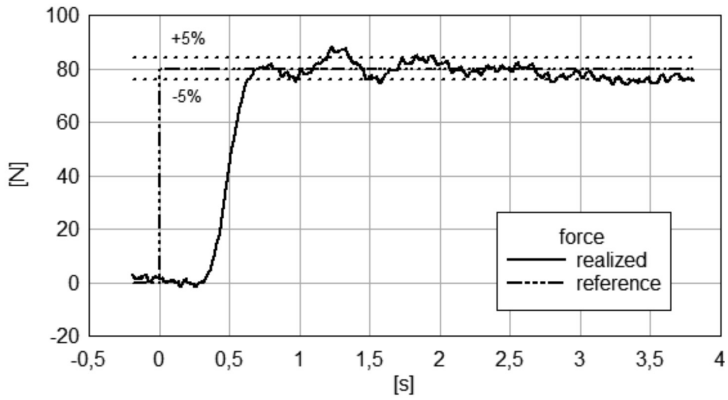


Fig. 10. The time history of the force realized by the operator subjected only to platform vibration with a frequency of 10 [Hz]

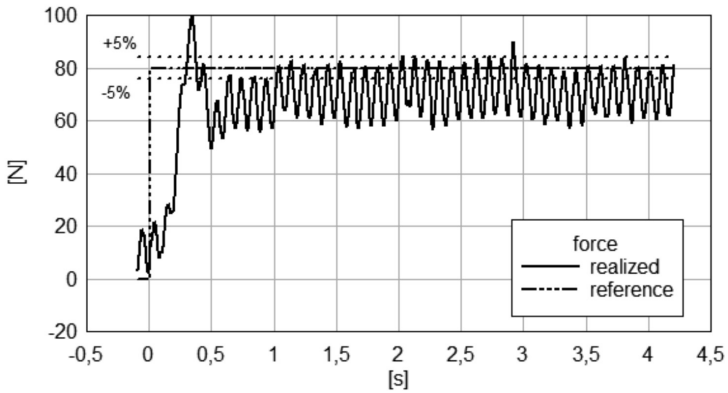


Fig. 11. The time history of the force realized by the operator subjected simultaneously to platform and tool vibration with the same frequency of 10 [Hz]

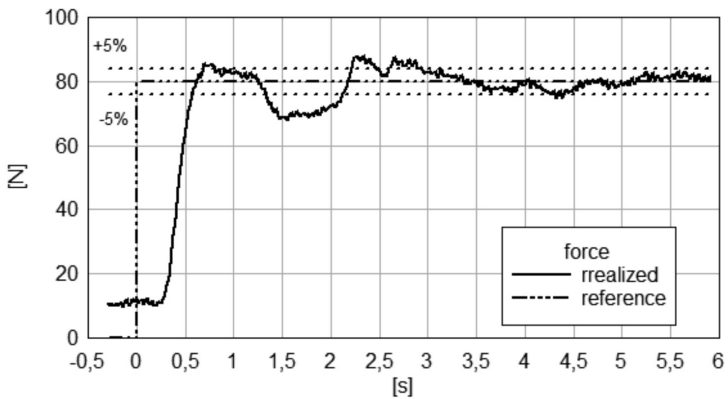


Fig. 12. The time history of the force realized by the operator only subjected to platform vibration with a frequency of 15 [Hz]

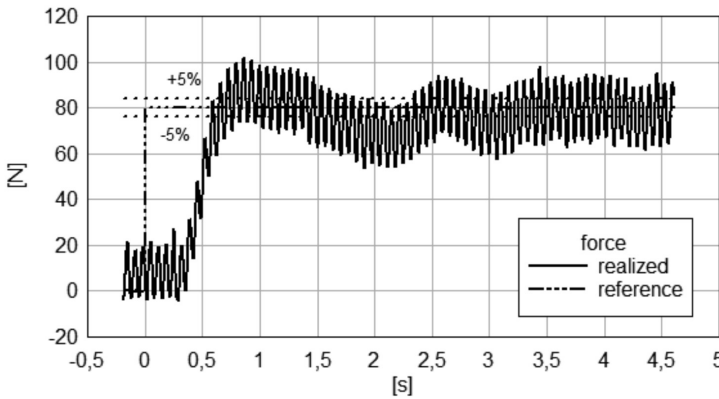


Fig. 13. The time history of the force realized by the operator subjected to platform and tool vibration simultaneously with the same frequency of 15 [Hz]

4. Discussion

The timing signals of the input force and the realized force have been processed in the D-plot software (HydeSoft USA). Because of the high gain signals from the bridge failures and performing measurements in a hall in which other used devices were submitted to some excitations (general and local vibrations), the signals from the sensor force had to be pre-filtered to remove the interference of external perturbations. Scaling was then made using earlier measurement calibration. The timeline was moved so that the sudden force stroke began at time 0 [s]. For each time history, two reference lines were generated with values equal to the input step force value of 80 [N] $\pm 5\%$. Thus, prepared time responses were used to analyze the quality of tool control by the operator in individual trials. The measures of quality tool control executed by the participants of the test were represented by typical parameters existing in control system engineering such as rise time, settling time, overshoot and integral square error (ISE) based on the difference $e(t)$ between realized $r(t)$ and reference $f(t)$ forces shown in formula (1).

$$e(t) = r(t) - f(t) \quad (1)$$

The integral square error was calculated according to formula (2). The time of integration for each test was aggregated from $t = 0$ to $t_k = 4.5$ [sec].

$$ISE = \int_0^{t_k} e^2(t) dt \quad (2)$$

Figure 15 shows an example of a time history of a realized force with the related ISE index in time domain from 0 to 4.5 [sec], equal to the area of the field presented in grey.

These parameters were calculated and presented on the basis of all registered time responses. During the analysis of the test results of conditions with distortion in the form of local vibration tools, a problem appeared relating to the settling time evaluation. It happened that some operators repeatedly failed to find the exerted force within the defined a priori

channel limited by the two reference lines $\pm 5\%$ of the reference force value. Another measure of quality control used during the analysis was the ISE performance index. The ISE was calculated for the chosen a priori, fixed settling time durations. Both the value of the possible ranges of adjustment in individual trials, as well as the value of ISE, were tabulated. Drawn-up scoreboards were used for statistical calculations in which the medians and ranges of considered values of parameters were assessed. The results of the experiments were presented in the form of bar charts showing the median and ranges of the results for individual trials in Figures 15–17.

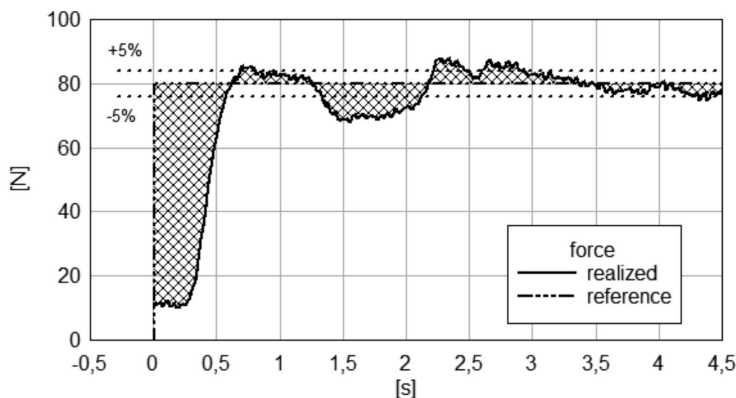


Fig. 14. Example of time history of realized force with the related ISE index

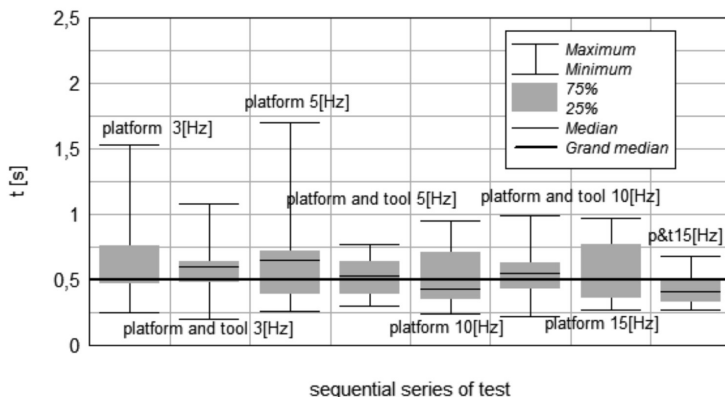


Fig. 15. Medians and ranges of rise time for subsequent tests

Rise time is an indicator, which gives information about the time in which the considered system managed to achieve an adjustable value in the range of 0.1 to 0.9 of its final value. In the case of the human-tool system, it also includes information about the human response time and on the nature of this reaction, e.g. whether it is fast and violent or slow. Distortions in the form of ground shakes and tool shakes can influence and affect the human-operator's reaction causing lack of concentration and difficulties in controlling the tools. The above

charts indicate a longer response time and a greater dispersion of results for lower frequency vibration platforms and tools. A large dispersion of the results and a long rise time especially apply to tests for vibration of the platform itself - that is, the effect of the whole body vibration with a frequency of 5 [Hz]. These results are consistent with indicated standard curves [6], where a frequency of 5 [Hz] is particularly troublesome for the human being.

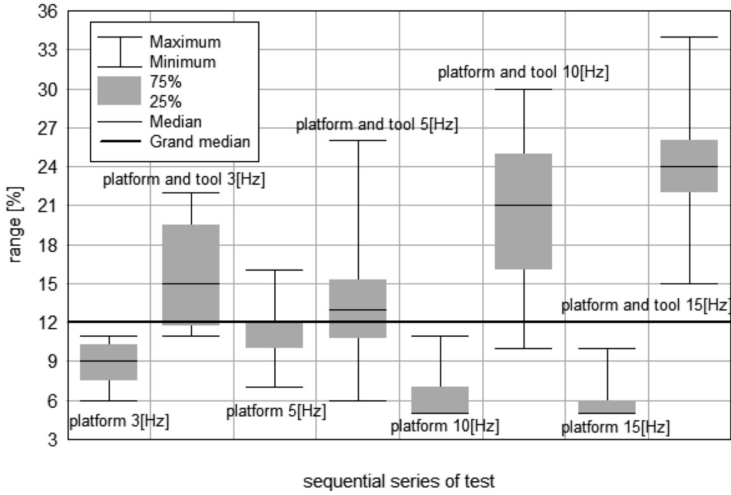


Fig. 16. Possible control range for subsequent tests

A typical indicator of control quality adjustment can be the time within which the test begins to set the size to a layout of $\pm 5\%$ and keeps the value within this range. Unfortunately, in the described studies of the human-tool system, reaching the desired value in the required range was unsuccessful in many cases. Therefore, the assessment of all the attempts by a single

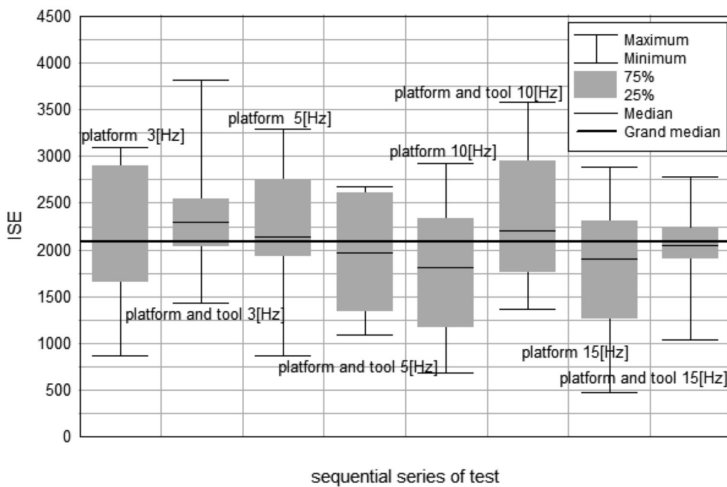


Fig. 17. Values of ISE index for subsequent tests

criterion, such as time regulation, was not possible. Instead, another assessment of operator action was proposed by the statistical charts representing the extent to which the operator tried to place exerted force into the required range.

The index ISE allows for aggregating errors during each trial and comparison of all attempts made. The same time (4.5 [sec]) was assumed for the comparison of all tests. Figure 17 presents the corresponding results.

5. Conclusions

The human-operator as the control element in human-machine systems, which is presented in this paper, largely affects the dynamic characteristics of the system as a whole. The graphs show that the biggest impact here is had by local (HAV) vibration of tools and accompanying dynamic forces between the handle and the vibrating tool. An increase in the frequency of the tools' vibration increases the adjustment range. The influence of platform vibrations on the adjustment range is relatively small. Typical for dynamic systems without human interaction parameters, such as settling time, rise time or overshoot, are fundamentally different from those of the human-machine parameters in terms of both quality and quantity that can be noted in Figs 5–13. This is the result of the inherent mental features of the individual operator. As a result of this, each dynamic layout containing the human must be assessed as the system with parameters stochastically variable with time and described by using stochastic differential equations. However, this is related to many mathematical and experimental difficulties concerning the probability distributions of parameters of the system, and therefore, scientific works with this approach have been relatively over-looked in previous literature.

References

- [1] Basista Z., *Modelowanie i symulacja układu człowiek-narzędzie-podłoże*, Zeszyty Naukowe „Mechanika nr 83”, Politechnika Krakowska, Kraków 2001, 21–30.
- [2] Basista Z., Książek M., *Estimation of comfort parameters of an active vibration isolation system of handle of percussive power tool*, Proc. “INTER-NOISE’2004”, Prague 2004.
- [3] Basista Z., Książek M., Tarnowski J., *Testowe badania doświadczalne reakcji człowieka-operatora narzędzia ręcznego przy sinusoidalnym sygnale wejściowym*, Czasopismo Techniczne, 1-M/2008, 27–35.
- [4] Basista Z., Książek M., Tarnowski J., *Experimental investigations of human-operator as a pressure force regulator in man-hand tool system*, Archives of Control Sciences, Vol. 19 (LIV), No. 1/2009, Polish Academy of Sciences, Committee of Automatic Control and Robotics.
- [5] Basista Z., Książek M.A., Tarnowski J., *Investigations of Influence of Vibration on Human-Operator Control Functions*, Mechanics, Quarterly, 2010, Vol. 29, 1–5.

- [6] ISO 2631 Standard: *Mechanical Vibration and Shock – Evaluation of human exposure to whole body vibration.*
- [7] Książek M.A., Tarnowski J., *Wpływ amplitudy wibracji narzędzia ręcznego oraz struktury układu wibroizolacji na proces sterowania narzędziem – badania doświadczalne*, Technical Transactions, 1-M/2011, 97–104.
- [8] McRuer D.T., Jex H.R., *A review of quasi-linear pilot models*, IEEE Transactions on Human Factors in Electronics, Vol. HFE 8, No. 3, September 1967, 231–249.
- [9] Sheridan T.B., Ferrell W., *Man-Machine Systems*, The MIT Press, Cambridge 1974.
- [10] Sövényi Sz., Gillespie R.B., *Cancellation of biodynamic feedthrough in vehicle control tasks*, IEEE Transactions on Control Systems Technology, Vol. 15, No. 6, November 2007, 1018–1028.

Filip Lisowski (filip.lisowski@mech.pk.edu.pl)
Faculty of Mechanical Engineering, Cracow University of Technology

OPTIMIZATION OF THREAD ROOT UNDERCUT
IN THE PLANETARY ROLLER SCREW

OPTYMALIZACJA PODCIĘCIA KARBU GWINTU
W PLANETARNEJ PRZEKŁADNI ŚRUBOWEJ ROLKOWEJ

Abstract

The paper presents the optimization problem of a thread root undercut in the roller of planetary roller screw using FEM. The depth and shape of the undercut as well as the radii of thread profiles curvature were optimized for the series of cooperating threads. The maximum HMH reduced stress in the undercut was accepted as an objective function. The limitation to the maximum contact pressure was assumed. The procedure aimed at limiting the range of variables was accepted in order to improve the efficiency of optimization method.

Keywords: planetary roller screw, optimization, thread root undercut

Streszczenie

W artykule przedstawiono zagadnienie optymalizacji podcięcia dna karbu gwintu rolki w planetarnej przekładni śrubowej rolkowej z zastosowaniem MES. Optymalizowano głębokość i kształt podcięcia oraz promienie zaokrąglenia zarysu gwintów dla szeregu współpracujących zwojów śruby i rolki. Jako funkcję celu przyjęto maksymalne naprężenie w karbie gwintu rolki przy ograniczeniu na maksymalne naciski kontaktowe na powierzchniach współpracujących gwintów. W celu poprawy efektywności metody optymalizacji przyjęto procedurę, która ma na celu zawężenie przestrzeni zmiennych.

Słowa kluczowe: przekładnia śrubowa rolkowa, optymalizacja, podcięcie karbu gwintu

Denotations

- d_s, d_r – pitch diameters of the screw and the roller [mm]
- x_{s1}, x_{s2} – dimensions of straight thread root undercut [mm]
- x_{e1}, x_{e2}, x_{e3} – dimensions of elliptical thread root undercut [mm]
- x_{t1}, x_{t2}, x_{t3} – dimensions of triangular thread root undercut [mm]
- R_s, R_r – radii of the screw and the roller thread flank [mm]
- σ_{HMH}^{\max} – maximum Huber-Mises-Hencky reduced stress in the thread root of the roller [MPa]
- $\sigma_{HMH}^{\max u}$ – maximum Huber-Mises-Hencky reduced stress in the undercut of the roller's thread root [MPa]
- C_{press}^{\max} – maximum contact pressure on thread (model without undercut) [MPa]
- $C_{press}^{\max u}$ – maximum contact pressure on thread (model with undercut) [MPa]

1. Introduction

Planetary Roller Screw (PRS) is a type of linear actuator used to convert linear motion to rotational motion or in the other way round. Thanks to high operating parameters, the mechanism is used to carry heavy loads in demanding mechanical engineering applications [4]. The axial load between the screw and the nut is transferred through several rollers uniformly distributed around the screw. To synchronize the operation of rollers, two planetary gear transmissions are applied. Since the planetary gears and the ring gears are integral parts of the rollers and the nut, the design of gears engagement has a direct impact on the cooperation of the screw, rollers and nut threads [7].

In recent years, authors of several publications have addressed problems related to load distribution, thread outline as well as dynamic or contact analysis. In the paper [9], a computational model was presented to determine the load distribution between cooperating elements accepting an arbitrary number of rollers. The model was intended for preliminary design. The analysis of displacements and load distribution based on the simplified model was presented in [8]. The authors of publication [1] developed a hybrid model, using one-dimensional finite elements and nonlinear spring elements, required for computation of load distribution and axial stiffness. The authors of publication [3] analysed dynamic effects and efficiency of PRS. In the paper [6], deformations of single cooperating pair of screw-roller and nut-roller threads were estimated. The authors of publication [10] modeled elasto-plastic contact problems in the PRS and studied the effect of the profile radius of the roller thread on contact characteristics. In article [11], a model to determine contact positions and clearances of mating thread surfaces was proposed.

The goal of this paper was to apply the finite element method in the optimization of a thread root undercut for a 2D problem. The undercut was accepted in the roller's thread. Three shapes of the undercut (straight, elliptical and triangular) and their impact on the maximum reduced stress in the notch and contact pressure were considered.

2. Optimization problem

In order to solve an optimization problem, a 2D finite element model including 10 cooperating threads, the screw and the roller was accepted as shown in Fig. 1. The model consisted of around 24 000 nodes and 70 000 elements (depending on geometry of the undercut). The pitch diameters of the screw and the roller as well as the thread pitch were assumed as: $d_s = 30$ mm, $d_r = 10$ mm, $p = 3$ mm. The 8-node PLANE82 elements available in ANSYS software were used. The plane strain was accepted. The contact elements CONTA172 and TARGET169 were accepted. The coefficient of friction in the plane of the model was set to $\mu = 0.1$. The axial load $F = 500$ N was applied to the edge of the roller core. Young modulus $E = 2.11 \cdot 10^5$ MPa and Poisson ratio $\nu = 0.3$ were accepted.

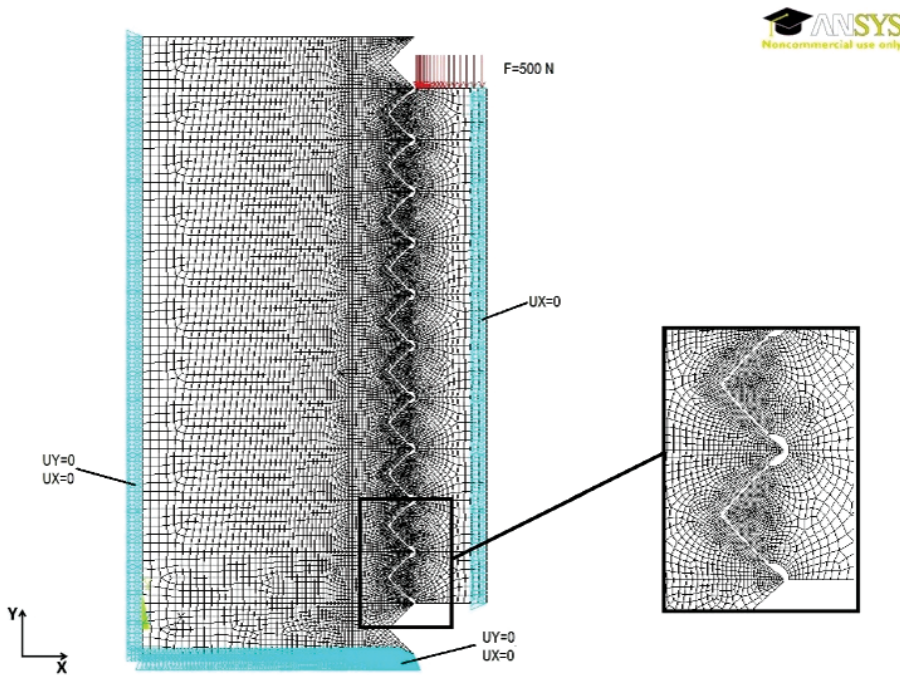


Fig. 1. Finite element model of the screw and the roller threads with boundary conditions

2.1. Optimization procedure

In order to improve the efficiency of optimization method, the procedure aimed at limiting the range of variables was accepted. To determine the starting points, a series of hundred calculations was performed. The values of design variables were randomly generated from the assumed range. The geometries resulted in the lowest HMM reduced stress were accepted as starting points. Optimization problem was solved by applying the gradient method available in ANSYS.

2.2. Objective function

As an objective function, Huber-Mises-Hencky reduced stress in the thread root undercut was accepted. The aim of the optimization was to determine the minimum of the function given by Eq. 1.

$$Q(x_{ij}, Rr, k) = \sigma_{HMH}^{\max, u} \quad (1)$$

$$Q \rightarrow \min \quad (2)$$

where:

- Q – objective function,
- $\sigma_{HMH}^{\max, u}$ – Huber-Mises-Hencky reduced stress in the thread undercut,
- x_{ij}, Rr, k – design variables.

2.3. Design and state variables

The authors of paper [2] noticed that, in order to keep the constant rolling diameters of cooperating elements, the thread profile of at least one of them has to be curved. The most advantageous distribution of the contact pressure is obtained when one of the thread profile is convex, whereas the other one is concave [5]. In this paper, the profile of the roller thread was assumed to be convex whereas the profile of the screw to be concave. The geometries of straight, elliptical and triangular thread root undercut are presented in Figs. 2–4. The values of design variables accepted for starting points as well as resulted maximum HMH reduced stress and maximum contact pressure for these points are presented in Tables 1–3.

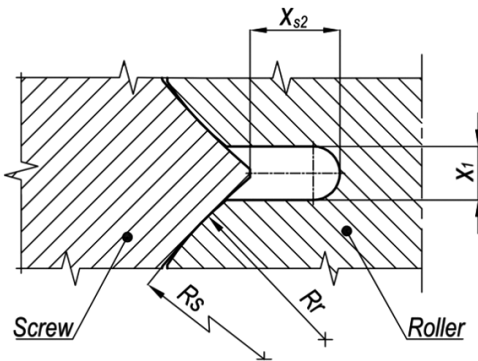


Fig. 2. Design variables and dimensions of threads with straight undercut

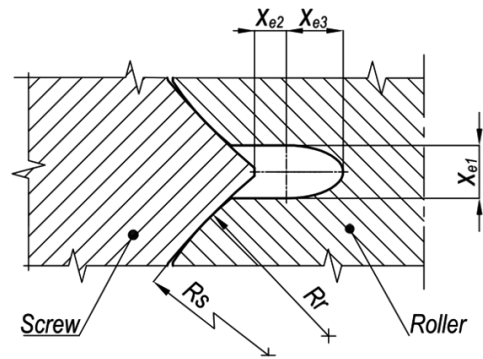


Fig. 3. Design variables and dimensions of threads with elliptical undercut

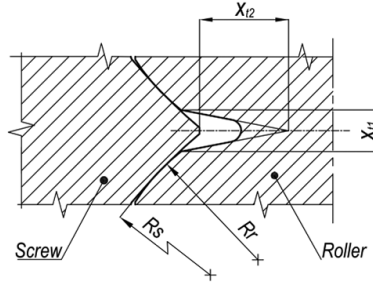


Fig. 4. Design variables and dimensions of threads with triangular undercut

Table 1. Design and state variables and optimization starting points (straight undercut of roller's thread root)

Design variables	Sp1	Sp2	Sp3	Sp4	Restrictions
x_{s1}	0.75	0.88	0.81	0.96	$0.1 < x_{s1} < 1$
x_{s2}	0.10	0.10	0.10	0.10	$0.1 < x_{s2} < 1$
R_r	8.16	14.48	15.14	15.86	$2 < R_r < 20$
k	1.64	1.26	1.23	1.60	$1.1 < R_r < 2$
State variables					
R_s	13.38	18.58	18.62	25.38	–
$C_{press}^{\max, u}$	370	243	216	282	$C_{press}^{\max, u} < 0.6 C_{press}^{\max}$
Obj. function					
$\sigma_{HMH}^{\max, u}$	183	169	174	166	–

Table 2. Design and state variables and optimization starting points (elliptical undercut of roller's thread root)

Design variables	Sp1	Sp2	Sp3	Sp4	Restrictions
x_{e2}	0.76	0.88	0.81	0.84	$-1 < x_{e2} < -0.1$
x_{e3}	1.40	1.30	1.02	1.04	$0.1 < x_{e3} < 1$
R_r	16.70	19.25	18.14	11.93	$2 < R_r < 20$
k	1.27	1.74	2.00	1.42	$1.1 < R_r < 2$
State variables					
x_{e1}	1.00	1.00	1.00	1.00	
R_s	21.21	33.50	36.28	16.94	–
$C_{press}^{\max, u}$	312	297	324	311	$C_{press}^{\max, u} < 0.6 C_{press}^{\max}$
Obj. function					
$\sigma_{HMH}^{\max, u}$	206	216	222	223	–

Table 3. Design and state variables and optimization starting points
(triangular undercut of roller's thread root)

Design variables	Sp1	Sp2	Sp3	Sp4	Restrictions
x_{t2}	1.00	1.02	1.06	1.01	$0.1 < x_{t1} < -1$
x_{t3}	0.45	0.36	0.36	0.37	$0.25 < x_{t2} < 0.45$
R_r	20.00	10.21	16.57	9.37	$2 < R_r < 20$
k	1.10	1.56	1.68	1.48	$1.1 < R_r < 2$
State variables					
x_{t1}	1.00	1.00	1.00	1.00	–
R_s	22.00	15.93	27.84	13.87	
$C_{press}^{max_u}$	191	326	282	281	$C_{press}^{max_u} < 0.6 C_{press}^{max}$
Obj. function					
$\sigma_{HMH}^{max_u}$	160	220	199	193	–

2.4. Results

The dimensions of the optimal thread root undercut and resulted maximum HMH reduced stress in the thread root undercut as well as maximum contact pressure for the best results obtained for particular starting points are listed in tables 4–6. The results obtained for the geometry without undercut ($\sigma_{HMH}^{max_u} = 308$ MPa, $C_{press}^{max} = 184$ MPa) were accepted as a reference point. The decrease of the maximum HMH reduced stress in the roller's thread undercut and the decrease of the maximum contact pressure for all of the considered shapes of thread root undercut are compared in Fig. 5. For the best result of the optimization problem, obtained for the triangular shape of undercut, the decrease of the maximum HMH reduced stress was 50% with an increase of the maximum contact pressure of 27%. It should be also noticed that the second best result was obtained for the straight undercut, where the decrease of the maximum HMH reduced stress equalled 48% and the decrease of the maximum contact pressure equalled 4%.

The distribution of HMH reduced stress obtained for the best result of optimization is shown in Fig. 6. Figs. 7–8 present the distribution of maximum HMH reduced stress in the thread root undercut and maximum contact pressure for all of the cooperating threads. Threads numeration starts from the top of model, where the load was applied.

Table 4. Design and state variables for the best optimization results
(straight undercut of the roller's thread root)

Design variables	Sp1	Sp2	Sp3	Sp4
x_{s1}	1.00	1.00	1.00	1.00
x_{s2}	0.10	0.10	0.10	0.40
R_r	17.04	15.51	15.77	10.86
k	1.19	1.20	1.12	1.15
State variables				
R_s	20.28	18.61	17.66	12.49
$C_{press}^{max_u}$	181	206	176	238
$\sigma_{HMH}^{max_u}$	179	162	160	266

Table 5. Design and state variables for the best optimization results
(elliptical undercut of the roller's thread root)

Design variables	Sp1	Sp2	Sp3	Sp4
x_{e2}	-0.85	-0.40	-0.90	-0.90
x_{e3}	1.40	1.00	1.00	1.00
R_r	16.62	16.68	9.96	7.96
k	1.27	1.15	1.10	1.10
State variables				
x_{e1}	1.00	1.00	1.00	1.00
R_s	21.11	19.18	10.96	8.76
$c_{press}^{max_u}$	251	238	206	226
$\sigma_{HMH}^{max_u}$	305	266	196	201

Table 6. Design and state variables for the best optimization results
(triangular undercut of the roller's thread root)

Design variables	Sp1	Sp2	Sp3	Sp4
x_{t2}	1.05	1.05	2.00	1.00
x_{t3}	0.45	0.45	0.45	0.45
R_r	15.93	7.05	16.55	6.05
k	1.21	1.19	1.23	1.10
State variables				
x_{t1}	1.00	1.00	1.00	1.00
R_s	24.05	8.39	20.36	6.66
$c_{press}^{max_u}$	206	252	208	233
$\sigma_{HMH}^{max_u}$	157	155	174	154

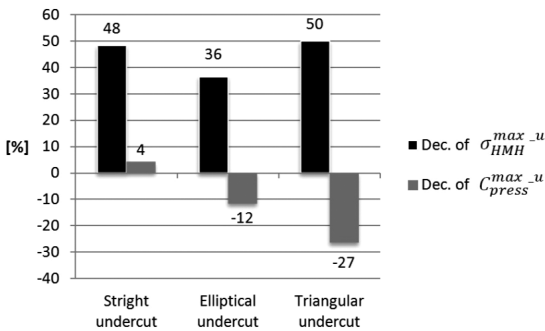


Fig. 5. Decrease of the maximum reduced stress in the thread root undercut and decrease of the maximum contact pressure on threads

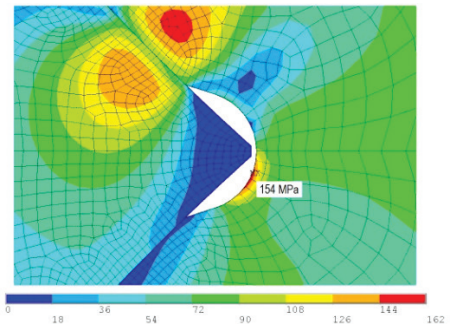


Fig. 6. Maximum HMH reduced stress in the triangular thread root undercut

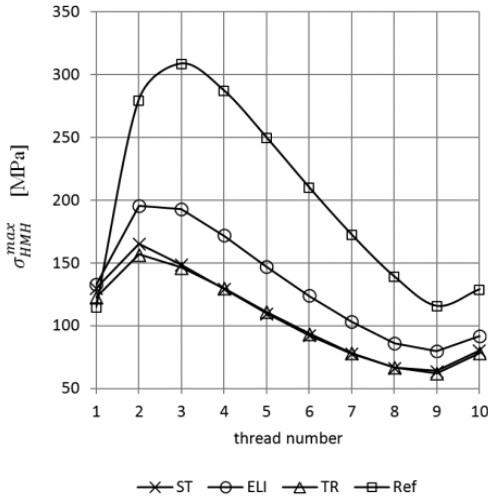


Fig. 7. Distribution of maximum HMM reduced stress in the roller's thread root

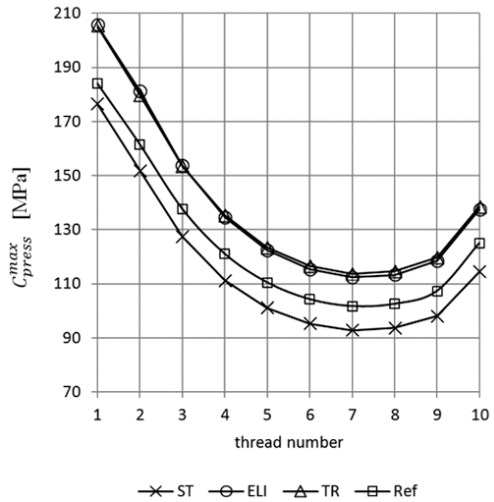


Fig. 8. Distribution of maximum contact pressure on threads

3. Conclusions

The results of the optimization problem, obtained by applying the finite element method indicated that the use of a thread root undercut in a roller is advantageous in the reduction of stress concentration in a thread notch. The best result was obtained for the triangular shape of an undercut. Concerning the cooperation of 10 pairs of the screw and roller threads, it can be concluded that dimensions of a triangular thread root undercut, referred to the thread pitch, should be accepted as follows: $x_{i1}/p \approx 0.33$, $x_{i2}/p \approx 0.35$, $x_{i3}/p \approx 0.15$.

Furthermore, it should be noted that the second best result was obtained for a straight undercut. In that case, the decrease of the maximum HMM reduced stress was slightly worse but the maximum contact pressure decreased by about 4%. Dimensions of straight thread root undercut should be accepted as follows: $x_{s1}/p \approx 0.33$, $x_{s2}/p \approx 0.03$.

References

- [1] Abevi F., Daidie A., Chaussumier M., Sartor M., *Static load distribution and axial stiffness in a planetary screw mechanism*, Journal of Mechanical Design, 2015, Vol. 138, doi: 10.1115/1.4031859.
- [2] Hojjat Y., Mahdi A.M., *A comprehensive study on capabilities and limitations of rollers crew with emphasis on slip tendency*, Mechanism and Machine Theory, Vol. 44, No. 10, 2009, 1887–1899.
- [3] Jones M.H., Velinsky S.A., *Dynamics and Efficiency of the Planetary Roller Screw Mechanism*, Journal of Mechanisms and Robotics, 8(1), 2014, DOI:10.1115/1.4030082.

- [4] Lisowski F., *Analiza obciążeń oraz optymalizacja konstrukcji wybranych śrubowych przekładni planetarnych*, Wydawnictwo Politechniki Krakowskiej, Kraków 2015, ISBN 978-83-7242-865-3, (in Polish).
- [5] Lisowski F., *Optimization of a curvilinear thread profile in a planetary roller screw*, Technical Transactions, 2-M/2015, 149–156.
- [6] Lisowski F., *Numerical computation of stresses and deformations in the planetary roller screw components*, Technical Transactions, 2-M/2015, 141–148.
- [7] Lisowski F. Ryś J., *A methodology of designing the teeth conjugation in a planetary roller screw*, Archive of Mechanical Engineering, Vol. LXIII, No. 4, 2016, DOI: 10.1515/meceng-2016-0033.
- [8] Lisowski F., *The Analysis of displacements and the load distribution between elements in a Planetary Roller Screw*, Applied Mechanics and Materials, 2014, 680, 361–364.
- [9] Ryś J., Lisowski F., *The computational model of the load distribution between elements in a planetary roller screw*, Journal of Theoretical and Applied Mechanics, Vol. 52, No. 3, 2014.
- [10] Tong R.T., Guo H., Liu G., Yao Q., *Elasto-plastic contact characteristics of the Planetary Roller Screw Mechanism*, Proceedings of the International Conference on Power Transmissions 2016 (ICPT 2016), Chongqing, P.R. China, 27–30 October 2016, 181– 186, DOI: 10.1201/9781315386829-28,
- [11] Tong Fu X., Liu, G., Ma, S., Tong, R., Lim, T.C., *A comprehensive contact analysis of planetary roller screw mechanism*, Journal of Mechanical Design, Vol. 139, Issue 1, 2017, Article number 012302.

Przemysław Młynarczyk (pmlynarczyk@pk.edu.pl)

Piotr Cyklis

Laboratorium Termodynamiki i Pomiarów Maszyn Ciepłych, Faculty of Mechanical Engineering, Cracow University of Technology

APPLICATION OF POROUS MEDIA FLOW MODEL FOR THE REGENERATOR FLUIDISED BED SIMULATION

ZASTOSOWANIE MODELU PRZEPLYWU PRZEZ WARSTWĘ POROWATĄ JAKO SYMULACJE PRZEPLYWU PRZEZ ZŁOŻE FLUIDALNE

Abstract

Modeling a flow thorough a fluidized bed is a complicated, time-consuming and power-demanding task. However, in some cases such a flow could be simplified as a porous media flow, when we treat it as a fixed bed. This publication presents a comparison between free flow and porous media flow in order to assess the effect on the surface layer erosion.

Keywords: Porous media flow, regenerator flow, fluidized bed

Streszczenie

Modelowanie przepływu przez złożo fluidyzacyjne jest zadaniem skomplikowanym, bardzo czasochłonnym oraz wymagającym dostępu do bardzo dużych mocy obliczeniowych. W niektórych jednak przypadkach modelowanie tego typu przepływu można uprościć do przepływu przez warstwę porowatą, tak jakby złożo miało postać stałą. W artykule przedstawiono porównanie przepływów bez złoża oraz ze złożem stałym w celu oszacowania wpływu na erozję warstwy wierzchniej.

Słowa kluczowe: Przepływ porowaty, regenerator, złożo fluidyzacyjne

Nomenclature

v – velocity

μ – viscosity

γ – flow porosity

1. Introduction

The fluidized bed is one of the commonly used technologies for combustion, regeneration or cement production, which is a floating mixture of gas and solid particles. Solid particles have usually abrasive properties, especially with high flow velocity near walls. The shape of inner elements influences velocity field near walls. The velocity field is a crucial factor for the determination of erosion threat. The simulation of the fluidized bed requires really high computational effort, exceeding the possibilities of standard computers and software. Therefore, the idea to substitute fluidized bed by the porous flow was proposed in this investigation.

1.1. Internal lining erosion issues

Fluidized bed vessels are often built of steel with internal lining especially chosen to reduce vessel temperature and abrasive action of particles. There are several companies which specialize in different types of lining. Some of them are designed for thermal insulation, others for erosion reduction. It is important to select a proper kind of lining since erosion resistant linings have higher conductivities. Internal erosion may, in the most dangerous cases, formulate “gas paths” inside the lining up to the vessel shell. In this case particles directly hit the steel causing erosion and possible cracks. Therefore, it is extremely important for safety reasons to avoid this effect. One of the forecasting tools which can be used is the simulation of internal vessel fluidized bed flow. With the results of simulation, the most dangerous places can be determined. Then the internal shape may be modified or a proper anti abrasive lining applied. The solution of a fluidized bed is usually too complicated for the reactor/regenerator vessels. In this paper, the porous bed flow model is proposed as a tool for inner flow simulation. This provides reasonable computational effort giving the answers for modifications. The results have been checked up against a real regenerator case, where the erosion occurred near the hatch.

1.2. Fluidized bed modeling

In the hydrodynamic model of a fluidized bed, relations between phases and mass and heat transfer phenomena are used to describe the motion, distribution and relation between gas and solids. Several cases of fluidized beds can be analyzed:

- ▶ Fixed bed with determined packed bed height – where the gas velocity is low and the bed is static,

- ▶ Bed with minimum fluidization – where the beginning of the fluidization of the particle bed can be observed,
- ▶ Bubbling bed – where the flow starts to be unstable,
- ▶ Bed with minimal solid fraction treated rather as a pneumatic transport with minimal solid fraction [1].

The fluidized bed is also characterized by the relation between pressure drop and gas velocity. In the pneumatic transport of solid particles, pressure drop decreases when gas velocity is higher than particles velocities. In the fixed bed, pressure drop increases when gas velocity increases. Therefore, for the fixed bed, the calculation of pressure loss is similar to porous volume flow. The so called packed-beds are mostly used in heterogeneous catalytic reactors [2].

In fluidized bed modeling, four different regimes are used to determine particles characteristics. This regimes were described by Geldard [3] and they are related to particles dimensions.

The minimum fluidization condition is determined by physical properties, where pressure drop, porosity, gas velocity and bed expansion are defined. These characteristics allow for the determination of particle diameter and velocity, which influence heat and mass transfer between phases. These phenomena are related mostly to the contact between different phases [1]. Depending on the calculation aim, numerical simulations of the fluidized bed can be based on different approaches. Sometimes basic equations like mass, energy and momentum conservation equations must be coupled with additional sources which describe the hydrodynamic model of phases interaction or another appropriate model. In the literature, many different approaches are presented. In this investigation, porous media flow is used to observe how much the flow thorough a fixed bed influences the lining layer abrasion. In the literature there are several models of porous media flow and its influence on different flow parameters like pressure drop, heat transfer etc. [4, 5].

2. Numerical model

Several models can be used for the fluidized bed simulation. For the specific problem which is the lining layer abrasion, porous media flow will be used to define the influence of flow parameters on the layer abrasion scale. In this paper, the results obtained in FLUENT/ ANSYS simulation are presented.

2.1. Porous media flow

The “porous” region in a model determines empirically additional flow resistance in the volume. It means that the porous media model adds a momentum source term to the governing momentum equations. This term is composed of two parts: an inertial loss term and a viscous loss term [6]:

$$S_i = - \left(\sum_{j=1}^3 - (D_{ij}) D_{ij} \mu v_j + \sum_{j=1}^3 C_{ij} \frac{1}{2} \rho |v| v_j \right) \quad (1)$$

where:

- $|v|$ – velocity magnitude,
- D – viscous loss term predefined matrix,
- C – inertial loss term predefined matrix.

This approach creates a pressure drop in the porous cell, which is proportional to the fluid velocity in the cell. In the case of simple homogeneous media, it takes the following form:

$$S_i = - \left(\frac{\mu}{\alpha} v_i + C_2 \frac{1}{2} \rho |v| v_j \right) \quad (2)$$

where:

- α – permeability.

For the power law model, different equations are used to define the velocity magnitude, but the authors do not consider this approach in this case.

In the laminar flows through porous media, pressure drop is proportional to velocity, but constant C_2 from the equation (2) is equal to zero. This gives us a pressure drop equation which is equal to the first part of the equation (2). The same constant for the turbulent flows is used as a pressure loss coefficient per length through the flow direction. In the FLUENT/ANSYS software, the porous medium, by default, has no influence on the turbulence generation and dissipation rates. The user can introduce the turbulence suppression if they consider it necessary.

While modeling the porous flow as a viscous flow, effective viscosity is introduced in the momentum equations as:

$$\mu_e = \mu_r \mu \quad (3)$$

Where μ_r is the relative viscosity which can be calculated in the FLUENT/ANSYS using one of implemented sub models:

Bruegem Correlation:

$$\mu_r = \begin{cases} \frac{1}{2} \left(\gamma - \frac{3}{7} \right) & \text{when } \lambda \geq \frac{3}{7} \\ 0 & \text{when } \lambda < \frac{3}{7} \end{cases} \quad (4)$$

Brinkman Correction:

$$\mu_r = 1 - 2.5(1 - \gamma) \quad (5)$$

or Einstein Formula:

$$\mu_r = 1 + 2.5(1 - \gamma) \quad (6)$$

To calculate thermal dependencies between porous medium and fluid, effective thermal conductivity must be defined. In the FLUENT/ANSYS software, effective thermal

conductivity in the porous medium is computed as the volume average of the solid and fluid conductivity:

$$k_{eff} = \gamma k_f + (1 - \gamma) k_s \quad (7)$$

where:

k_s – thermal conductivity of solid,

k_f – thermal conductivity of fluid.

Further in this paper, the possibility of using the porous media flow model to assess fixed bed flow influence on the internal lining erosion is presented.

2.2. Geometry and mesh

To achieve the expected results from numerical simulations, a simplified regenerator model geometry was created. It is a simple volume without additional elements (like cyclones, pipes etc.). Internal lining erosion occurs especially near different cavities, corners etc. In most cases such a cavity constitutes a cylinder volume which is a part of a hatch structure. Geometry used in this investigations is presented in Fig. 1. It is 16 meters high with the radius equal to 3.5 m.

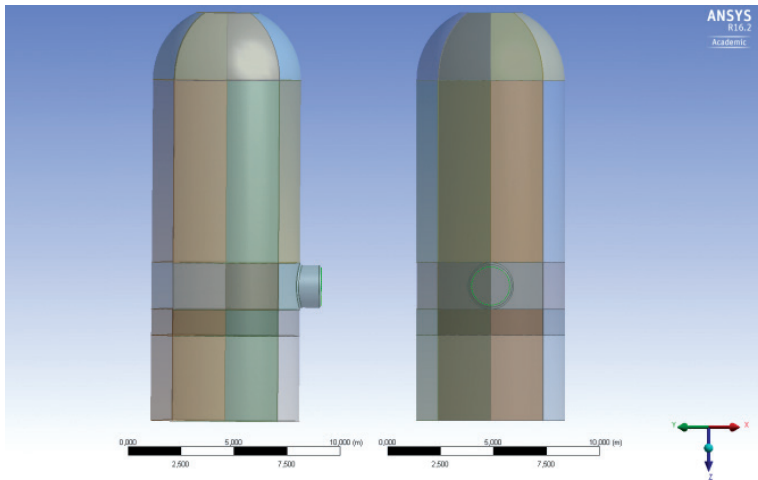


Fig. 1. Regenerator geometry – side and front view

The mesh generated for presented geometry should be as fine as possible. The presented approach has to be simple, fast and done in the simplest commercial tool like FLUENT/ANSYS. Therefore, also the grid has to be done in this software. Unfortunately, Ansys Mesher in the 6.2.version has a problem with defining fine hexagonal mesh with the boundary layer in the presented volume when there is an additional cavity. In this case, the fine mesh was defined in the model heights below and above the hatch. The tetrahedral mesh was created for the hatch heights. The fine mesh for the cylinder volume is presented in detail in Fig. 2 and details of the mesh near hatch are presented in Fig. 3.

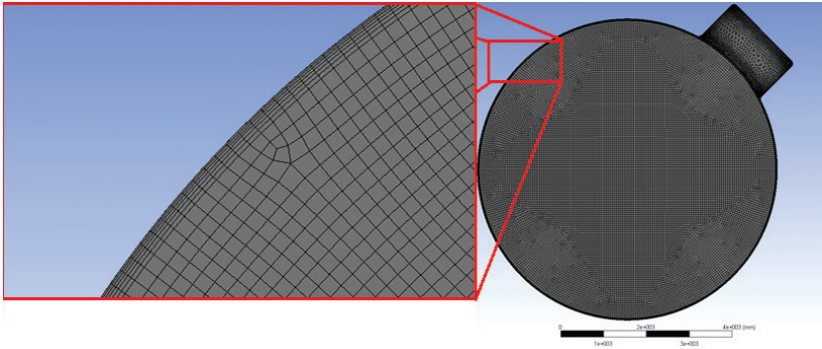


Fig. 2. Mesh with details (Bottom view)

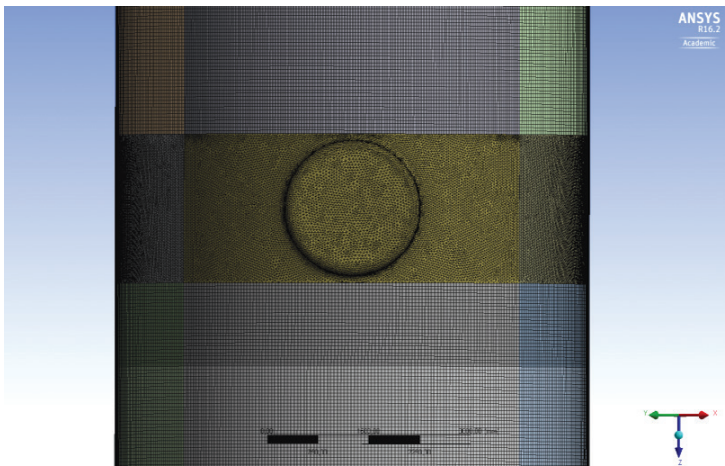


Fig. 3. Mesh detail (front view)

2.3. Flow parameters

Two different approaches were used for the regenerator flow simulation. First is the simulation of free flow of air, which can correspond to a flow where there is no fixed bed, and the second approach, where the fixed bed is modeled as a porous volume. By comparison of these two approaches, spots where the lining layer is more exposed to abrasion can be determined. Boundary conditions are presented in Table 1.

Table 1. Boundary conditions

Boundary condition	Type	Values
Inlet	Mass flow	$\dot{m} = 40 \text{ kg/s}$; gauge pressure 224 kPa
Outlet	Pressure outlet	gauge pressure 220 kPa;
Walls	Adiabatic walls	–

To describe the flow viscosity, k-ε turbulence model is applied. Brinkman correction described in equation (5) is used to calculate relative viscosity in the porous zone. For the porous media flow, the porous zone is defined at inflow zone under the hatch.

3. Results

The most important parameters which determine lining layer erosion could be velocity/dynamic pressure or turbulent kinetic energy which may occur near the eroded region. In Figs. 4 and 5 the velocity vectors are presented.

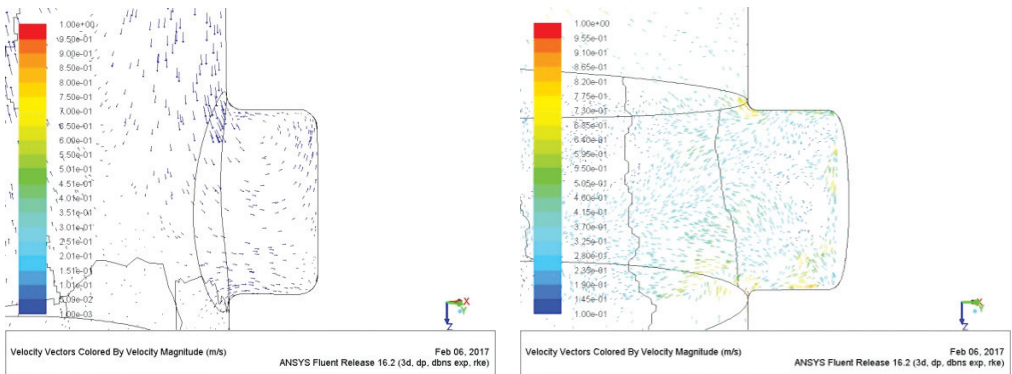


Fig. 4. Velocity vectors – with porous volume, coarse mesh, $v_{max} \sim 0.1$ m/s (left), refined mesh, $v_{max} \sim 0.75$ m/s (right)

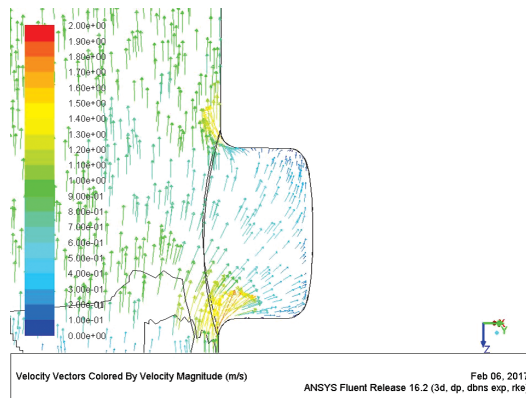


Fig. 5. Velocity vectors – pure gas, $v_{max} \sim 1.4$ m/s

As it can be seen in Figs. 4 and 5, in the presented case the porous volume, which could be treated as a fluidized fixed bed, gives a more stable flow through the regenerator geometry. For the ideal gas flow model, some areas with higher velocity vectors magnitudes can be observed near the hatch region. This contributes to the lining layer abrasion, which in a real vessel lining occurred exactly in this region.

4. Conclusions

In the paper, the possibility to simulate a fluidized, fixed bed flow as a porous media flow is presented. In each application where the process comprises the flow through a fluidized bed, the problem with internal lining layer erosion and abrasion can be expected.

Hazardous regions are identified by means of simulation. Numerical simulation of a fluidized bed is very demanding for modeling, needs high computational effort and takes a large amount of time. This is even more demanding for real industrial cases with high capacity installation and a hardly defined process. Simulation of a fluidized fixed bed as a porous flow considerably reduces the time of computation. In the presented case, the comparison between the porous media flow and ideal gas flow confirmed the real process issue where the abrasion occurred in the hatch region exactly in part where velocity vectors resulting from simulation are of highest value near the lining inner surface. The simulation of the porous flow showed high dependency of the mesh density and quality. In case of the coarse mesh, the results were extremely different from reality, though the simulation convergence has been reached.

References

- [1] Philippsen C.G., Vilela A.C.F., Zen L.D., *Fluidized bed modelling applied to the analysis of processes: review and state of the art*, Journal of Materials Research and Technology 4(2), 2015, 208–216.
- [2] Calis H.P.A., Nijenhuis J., Paikert B.C., Dautzenberg F.M., van den Bleek C.M. *CFD modelling and experimental validation of pressure drop and flow profile in a novel structured catalytic reactor packing*, Chemical Engineering Science 56, 2001, 1713–1720.
- [3] Geldart D., *Types of gas fluidization*, Powder Technology, Vol. 7, Iss. 5, 1973, 285–292.
- [4] Kedouci M.A., Kharroubi B., Khelfaoui R., Bendida A., Dennai B., Maazouzi A., *Simulation of water filtration in porous zone based on Darcy's law*, Energy Procedia 36, 2013, 163–168.
- [5] Wang F., Tan J., Wang Z., *Heat transfer analysis of porous media receiver with different transport and thermophysical models using mixture as feeding gas*, Energy Conversion and Management, 2014, 159–166.
- [6] ANSYS Fluent Documentation, v. 16.2.

Andrzej Skowronek (skowronek@mech.pk.edu.pl)
Faculty of Mechanical Engineering, Cracow University of Technology

APPLICATION OF THE MULTI-GENERATING METHOD
TO SUPPORT THE QUALITY OF SMART DESIGNS OF EXPERIMENT

ZASTOSOWANIE METODY WIELOKROKOWEGO GENEROWANIA
WSPOMAGAJĄCEJ JAKOŚĆ ELASTYCZNYCH PLANÓW EKSPERYMENTU

Abstract

The article presents a method used in the process of generating smart designs of experiment in a dedicated computer program with the application of pseudo-random numbers, the use of which may have a considerable impact on the quality of generated designs. In order to increase the probability of generating the optimal design for the defined parameters of generating, a special method was applied, in which several designs were generated and the best of them selected, based on the equipartitional analysis parameters. The results confirm a significant positive influence of the analyzed method on the smart design's quality.

Keywords: smart design of experiment, experimental research

Streszczenie

Artykuł przedstawia metodę używaną w procesie generowania elastycznych planów eksperymentu w specjalnym programie komputerowym z zastosowaniem liczb pseudolosowych, których użycie może mieć znaczący wpływ na jakość planów. W celu zwiększenia prawdopodobieństwa wygenerowania planu optymalnego dla ustalonych parametrów w generowaniu planu, zastosowano specjalną metodę, w której generowanych jest wiele planów i wybierany najlepszy na podstawie parametrów tzw. analizy ekwipartycyjnej. Uzyskane wyniki potwierdzają znaczący pozytywny wpływ metody na jakość elastycznych planów eksperymentu.

Słowa kluczowe: elastyczne plany eksperymentu, badania eksperymentalne

1. Introduction

Experimental research is one of the commonly used source of obtaining information. Special techniques, known as design of experiment methodology (DoE), are applied to conduct experimental research. Planning of experimental research is based on the application of special designs of experiment, which allow for a significant reduction in size of experiment (runs of experiment, observations, number of measurements, etc.). It may be particularly important in the case where a researcher is not able to perform the research for all combinations of input levels, which could be, for example, a result of restrictions imposed on the time of experiment's realization, its high costs or just inability to realize certain combinations of input factors' levels. It should be noted that reducing the size of the experiment does not necessarily lead to the reduction in the amount of information obtained as a result of the experiment conducted with the application of DoE techniques.

Depending on the goal of experimental research, various types of designs can be used [1–3]. When using the traditional design of the experiment, the researcher must accept its characteristics and execute the experiment strictly according to the design which has been selected. In particular, such design's characteristics as the number of units, the input factor levels and their number cannot be changed, as this could make the experiment difficult or even impossible to realize. Quite a different approach to the conception of experiment planning is applied when smart designs of experiments are used [4]. The researcher is allowed to set the number of design's units and the number of input levels. Moreover, one can impose restrictions on the input space and avoid combinations of factor levels which are not allowed or not feasible to be implemented. The main idea of smart designs of experiment is the possibility of easy application in experimental research. The researcher only needs to define the most important features of the experiment, such as the number of runs, the number of input factors, levels of input factors and possibly some restrictions put on the input space.

2. The Idea of Smart Designs of Experiments

Smart designs of experiment are generated in a dedicated computer application, based on three important principles: adaptation, randomness and equipartition [4, 5]. The first principle means the possibility of adjusting the design's characteristics to the conditions of the experiment and characteristics of the analyzed object. The researcher is able, for example, to set the number of design's units and the number of its levels for each input. The second principle means that smart designs are created in a non-deterministic manner: both the generation of input levels and the selection of design's units are conducted with the use of pseudo-random numbers. However, there are some limitations put on the random way of generation of design's units:

- ▶ a parameter called “important difference” (Δx), a minimal permissible distance between the last generated value and existing values of each input factor levels,

- ▶ a parameter called “minimal Euclid’s distance” ($esmin$) – it is Euclid’s distance to the nearest “neighbor-unit” in the input space, calculated for each design’s unit, each unit must fulfill the $esmin$ condition: $es \geq esmin$

The conceptions of both parameters described above are based on the Euclid’s distance measure and they use the fact that a set of experimental design units in the input space is equivalent to the set of points in the orthogonal coordinate system as well as the combinations of input levels (which make up the units of designs) are equivalent to the points coordinates. The Δx and $esmin$ parameters support equipartition of the design’s units in the input space. If there are no other assumptions, design’s units should cover regularly the whole input space (the third rule). The equipartition of design’s units means regularity and uniformity of the design’s units in the input space, which reduces the likelihood of occurrence of empty spaces (without any design’s unit), and is strongly required if you want to obtain as much data on the research object as possible and find out the research object function which specifies how inputs affect the output. The equipartition of units is the main smart design optimality criterion.

To estimate the regularity of the distribution of the design’s units (equipartition), the method of equipartitional analysis (EPA) is used [4, 5]. This analysis provides parameters that allow you to make a qualitative assessment of the generated designs. The high equipartition of the units distribution in the input space means the high quality of the design. In the equipartitional analysis, the created design of experiment is compared to the master-design, whose units are distributed perfectly regularly in the input space. The master-design always has the same number of inputs as the analyzed designs and the same number of input factors’ levels, but the number of master design’s units is usually significantly higher and equal to the product of numbers of all input levels (number of all combinations of input factors’ levels). For example, in case of design consisting of 10 units, 6 levels for the first factor and 8 for the second factor, the master design consists of 48 units (all combinations of 6 factors’ levels for the first input factor and 8 for the second factor). The input factors’ levels of the master-design are calculated for each input factor by regular division of the length of input factors’ ranges and the number of factors’ levels (Fig. 1).

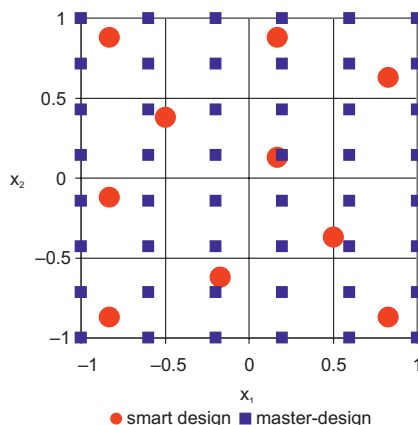


Fig. 1. Smart design and master design

For each unit of the master-design (x^m), one can evaluate the Euclid's distances to all units of the analyzed smart design (x^s):

$$e(x^m, x^s) = \sqrt{\sum_{i=1}^d (x_i^m - x_i^s)^2} \quad (1)$$

where:

d – number of input factors.

Having calculated matrix E of Euclid's distances between master design units and smart design units:

$$E = \begin{bmatrix} e(x_1^m, x_1^s) & e(x_1^m, x_2^s) & \dots & e(x_1^m, x_{ns}^s) \\ e(x_2^m, x_1^s) & \dots & & \\ \dots & & & \\ e(x_{nm}^m, x_1^s) & e(x_{nm}^m, x_2^s) & \dots & e(x_{nm}^m, x_{ns}^s) \end{bmatrix} \quad (2)$$

where:

nm – number of master design units,

ns – number of smart design units,

one can evaluate vector $E1$ of the Euclid's distances between all master design units and their nearest smart design unit:

$$E1 = [\min(e(x_1^m, x_1^s), \dots, e(x_1^m, x_{ns}^s)), \dots, \min(e(x_{nm}^m, x_1^s), \dots, e(x_{nm}^m, x_{ns}^s))] \quad (3)$$

For such a collection ($E1$ vector, called equipartitional set), one can evaluate a lot of statistical parameters, e.g. descriptive statistics [6] or make one of the statistical tests [7], which could be an equipartition criterion in this analysis. Two parameters have been used: the maximal ($e1max$) and mean ($e1mean$) value of the equipartitional set. The $e1mean$ parameter describes the central tendency of the equipartitional set whereas the $e1max$ parameter provides the information whether there are any huge empty areas in the input space (without any design's units), which is important taking into consideration the assumption that the design's units should regularly cover the whole input space. The dependence between both parameters and the design's quality (quality means equipartition, perfect regularity of the design's units distribution in the input space) was verified and described in [5]. The conclusion was that the less value of equipartitional parameters means the more regular distribution of design's units in the input space. Assuming that smart designs quality is identified with regularity and uniformity of design's units distribution in the input space (equipartition), the quality can be evaluated using equipartitional analysis parameters, for example $e1max$ and $e1mean$, which should be minimized. Both parameters can be used separately and each could be the main criterion of design quality. However, it is recommended to use them together.

There are three methods of generating the inputs' levels used to create smart design's units in the current version of designs' generator. In the Z-method, inputs' levels are generated as pseudo-random values from the normalized range $[-1, 1]$ and checked if they pass the important difference condition test. If a value (factor's level) fails the test, it is removed and the next one is generated to reach the right amount (assumed number of factor levels). In

the “R” method, the input factors’ levels are calculated by dividing the input ranges by the demanded numbers of input factors’ levels. The first level is calculated as the minimum of the input range, whereas the last level is calculated as the maximum of the input range. In the R2-method, the idea of levels calculation is that each level should be the center point of equal areas of influence. The first and the last levels are not equal to the minimum or maximum of the input factor’s range.

The smart design’s generator in the current version has implemented functionalities which support the selection of the optimal values of important generation’s parameters: the important difference (Δx , used in Z-method of levels’ generating) and the minimal Euclid’s distance (*esmin*), used to enhance high regularity and equipartition of design’s units in the input space [8]. When using the previous versions of the generator, a researcher must set Δx and *esmin* parameters by himself, which could make the generated design not optimal – designs’ units do not cover equally the whole input space in the case of setting to small values of generation parameters, or it is not possible to obtain the design with the assumed properties (number of units) otherwise. In the current version, the problem has been fixed since the initial values of both parameters (Δx and *esmin*) are calculated automatically.

3. A procedure of multi-generation of the smart design of experiment

Smart designs of experiment are generated in a special computer program with the application of pseudo-random numbers, the use of which may have a considerable impact on the quality of the generated designs. Computer-generated pseudo-random numbers, which have properties similar to random numbers, are deterministic. The choice of a seed value, which is used to initialize a pseudo-random number generator, seems to be crucial. A generated sequence of pseudo-random numbers can be reproduced if the used seed value is not changed [9], which should be considered an advantage. But on the other hand, randomly generated series of numbers used in the procedure of smart designs generating can cause a significant change in potential possibilities of generating a design. It may result in obtaining a better or worse quality design for the same settings of generation, which of course is a disadvantage.

In the smart designs’ generator, pseudo-random numbers are applied in the module of generating the input factors’ levels using the Z-method and in the module of unit selection from the set of candidate units (a set of units created as all combinations of all factors’ levels). Designs generated with the same seed of a pseudo-random number generator, the same parameters of generation (values of Δx and *esmin*, method of input’s levels generating) and the same design’s characteristic (the number of inputs, the number of input’s levels, the number of design’s units and method of levels generating) will be identical. However, in the case of using a different seed value, it is possible (but rather certain) to obtain various designs for the same settings defined for the generating process. Moreover, there is no certainty whether designs obtained for defined parameters of generating are really optimal (best quality) and the difference in their quality could be sometimes significant. Considering the above, it seems to be necessary to generate several designs and select one, based on EPA-parameters (*e1max* and *e1mean*), which are the



measures of designs' quality. That is the idea of multi-generating smart designs of experiment. Thus, the role of a multi-generating procedure is to eliminate or at least reduce the impact of the use of pseudo-random numbers on the generated designs' quality.

Users of smart designs generator can set a pseudo-random numbers generator seed value by themselves or can let it generate automatically, based on the real-time clock, which is a default and recommended option. To regenerate the identical design again, only its seed value must be known. The researcher can select the EPAparameter which he prefers to identify the best design. In the current version of smart designs generator, the procedure of multi-generating consist of up to 20 design generating attempts to get 10 candidate-designs using various seed values. The initial seed value is generated using system time and increases by 1 for each attempt of design generation. For each design, EPA-parameters ($e1max$, $e1mean$) are calculated and saved. After completing 10 candidate-designs (or after completing 20 attempts of generating) the best one is selected based on EPA-parameters. The one with the lowest values of $e1max$ and $e1mean$ parameters is saved as a result of the multi-generation procedure. However, theoretically it is possible to obtain no design or only one or two designs. In such cases, it is recommended to repeat the generating procedure once again.

4. Computer simulation to evaluate the effectiveness of the considered method

In order to evaluate the effectiveness of the analyzed method and its influence on the quality of generated designs, a computer simulation was performed. In the simulation, 108 smart designs were generated, using the Z, R and R2-methods of generating the input factors' levels, various numbers of factors' levels and various numbers of units (see Table 1). For each combination of four mentioned design's characteristics (number of factors, number of factors' levels, number of units, method of levels generating) a generation process was executed 2 times to check if the obtained results are both stable and repeatable.

Table 1. Combinations of design's characteristics applied in simulation

Number of input factors	Number of factors' levels	Number of designs' units	Methods of levels' generating
2	5, 5	10, 15, 20	Z, R, R2
2	6, 8	10, 15, 20	Z, R, R2
3	5, 5, 5	10, 30, 50	Z, R, R2
3	6, 7, 8	10, 30, 50	Z, R, R2
4	5, 5, 5, 5	100, 200, 300	Z, R, R2
4	5, 6, 7, 8	100, 200, 300	Z, R, R2

Despite 20 attempts to generate 10 designs, it can happen for certain combinations of designs' characteristics and initial seed values that less than 10 designs fulfilling all assumptions are generated. It was assumed in the simulation that if the number of designs achieved in the

procedure of multi-generating is less than 3, it was repeated, but only up to 2 times. If during 3 runs less than 3 designs were generated for some combination of design's characteristics, no further action was taken.

The aim of application of multi-generation procedure is supporting smart designs' quality, which is evaluated based on two EPA-parameters: $e1max$ and $e1mean$. This is the reason why both EPA-parameters were used to assess the effectiveness of the analyzed method. The effectiveness was calculated in percentage as the relative difference between values of EPA-parameters obtained for the design qualified as the worst one (the highest values of both EPA-parameters) and values of EPA-parameters obtained for the design qualified as the best one (the lowest values of $e1max$ and $e1mean$ parameters) from a set of multi-generated candidate designs (up to 20 attempts of generating to get 10 designs) for each combination of 4 designs' characteristics. In case when the value of $e1max$ parameter for some design is higher and the value of $e1mean$ parameter is lower than for the compared design in candidate-design set, the higher value of $e1max$ EPA-parameter has determined the worse design. For both sets of relative differences, (for $e1max$ and $e1mean$ EPA-parameters) two basic descriptive statistics were calculated: maximal value of effectiveness ($effmax$) and average value of effectiveness ($effavg$).

5. Results of the simulation

The summary of simulation results according to various criteria are shown in Table 2 and Table 3.

Table 2. Results of simulation obtained in the first and second run of experiment

Runs	Method's effectiveness evaluated using EPA-parameters in [%]			
	$e1max$		$e1mean$	
	$effmax$	$effavg$	$effmax$	$effavg$
1. run	39	17	18	4
2. run	43	20	26	4
overall	43	19	26	4

The effectiveness calculated in simulation for all 108 cases reached on average 19% for $e1max$ parameter and 4% for $e1mean$ parameter, whereas the maximal effectiveness for $e1max$ parameter reached 43% and 26% for $e1mean$ parameter. It is important, because decreasing EPA-parameters means improving the design's quality.

As it was described above, every generating process (for all combinations of designs' attributes) was executed twice. Let us now focus on Table 2, which shows the results obtained in the first run, second run and overall. The values of improvements obtained in both runs are similar, which confirms that the effects of application of the analyzed method are stable and repeatable.

Table 3. Results of simulation depend on the method of levels' generation

Method of levels generating	Method's effectiveness evaluated using EPA-parameters in [%]			
	e1max		e1mean	
	effmax	effavg	effmax	effavg
Z	41	18	26	7
R	43	17	12	2
R2	43	20	13	3

Comparing the results obtained for all 3 various methods of generating the factors' levels (Table 3), one can observe similar effectiveness values, especially those achieved for *e1max* parameter. For *e1max* parameter, the R2-method of generating produces the highest effectiveness, whereas for *e1mean* parameter the best results are obtained in case of the Z-method. However, you must remember that the levels of the factors in the Z-method are re-generated on each attempt of smart design creating, as opposed to the methods of R and R2, where the generated sets of factor levels are the same for the whole procedure of designs' multi-generating (up to 20 attempts, if necessary) to select the best one when the multi-generation method is active. The re-generating of levels in the Z-method can cause high variability of the results and high values of effectiveness achieved for *e1mean* parameter.

Table 4 shows relative frequencies of effectiveness cases calculated for both EPA-parameters. For *e1mean* parameter, cases with effectiveness of less than 5% are dominating, whereas for *e1max* parameter cases with effectiveness between 10% and 30% are dominating. As can be noticed, larger values of effectiveness were obtained for the *e1max* parameter, but considering the manner of calculating both statistics it appears foreseeable and justified.

Table 4. Relative frequencies of effectiveness cases for EPA-parameters

EPA-parameter	Relative frequencies of effectiveness cases for EPA-parameters (in %)				
<i>e1max</i>	range	≤ 10%	≤ 30%	≤ 50%	> 50%
	frequency	21	64	15	0
<i>e1mean</i>	range	≤ 5%	≤ 10%	≤ 15%	> 15%
	frequency	74	14	7	5

If only one design for some combination of design's characteristics and initial seed value was generated (3 of 108 cases in the simulation), the effectiveness is 0%. However, it does not mean design's poor quality. The procedure of generating smart designs of experiment includes various tools supporting quality of design, e.g. important difference condition, minimal Euclid's distance condition, automatic selection of important difference and minimal Euclid's distance values (see chapter 2). Comparing these designs to designs generated on the other run or with the application of the other method of factor levels generating, there were usually no significant differences of both EPA-parameters. It suggests a tendency that generating

only 1 design during 20 attempts provides usually some of good quality, notwithstanding the fact that multi-generating procedure does not work. In cases where several designs were obtained in up to 20 attempts of generating, a larger variety of results is usually observed. In such cases, the procedure of multi-generating works very well. There are also 9 cases where only 2 designs were generated. However, in 8 cases from these 9, some effectiveness of at least one of two EPA-parameters was observed. Generally, in 88% of cases, some effectiveness of eI_{max} parameter was observed, and in 64% of cases some effectiveness was observed for both EPA-parameters.

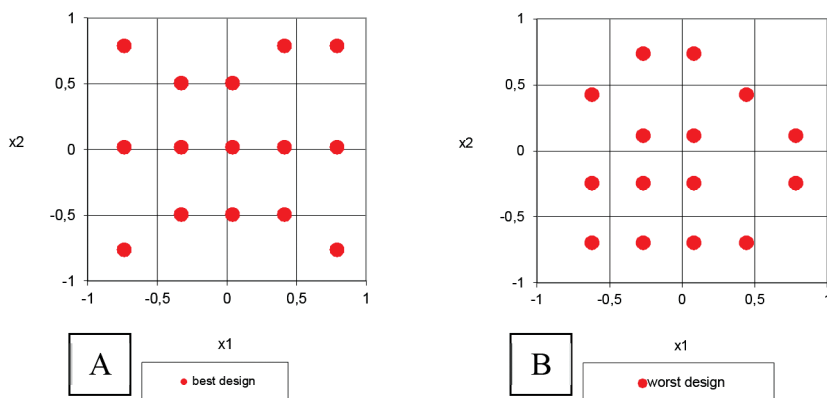


Fig. 2. Design qualified as the best of series (A) and as the worst of series (B) in multi-generation method

Figure 2 shows the distribution of the design's units in the 2-dimensional input space for a smart design generated with the following assumptions: 2 input factors, 15 units, 5 levels for each factor, Z-method of factor levels generating. The best design was selected from among 5 designs, the achieved effectiveness of multi-generating method amounted to 36% for eI_{max} and 26% for eI_{mean} , which are one of the highest values in case of eI_{max} parameter and the top value in case of eI_{mean} parameter. The design qualified as the best of series generated with the application of multi-generation method is shown in Figure 2-A, whereas the design qualified as the worst in the same series is shown in Figure 2-B. It seems that the points representing design' units are distributed really more equally (uniformly) in Figure 2-A than in Figure 2-B, which confirms the effectiveness of the method analyzed.

6. Conclusions

The results of simulation have confirmed a significant impact of the multi-generation method on enhancing smart designs of experiment's quality. The application of the considered method allows you to select the optimal design among several generated for the defined design's characteristics and, as a result, to avoid accidental impact of random numbers, and thus supports the increase in the quality of smart designs of experiment.

Considering eI_{max} parameter, the decrease of its value is usually very high and reaches more than 10% in 79% of cases in the simulation. Considering eI_{mean} parameter, the decrease is not too huge but significant as well. Significant values of effectiveness obtained for eI_{mean} parameter can suggest reducing empty areas in the input space as a result of the application of analyzed multi-generating procedure.

When it is impossible to generate more than one design in 20 attempts, the only generated design is usually of good quality, notwithstanding the fact that the multi-generating procedure does not work in such a case. But if several designs are obtained in up to 20 attempts of a multi-generating procedure, a high variety of EPA-parameters is usually observed. In such cases, the procedure of multi-generating works very well and leads to enhancing the quality of smart designs.

You should also remember that the occurrence of empty zones in the input space may be the reason why the designs are generated with values of parameters set by the researcher, in particular: a defined number of units, defined number of input factor levels and their specified values, which could in fact more or less promote uniformity of design's units in the input space and could have a negative impact on the efficiency of the analyzed method. We do not know exactly of what quality would be a smart design generated without the application of the multi-generating procedure, maybe quite good, maybe very high, but certainly the application of the multi-generating procedure cannot cause a decrease in the design's quality. The likelihood of an increase in design's quality is significant and the damaging influence of pseudo-random numbers is seriously reduced.

References

- [1] Montgomery D.C., *Design and Analysis of Experiments*, John Wiley & Sons, Hoboken 2012.
- [2] Hinkelmann K., Kempthorne O., *Design and Analysis of Experiments. Volume 1. Introduction to Experimental Design*, John Wiley & Sons, Hoboken 2008.
- [3] Hinkelmann K., Kempthorne O., *Design and Analysis of Experiments. Volume 2. Advanced Experimental Design*, John Wiley & Sons, Hoboken 2005.
- [4] Polański Z., *Empirical research – methodology and computer aiding*, [in:] *Modern metrology*, J. Barzykowski (ed.), WNT (in Polish, Warszawa 2004).
- [5] Skowronek A., *Optymalizacja procesu generowania elastycznych planów eksperymentu (Optimization the process of generating the flexible designs of experiment)*, *Czasopismo Techniczne*, 1-I/2007, 63–74 (in Polish).
- [6] Johnson R.A., Bhattacharyya G.K., *Statistics: Principles and Methods*, John Wiley & Sons, Hoboken 2010.
- [7] Sheskin D.J., *Handbook of parametric and nonparametric statistical procedures. 3rd ed.*, Chapman&Hall/CRC, Florida 2004.
- [8] Skowronek A., *A method of self-adaptation calculating the value of the smart designs of experiment generation's parameter*, *Polish Journal of Environmental Studies*, Vol. 18, No. 3B, 2009, 327–331.
- [9] Dixit J.B., *Solutions to Programming in C and Numerical Analysis*, Laxmi Publications, 2006.